Characterization of Invadolysin in *Drosophila* and human cells: New insights into a novel, essential metalloprotease

Shubha Gururaja Rao

A thesis submitted to the University of Edinburgh in conformity with the requirements for the degree of Doctor of Philosophy

2008

Declaration

I hereby declare that this thesis is entirely my own composition and the experimental work described herein has been exclusively performed by myself unless otherwise stated in the text.

I also declare that the contents of this thesis have not been submitted for any other degree of professional qualification.

Shubha Gururaja Rao

March 2008

Dedicated to Meerakka

"We don't know that yet"
Margarete Heck

"Satyameva Jayate (Truth Alone Triumphs)"
(Mundaka Upanishad)

Acknowledgements

First and foremost, I would like to thank my supervisor Prof. Margarete Heck for her inspiring guidance and support during this work. I am very grateful to Sir Ken Murray and The Darwin Trust of Edinburgh for giving me the opportunity to study at the University of Edinburgh and for financially supporting me during my studies.

I am thankful to past and present members of the lab, Drs. Sharron Vass, Neville Cobbe, Francesca DiCara, Bin Yu, Kathryn Marshall, and Shrobona Bhattacharya, as well as fellow Ph.D. students Ching-Wen Chang, Edward Duca, and Ekin Bolukbasi for their help, guidance, support and company. I specially thank Dr. Bryce Nelson for his encouragement and guidance. I also sincerely thank Prof. Bill Earnshaw for his advice and inspiration. I thank Dr. Mike Cousin and Dr. Maria Vogelauer for their useful suggestions.

I thank my parents Mrs. Sathyabhama and Mr. T. R. Gururaja Rao, my doddamma Late. Mrs. Chitravathi, my doddappa Mr. L. G. Gururaja Rao, my two other parents Mrs. Harvinder Kaur and Capt. Sohan Singh, and Mrs. Prabhavathi and Mr. K.S. Ramanujam for their blessings. I also thank my brother in law Mr. Ravikumar, nieces Rashmi and Pranathi, Mrs. Hema Shetty and Mr. Bharat Shetty, and other family members Poornima, Srinivasan, Fozia, Mintu, Pavi for their love and care. I specially thank all my teachers in India who guided and motivated me to pursue higher studies in science.

I heartily thank my two dear friends Smitha and Sumati for being there for me not only during my Ph.D. but always. I also thank my other friends Latha, Rupa, Shwetha for always wishing me the best. My friends at Roorkee Anju, Deepak, Osman, Mankesh, and Mukut Chacha and Prof. Dhaliwal have been an incredible support for me to pursue this Ph.D.

There are two people without whose contribution my Ph.D. would be incomplete. I would like to thank the two idols of my life Drs. L. G. Meera and Harpreet Singh for inspiring, loving and guiding me all through.

Last, but the most, I would like to thank the super energy that balances the world without which none of this would be accomplished.

Abstract

Metalloproteases are enzymes that cleave other proteins and require a metal ion for their activity. They play a major role in the regulation of several cellular processes. I have analysed the functions of a novel, conserved metalloprotease named Invadolysin, previously reported by the Heck laboratory to be involved in mitosis and cell migration.

I carried out a second site non-complementation screen in *Drosophila melanogaster* to identify the interactors of Invadolysin utilizing the availability of a collection of genome-wide deficiency stocks. As a result of this screen, I identified *non-stop*, a ubiquitin protease, as a genetic interactor of *invadolysin*. I characterized similar mutant phenotypes of *invadolysin* and *non-stop* and showed that the abnormal chromosomal architecture observed in both mutants might be a result of histone ubiquitination.

I also investigated the involvement of Invadolysin in Notch pathway. The Notch extracellular domain levels were normal in the *invadolysin* mutants, but the intracellular domain levels were greatly reduced suggesting that the Notch pathway was inactive, or compromised. The levels of the Notch ligand Delta were abnormally high in *invadolysin* mutants, suggesting a block of Notch activity through *cis*-inactivation due to a possible failure in endocytosis of the Delta ligand. In human cells, I showed that Invadolysin partially co-localized with Rab11 and Itch proteins, which have been shown to influence the Notch pathway.

Considering the possible involvement of Invadolysin in Delta endocytosis, I examined the colocalization of Invadolysin with endocytosis machinery in human cells. I found that Invadolysin rings partially localized with Caveolin-1, and the caveolar endocytosis marker cholera toxin B was found inside the Invadolysin ring-like structures, suggesting that the inner region of Invadolysin rings might be a lipid based entity. When the lipid droplet marker BODIPY was utilized with Invadolysin, I established that Invadolysin surrounds lipid droplets.

Together, these studies have identified a previously unknown involvement of Invadolysin in the regulation of chromosome architecture, and the Notch pathway. The localization of Invadolysin to lipid droplets suggests its site of action and provides novel avenues to the study of this intriguing and essential metalloprotease.

Table of Contents Page

Abbreviations

A	absorbance
bp	base pair
BODIPY	4,4-difluoro-4-bora-3a,4a-diaza-s-indacene
BSA	Bovine Serum Albumin
cDNA	complementary DNA
CLAP	Chymostatin, Leupeptin, Antipain, Pepstatin A
C-terminus	Carboxyl terminus
CTxB	Cholera Toxin B subunit
DAPI	4', 6-diamidino-2-phenylindole
DEPC	Diethyl pyrocarbonate
Df	Deficiency of chromosomal region
DMEM	Dulbecco's modified Eagle's medium
DMSO	Dimethyl sulphoxide
DNA	Deoxyribonucleotide
dNTP	2'-deoxyribonucleoside 5'-triphosphate
dsRNA	Double stranded RNA
dsRNAi	Double stranded RNA-mediated interference
DTT	Dithiothreitol
EBR	Ephrussi Beadle Ringer's Solution
ECL	Enhanced Chemiluminescence
EDTA	Ethylenediamine-N,N,N',N'-tetraacetic acid
EGTA	Ethylene glycol bis(2-aminoethyl ether)- N,N,N',N'-tetraacetate
EM	Electron Microscopy
EMS	Ethylmethane Sulfonate
EST	Expressed Sequence Tag
FBS	Fetal Bovine Serum
GFP	Green Fluorescent Protein
HCl	Hydrochloric acid
HEPES	N-(2-hydroxyethyl)piperazine-N'-(2-ethanesulfonic acid)

His	Histidine
hr or hrs	hour or hours
HRP	Horseradish peroxidase
kb	kilobase-pairs(s)
kDa	kiloDalton(s)
l	litre
LB	Luria-Bertani medium
LD	Lipid droplet
M	molar
mg	milligram
mins	minutes
ng	nanogram
nm	nanomolar
N-terminus	Amino terminus
°C	Degree Celsius
OA	Oleic acid
OD	Optical Density
ORF	Open Reading Frame
PAGE	Polyacrylamide Gel Electrophoresis
PBS	Phosphate Buffered Saline
PCR	Polymerase Chain Reaction
pmol	picomoles
PMSF	Phenylmethyl Sulfonyl Fluoride
RNA	Ribonucleic acid
RNase	Ribonuclease
Rpm	Revolutions per minute
RT	Room Temperature
RT-PCR	Reverse Transcriptase - Polymerase Chain Reaction
SAR	Scaffold Attachment Region
SDS	Sodium Dodecyl Sulfate
SDS-PAGE	Sodium Dodecyl Sulphate Polyacrylamide Gel Electrophoresis
SMC	Structural Maintenance of Chromosomes

TAE	Tris acetate buffer with EDTA
TBE	Tris borate buffer with EDTA
TCA	Trichloroacetic acid
TE	Tris buffer with EDTA
Tris	Tris[hydroxymethyl]aminomethane
Triton X-100	Octylphenol ethoxylate
Tween-20	Polyoxyethylene-sorbitan monolaurate
UAS	Upstream Activating Sequence
v/v	volume per volume
vs	versus
w/v	weight per volume
wt	wild type
µg	microgram
µl	microlitre
µm	micrometer
µM	micromolar

Organisms

C. elegans	*Caenorhabditis elegans*
D. melanogaster	*Drosophila melanogaster*
E. coli	*Escherichia coli*
H. sapiens	*Homo sapiens*
L. major	*Leishmania major*

Cell lines

A375	Human malignant melanoma
HeLa	Human cervical adenocarcinoma
Huh7	Human hepatoma
PEO14	Human ovarian carcinoma

Table of Figures

Chapter 1: Introduction

My Ph.D. research in the Heck laboratory focused on the functional analysis of a novel metalloprotease Invadolysin (also known as IX-14) known to be involved in mitosis and cell migration (McHugh *et al.*, 2004), in *Drosophila melanogaster* and human cells. This thesis presents my work in five results chapters along with a discussion and a chapter on the Materials and Methods used for the study. Before these chapters, I am introducing *D. melanogaster*, the important model system I have used and the processes where we believe Invadolysin plays a role such as cell cycle and chromosome condensation. Invadolysin is a metalloprotease and hence a section of my Introduction is dedicated to proteases. I have also briefly reviewed additional cellular processes where Invadolysin might be playing a role according to my research, such as Notch signalling and lipid droplet biology. I conclude my introduction with a discussion of the background of Invadolysin.

***Drosophila* as a model organism**

D. melanogaster (fruit fly) is the most extensively studied model organism in biological research. It is used in various fields such as evolution, physiology, neurobiology, genetics, developmental biology, and so on. Thomas Hunt Morgan started using flies for research in the beginning of the 20th century to study the chromosomal theory of inheritance. Since then, use of fruit flies in research has grown immensely.

One important aspect that makes *Drosophila* such a widely used organism is the fact that 77% of human disease genes have strong matches to sequences in the *Drosophila* genome (Reiter *et al.*, 2001) (http://superfly.ucsd.edu/homophila/). There are *Drosophila* disease models for several diseases such as Parkinson's, diabetes and cancer (Feany and Bender, 2000; Leopold and Perrimon, 2007; Tenenbaum, 2003). The *Drosophila* genome was published in 2000 (Adams *et al.*, 2000) and revealed that there are around 13,000 genes in its 132 Mb euchromatic genome. Other advantages of using *Drosophila* as a model organism are that the flies are small and easy to maintain in the laboratory, the generation time is about 10 days, the sexes are dimorphic and easy to distinguish. It is economical to maintain fruit flies in the laboratory and they reproduce efficiently in defined medium at room temperature. *Drosophila* males do not undergo recombination and there are genetically engineered "balancer" chromosomes that have multiple inversions to prevent recombination and to maintain homozygous mutations. There are thousands of mutations available in worldwide stock centres allowing the analysis and manipulation of the majority of genes.

Drosophila allows the study of various cellular processes, offering its range of differentiated cell types and tissues. The proliferating tissues, such as larval neuroblasts and imaginal discs have a conventional cell cycle with G1, S, G2 and M phases and components of the cell cycle are highly conserved. These proteins can thus also be studied at various stages of development. Spermatogenesis and oogenesis in *Drosophila* are two different modes of meiosis and they provide an interesting research material to study this reductional cell division. The compound eye of *Drosophila* is made up of 800 individual units and is an exciting organ to study since these complex eyes develop from a monolayer of precursor tissue (Tio *et al.*, 1996). Fruit flies are also used to study the development of a multicellular organism from a simple fertilized egg, as is the case in all metazoans. There are only four chromosomes in *Drosophila* that are easy to visualize. Many of the larval tissues are polyploid and as a consequence the salivary gland chromosomes (which are also polytene chromosomes) of third instar larvae have replicated chromatids (1000-2000) lie alongside each other with a characteristic banding pattern making huge chromosomes. This gives rise to differential packaging and transcriptional activity on these chromosomes, providing a good model to study chromosome architecture.

In addition to the whole organism, there are several *Drosophila* cultured cells available such as Schneider cells that allow the study of cellular processes at the single cell level. Double stranded RNA mediated interference in cultured cells is a simple and powerful tool to "knock-down" protein expression and thereby study protein function.

Life cycle of *Drosophila melanogaster*

The *Drosophila* life span in the lab is about 30 days at room temperature (25˚C). They undergo a complete metamorphosis cycle, whereby they pass through embryo, larval and pupal stages before becoming adults (Figure 1.1). They survive at temperatures of 16˚C up to 30˚C and the length of the life cycle depends on temperature where the life span is longer at lower temperatures. At 25˚C, the flies spend about 5 days in embryo and larval stages and 4 days in pupal stages (total 9-10 days for the eclosion of adults). The female *Drosophila* lays eggs shortly after fertilization. The egg undergoes 13 rapid and synchronous nuclear divisions consisting of only S and M phase known as syncytial divisions (Foe, 1989). These divisions are completed in two hours. There after, cell membranes form around the nuclei resulting in the formation of cellular blastoderm. Maternally loaded mRNAs and proteins are mostly used for this process, whereas for further divisions zygotically produced material is required (Bate and Arias, 1993).

Approximately 24 hours after fertilization, the first instar larvae hatch. The first instar immediately begins feeding on the surface of the medium and begins into burrow in the medium after molting into the second instar stage after 48 hours of egg laying. The second instar larvae burrow into the media most of the time leaving only the spiracles exposed. After 72 hours, the second instar molts into the third instar that feeds for two days and then emerges out of the medium to "wander" on the vial walls for a suitable place to pupariate. Hence these larvae are called the wandering third instars. Pupariation occurs at 120 hrs after egg laying. The pupariation period is 4-5 days and the complete development takes place inside the pupa. The adult fly ecloses out of the pupal case with unexpanded wings and unpigmented body. Wing

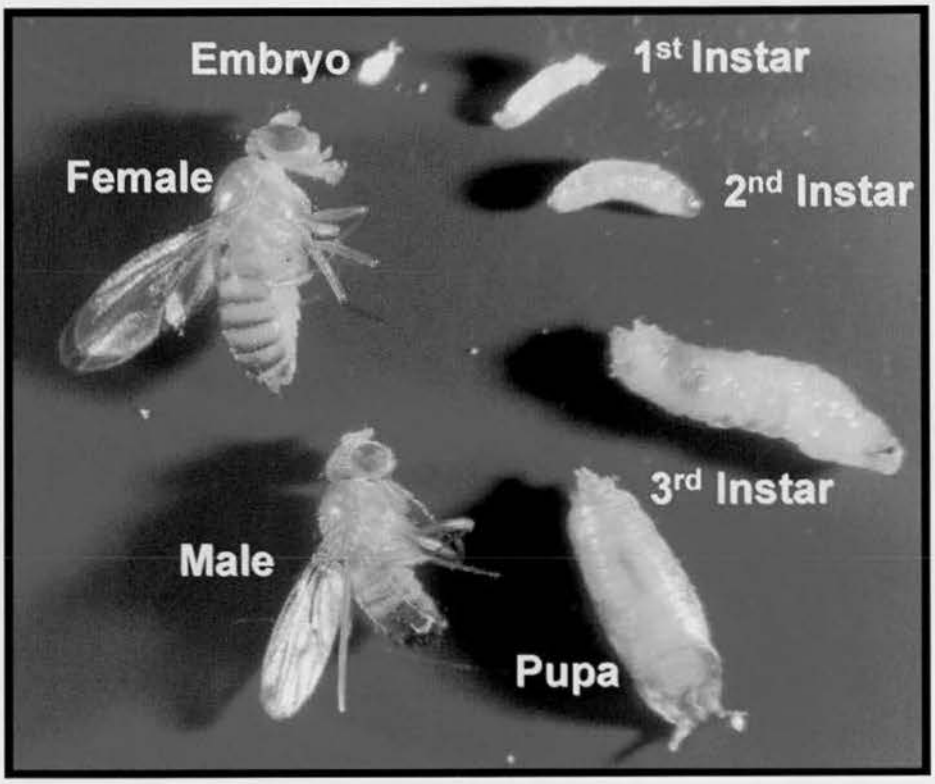

Figure 1.1. Life cycle of *Drosophila melanogaster.*
The fertilized egg develops into an embryo that hatches into a first instar larva. The first instar undergoes feeding and a growth phase, molts into second and third instar larvae and finally forms an immobile pupa. Metamorphosis takes place inside the pupal case and the adult fly ecloses out of the pupal case.

expansion occurs with in an hour of eclosion and full pigmentation occurs in 2-3 hrs (Ashburner *et al.*, 2005; Greenspan, 1997; Roberts, 1998).

The power of genetics

The reason that *Drosophila* is one of the best model organisms in biological research is largely due to the power of genetics. There are a number of genetic techniques devised in the past century that have lead to the elucidation of complex genetic interactions of signalling pathways and developmental stages (St Johnston, 2002). In the early stages of research, Drosophilisists isolated only spontaneously occurring phenotypically obvious mutations, but better molecular ways to generate more subtle mutations were developed later.

Ethyl methyl sulfonate (EMS) mutagenesis and the transposon (P-element) allele generation are the most popular strategies to create mutant alleles of genes. These mutations can be used to identify genes that function in a particular process having a set of phenotypes as the readout. P-elements are transposons that exist within the *Drosophila* genome and when allowed to transpose, generate mutant alleles. P-elements can also be engineered for ectopic expression of a given gene under tissue- of temporal-specific promoters. A large number of P-element alleles have been generated in large scale screens and are currently available in the stock centres (Spradling *et al.*, 1999).

One very powerful saturation screen mutagenesis was for mutations that affected patterning of the embryo (Nusslein-Volhard and Wieschaus, 1980). Since then, there have been several genetic screens focussing on a variety of processes. One of the most useful tools for carrying out genetic screens in *Drosophila* is the

"deficiency" collection. There are various stock centres in Bloomington, Kyoto and Szeged that offer a large collection of deficiency stocks covering the whole genome. A deficiency is a deletion that removes a large number of genes at a time from a few to hundreds possibly. Most of the Drosdel deficiencies from Szeged are molecularly mapped (Ryder *et al.*, 2007; Ryder *et al.*, 2004). By using the collection of these deficiencies, large scale and genome wide screens can be carried out.

A Second site non-complementation screen is a screen whereby a particular mutation can be brought together with another mutation or a deficiency and the transheterozygous progeny in such a combination can be tested for a particular phenotype of lethality (Fuller *et al.*, 1989). The phenotype or the lethality of the transheterozygous progeny would suggest a genetic interaction between the gene of interest and one or more genes deleted in the deficiency.

There are several systems that have been adapted in fruit flies and the best example is the yeast *UAS*-GAL4 system (Brand and Perrimon, 1993; Duffy, 2002) (Figure 1.2). GAL4 is a yeast transcriptional activator, which can be used to activate gene expression in *Drosophila* if a gene of interest is downstream of an upstream activating sequence (*UAS*). GAL4 specifically binds *UAS* and promotes the expression of the gene that is downstream of *UAS*. The expression of GAL4 itself can be controlled by using a tissue specific promoter with it, ensuring that GAL4 is only expressed in a particular tissue or at a particular time. Hence the ectopic expression of any *Drosophila* gene can be controlled spatially and temporally using this system. There are hundreds of GAL4 "driven" lines available that can be used to express a gene at a particular time in a specific tissue.

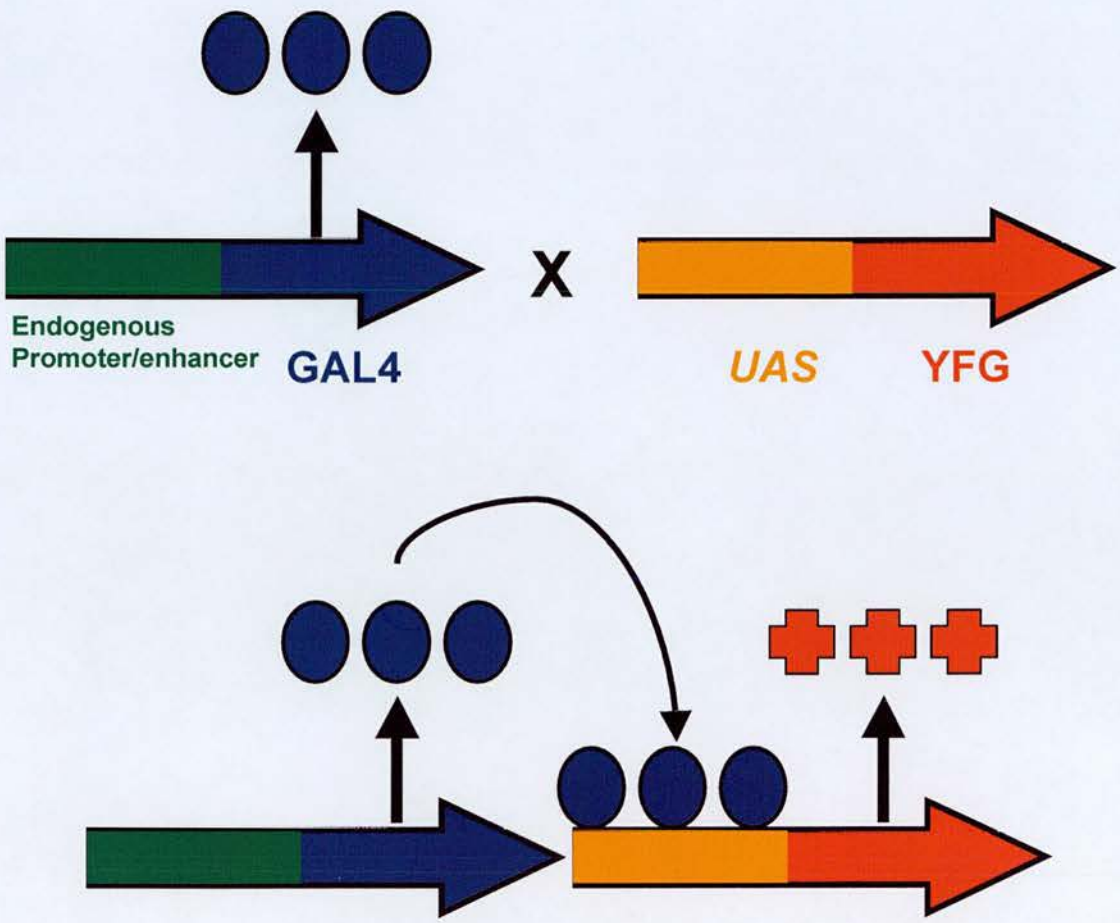

Figure 1.2. Schematic of *UAS*-GAL4 system.
When flies containing GAL4 (a transcriptional activator, shown in blue) with an endogenous tissue specific promoter (shown in green) are crossed to flies containing *UAS* (Upstream activating sequence, shown in orange) with the gene of interest, your favourite gene (YFG, shown in red), GAL4 is expressed in the promoter specific tissue in the progeny. GAL4 binds to *UAS* sequence activating the expression of YFG.

Enhancer and suppressor screens have been successful in identifying the components of several pathways. A gene can be overexpressed using *UAS*-GAL4 system in a particular tissue to result in a visible phenotype (Brand and Perrimon, 1993; Lee *et al.*, 2001). The *Drosophila* eye is the most popular choice for this kind of experiments. Over-expression of a gene in the ommatidia may result in a rough eye. The rough eye phenotype can be used as the starting point for an enhancer/suppressor screen where the overexpression can be examined in context of genome wide mutations. The mutations that enhance or suppress the phenotype can be identified as regulators of the gene of interest.

Another useful technique widely used in flies is the yeast FLP/FRT system (Theodosiou and Xu, 1998). This system is also adapted from yeast where FLP is a recombinase that can bring about recombination of sequences between short Flipase Recognition Target (FRT) sites. Mitotic recombination may generate a clone of cells that are homozygous mutant for a gene in an otherwise heterozygous animal (Figure 1.3). FLP can be expressed under the control of a heat shock promoter. Either the mutant clone or the wild type cells can also be marked with GFP to make it easier to follow the cells. A refinement of the FLP/FRT system is the "dominant female sterile technique". It uses the dominant mutation to kill the non-recombinant germ cells and hence females will only lay homozygous mutant germ line clones. This system is very useful to study maternal effect phenotypes of lethal genes and has identified many genes involved in embryogenesis that were missed by other screens due to maternal loading.

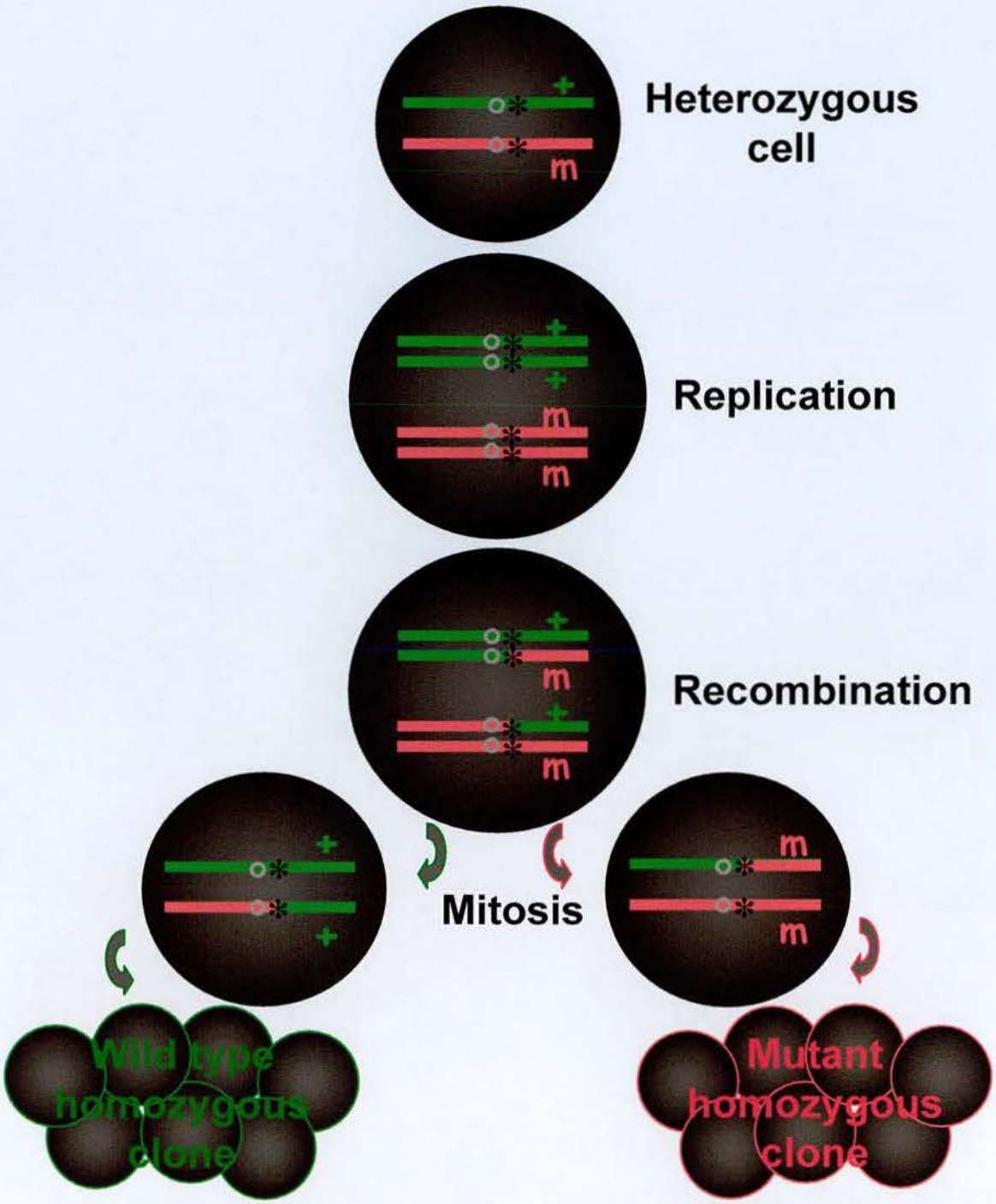

Figure 1.3. Schematic of FLP/FRT system.
In a heterozygous parental cell (with mutation 'm'), FLP induces mitotic recombination between FRT sites (shown as black asterisks) on homologous chromosome arms. Segregation of recombinant chromosomes at mitosis produces two daughter cells; a mutant cell bearing two copies of the mutant allele and a wild-type cell containing only the wild-type form of the gene. Subsequent cell divisions result in clones from each of these original daughter cells.

RNA interference (RNAi) is not only used in *Drosophila* cultured cells but also in flies (McGuire *et al.*, 2004). Gene transcripts can be knocked down in flies by generating flies that contain 300-500 base pairs of the target gene cDNA in an RNAi vector. The expression of this cDNA results in hairpin RNA that can induce RNAi (Clemens *et al.*, 2000; Kennerdell and Carthew, 1998). The RNAi in flies can also be combined with the *UAS*-GAL4 system to generate an inducible RNAi system and hence RNAi can be carried out in specific tissues at specific times (Lam and Thummel, 2000).

There is also a large collection of interaction data for fly proteins generated from yeast two hybrid interaction studies (Giot *et al.*, 2003). This is very helpful in preliminary analysis of the function of a given protein.

In conclusion, the ease of generating mutations in *Drosophila* and the efficiency of genetic screens make it the most suitable organism for large-scale genetic screens. Most proteins carry out more than one function and hence being able to study these functions using a range of alleles, with weak to strong phenotypes, is a very important tool to dissect pathways and functions of proteins in basic research.

The Cell Cycle

The cell cycle is the process whereby one cell makes a copy of itself, and divides into two daughter cells. The cell cycle is divided into four phases, namely S phase (DNA synthetic phase) in which the DNA is replicated, M phase in which the cell actually divides into two, and G1 and G2, which are the two 'Gap' phases between the end of mitosis and DNA replication and between replication and entry into mitosis respectively. Interphase is the general term for cells at G1, S or G2 phases. All of these phases have an important role in bringing about proper division of cells.

G1 phase

Cells make a decision whether to divide or to permanently or temporarily remain in a non-dividing state in G1 phase. They differentiate into specialised cells if they decide to be in a non-dividing state. Several cyclin-dependent kinases that regulate the cell cycle are activated in this phase by binding to cyclins which undergo dynamic changes during the cell cycle (Doree and Hunt, 2002; Morgan, 1997). Thus the check points between G1 phase and mitotic phase are regulated by these kinases. Cell cycle checkpoints are important to safeguard the accurate transfer of genetic material to two daughter cells (Pollard and Earnshaw, 2007).

S Phase

The genetic material is accurately replicated and transferred to daughter cells when the cells divide by mitosis. DNA gets replicated during the synthetic phase (S phase) prior to G2 and cell division. Replication begins at specific points on the

chromosomes called the origins of replication. Prokaryotes have a single origin of replication whereas eukaryotes have multiple origins of replication. In budding yeast, replication begins in autonomously replicating sequences (ARS) and a pre-replication (pre-RC) complexes assemble before S phase starts (Seki and Diffley, 2000; Toone *et al.*, 1997). There is evidence of pre-RC complexes in mammals as well (Diffley and Labib, 2002; Gerbi and Bielinsky, 2002). Several protein kinases are involved in the initiation of S phase in mammals (Zhang, 2007).

There is a specific pattern of DNA synthesis that takes place during S phase. The less condensed euchromatin replicates in the beginning of S phase and the highly condensed chromatin (heterochromatin) replicates at the end. Also during S phase, the cohesin complex establishes a physical link between sister chromatids (Blow and Dutta, 2005; Blow and Tanaka, 2005), and the centrosomes are duplicated (Doxsey, 2001).

G2 Phase

G2 is the interval between the end of S phase and the beginning of M phase. This phase consists of a protein kinase cascade that results in activation of cyclin dependant kinases (Cdks), that are required for mitotic entry; the main purpose of this phase is to proof-read the DNA sequence and prepare for mitosis. The centrosomes separate to become the spindle poles and initiate bipolar microtubule organisation.

DNA Damage Checkpoint

The DNA damage checkpoint is the mechanism by which damaged DNA is recognised and the cell is arrested at Gap phases, S phase may be slowed down and the expression of DNA repair genes is triggered (Elledge, 1996). If the damage is not reversible, the cell division is permanently halted by cellular senescence directed by signalling pathways. This is one example of a cell cycle checkpoint (Lukas *et al.*, 2004).

Mitosis

Mitosis is subdivided into five phases through which two daughter cells are formed from a single cell. The phases are prophase, metaphase, anaphase, telophase and cytokinesis (Figure 1.4).

Prophase

This is the first visible stage of mitosis and several changes happen in the nucleus and cytoplasm during this phase. The chromosomes condense starting from the nuclear periphery and may become visible as sister chromatids. The kinetochore proteins take their place on the primary constriction (centromere) of the chromosomes. Kinetochore is a structure on the centromeric hetetochromatin and it mediates the movement of chromosomes during mitosis (Ault and Rieder, 1994; Pollard and Earnshaw, 2007). Histone H3 gets phosphorylated by aurora B kinase (Adams *et al.*, 2001) and unfolding of the local chromatin due to histone phosphorylation may permit the binding of the condensin complex (Hirano, 2002). Histone H1 also gets phosphorylated by Cdk1-cyclinB (Swank *et al.*, 1997). The

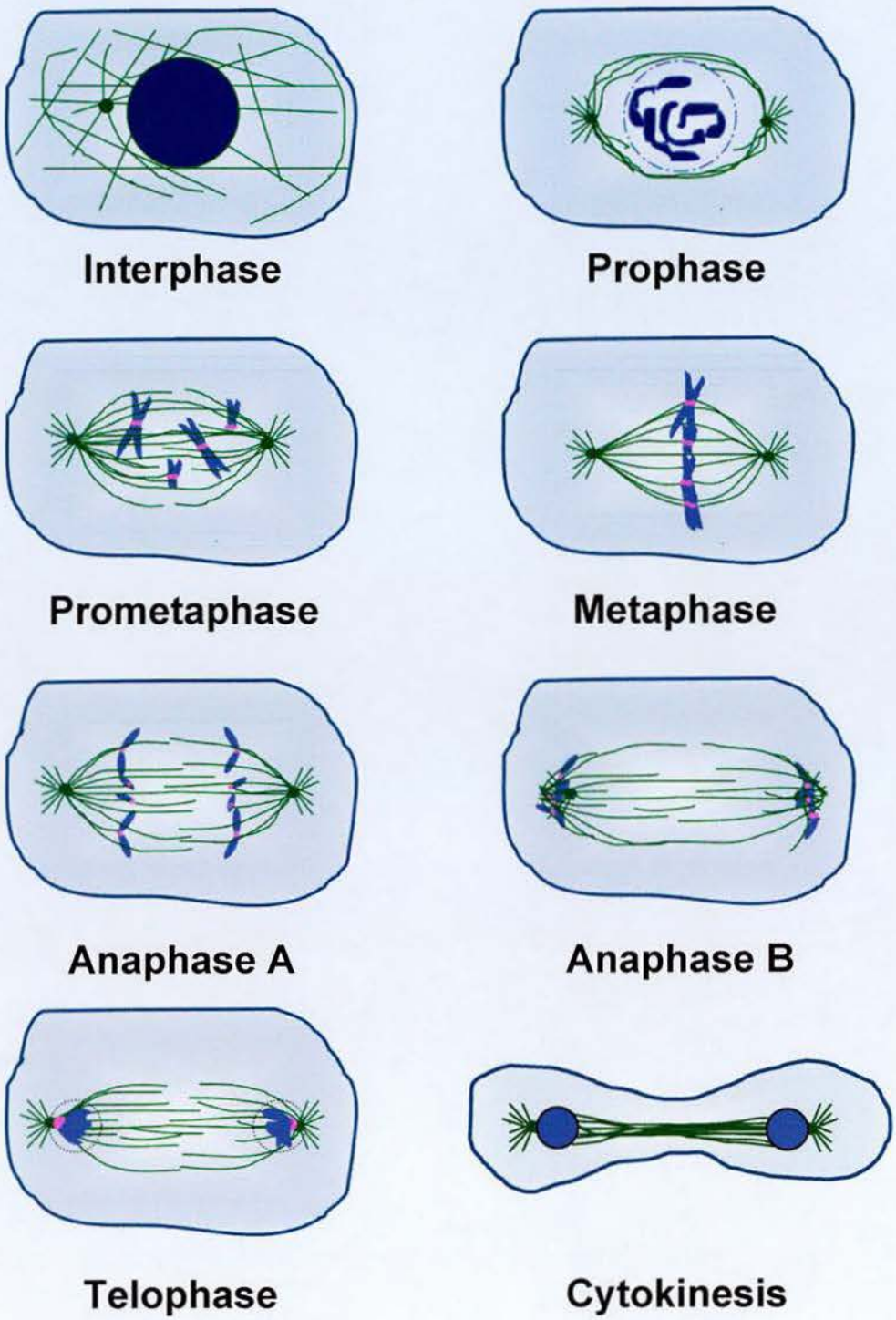

Figure 1.4. Mitosis in metazoan cells.
Mitosis in metazoan cells consists of interphase, prophase, prometaphase, metaphase, anaphase, telophase and cytokinesis.
Chromosomes are shown in blue, spindles are shown in green and centromeres are shown in pink.

microtubule network in the cytoplasm gets re-organised into astral arrays around separated centrosomes. Actin filaments disassemble, endo-exocytosis are brought to a minimum and protein synthesis is also stopped (Pollard and Earnshaw, 2007).

Metaphase

Before the onset of metaphase, prometaphase occurs where the nuclear membrane disassembles and kinetochores and spindles start interacting to align chromosomes. Each one of the sister chromatids gets oriented to one spindle pole. During metaphase, all chromosomes become attached to microtubules lining up in the middle of the spindle poles. This arrangement of chromosomes is called a metaphase plate. The spindle assembly checkpoint or the metaphase checkpoint ensures all the chromosomes are properly attached to both poles before the onset of anaphase.

Anaphase

During anaphase, the sister chromatids move to opposite poles (Anaphase A) and the poles move apart (Anaphase B). Anaphase entry is mediated by a reduction in Cdk1 activity by APC/C directed cleavage of proteins including securin and cyclin B (Irniger, 2002). The microtubules attached to the kinetochores shorten and motor proteins help the chromosomes move in anaphase A. In anaphase B, the spindle poles separate from each other. The interpolar spindles organise as the central spindle between the separating chromatids.

Telophase

The chromatids arrive at opposite poles of the cell, and new nuclear envelopes form around the segregated chromosomes. The chromosomes decondense and are no longer visible as distinct entities. Cytokinesis or the partitioning of the cell begins during this phase.

Cytokinesis

In animal cells, cytokinesis results when a fibrous ring composed of actin and myosin and other proteins around the center of the cell contracts, pinching the cell into two daughter cells, each with one nucleus. In plant cells, the rigid cell wall requires that a cell plate be synthesized between the two segregated daughter nuclei (Alberts *et al.*, 1994; Pollard and Earnshaw, 2007).

Chromosome condensation

Interphase chromatin condenses to give rise to usually distinct chromosomes in mitosis. Flemming first described mitotic chromosomes in 1879 (Flemming, 1879). It was believed that the chromosomes were invisible in interphase and during mitosis chromatin got bundled into a more condensed state. There has been a century of research focussed on the mechanism of chromosome condensation aided by the advent of electron and fluorescence microscopy and biochemical techniques.

DNA in a single human cell stretches to about 2 metres from end to end. This DNA has to fit into a nucleus of approximately 5-10 μm diameter and has to be compacted 10,000 times in length to make a metaphase chromosome (Heck, 1997). Hence there are levels of compaction involving a number of structural proteins that enable DNA to achieve this compaction. Several models have been proposed to explain this complicated compaction process (Belmont, 2002; Hirano, 2002). However, it still remains unclear the exact process by which mitotic chromosomes form.

Nucleosome

Interphase chromatin under low salt conditions appears as 'beads on a string' with a diameter of 10 nm by electron microscopy. The beads consist of an octamer of core histones (Histone 2A, Histone 2B, Histone 3 and Histone 4) and 166 bp DNA winding around the octamer in a left-handed super-helix. The histone octamer consists of a $[H3]_2$:$[H4]_2$ tetramer, flanked by two H2A:H2B heterodimers. The histones have compact histone fold of 70-80 amino acid residues and an N-terminal

tail of approximately 30 amino acids outside the nucleosome. Specific modifications of the N-terminal tail are important for modulation of chromatin structure (Woodcock and Dimitrov, 2001). Histone H1 or other linker histones bind to linker DNA between nucleosomes. Recently histone H1 has been shown to be necessary for full compaction of chromosomes *in vitro*. (Maresca and Heald, 2006). Histone phosphorylations and other modifications have been known to influence chromosome architecture (Ito, 2007).

The 10 nm 'beads on a string' compacts into a 30 nm fibre at the second level of chromosome compaction. Histone H1 is thought to promote the 30 nm fibre, a condensed filament of fibres that can be observed by electron microscopy. The 30 nm fibre is believed to compact into a 100-300 chromonema fibre, which has been observed by fluorescent microscopy in living cells and also by electron microscopy (Belmont and Bruce, 1994; Swedlow and Hirano, 2003). It is not known yet if the 300 nm chromonema fibre level is the next level after 30 nm level of compaction. How the chromonema fibre further compacts into a tight metaphase chromosome still remains a mystery.

The scaffold hypothesis

The proposal of the scaffold hypothesis (Figure 1.5) (Alberts *et al.*, 1994) over the last 30 years has attempted to elucidate the understanding of chromosome compaction. Paulson and Laemmli demonstrated the existence of a proteinaceous scaffold-like structure surrounded by a halo of DNA when histones were removed from mitotic chromosomes using a high salt extraction protocol (Paulson and Laemmli, 1977).

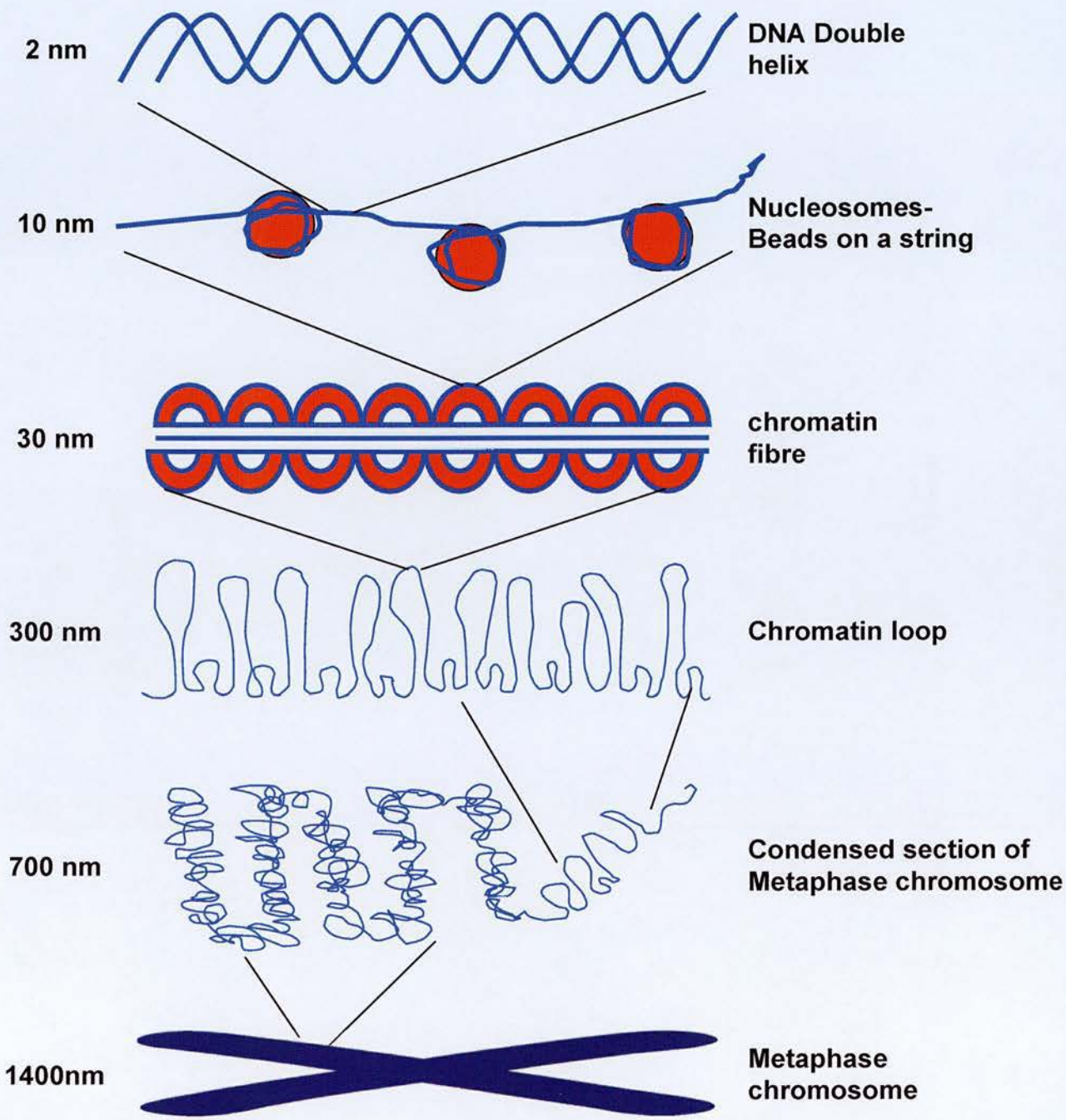

Figure 1.5. Model for the packaging of chromatin and the chromosome scaffold in metaphase chromosomes.
The winding of DNA around octamers of core histones to form nucleosomes constitutes the the 10 nm fibre. The 10 nm fibre further folds into a thicker (30 nm) filament called chromatin fibre. During interphase 30 nm fibres loop out from scaffolds. During metaphase, the scaffold folds into a further compacted structure (adapted from Alberts *et al.* 1994).

The DNA was observed as folded loops anchored to the proteinaceous scaffold. This gave rise to the hypothesis that the non-histone chromosomal proteins provide the framework for the final levels of DNA compaction. Specific scaffold attachment regions (SARs) in the DNA were discovered and they were shown to bind the chromosome scaffold with high affinity (Mirkovitch *et al.*, 1984). Synthetic peptides containing multiple AT-hooks (bind to AT-rich regions on DNA) have been shown to disrupt chromosome condensation by binding the SARs (Girard *et al.*, 1998) (Strick and Laemmli, 1995). Origins of replication have also been thought to act as the sites of chromosome condensation where DNA replication origins provide a template for the lengthwise compaction of chromosomes (Pflumm, 2002). Intriguingly, mitotic chromosome condensation defects have been observed in various DNA replication mutants (Krause *et al.*, 2001; Loupart *et al.*, 2000; Pflumm, 2002).

Purification of the chromosome scaffold revealed two major proteins Sc1 (170 kDa) and Sc2 (135 kDa), and a number of less abundant proteins (Gassmann *et al.*, 2004; Lewis and Laemmli, 1982). Sc1 was identified as DNA topoisomerase II (Earnshaw *et al.*, 1985; Gasser *et al.*, 1986) and Sc2 as a SMC protein (one of the subunits of the condensin complex) (Saitoh *et al.*, 1994). Protein extractions from mitotic chromosomes of different cell types have identified histones, topoisomerase IIα, chromokinesin, ATPase ISW1 and the condensin complex (Hirano *et al.*, 1997; Hirano and Mitchison, 1994; MacCallum *et al.*, 2002; Vernos *et al.*, 1995). ATPases present in the chromosome fractions are thought to be important for conformational changes of chromatin and to help their association and movement with microtubules (Swedlow and Hirano, 2003). Topoisomerase II is an ATP-dependent enzyme that

alters DNA topology by passing one double strand helix through another via a transient double-strand break (Wang, 2002). It is an essential protein localizing to the axial core of mitotic chromosomes (Earnshaw and Heck, 1985).

SMC family of proteins

The SMC family of proteins (Structural Maintenance of Chromosomes) are known to be condensin and cohesin complexes. The condensin complex consists of two SMC proteins (SMC2 and SMC4) and three non-SMC subunits (CAP-D2, CAP-G and CAP-H) (Cobbe and Heck, 2000). Initial genetic studies in yeast and *Drosophila* implied that condensin subunits are required for proper condensation and segregation of mitotic chromosomes (Losada and Hirano, 2001). However, recent studies have implicated this complex in stabilizing the shape of condensed metaphase chromosome rather than driving condensation per se (Hirota *et al.*, 2004; Hudson *et al.*, 2003). Metaphase chromosomes condense to a nearly wild type level in the absence of condensin (Bhat *et al.*, 1996; Savvidou *et al.*, 2005; Vagnarelli *et al.*, 2006) implying that there must be undiscovered molecular mechanisms regulating mitotic chromosome condensation (Belmont, 2006).

Cohesin is another complex identified to be involved in chromosome dynamics. The cohesin complex includes SMC1, SMC3, SCC1 and SCC3 proteins (Guacci, 2007). This complex is important for sister chromatid cohesion (Guacci *et al.*, 1997; Vass *et al.*, 2003). Cohesin is hypothesized to form a ring structure around replicated DNA at S-Phase. The cohesin ring is shown to be cleaved at anaphase onset by seperase (Gruber *et al.*, 2003; Haering *et al.*, 2002). However, this model

has been questioned in recent studies where chromatids can be resolved without cohesin dissociation (Guacci, 2007).

Thus detailed structural understanding of chromosome architecture still remains poorly understood (Belmont, 2006).With ambiguities surrounding the structural models for chromosome structure, more work needs to be done to address the mechanism of condensation.

Role of histone modifications in chromosome condensation

Histones are basic proteins that associate with DNA. Nucleosomes are made up of four kinds of histones (H2A, H2B, H3 and H4) and the linker histone H1 connects the nucleosomes. The compact structure of chromatin/chromosomes can allow access of transcription factors and this is an interesting area of study to know how chromatin organisation facilitates this process. There should be dynamic chromatin reorganisation events occurring in order to achieve this. Although histones make structural components of nucleosomes, their N-termini hang out from the nucleosomes, which can be accessed for various post-translational modifications. Histones undergo acetylation, methylation, phosphorylation, ADP-ribosylation, ubiquitination, sumoylation, deimination and proline isomerization. Acetylation and methylation are mainly linked to transcriptionally active or inactive states of genes where as phosphorylation is mainly linked to mitosis. Ubiquitination, sumoylation, ADP ribosylation, deimination and proline isomerisation are poorly understood, most being implicated to transcription so far (Kouzarides, 2007).

Chromosome condensation is also known to be regulated by histone modifications. Phosphorylation on serine 10 on Histone H3 (H3S10) has been linked to chromosome condensation during mitosis (Strahl and Allis, 2000). H3S10 phosphorylation by aurora kinase is the well known histone phosphorylation that appears at mitosis and is thought to be occurring by replacing Heterochromatin protein 1 at H3K9 monomethylation site (Fischle *et al.*, 2005). The other phosphorylation associated with chromosome condensation is H3 tyrosine 3 mediated by Haspin kinase and is required for metaphase chromosome alignment (Dai *et al.*, 2005) Intriguingly, H2B Serine 10, H2B Serine 14 and H4 Serine 1 have also been recently linked to chromosome condensation (Kouzarides, 2007). H4 lysine 16 acetylation affects chromatin decondensation (Shogren-Knaak *et al.*, 2006) where as a deacetylase SirT2 that localizes to chromatin also induces chromosome condensation (Vaquero *et al.*, 2006).

Histone modifications affect a number of nuclear events such as transcription, chromosome condensation and mitosis. However, how individual histone modifications affect a particular process both positively and negatively is yet to be elucidated. Much more research on histone code is required to throw light on the complex mechanism of chromatin and chromosome structure and gene regulation.

Proteases

The enzymes that cleave peptide bonds between amino acids are called proteases, proteinases, peptidases or proteolytic enzymes. They mediate several physiological processes by modulating the activity of other proteins. They participate in regulatory mechanisms and thereby bring about activation, inactivation or degradation of other proteins by cleaving them. Thus proteases are extremely important for homeostasis, regulation of signal transduction, and modulation of inter-protein and intercellular interactions. Pathways such as blood-clotting cascade, apoptosis and various signalling cascades involve major contributions of proteases.

Proteases are broadly classified into two classes, endo-peptidases and exo-peptidases. The difference between the endo and exo-peptidases is that the former cleaves peptide bonds in the internal region of its substrate protein where as the latter cleaves di- or tri-peptide bonds at the termini of substrate proteins. Based on the catalytically active residue of proteases, there are six classes. These are serine proteases, cysteine proteases, threonine proteases, aspartic acid proteases, glutamic acid proteases and metalloproteases. As indicated by their names, these proteases have either a specific amino acid or the help of a metal ion to bring about their activity. Metalloproteases are hydrolytic endopeptidases that require either zinc or calcium for their activity. A water molecule co-ordinates the metal ion and is essential for the activity.

Metalloproteases contain a short consensus sequence, HEXXH with two histidines acting as the ligands for the catalytic zinc and glutamate as a base (Gomis-Ruth, 2003). These are termed as zincins (or inverzincins if the active sites read HXXEH). Metalloproteases are also divided into clans M1-M76 (http://merops.sanger.ac.uk/).

Zincins are further classified as gluzincins, aspzincins and metzincins based on the nature and position of an additional third protein zinc ligand. The gluzincins have a 20 residue motif downstream of the HEXXH motif. The aspzincins have an aspartate residue as the third zinc ligand. The metzincins have a C-terminally elongated zinc binding motif HEXXHXXGXXH/D with an additional histidine or aspartate. They also possess a conserved methionine containing a 1,4-β turn called the Met-turn (Figure 1.6A). This gives them the name metzincins. The metzincins are subdivided into structurally characterized families as astacins, serralysins, adamalysins, snapalysins, matrix metalloproteinases, and leishmanolysins (Hooper, 1994; Stocker *et al.*, 1995). The matrix metalloproteinase and leishmanolysin families will be introduced with more detail.

Matrix metalloproteases (MMPs)

The first matrix metalloproteases were discovered 40 years ago, as the active agent engaged in tail resorption during frog metamorphosis (Gross and Lapiere, 1962). This enzyme was identified as a collagenase, and was further found in all vertebrates, involved in extracellular matrix (ECM) degradation. Naming of the matrix metalloproteases started with fibroblast collagenase being named MMP-1. There are 23 MMPs in human and 24 in mice (Page-McCaw, 2007). All these MMPs share a similar structural organisation with a signal peptide that targets them to the secretory pathway, a pro-peptide domain and the catalytic domain. They are classified as true collagenases, gelatinases and stromelysins. There is also a subfamily of MMPs that are categorised as membrane-type MMPs (MT-MMP). Of such MMPs are the transmembrane MMPs and GPI (glycosylphosphatidyl inositol)

anchored MMPs (Handsley and Edwards, 2005). MMPs are inactive when they are synthesized because of a prodomain. Activation of the prodomain occurs via a cysteine switch (Wasserman, 2005). A conserved cysteine residue in MMPs is bound to a zinc ion in the active site and prevents the binding and cleavage of the substrate keeping the enzyme in an inactive form. Dissociation of this cysteine from zinc results in the activation of the enzyme. This dissociation is called as the cysteine switch and this mechanism is applicable to all MMPs (Van Wart and Birkedal-Hansen, 1990).

In the 1960s and 70s MMPs were observed to be upregulated in many human diseases including cancer, rheumatoid arthritis and bone disease (Egeblad and Werb, 2002). However, recent evidence suggested that the relationship between MMPs and disease is more complicated than initially thought. Increased MMP activity was found to not only enhance progression of some tumours but also suppress it in other instances (Coussens *et al.*, 2002). Hence a need to further study the role of MMPs in normal physiology and disease remains.

Only two MMPs have been found in *Drosophila*; *Dm*MMP-1 and *Dm*MMP-2. *Dm*MMP-1 is embryonically expressed (Llano *et al.*, 2000) and *Dm*MMP-2 is expressed throughout development (Llano *et al.*, 2002). Tissue remodelling defects have been observed in the *Dm*MMP-1 mutant flies where the tracheal tubes fail to grow (Wei *et al.*, 2003). Ninjurin, a signalling protein, has been discovered associated with *Dm*MMP1 showing a possible role for MMPs in intercellular

signalling (Zhang, 2007). *Dm*MMP2 has been shown to be involved in histolysis where the mutants have shown larval tissues that should have been histolysed (Page-McCaw *et al.*, 2003).

MMPs uniquely have their tissue specific inhibitors (TIMPs) that act by forming a complex with the activated catalytic zinc in MMPs (Pender and MacDonald, 2004). Inhibitors from one organism can inhibit MMPs from another. This shows the striking conservation of MMPs and TIMPs between different organisms (Page-McCaw *et al.*, 2007).

Leishmanolysin

Leishmania sp. are a type of protozoa that cause 1.5-2 million cases of leishmaniasis per year in the world (Desjeux, 2001). Leishmaniasis is characterised by persistent fever, enlarged liver and spleen, and dark and scaly skin (Murray *et al.*, 2005). *Leishmania* species are transmitted by sand flies. The life cycle of *Leishmania* also requires a mammalian host to complete. The sand flies inject promastigotes into human body while sucking blood. Promastigotes are phagocytosed by macrophages where they become amastigotes. Amastigotes multiply in infected tissues causing the clinical manifestations mentioned above. Sand flies become infected by ingesting macrophages containing amastigotes in the blood. In the sand fly's midgut, amastigotes differentiate into promastigotes and migrate into the proboscis of the sand flies (Yao *et al.*, 2003). The cell-surface coat of *Leishmania* is responsible for the survival and proliferation of the organism in the adverse conditions of the sand fly's midgut and mammalian macrophages. One of the cell surface proteins in *Leishmania major* is leishmanolysin, a 63 kDa

glycosylated GPI-linked protein, also known as gp63 (Russell and Wilhelm, 1986). Gp63 cleaves CD4 molecules on the surface of human T cells and protects promastigotes from lysis by complement proteins. This suggests a role for gp63 as a virulence factor making it an attractive target for vaccine production (Bouvier *et al.*, 1995; Etges, 1992).

The crystal structure of leishmanolysin was published in 1998 (Schlagenhauf *et al.*, 1998). Leishmanolysin (Rawlings *et al.*, 2008) (MEROPS M8) was found to have homologues in *Drosophila*, mammals and recently in bacteria as well (Gomis-Ruth, 2003; McHugh *et al.*, 2004). Leishmanolysin is synthesised in an inactive form in the endoplasmic reticulum where the signal sequence is cleaved off post-translationally. Another processing step removes the 100 residue pro-domain, including a highly conserved cysteine switch, thus liberating the mature active protein.

Leishmanolysin has a large insertion of ~60 residues between the glycine and the third histidine residue of metzincin (Figure 1.6B). Leishmanolysin lacks the 2nd beta-strand present in typical metzincins, but has insertions of other alpha helices and beta-strands. The alpha helices A, B and C and beta strands I, III, IV and V are well-conserved. Leishmanolysin has the stereotypical arrangement of the typical zinc-binding histidines and underlying met-turn methionine, which qualifies it into the class of metzincin metalloprotease (Figure 1.6B).

Leishmanolysin is not classified as an MMP because the insertion between histidine and glycine makes the catalytic domain very different from that of MMPs. However, leishmanolysin has a similar cysteine switch mechanism of activation.

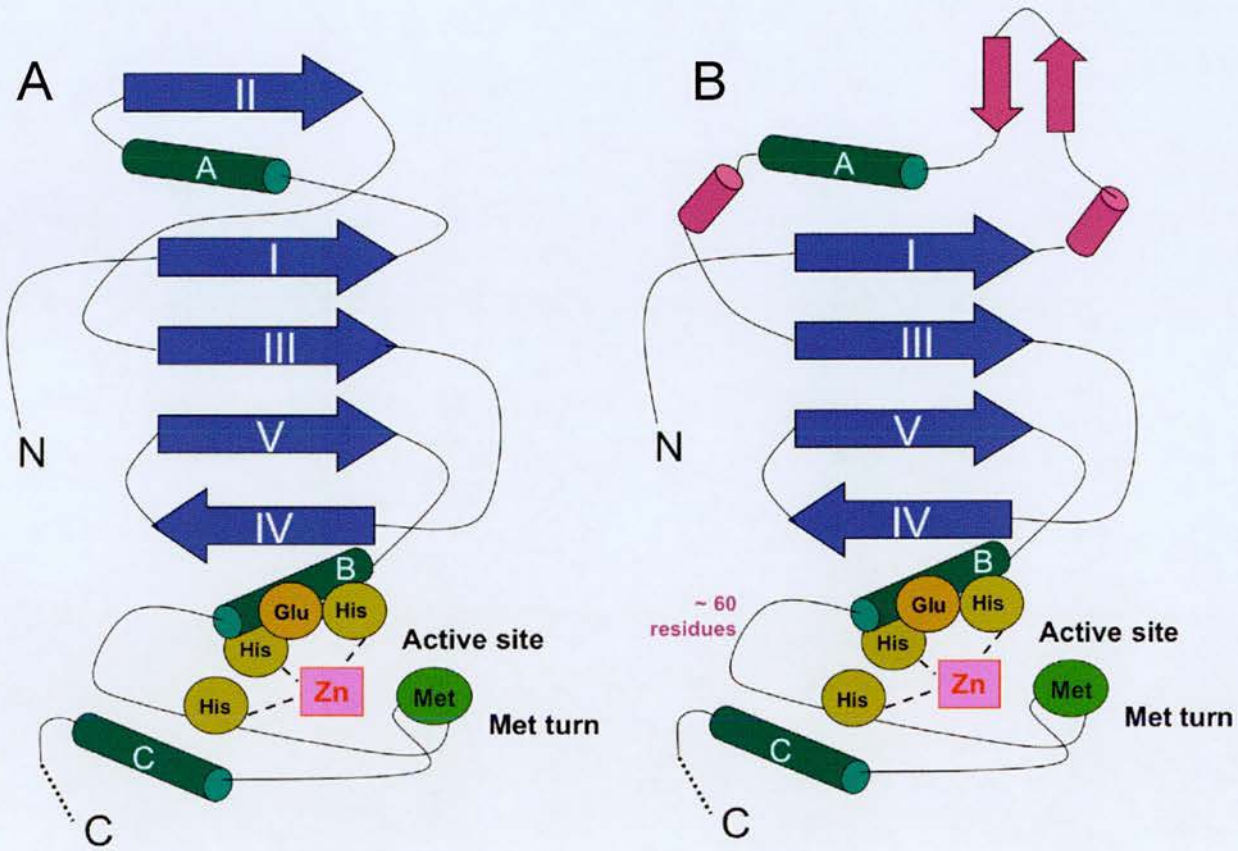

Figure 1.6. Schematic structure of a typical metzincin (A) and Leishmanolysin (B). The metazincins share a conserved structure of 3 α- helices (represented by green cylinders A, B, C) and 5 β-strands (represented by blue arrows I, II, III, IV, V). Three histidines bind a zinc ion to make the active catalytic site. A "met turn" follows the active site. Leishmanolysin lacks β-strand II but includes insertions of α- helices, β-strands and further (~60) residues (all represented in purple). Although some minor differences exist, the site and met turn are well conserved in Leishmanolysin. Therefore Leishmanolysin is classified into the metzincin class of metalloproteases (adapted from Gomis-Ruth, 2003).

Leishmanolysin can cleave casein, gelatin, hemoglobin, fibrinogen and CD4 molecules (Yao *et al.*, 2003). MRP (MARCKS-related protein) is also known to be cleaved by leishmanolysin (Corradin *et al.*, 1999). Myristoylated alanine-rich C kinase substrate (MARCKS) and MARCKS-related protein (MRP) are implicated in the coordination of membrane-cytoskeletal signaling events, such as cell adhesion, migration, secretion, and phagocytosis in a variety of cell types (Sundaram *et al.*, 2004).

Deubiquitinating enzymes

Another class of interesting proteases are the deubiquitinating enzymes (DUBs). Post-translational modification of proteins occurs by the addition of a small molecule, ubiquitin, which can decide the fate of proteins. Hence (DUBs) become an important group of proteases in biological research with their ability to remove the ubiquitin moiety adding an extra level of regulation to post-translational modifications. DUBs play an important role in regulating several pathways and diseases such as neurodegeneration or cancer. DUBs are also known for their role in regulating the ESCRT complex and thereby influencing endocytosis, a very important process in several cellular events (Clague and Urbe, 2006). DUBs have been recently studied in oncology as potential drug targets in order to selectively down regulate or ablate oncogene products (Nijman *et al.*, 2005).

There are more than 500 deubiquitinating enzymes in the human genome (Puente and Lopez-Otin, 2004). Of these, 84 are already known to be functional (Clague and Urbe, 2006). DUBs can be categorized as metalloproteases or cysteine proteases classes, although most DUBs are cysteine proteases (Nijman *et al.*, 2005).

Cysteine proteases rely on the thiol group of a cysteine for their activity. During catalysis, a cysteine nucleophile attacks a peptide bond existing between the ubiquitin molecule and substrate in case of the DUBs.

DUBs are further classified into five classes based on their ubiquitin protease domain. These include ubiquitin-specific protease (USP), ubiquitin C-terminal hydrolase (UCH), Otubain protease (OTU), Machado-Joseph disease protease (MJD) and JAMM motif proteases (JAB1/MPN/Mov34 metalloenzyme). All are cysteine proteases with the exception of JAMM motif proteases. JAMM proteases are metalloproteases that need a zinc ion for their activity. USPs represent the bulk of DUBs encoded by the human genome. It is believed that USPs increased in number, coevolving with their corresponding E3 ubiquitin ligases (Semple, 2003).

Recent research suggests that most DUBs regulate a limited number of pathways suggesting that they have specific substrates (Nijman *et al.*, 2005). The specificity might come from the substrate or ubiquitin moiety. Some DUBs are known to prefer K63 lysine link over K48 lysine link (Kee *et al.*, 2005), while others DUBs choose to cleave K48 linkages and not K63 (Hu *et al.*, 2005). Some DUBs also associate with their E3 ligase (ubiquitin ligase) counterparts to stabilize the ligases (Wu *et al.*, 2004).

Functions of DUBs

DUBs are implicated in endocytosis, proteasomal activity and chromatin structure. Deubiquitination of proteins targeted to the proteasome allows recycling of ubiquitin and is also essential for degradation of targeted proteins. Many DUBs have been shown to complex with the 19S proteasome regulatory component

(Borodovsky *et al.*, 2001). Nucleosomal proteins, i.e. histones, get ubiquitinated and deubiquitinated. Histone ubiquitination is linked to the regulation of transcription and gene silencing. H2B is deubiquitinated by UBP8 and UBP10 which correlate with transcriptional activation and telomeric silencing respectively (Emre *et al.*, 2005; Henry *et al.*, 2003). This suggests the requirement of dynamic histone modification by ubiquitin to regulate transcription. How other histones get ubiquitinated or deubiquitinated and how this process affects higher-order chromosome architecture is not yet clear. The *Drosophila* deubiquitinating enzyme *non-stop* (a homologue of yeast UBP8) is also implicated in axon-targeting and glial cell migration (Poeck *et al.*, 2001).

Another important process of DUB action is endocytosis. DUBs act on ubiquitinated receptors to rescue them from being targeted to the lysosomes and recycle the receptors to cell surface. For example, the *Drosophila* DUB "Fat Facets" deubiquitinates Liquid Facets and stabilizes it. The stabilization of Liquid Facets is important for endocytosis of the Notch ligand Delta (Overstreet *et al.*, 2004). Thus DUBs play an important role in reversal of ubiquitination and regulation of several cellular processes.

Notch signalling

Cell signalling is a complex coordinated system of communication between cells to mediate various cellular activities. Failure or aberrations in signal transduction lead to various disease states such as diabetes, cancer and autoimmunity diseases. There are various signalling pathways acting between cells, and Notch signalling is one of them. Notch signalling is required throughout development to regulate spatial patterning, timing and cell fate decisions (Baron, 2003). Notch is also known to promote development and proliferation of some cell types and, depending on the context of its action, it can act as an oncogene or a tumour suppressor (Weng and Aster, 2004).

Notch pathway proteins play important roles in processes ranging from glial cell migration (Edenfeld *et al.*, 2007) to differentiation (de la Pompa *et al.*, 1997). The Notch signalling pathway consists of the Notch receptor, its ligands Delta, Serrate or Jagged and a number of regulators of both ligand and receptors. There is only one Notch receptor in flies and four in humans. The number of ligands also varies between species where *Drosophila* has two (Delta and Serrate) and mammals contain five (Delta like 1,3,4 and Jagged 1,2) (Pintar *et al.*, 2007). However, the mechanism of action of this pathway is highly conserved throughout the animal kingdom (Schweisguth, 2004).

Notch is single-pass transmembrane protein with EGF and LNG repeats (Mumm and Kopan, 2000). It is a heterodimer with an extracellular domain (NECD) and an intracellular domain (NICD) associated non-covalently on the plasma membrane (Figure 1.7). The ligands from the signal donor cell bind to the Notch receptor in the signal recipient cell. The Notch pathway is activated with a series of cleavages termed S1, S2 and S3. The S1 cleavage occurs within the secretory

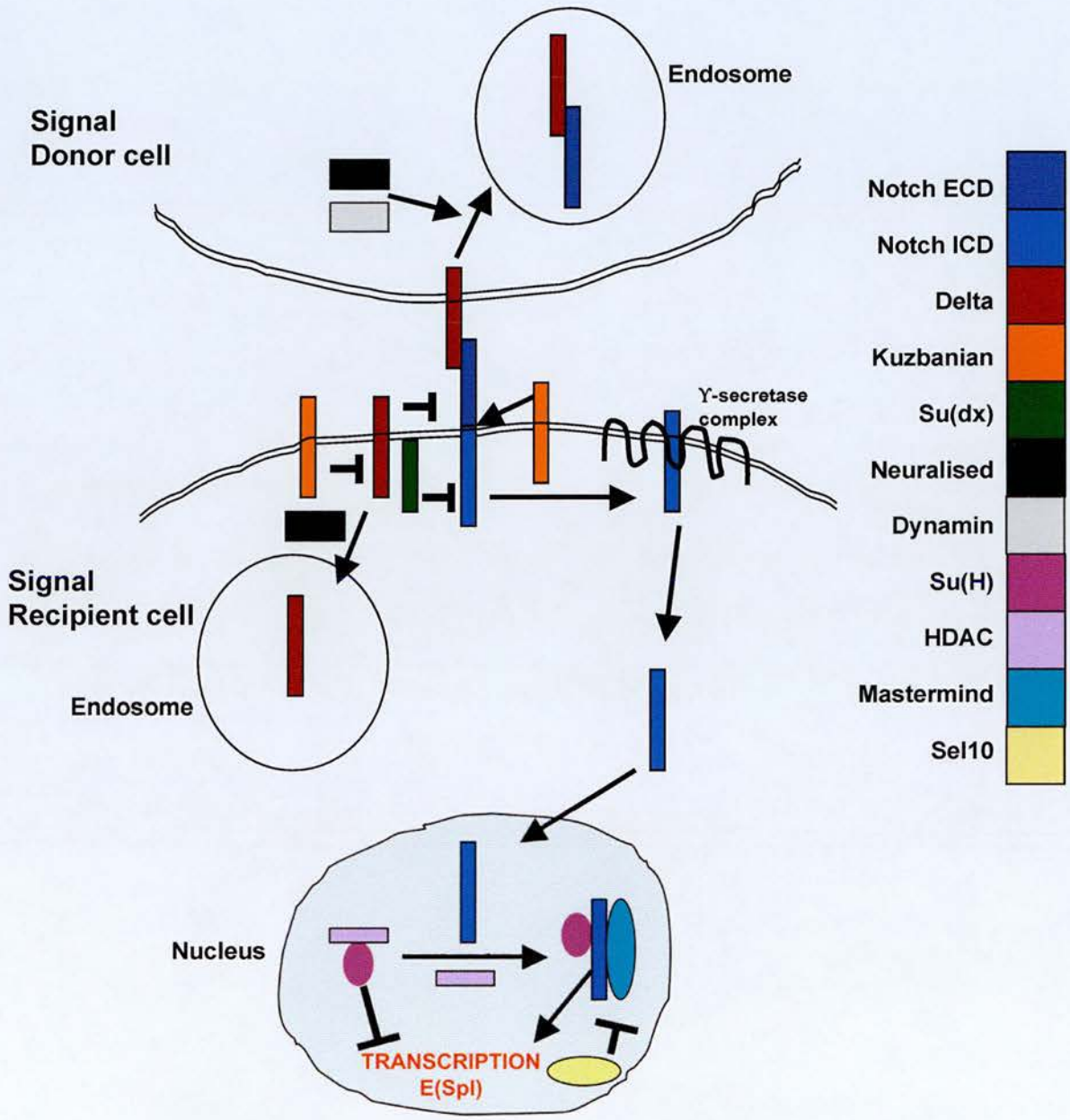

Figure 1.7. An overview of the Notch signaling pathway in *Drosophila.*
The Notch receptor at the cell surface undergoes a series of cleavages to release the intracellular domain upon ligand (Delta) binding. The intracellular domain enters the nucleus to bring about transcription of target genes. Both Notch and its ligands are regulated by multiple enzymatic activities (adapted from Baron, 2003).

pathway by a furin-like convertase occurring at a furin consensus site (Logeat *et al.*, 1998). This cleavage is not well characterized in *Drosophila*; it may not occur at all or at least not be necessary for signalling (Kidd and Lieber, 2002). Upon ligand binding to the extracellular domain, S2 cleavage of Notch occurs via an ADAM metalloproteases (Pan and Rubin, 1997). In *Drosophila* the ADAM metalloprotease involved in this process is Kuzbanian (Rooke *et al.*, 1996).

However, there are studies showing that soluble Delta constructs can act dominant negatively (Sun and Artavanis-Tsakonas, 1997). Delta can inhibit Notch signalling by a process called '*cis*-inactivation' or '*cis*-inhibition' where Delta binds the Notch receptor of the same cell with a dominant negative effect on signalling (Li and Baker, 2004). This also explains the observed role for Kuzbanian in the signal-receiving cell where it might be acting on Delta. ADAM metalloproteases are known to cleave Delta in mammals (Six *et al.*, 2003). The mammalian ADAM metalloprotease linked to S2 cleavage of Notch is TACE/ADAM17 (TNF-α converting enzyme). It has been found that the *Drosophila* TACE can also cause S2 cleavage (Brou *et al.*, 2000) but it is distinct from Kuzbanian type of S2 cleavage.

Ubiquitination and endocytosis are also important for Notch signaling (Gupta-Rossi *et al.*, 2004). The GTPase dynamin (known as *shibire* in *Drosophila*) is also implicated in Notch signaling. Dynamin is involved in promoting endocytosis and a dynamin dependent endocytosis of Delta in the signaling cell *trans*-endocytosis is hypothesized (Parks *et al.*, 2000). The ring finger ubiquitin ligase Neuralised is also implicated in both *cis* and *trans* endocytosis of Delta where it is known to promote Delta endocytosis by ubiquitination of Delta (Deblandre *et al.*, 2001; Lai,

2002). The expression of neuralised is more in correlation with the *cis*-endocytosis than the *trans*. The definitive roles of Neuralised are yet to be described.

After S2 cleavage, NICD undergoes S3 cleavage within the transmembrane domain to release the soluble version of NICD. Studies in mice, *Drosophila* and *C. elegans* have shown that presenilin proteins are processing the S3 cleavage (Donoviel *et al.*, 1999; Levitan and Greenwald, 1995; Struhl and Greenwald, 1999). Presenilin proteins are a large complex that cleave amyloid precursor proteins in mammals within the transmembrane domain (Haass and De Strooper, 1999). Presenilin does not co-purify with the activity responsible for the S3 cleavage of Notch in *in vitro* assays. The localization of presenilin in cultured cells is in the secretory pathway (Cupers *et al.*, 2001) and presenilin-independent Notch signalling is shown to occur (Berechid *et al.*, 2002). Hence it is believed that there might be another protease involved in the process.

Cleaved NICD translocates to the nucleus to activate its target genes. NICD enters the nucleus and interacts with the DNA binding protein complex CSL (CBF (C-promoter binding factor)-1, Suppressor of hairless, Lag-1). When there is no NICD, CSL represses the transcription of Notch target genes by interacting with a co-repressor complex that includes a histone deacetylase. NICD displaces the co-repressor complex from CSL, replacing it with a transcriptional activation complex that includes NICD, mastermind and the histone acetyl transferase p300 and pCAF p300/CBP (cyclic AMP response element binding protein) associated factor. NICD thus converts a transcription repressor complex into a transcription activator complex. The currently known target genes of the Notch pathway are Hes genes

(Hairy, enhancer of split), HRT/HERP/HEY families of genes and certain differentiation and cell-cycle related targets (Kadesch, 2004).

On its way to the nucleus the NICD is regulated by several steps. Ubiquitination can control the Notch pathway via several E3 ligases (Lai, 2002). Sel-10 E3 ligase stimulates phosphorylation-dependent ubiquitination of nuclear NICD to trigger proteasomal degradation. (Gupta-Rossi *et al.*, 2001). Mastermind, another ubiquitin ligase regulating the turnover of NICD is recruited by NICD itself which is a self-limiting activity of Notch (Fryer *et al.*, 2002). Another E3 ligase involved is Suppressor of Deltex (Su(dx)). Itch, a vertebrate homologue of the *Drosophila* Su(dx), genetically interacts with Notch1 in mice and is also involved in inflammatory responses which have not been yet linked to the Notch pathway (Matesic *et al.*, 2006). Itch localizes to early endosomal system (Angers *et al.*, 2004).

The Notch pathway is vitally important for development and diseases. Aberrant Notch signalling is involved in many neurodegenerative disorders and cancers. The involvement of various regulatory steps provide a potential target for several human diseases. Since Notch is known to crosstalk with several signalling pathways it is important to understand this pathway to study the basis of disease and development. Hence there is a wide scope for studies of the Notch pathway to more clearly understand regulation of the pathway, its target genes, and their functions.

Lipid Droplets

Lipid droplets (LD) are organelles that exist in most eukaryotic cell types to store neutral lipids. Their size and number vary between different cell types with adipose tissue containing the highest amount, where they are called adiposomes. The size is typically between 0.05 μm to 200 μm (Murphy, 2001). They are usually surrounded by a monolayer of phospholipids. They also have other names such as fat globules, lipid bodies, oil bodies, etc. in different organisms and cell types. They are formed in response to elevated levels of fatty acids in cultured cells and *in vivo*. They originate from the endoplasmic reticulum where lipids are synthesised. Mature LDs bud from the ER membrane to form independent structures in the cytoplasm (Blanchette-Mackie *et al.*, 1995; Tauchi-Sato *et al.*, 2002).

Composition of lipid droplets

Recent research in LD biology has shown that lipid droplets are not just 'great balls of fat' (Beckman, 2006). They consist not only a core of neutral lipids (mainly triglycerols or cholesteryl esters) but also several protein components. Some of the well-studied LD components are members of PAT-domain family of proteins (perilipin, ADRP, TIP47-related protein domain) (Martin and Parton, 2006). The PAT domain is a similarity in sequence shared by the founding members of this family: perilipin, ADRP (Adipose Differentiation Related Protein or Adipophilin), and TIP47 (Tail Interacting Protein of 47kDa). PAT domain proteins are evolutionarily conserved and *Drosophila* LSD2 (Lipid Storage Droplet-2) is one of the best studied (Welte, 2007). Perilipins are structural components of LDs known to stabilize the storage of lipids and *perilipin* null mice are lean and resistant to

obesity (Brasaemle *et al.*, 2000). ADRP is associated with cholesterol and fatty acid binding to promote the accumulation of tryglycerols and uptake of fatty acids (Gao and Serrero, 1999; Imamura *et al.*, 2002). TIP47 is known to transport the mannose-6-phosphate receptor from endosomes to the Golgi and also coats the membrane of LDs (Barbero *et al.*, 2002; Miura *et al.*, 2002).

Other proteins that are found on the LD membrane are S3-12 (Wolins *et al.*, 2005), ATGL (Adipose TriGlyceride lipase), (Smirnova *et al.*, 2006) and CGI-58 (a hydrolase) (Yamaguchi *et al.*, 2007). Whether all of these proteins are only on the surface of the LDs or also reside inside them is controversial as some electron microscopic studies have found these proteins in the core of LDs (Robenek *et al.*, 2005).

Lipid droplets can be easily isolated with high purity due to their unique density and their ability to float on the top of the sucrose gradient. There have been a number of mass spectrometric analyses of the LD proteome over the last three years (Beller *et al.*, 2006; Brasaemle *et al.*, 2004; Cermelli *et al.*, 2006; Fujimoto *et al.*, 2004; Liu *et al.*, 2004). These studies have identified several proteins that were thought to be unique to other subcellular organelles. Some of these proteins are only the temporary members of the LDs and delocalize under different physiological conditions. The well-known nuclear histones, have been identified in *Drosophila* embryonic LDs (Beller *et al.*, 2006; Cermelli *et al.*, 2006). Caveolins which are associated predominantly with endocytosis (Martin and Parton, 2005), GTPases such as Rab18 and Arf1 (Nakamura *et al.*, 2005; Ozeki *et al.*, 2005), hepatitis C core protein (Shi *et al.*, 2002) and heat shock proteins (Jiang *et al.*, 2007) have been shown to be localized in the LDs as 'refugee' proteins (Welte, 2007).

Functions of lipid droplets

With this increasing list of a variety of proteins found in the LDs, the function of LDs can easily be visualized beyond lipid storage. LDs are now thought to be a site for sequestration of refugee proteins. For example, the nuclear histones are found in *Drosophila* embryo LDs may be excess protein stored and sequestered in LDs. LD sequestration of histones might also be degrading or inactivating them. Another possibility is that LDs act as storage organelles for proteins in addition to lipids (Cermelli *et al.*, 2006).

LDs have also been linked to autophagy and proteasomal degradation. Apolipoprotein B (ApoB) accumulates on lipid droplets during proteasomal inhibition. This might occur in order to avoid formation of aggregates of excess ApoB in the cells, which could be toxic to them. Both autophagic and proteasomal components accumulate on LDs upon proteasomal inhibition. This also suggests that the LDs might play anchoring role to these degradation processes (Ohsaki *et al.*, 2006). LDs are also viewed as the garbage dumps where misfolded proteins accumulate (e.g. Arl8b), (Hofmann and Munro, 2006). Ubiquitinated ApoB is also known to accumulate on LDs when its degradation is inhibited (Ohsaki *et al.*, 2006). Lipoproteins are the extracellular versions of LDs that consists of neutral lipids and proteins. Lipoproteins are involved in carrying lipids across cells to pass signals (Panakova *et al.*, 2005).

With multiple studies identifying several proteins in LDs that are important for the function of other organelles, the importance of LDs is fast increasing. This generates the need to study the detailed biology of LDs in greater detail. LDs are also becoming associated with several human disease states. LD numbers increase in osteoarthritis, liver degeneration, cartilage over-proliferation and breast cancers (Welte, 2007). LDs in neurons are very few in number and this might contribute to the accumulation of inclusion bodies in neurodegenerative diseases where LDs might be important for the degradation or processing of aggregation-prone proteins (Ohsaki *et al.*, 2006). LDs are linked to viral infections where the viral capsid proteins of hepatitis C virus associate with LDs to generate infectious particles and the assembly of viral particles takes place in the vicinity of LDs (Miyanari *et al.*, 2003).

These recent studies have clearly shown that LDs are highly dynamic organelles. They may co-ordinate several cellular processes either directly or indirectly. LDs cross talk with lysosomes, endosomes and caveolae by transiently sharing proteins and influence cellular processes from lipolysis to membrane trafficking. Hence LD proteins need to be characterized in detail and a better understanding of the nature of interactions between 'refugee' proteins and LDs also needs to be achieved. This presents a vast potential for future research to help understand the crosstalk between various biological processes. The increasing number of research papers being published on LDs is only an indication of the importance of LD research.

Background of IX-14 (Invadolysin)

IX-14^{1} is a late larval mutation in *Drosophila* published in 1971 from an ICR-170 (an acridine compound causing frameshift mutations) chemical mutagenesis screen for mutations defective in imaginal discs (Shearn *et al.*, 1971). The mutation was mapped to the right arm of the third chromosome. Initial analysis of the mutation showed that there was a metaphase arrest in mutant brains and the mitotic chromosomes were hypercondensed. The chromosomes were also reported to show a low level of breakage (Gatti and Baker, 1989).

The Heck lab carried out further work on the *IX-14*^{1} mutation. A former Ph.D. student in the lab, Sue Ann Krause generated a P element insertion allele of *l(3)IX-14*^{1} by local hopping of a nearby P element. This allele was termed *l(3)IX-14*^{4Y7}. A detailed analysis of the two alleles was carried out and published previously (McHugh *et al.*, 2004). Both *l(3)IX-14*^{1} and *l(3)IX-14*^{4Y7} showed similar defects and were non-complementing. The neuroblast chromosomes were hypercondensed lengthwise and a loosely condensed halo of chromatin surrounded the chromosomes. The salivary gland chromosomes had lost the distinctive banding pattern along the chromosome arms and the arms were twisted and frayed. The chromocentre of polytene chromosomes was hard to distinguish; the polytenes themselves were smaller than the wild type. Colchicine treatment could double the mitotic index in both wild type and mutant neuroblasts. This suggested that there is also a defect in the cell cycle earlier than metaphase arrest. BrdU incorporation was low in *IX-14* mutants suggesting a cell cycle block or delay before mitosis. The reduction in size of the polytene chromosomes might be due to under-replication. *l(3)IX-14*^{1} also had "redder" eyes in a position effect variegation experiment compared to the w^{m4} allele. This suggested that *l(3)IX-14*^{1} was a suppressor of variegation "opening" the

heterochromatin and allowing greater expression of the reporter gene possibly through affecting chromatin structure. Spindle and centrosomal abnormalities were also observed in both *l(3)IX-14* alleles. The spindles were monopolar, asymmetric bipolar, or completely disorganised. Mutant mitotic cells showed either one centrosome or two un-separated centrosomes in a dumbbell shape. dsRNAi in *Drosophila* cultured cells phenocopied the mutant spindle phenotypes. Very few anaphases were observed in the mutants and there was a higher level of cells that entered apoptosis as shown by TUNEL labelling (Terminal deoxynucleotidyl transferase biotin-dUTP Nick End Labeling).

Chromosome condensation and spindle assembly are accompanied by the disassembly of the nuclear envelope. Nuclear envelope proteins such as lamin DmO (B-type) and otefin (LEM domain containing protein) accumulated to higher levels in the mutant neuroblasts. The increase in the level of these proteins was detected by immunoblots as well as immunofluorescence. IX-14 was also shown to cleave lamin. *in vitro* synthesized DmO lamin was cleaved by *in vitro* synthesized IX-14. This activity could be blocked by the addition of the zinc chelator ortho-phenanthroline.

In an attempt to identify the gene, *l(3)IX-14*^{1} allele was mapped to the 85E10-F16 region using deficiencies with known break points. The gene was identified by inverse PCR and cloned. A 3.6 kb cDNA was identified from the *Drosophila* adult head library EST. The P-element insertion was mapped to 40 bp upstream of the transcription start region. Hence *l(3)IX-14*^{4Y7} could be a hypomorphic or null allele of *l(3)IX-14*^{1}. Northern blot analysis showed that no expression of *IX-14* mRNA was

found in either of the alleles suggesting that both the mutations were strong hypomorphic or null mutations.

The *Drosophila IX-14* gene has 9 exons spread over 15 kb of genomic DNA. The first intron is approximately 8.6 kb. The protein is predicted to be about 71 kDa in size as it is encoded by an ORF of 2052 nucleotides (683 aa). Sequence analysis of the protein originally showed one conserved sequence belonging the protozoan *Leishmania major*, named Leishmanolysin. Later multiple orthologues were identified in higher eukaryotes. Leishmanolysin belongs to the M8 class of metalloproteases and is a major gp63 surface protein of the pathogen *L. major*. Leishmanolysin is the founding member of the M8 family. The protein is a metalloprotease with a conserved HEXXH catalytic motif conserved in all organisms. The worm, human, mouse and fly orthologues are included in the figure (Figure 1.8A). The N and C-terminal regions are more divergent but the blocked numbered regions are shared among all the higher eukaryotes, but not in Leishmanolysin. There are 14 remarkably conserved cysteines throughout all the organisms. The conserved cysteines suggest that the core of 1X-14 should be similar to that of leishmanolysin (Figure 1.8B) (Schlagenhauf *et al.*, 1998). This also suggests that the insertions indicated with black numbered spheres on the modelled crystal structure of gp63 should lie on the surface. These regions could be predicted to mediate interactions with substrates, regulators or other binding partners. These are also potential targets for insertion of tags or to make antibodies. The internal zinc ion, essential for protease activity, is shown by a magenta sphere. There is a signal sequence in the N-terminus of the *Dm* gene that should direct its localization to the endoplasmic reticulum through docking with the signal recognition particle.

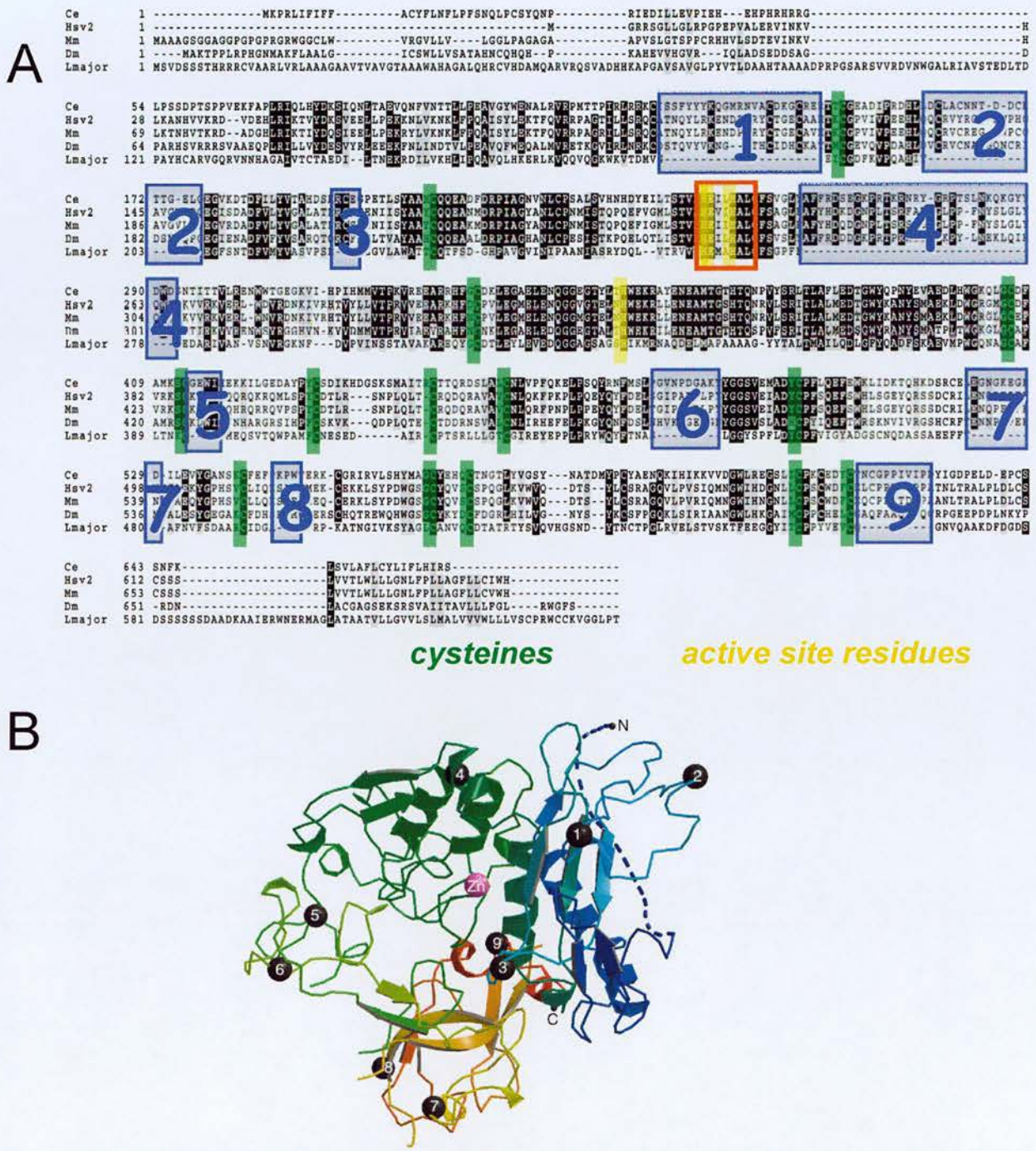

Figure 1.8. T-COFFEE alignment of Invadolysin homologues and the structure based on Leishmanolysin (Adapted from McHugh *et al.* 2004).

A. T-COFFEE alignment showing homologues of IX-14/Invadolysin conserved between *Caenorhabditis elegans* (Ce), *Homo sapiens* (variant 2, Hs V2), *Mus musculus* (Mm), *Drosophila melanogaster* (Dm) and *Leishmania major* (Lmajor) with the conserved HEXXHXXG (and third required H) zinc-metalloprotease motif (red box). There are 14 conserved cysteines (green) between all the homologues. Nine regions (insertions relative to Leishmanolysin) shared among the higher eukaryotic orthologues (absent in Leishmanolysin) are indicated by blue boxes with the numbers. **B**. Structure of Leishmanolysin. The black numbered spheres represent the insertions (correlating to the blocked number regions in A that map by prediction to the surface of the Leishmanolysin structure. The internal magenta sphere represents the zinc ion required for catalysis.

There is also a C-terminal GPI anchor consensus that may modify the protein helping it to insert in the plasma membrane. The sequence also contains some potential destruction motifs (D-box and KEN-box), which direct the protein to ubiquitin-mediated degradation possibly in a cell cycle regulated manner. There is also a SUMO-ylation signal just after the HEXXH catalytic motif. A loss of protease activity was detected in mutant larval brain extracts in zymogram gels at the predicted size of the protein, supporting the fact that IX-14 is a protease.

So far there is only one known of *IX-14* variant in *Drosophila*, but there are four variants in humans variant 1, variant 1Δ37, variant 2 and variant 2Δ37 (Figure 1.9). The human IX-14 variant 1 and the variant 1Δ37 differ from each other with the Δ37 variant missing the exon 12 that codes for 37 amino acids. Variant 2 and variant 2Δ37 differ for the same reason. The difference between variant 1 and 2 is with respect to the first exon where variant 1 has a longer N terminus and variant 2 has an alternative reading frame embedded within the first exon. Variant 1 EST was obtained from testis and brain and variant 1Δ37 was from embryonic stem cells, colon and melanoma. Variant 2 EST was obtained from testis and placenta. The variant 2Δ37 was found by RT-PCR from HeLa cells by Dr. Neville Cobbe (Heck laboratory).

The localization of the protein was originally studied in both *Drosophila* S2 and HeLa cells. The antibodies recognised peculiar ring-like structures in the cytoplasm of human cells (Figure 1.10A). These ring-like structures did not colocalize with proteasomes, peroxisomes, mitochondria, Golgi, signalosomes and lysosomes, which can have a ring-like appearance. It was postulated that these structures might be invadopodia. Invadopodia are actin-based projections that are

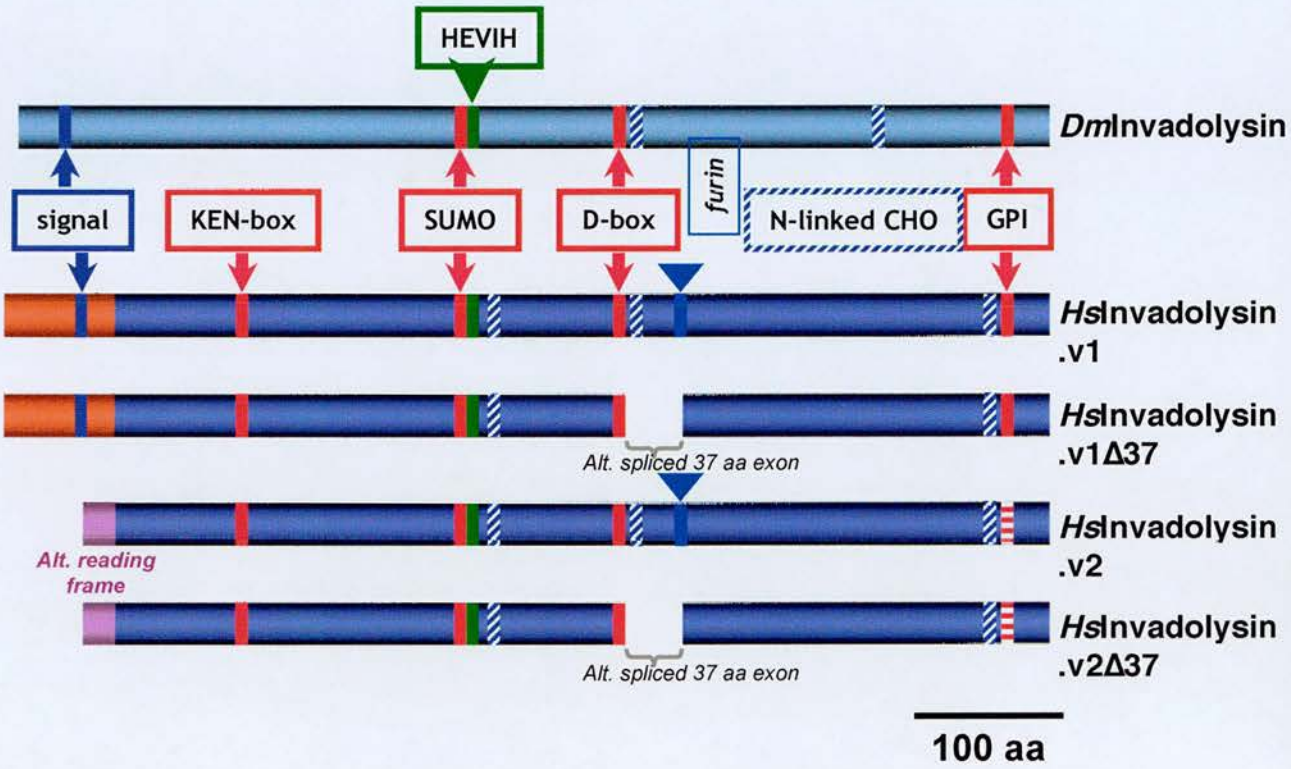

Figure 1.9. IX-14/Invadolysin variants in *Drosophila* and human.
To date, only one varient has been identified in *Drosophila* whereas four splice variants have been identified in human. They all share some common motifs such as HEXXH protease motif, sumoylation motif and, KEN- and D-Boxes. In human, variant 1 and variant Δ37 contain a signal sequence. The signal sequence is missing in variant 2 and variant Δ37, which start with an alternative reading frame. In addition there is an alternatively spliced 37 amino acid region encoded by exon 12. The presence or absence of this region is referred to by a Δ sign. The scale bar represents 100 amino acids.

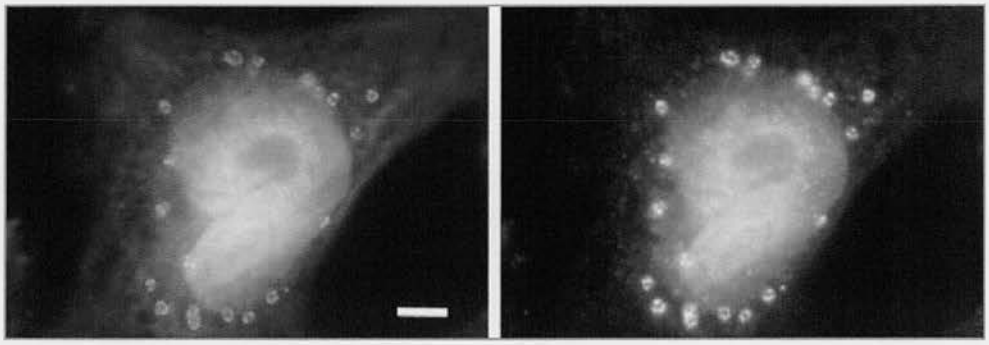

Figure 1.10A. IX-14/Invadolysin localization in human cells.
Invadolysin localizes to ring-like structures in HeLa cells. Invadolysin is shown in green and red is actin (McHugh *et al.* 2004).

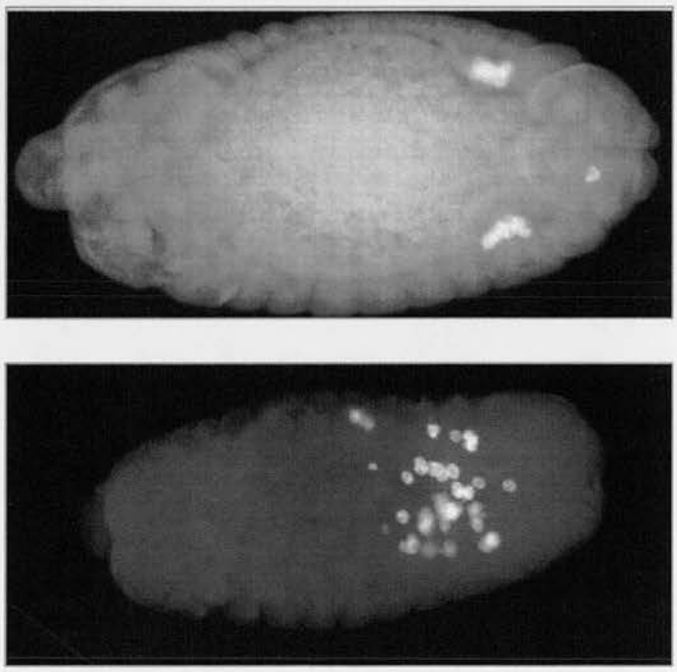

Figure 1.10B. *IX-14*/*invadolysin* mutants embryos have a germ cell migration defect.
The germs cells in wild type form gonads (upper panel). In the *invaolysin* (*IX-14*) mutants, germ cells are formed but they fail to migrate to form the gonads.
Germ cells are labeled with Vasa (a germ cell marker protein) antibodies.
(McHugh *et al.* 2004).

important for extracellular matrix degradation in transformed cells (Baldassarre *et al.*, 2003; Buccione *et al.*, 2004). Taking into account the homology to Leishmanolysin and the proposed localization to invadopodia, the protein was named as Invadolysin (McHugh *et al.*, 2004). However, further experiments by Dr. Kathryn Marshall (Heck lab) showed that these ring like structures were not invadopodia as the regions extracellular matrix degradation did not colocalize with the rings. The rings also did not colocalize with invadopodia markers such as cortactin. Hence these structures remained to mystery in the lab.

A role for the protein in cell migration was suggested with the observation of striking localization pattern in human macrophages. The protein localized to the leading edge of macrophages. In stationary macrophages, the protein was in the cytoplasm but when macrophages were migratory the protein dramatically localized to the leading edge. This supported the idea that IX-14 might be involved in migration. Hence germ cell migration was examined in *Drosophila* (Figure 1.10B). Interestingly, germ cell migration was defective in mutant embryos. The germ cells were formed but did not migrate properly to make gonads and hence gonads were also absent in the mutant larvae (McHugh *et al.*, 2004). The germ cell migration defect could also be observed using time-lapse video microscopy using vasa-GFP marked *IX-14* mutant embryos (Ivan Clark). Thus phenotypic analysis of *IX-14/invadolysin* mutants and the localization of Invadolysin in human cells indicated that Invadolysin might be involved in both mitosis and migration.

Aims of the Ph.D. project

As described in the original paper published by the Heck Lab on IX-14/Invadolysin, it was clear that the mutants showed a wide range of phenotypes. Thus it was concluded that the protein has pleotropic functions. The reasons that it was a lethal mutation in *Drosophila* and its involvement in both mitosis and migration made it a very interesting protein.

When I started my Ph.D., though there was a lot known about the mutant phenotypes of IX-14/Invadolysin, there was little known about the function of Invadolysin other than it should act as a metalloprotease. Hence my general aim was to investigate the function of IX-14/Invadolysin.

One way of understanding the function of a protein is to identify its interactors. Hence my first aim was to carry out a genome-wide second-site non-complementation screen in *D. melanogaster* with *IX-14* mutant alleles in order to isolate the mutations that fail to complement the original mutation. The isolated mutations should be the genetic interactors of *IX-14*. Understanding the relationship between *IX-14* and its interactors should give more clues to the functions of *IX-14*. The results of these experiments are described in the Results Chapters 3 and 4. Second aim was to study the pathways *IX-14* is involved in and results are presented in the Result Chapter 5. The ring-like structures seen in human cells were not known to colocalize with any organelle. Another of my aims was to determine what these structures were. This work is described in Result Chapter 6. Another minor aim of my research also involved generating reagents to further study IX-14/Invadolysin in flies. This included antibodies and over-expressing *IX-14* in fly eyes and generating constructs. These experiments are collectively presented in Chapter 7.

Chapter 2: Materials and Methods

Drosophila melanogaster stocks

Strain	Source
Canton S	Bloomington *Drosophila* Stock Center (USA)
l(3)IX-14^{1}/TM3	Heck laboratory
l(3)IX-14^{1}/TM6B	M. Gatti, Rome
l(3)IX-14^{4Y7}/TM3	Heck laboratory
l(3)IX-14^{4Y7}/TM6B	Heck laboratory
UAS-IX-14	Heck laboratory
Drosdel deficiency kit	Szeged *Drosophila* Stock Center (Hungary)
Df(3L)Exel6134	Bloomington *Drosophila* Stock Center (USA)
Df(3L)H99	Bloomington *Drosophila* Stock Center (USA)
CG13702-AICR2(f03116)	Bloomington *Drosophila* Stock Center (USA)
CG32197-Met75Ca/TM6B	Bloomington *Drosophila* Stock Center (USA)
CG18231(f03022)	Bloomington *Drosophila* Stock Center (USA)
not^{1}/TM6B	B. Poeck, Würzburg
not^{02069}/TM6B	B. Poeck, Würzburg
GMR-Gal4	Bloomington *Drosophila* Stock Center (USA)
actin-Gal4	Bloomington *Drosophila* Stock Center (USA)
tubulin-Gal4	Bloomington *Drosophila* Stock Center (USA)
UAS-Bre1	M. Beinz, Cambridge

Common Reagents and Buffers

Aprotinin

Stock at 1.4 mg/ml in 0.9% NaCl and 0.9% benzyl alcohol, used at 1.4 µg/ml (Sigma)

BSA

Bovine Serum Albumin, 30% stock solution (Sigma, A3299)

BODIPY 493/503 (4,4-Difluoro-4-bora-3a,4a-diaza-*s*-indacene) (Invitrogen)

10 µg/ml in absolute alcohol (stock solution), used at 100 ng/ml (1:100 dilution)

Cholera toxin B-Alexafluor 555 conjugate (Molecular Probes)

1 mg/ml in PBS (stock solution), used at 10 µg/ml (1:100 dilution)

CLAP

1 mg/ml chymostatin, 1 mg/ml leupeptin, 1 mg/ml antipain, 1 mg/ml pepstatin A (Sigma) in DMSO (dimethyl sulfoxide), used at 10 mg/ml

Coomassie Brilliant Blue Stain

0.5% Coomassie Blue (Sigma) in 100% methanol

Coomassie Blue Stain Diluent

35% methanol, 14% acetic acid

BIBL. UNIV. EDIT. EX

Coomassie Blue Fast Destain

35% methanol, 10% acetic acid

Coomassie Blue Slow Destain

10% methanol, 7% acetic acid

DAPI

4',6-diamidino-2-phenylindole (Sigma), stock solution at 1 mg/ml in dH_2O, stored at –20˚C, used at 0.1 µg/ml (1:10,000 dilution)

DTT

Stock solution at 1M dithiothreitol (Fisher) in dH_2O stored at –20˚C

Dulbecco's Phosphate Buffered Saline (PBS) (10X)

1.37 M NaCl, 26.8 mM KCl, 14.7 mM KH_2PO_4, 64.6 mM Na_2HPO_4, pH 7.4

EDTA

Ethylenediamine-N,N,N',N'-tetraacetic acid, Stock solution 0.5 M solution in dH_2O, pH 8.0

EGTA

Ethylene glycol-bis (2-amino-ethyl ether)-N,N,N',N'-tetraacetic acid, Stock solution 0.25 M in dH_2O, pH 6.8

Ephrussi-Beadle Ringer's solution (EBR) (10X)

1.3 M NaCl, 47 mM KCl, 19 mM $CaCl_2$, 100 mM HEPES, pH 6.9

Ethidium Bromide (EtBr)

Stock solution at 10 mg/ml in dH_2O, used at 300 ng/ml

Formaldehyde

16% Formaldehyde ampules (methanol free) (TAAB, F017)

LB (Luria-Bertrani broth)

1% Bacto-tryptone, 0.5% Bacto-yeast extract, 1% NaCl, pH 7.4

Molecular weight markers

SeeBlue Plus2 prestained standard for proteins (Invitrogen, LC5925)

100 kb DNA ladder (Promega, G210A)

1 kb DNA ladder (Promega, G571A)

MOPS SDS-PAGE electrophoresis buffer (20X)

1 M 3-(N-morpholino) propane sulphonic acid, 1 M Tris base, 2% SDS, 20.5 mM EDTA, pH 7.7

Mowiol mounting solution

10% Mowiol 4-88 (Calbiochem), 20% Glycerol in PBS

PBS-Tx

Dulbecco's PBS with 0.1% TritonX-100 (diluted from 10% w/v stock solution of TritonX-100 in water)

PBS-Tw

Dulbecco's PBS with 0.1% Tween-20 (diluted from 10% w/v stock solution of Tween-20 in water)

PMSF (Phenylmethylsulfonyl fluoride) (Sigma)

0.1 M stock solution in ethanol, used at 1mM concentration

SOB

2% Bacto-tryptone, 0.5% Bacto-yeast extract, 8.6 mM NaCl, 50 mM $MgCl_2$, 2.5 mM KCl, pH 7.4

Stripping solution

100 mM β-mercaptoethanol, 2% SDS, 62.5 mM Tris, pH 6.7

TBS (Tris-buffered saline) (1X)

137 mM NaCl, 20 mM Tris base, pH 7.6 (with HCl)

TBS-Tw

TBS with 0.05% Tween-20

TAE (1X)

40 mM Tris-acetate, 1 mM EDTA, pH 8.0

TBE (1X)

45 mM Tris-borate, 1 mM EDTA, pH 8.0

TE (1X)

10 mM Tris-HCl, 1 mM EDTA, pH 8

Towbin buffer (protein transfer solution)

25 mM Tris (Sigma 7-9, code-T1378), 20% methanol, 250 mM Glycine (Sigma)

0.1% SDS

Transferrin-Alexafluor 633 conjugate (Molecular Probes)

1 mg/ml in PBS, used at 10 μg/ml (1:100 dilution)

3X SDS-PAGE sample buffer

6% SDS, 150 mM upper buffer (0.5 M trizma-base, pH 6.8), 30% Glycerol, 0.03%

Bromophenol blue, 6 mM EDTA

5X loading dye for DNA agarose gels

17.5% Ficoll 400, 100 mM EDTA, pH 8.0, 2.5% SDS, 0.25% Bromophenol blue,

0.25% Xylene cyanol FF

Maintenance of *Drosophila* stocks

Flies were collected in bottles or vials containing 'Dundee' maize medium (14 litres water, 150 g agar, 1100 g glucose, 620g brewer's yeast, 1000 g maize meal, 80 g dried yeast, 38 g nipagin (p-hydroxy benzoic acid methyl ester), 380 ml absolute alcohol, 45 ml propionic acid). To fatten flies before embryo collection or larval dissection, yeast paste diluted with fruit juice (mango, banana and orange from Sainsbury's) was placed in the vial. Flies were usually kept at room temperature (RT) or 25°C with tipping into a new vial once every 10 days or at 18°C with tipping into a new vial once every month. Genetic crosses were performed using virgin female flies collected as soon as possible after eclosion.

Fly crosses (general)

Virgin females (about 5-10) from one stock were collected and crossed with 2-3 males from the desired stock. Flies were left to mate and lay eggs for 3 days. The parents were removed from the vials and the progeny were allowed to emerge in the same vial. The crosses were carried out at 18, 25, 27 or 29°C according to the requirements of the experiment.

Second site non-complementation (Deficiency) screening

Virgin females (about 5-10) from the stocks of *IX-14* mutant lines over a third chromosome balancer were crossed with males from each of the 225 deficiency lines from the Drosdel deficiency kit (Szeged). Flies were left to mate and lay eggs for 3 days. The parents were removed from the vials and the progeny were allowed to emerge in the same vial. These crosses were carried out at RT and after 12 days,

the flies that eclosed were scored for the presence or absence of balancer chromosomes. Males and females were evaluated separately.

Determination of larval longevity of *non-stop* mutants

Male and female flies of the desired genotype were kept together in vials of yeast-glucose-agar medium supplemented with yeast paste for 2 days. They were transferred into a fresh vial on the third day and left to lay eggs for a day. The parents were removed from the vials and the embryos were allowed to hatch. The number of days the homozygous larvae survived was recorded.

Preparation of larval samples for SDS-PAGE

10-15 wandering third instar larvae of the appropriate genotype were removed from culture vials and transferred to 1.5 ml Eppendorf tubes and rinsed three times in 1X EBR. 300 µl of cold lysis buffer (1X EBR, 10 mM EDTA, 10 mM DTT, 10 µg/ml each of Chymostatin, Leupeptin, Antipain, and Pepstatin [CLAP], 1 mM phenylmethanesulfonyl fluoride [PMSF], and 1 unit Aprotinin) was added to the tubes. The larvae were then homogenised using a hand pestle starting at lowest speed and gently increasing the speed to the maximum for ~2 minutes on ice. 150 µl of hot (70°C) 3X SDS-PAGE Sample Buffer +10 µl of 1M DTT was added to the homogenate and the tube was placed at 100°C for 10 minutes. Particulate matter was centrifuged at 13,000 rpm for 2 minutes at 4°C in a benchtop centrifuge, and the supernatant transferred to a fresh tube. Samples were stored at –20°C until required. Protein samples were resolved by SDS-PAGE on bis-tris pre-cast gels (Novex) at

180 volts for 45 minutes, transferred to nitrocellulose filter membranes (Schleicher & Schuell), and processed for immunoblotting.

Transfer of SDS-PAGE gels onto nitrocellulose membrane

After electrophoresis, the resolved proteins were transferred to Protran nitrocellulose membrane (Schleicher and Schuell) by electroblotting, in preparation for probing with antibodies. 4 litres of Towbin buffer were prepared. Of these 4 litres, 250 ml were decanted for wetting the Protran membrane and 18.5 ml 20% SDS were then added to the remaining 3.75 litres to give a final concentration of 0.1% SDS). The blot was then assembled in the transfer cassette, in the following order: (negative pole)- sponge- Whatman blotting paper- gel- nitrocellulose membrane- Whatman blotting paper- sponge- (positive pole). The cassette containing the gel and nitrocellulose were placed in the transfer tank (BioRad Trans-Blot) and the transfer was performed at 40 volts/550 mA for 3.5 hours at 4°C. After transfer, the membrane was rinsed with dH_2O and stained with Ponceau-S (0.2% Ponceau-S in 3% trichloroacetic acid) for two minutes at RT with shaking. The membrane was rinsed with dH_2O. The membrane was stored at 4°C or washed once with PBS-Tw or TBS-Tw and used immediately for immunoblotting.

Immunoblotting

Protein extracts were resolved by SDS-PAGE (4-12% or 10% precast gels by Novex) and transferred onto nitrocellulose membranes in a Trans-Blot apparatus (BioRad). Non-specific binding to membrane was blocked in TBS-Tw and 5% (w/v) semi-skim powdered milk (Sainsbury's) for 1 hr at RT and then incubated for 1 hr at

RT with the primary antibody in TBS-Tw. After washing three times for 5 minutes with TBS-Tw, the membranes were incubated in the appropriate horseradish peroxidase-linked (HRP) secondary antibody (1:10,000) for 1 hr in TBS-Tw at RT. Finally the membranes were washed as above with TBS-Tw or in TBS with 0.2% triton X-100 and immune-complexes were detected by enhanced chemiluminescence (ECL, Amersham Biosciences). For the analysis of larvae, 1/2 larva was loaded per lane for wild type (Canton S) and *non-stop* mutants and 1.5 larvae for *invadolysin* mutants.

Stripping of probed nitrocellulose membrane

Nitrocellulose membranes that were already used for immunoblotting were stripped of the primary antibody in order to be used for further immunoblotting with different primary antibodies. The membrane was washed twice in TBS-Tw for 15 minutes each time and incubated in Stripping Solution for 30 minutes at 65°C. The membrane was then rinsed several times with TBS-Tw and washed twice for 10 minutes each time in TBS-Tw and then for 1-2 hours at room temperature (or overnight at 4°C) with TBS-Tw. The membrane was ready to be used for another probing.

Preparation of electrocompetent cells

A 2 ml overnight culture of the appropriate bacterium (BL21 or XL-1 Blue) was grown with shaking at 37°C in SOB medium. 0.5 ml of the overnight culture were diluted into each of two 2 litre flasks containing 500 ml SOB. The larger cultures were grown with shaking at 37°C to an optical density (OD_{600}) of 0.8 (about

four hours). The flasks were chilled on ice for about 15-30 minutes. All subsequent steps were performed on ice (it is important that the bacterial cells remain cold, otherwise their competence is affected).

The bacterial cells were harvested by centrifuging in sterile, chilled 250 ml bottles for 15 minutes at 2500 rpm in a Beckman JLA 10.500 rotor at 4˚C. The supernatant was removed and the cell pellet for each culture was resuspended in 500 ml ice-cold sterile 10% glycerol (in distilled water). The resuspended culture was centrifuged again at 2500 rpm for 15 minutes at 4˚C and the supernatant was removed. Each pellet was resuspended in 4.5 ml of 10% glycerol and aliquots of 200 µl were snap-frozen in liquid nitrogen and stored at -80˚C.

Electroporation

Electroporations were performed in appropriate cuvettes (0.2 cm, Invitrogen) using a BioRad electroporator. Tubes of electrocompetent cells (aliquots of 200 µl) were thawed on ice. At the same time, the required number of 1.5 ml Eppendorf tubes and 0.2 cm disposable cuvettes were placed on ice to cool at 4˚C. 80 µl of competent cells were added to the 1.5 ml tubes and an appropriate amount of DNA (1-2 µg) was added and mixed. Cuvettes were tapped so that the sample went to the bottom and then electroporated at the following conditions: resistance set at 200 Ohms, capacitance set at 25 µFD and voltage set at 2.5 kV. After electroporation, 1 ml of LB medium was immediately added to each cuvette. The mixture was then transferred to 1.5 ml tubes and incubated at 37˚C for 30 minutes. Dilutions of the cultures were plated out on agar plates containing the appropriate antibiotic.

Plasmid DNA extraction

For small scale plasmid DNA isolation, 1 colony of *E. coli* (XL1-Blue, DH5α) was inoculated into 3 ml of LB and culture were grown overnight at 37°C with shaking. 2 ml of this culture was used for plasmid DNA extraction and the remainder was used for making frozen glycerol stocks (700 µl of culture and 300 µl of 100% sterile glycerol). All small scale plasmid DNA extractions (mini-preps) were performed using the UltraClean™ Plasmid Miniprep Kit from Mo Bio or QIAprep Spin® MiniPrep Kit from Qiagen, according to manufacturer's instructions. Larger scale extractions of up to 50 ml cultures were performed using either the UltraClean™ Midiprep columns from MoBio or the Qiafilter® Plasmid Midi Kit from Qiagen, according to the manufacturer's instructions.

Restriction digestion of DNA plasmids

Restriction digestion of DNA plasmids was performed in 1.5 ml Eppendorf tubes as follows:

DNA (plasmid preps)	1-2 µl
New England Biolabs enzyme(s) (20,000 U/ml)	1 µl
Bovine serum albumin (10 mg/ml)	0.2 µl
New England Biolabs 10X buffer	1 µl
Sterile deionised water	up to 20 µl

Unless otherwise indicated, the 10X reaction buffer provided with the enzyme was used. Digestions were normally performed at 37°C for 2-4 hours. The

size of the cloned insert was estimated by running an aliquot of the plasmid digest on a 1% agarose gel in TAE or TBE along with appropriate molecular weight markers.

Agarose gel electrophoresis

Agarose gels were usually prepared at a concentration of 1% SeaKem LE Agarose (BioWhittaker Molecular Applications) containing 300 ng/ml of ethidium bromide in 1X TBE or TAE buffer. Gels were electrophoresed in electrophoresis tanks (Owl Scientific Plastics) in 1X TBE or TAE buffer. Different gel sizes were used according to the number of samples and/or the degree of separation required. Gel size: mini (50 ml, run at 70-80 V), midi (100 ml, run at 100 V) and maxi (300 ml, run at 150 V).

Purification of DNA from agarose gels

Electrophoresis was performed in low-melt agarose gels (MacroSieve LM agarose, Flowgen) containing 300 ng/ml ethidium bromide. 1X TBE buffer was used and the desired bands were excised under UV irradiation using a razor blade and placed into 1.5 ml Eppendorf tubes. DNA was purified from the agarose gel by using Qiagen's QIAquick® Gel Extraction Kit as per manufacturer's instructions. Samples were weighed and the appropriate volume of Binding buffer was added. The gel was incubated for 5 to 10 minutes at 50°C and finally DNA was isolated by following the manufacturer's instructions (using Qiagen's QIAquick® Gel Extraction Kit).

Amplification of plasmid DNA by PCR

Most PCR reactions were performed by using the *Pfu* DNA polymerase (Promega). The following basic protocol for a typical 50 µl reaction was used.

Pfu DNA polymerase buffer with 20 mM $MgSO_4$ (10X)	5 µl
dNTPs (1.25 mM each)	4 µl
primer mix (2 µM each)	12.5 µl
Pfu DNA polymerase (2-3 U/µl)	0.5 µl
DNA template (50-200 ng)	variable
Sterile deionised water	up to 50 µl

PCR reactions were performed in a Biometra Personal Cycler or a Biometra Gradient Cycler according to the following protocol:

Initial Denaturation	95°C	2 minutes	
Denaturation	95°C	30 seconds	x 30 cycles
Annealing	56-58°C	30 seconds	
Extension	72°C	2-4 minutes	
Final extension	72°C	10 minutes	
Hold	4°C		

Purification of DNA from PCR reactions

DNA products from PCR reactions were usually purified by using the UltraClean™ PCR Clean-up™ Kit (MoBio) or QIAquick® PCR Purification Kit (Qiagen). This method was preferred when only a single PCR product was amplified

in a reaction. The entire PCR reaction was used and 5 volumes of the SpinBind reagent were added. The DNA was finally purified using the Spin Filter columns by following the manufacturer's instructions and the DNA was eluted in 25 µl of elution buffer.

Ligations

All ligations were performed using T4 DNA ligase from Promega or New England Biolabs with appropriate reaction buffer at 16-18˚C overnight. An insert:vector molar ratio of 3:1 was routinely used.

Sequencing of DNA samples from plasmids

Sequencing reactions were performed using 250-500 ng of template DNA in conjunction with 3.2 pmol of the appropriate primer and 4 µl of Big Dye terminator cycle sequencing kit version 3.1 (Perkin Elmer, Applied Biosystems), in a total reaction volume of 20 µl. The reactions were performed in a Biometra Personal Cycler according to the following protocol:

95˚C	5 minutes	
96˚C	30 seconds	x 25 cycles
55˚C	15 seconds	
60˚C	4 minutes	
Hold	15˚C	

The reactions were then transferred to 1.5 ml tubes and taken to the University of Edinburgh sequencing facility at ICB or Ashworth buildings for loading onto an ABI prism sequencer.

RNA extraction

RNA from larvae was extracted using RNeasy ® Mini Kit (Qiagen) according to manufacturer's instructions or using the Trizol method as described below.

DEPC-treated water was prepared before extractions using sterile, deionised water. DEPC was added to a final concentration of 0.01%, stirred overnight/1 hr at RT and autoclaved. Plastic/corex items were rinsed with chloroform and then with DEPC-treated water.

Third instar larvae were collected and washed with PBS. They were homogenised in Trizol using a Polytron (Kinematica) at RT starting at lowest speed and gently increasing the speed to the maximum for ~2 minutes. The lysate was passed several times through a pipette to further homogenise it. 0.2 ml of chloroform was then added per ml of Trizol. This was capped, shaken by hand for 15 seconds and incubated at RT for 2-3 minutes. This was centrifuged in a benchtop centrifuge at 4˚C at 13,000 rpm for 15 minutes. The aqueous (upper) phase, about 60% the original Trizol volume, was decanted to a fresh tube. Isopropyl alcohol was added to the aqueous phase, 0.5 ml per 1ml Trizol. This was incubated for 10 minutes at RT and spun in a benchtop centrifuge at 4˚C at 13,000 rpm for 10 minutes. The RNA precipitate formed a gel-like pellet. The supernatant was discarded and the pellet was washed with 75% ethanol, vortexed and centrifuged at 10,000 rpm for 5 minutes

in a benchtop centrifuge at 4°C. The pellet was air dried for 5-10 minutes. The pellet was dissolved in DEPC-treated water in 2-5 times volumes of the pellet. The suspension was then incubated for 10 minutes at 55-60°C and dissolved in RNAase free water. The $A_{260:280}$ was measured using spectrophotometer (Cecil 2040 or NanoDrop®). The concentration was evaluated as A_{260} x 40 x dilution factor. A value between 1.8 to 2.0 for the ratio or A_{260}/A_{280} was taken as pure RNA.

DNase treatment of total RNA

Total RNA was treated with DNAse I, (Amplification Grade, Invitrogen) prior to reverse transcription as follows:

DNAase I, Amp Grade 1U/µl	1µl
10X DNaseI Reaction Buffer	1µl
total RNA	1µg
DEPC-treated Water	up to10 µl

The reaction mixture was incubated for 15 minutes at RT and the DNAse I was inactivated by the addition of 1 µl of 25 mM EDTA solution. The reaction was heated at 65°C for 10 minutes and the RNA was ready to be used for reverse transcription, prior to PCR amplification.

Reverse Transcriptase-PCR of total RNA isolated from larvae

Reactions were performed using the Access RT-PCR system (Promega) under the following conditions:

Nuclease-free water	31.5 µl
AMV/*Tfl* 5 X Reaction buffer	10 µl
dNTP mix (10 mM each)	1 µl
Primer mix (50 mM each)	2 µl
$MgSO_4$ (25 mM)	2 µl
AMV reverse transcriptase (5 U/µl)	1 µl
Tfl DNA Polymerase (5 U/µl)	1 µl
RNA template	1.5 µl

The reactions were performed in a Biometra Personal Cycler or a Biometra Gradient Cycler according to the following protocol:

First strand DNA synthesis:

Reverse transcription	48°C	45 minutes
AMV RT inactivation	94°C	2 minutes

Second strand synthesis and PCR amplification:

Denaturation cycle	94°C	30 seconds	30 cycles
Annealing cycle	55-60°C	1 minute	
Extension cycle	68°C	2 minutes	
Final extension	68°C	7 minutes	
Hold	4°C		

10 µl of each reaction was analysed by 1% agarose gel electrophoresis.

Coomassie Blue staining of protein gels

To observe protein bands, polyacrylamide gels were stained with Coomassie Blue (0.5% Coomassie Blue in methanol) diluted 1:5 in Stain Diluent Solution (35% methanol, 14% acetic acid in dH_2O) for 1 hour (or overnight) at RT. The gel was then destained with Fast Destain solution (35% methanol, 10% acetic acid in dH_2O) for 1 hour at RT and destained further with Slow Destain solution (10% methanol, 7% acetic acid in dH_2O) for 1 hour (or overnight) at RT. For drying, the gel was then placed between two layers of cellulose acetate (IDEA Scientific company), which were clamped together using a plastic square box making sure that no bubbles were present. The gel was placed in a fan incubator (BioRad) to dry for three hours.

Immunofluorescence of larval brains

Third instar larvae were collected from approximately staged vials and washed in EBR in a dissecting dish to remove excess food. Individual larvae were transferred to a new well containing EBR and brains were dissected under a dissecting microscope. 4-5 dissected brains were placed into a new well containing EBR until ready, but never for more than 10 minutes. The brains were hypotonically swollen for 3 minutes in 0.25X EBR and fixed for 5 minutes in 4% formaldehyde, 5% acetic acid, 0.1% Triton-X 100 in 0.16X EBR by placing them in a drop on a siliconised coverslip. A poly-L-lysine slide was inverted onto the coverslip and the brains were squashed during the fix repeatedly by pressing very hard on the slide with thumb. The slide was dipped in liquid nitrogen until frozen and the coverslip was breathed on to warm briefly and flicked off with a razor blade. The slide was placed immediately into a Coplin jar containing PBS for 2 minutes and it was then

permeabilised 3 times for 10 minutes each in PBS-Tx. Blocking was performed in 3% BSA in PBS for 1 hour at RT. After blocking, the slide was washed for 5 minutes in PBS-Tx at RT and then incubated 1-2 hours at RT or overnight at 4˚C in the primary antibody diluted in PBS + 0.3% BSA. The slide was washed 6 times for 5 minutes each in PBS-Tx and the appropriate secondary antibody (diluted in 0.3% BSA in PBS) was applied for 1-2 hours at RT. The slide was then washed 6 times, 5 minutes each, in PBS-Tx. The brains were also stained with DAPI (0.1 μg/ml) included with the secondary antibody. Slides were finally drained and mounted in Mowiol, allowing 30 minutes for the Mowiol to set before examination with a fluorescence microscope (Olympus Provis).

Bonaccorsi *et al.* fixation of larval brains

This protocol has been adapted from Bonaccorsi *et al* (Bonaccorsi *et al.*, 2000) and is recommended for the analysis of mitotic spindles in *Drosophila* neuroblasts. Brains were dissected from second or third instar larvae in EBR as described above and fixed in 4% formaldehyde in PBS for 30 minutes at RT in a dissecting dish. Following this, the brains were transferred to a new well containing 45% acetic acid (in dH_2O) for 3 minutes, then transferred to a drop (10-15 μl) of 60% acetic acid on a siliconised coverslip and squashed gently onto a poly-L-lysine slide. The slide was flash-frozen in liquid nitrogen and the coverslip was removed. The slide was placed in a Coplin jar with 100% ethanol at – 20˚C for 10 minutes. The brains were then permeabilised in PBS-Tx for 10 minutes at RT, washed twice in PBS, 5 minutes each, and then blocked in PBS + 3% BSA. Primary and secondary antibody incubations, washes and DAPI staining were performed as described above.

DAPI staining of larval brains

Brains were dissected from second or third instar larvae in EBR as described above and fixed twice in 45% acetic acid, for 90 seconds each, in a dissecting dish. The brains were then transferred to a drop of 45% acetic acid (5 µl per drop) on a siliconised coverslip and a poly-L-lysine slide was inverted on top of the coverslip (total fixation should not exceed 3 minutes). The brains were squashed by pressing on the inverted slide (placed between folded Kim-wipe paper) and flash-frozen by dipping in liquid nitrogen. The coverslip was breathed on to warm and flicked off with a razor blade and immersed immediately in a Coplin jar containing PBS for 5 minutes to wash off the acetic acid. The slide was transferred to a jar containing 0.1 µg/ml DAPI in PBS-Tx for 10 minutes and then washed 3 times, 5 minutes each with PBS-Tx. Slides were finally drained and mounted in Mowiol, allowing 30 minutes for the Mowiol to set and examined under the fluorescence microscope (Olympus Provis).

Preparation of polytene chromosome spreads

Flies were fattened for one generation with a paste of fresh yeast added to their usual medium. Salivary glands from the resulting wandering third instar larvae were dissected as quickly as possible in EBR. They were transferred to a 20 µl drop of 45% glacial acetic acid on a siliconized coverslip for 30 seconds, and then to a 20 µl drop of 1:2:3 (1 part glacial acetic acid, 2 parts of water and 3 parts of lactic acid) on a siliconized coverslip for 4-5 minutes. A clean poly-L-lysine slide was gently placed face down over the coverslip to pick it up and the back of the slide was tapped with the eraser of a pencil to release the chromosomes. The progress of spreading

was examined by phase contrast microscope at 40X magnification. Once a satisfactory spread had been achieved, the slides were dipped in liquid nitrogen. The coverslip was flicked off with a razor blade (immediately after breathing on the back to defrost it). The slides were then placed PBS in a Coplin jar for two minutes and subsequently incubated in 0.1 μg/ml of DAPI in PBS-Tx for 3 minutes. The unbound DAPI was washed off by rinsing in PBS-Tx for three minutes before mounting the samples in Mowiol.

Immunofluorescence of cultured human cells

General

To stain for Invadolysin or other proteins, cells were seeded on round coverslips (13 mm in diameter) in 6-well dishes and grown under normal conditions using DMEM (Dulbecco's Modified Eagle's Medium from Gibco) with 10% FBS (Sigma). The next day, the coverslips were fixed in fresh 4% formaldehyde in PBS for 3 minutes, the formaldehyde was rinsed off with PBS for 2 minutes, cells were permeabilised in PBS + 0.5% Triton X-100 for 3 minutes, washed 2 times for 3 minutes in PBS-Tx and blocked in 3% BSA in PBS at RT for 1 hour. After the coverslips were washed 5 minutes in PBS-Tx, the primary antibody incubation was performed at the appropriate dilution in PBS + 0.3% BSA at RT for 1 hour. The coverslips were then washed 3 times for 5 minutes in PBS-Tx before the secondary antibody was applied at the appropriate dilution in 0.3% BSA in PBS at RT for 1 hour (100 ng/ml BODIPY was used with secondary antibodies to stain lipid droplets). Finally the coverslips were washed 4 times for 5 minutes in PBS-Tx (including DAPI at 0.1 μg/ml in the penultimate wash) and the coverslips were mounted on slides in Mowiol while the edges were sealed with nail varnish.

TIP47 and ADRP

To stain for TIP47 and ADRP, cells were seeded on round coverslips (13 mm in diameter) in 6-well dishes and grown under normal conditions using DMEM. The next day, coverslips were fixed in fresh 3% formaldehyde, 0.1M Phosphate buffer (pH 7.4) for TIP47 or 3% formaldehyde plus 0.025% gluteraldehyde in 0.1M Phosphate buffer (pH 7.4) for ADRP for 10 minutes. The formaldehyde was rinsed off with PBS for 2 minutes and cells were permeabilised in 0.01% digitonin in PBS for 30 minutes, washed 2 times for 3 minutes in PBS and blocked in 3% BSA in PBS at RT for 30 minutes. After the coverslips were washed 5 minutes in PBS, the primary antibody incubation was performed at the appropriate dilution in PBS + 0.3% BSA at 37˚C for 30 minutes. Then the coverslips were washed 3 times for 5 minutes in PBS before the secondary antibody was applied at the appropriate dilution in 0.3% BSA, PBS at 37˚C for 30 minutes (100ng/ml BODIPY was used with secondary antibodies to stain lipid droplets). Finally the coverslips were washed 4 times for 5 minutes in PBS (including DAPI at 0.1 μg/ml in the penultimate wash) and the coverslips were mounted on slides in Mowiol while the edges were sealed with nail varnish.

Endocytosis assay on human cells

Cells were seeded on round coverslips (13 mm in diameter) in 6-well dishes and grown under normal conditions using DMEM + 10% FBS. The next day, cells were serum starved for half an hour in DMEM (no FBS in the media). Endocytosis markers were added to the cells (Cholera toxin B or Transferrin, from Molecular Probes) at a

dilution of 1 in 100 from the stock solution of 1 mg/ml (10 μg/ml final concentration) with the media. The cells were incubated at 37˚C for 10 minutes and the dyes were washed off with PBS five times. Then the cells were fixed in 4% formaldehyde for 3 minutes and immunofluorescence was carried out as normal.

Microscopy

All slides were examined with an Olympus Provis microsope, equipped with epifluorescence optics. Images were captured with an Orca II CCD camera (Hamamatsu) and Smart-capture 3 software (Digital Scientific). All images were processed using Adobe Photoshop software.

Histone extractions

Histones were extracted from larvae following the protocol described in (Bonaldi *et al.*, 2004). The larvae (about 20) were resuspended in 40 ml of hypotonic buffer (15 mM HEPES-KOH pH 7.6, 10 mM KCl, 5 mM $MgCl_2$, 0.05 mM EDTA, 0.25 mM EGTA, 1 mM DTT, 0.2 mM PMSF, 5 mM Na butyrate, 10% glycerol and protease inhibitors) and homogenized using a hand pestle. The lysate was centrifuged for 10 minutes at 10,000 rpm in a HB-4 rotor at 4˚C. This resulted in a biphasic pellet with a loose nuclear pellet on top and a tight yellow pellet at the bottom. The supernatant was discarded and the nuclear pellet was carefully resuspended in a final volume of 50 ml of SUC buffer (15 mM HEPES-KOH pH 7.6, 10 mM KCl, 5 mM $MgCl_2$, 0.05 mM EDTA, 0.25 mM EGTA, 1 mM DTT, 0.2 mM PMSF, 350 mM sucrose, 5 mM Sodium butyrate and protease inhibitors). The

nuclear pellet was washed twice in 50 mL of SUC buffer and finally resuspended in 30 ml of SUC(-) (without sucrose) buffer (15 mM HEPES-KOH pH 7.6, 10 mM KCl, 5 mM MgCl2, 0.05 mM EDTA, 0.25 mM EGTA, 1 mM DTT, 0.2 mM PMSF, 5 mM sodium butyrate and proteases inhibitors) without sucrose.

Core histones, together with linker histones and HMG proteins, were then extracted by adding 0.5 volumes of ice-cold 0.8 M HCl. After an overnight extraction on a rotating wheel at 4˚C, the sample was centrifuged for 10 minutes at 13,000 rpm on a benchtop centrifuge. The histones and all other acid-soluble proteins remained in the supernatant. Residual histones were re-extracted for 3–4 hrs in ice-cold 0.4 M HCl. The proteins in the supernatant were incubated with 10% TCA (trichloro acetic acid), incubated on ice for 30 minutes and centrifuged at 13,000 rpm at 4˚C using a benchtop centrifuge for 15 minutes. The supernatant was carefully removed and 300 µl of acetone was added and centrifuged at 13,000 rpm at 4˚C using a benchtop centrifuge. The supernatant was removed and the pellet was resuspended in SDS-PAGE sample buffer with DTT. Samples were boiled for 5 minutes at 100˚C on a heat block before loading on to a gel.

List of Primers

Gene	Sequence
Delta	5′-ATGGGAAACTGACCTTGCAC 3′-GTCGTCCAGTGGTTCTTGGT
E(Spl)	5′-GAAGGTGAAGAAGCCAATGC 3′-CGTTGACGGCATTCATGTAG
Invadolysin	5′-ATGGCCAAAACGCCCCCGCTC 3′-ACGCCCTTGGTCTCTCGCACC
Poly	5′-ATGGCCACCTCAGTCCTGCTA 3′-GACTTTGACCCCAATTTCGCC

Primers for FLAG-tagged constructs	5′- G AGATCT ATG GCC AAA ACG CCC CCG CTC 5′- G AGATCT ATG CAG ACA CTG ATC TCC ACC G 5′- G AGATCT ATG TTC TCC GTG AGC TTG TAC G 3′- G GCGGCCGC TTA CTT GTC GTC GTC GTC CTT ATA GTC TCC TCC TCC TCC TCC TCC ACT GAA TCC CCA TCG CAG GCC G 3′- G GCGGCCGC TTA CTT GTC GTC GTC GTC CTT ATA GTC TCC TCC TCC TCC TCC TCC CTT TAC GGT GGA GAT CAG TGT C 3′- G GCGGCCGC TTA CTT GTC GTC GTC GTC CTT ATA GTC TCC TCC TCC TCC TCC TCC GAA TGC GTA CAA GCT CAC GGA G

List of Antibodies

Primary antibodies

Antibody	Host animal	Source (catalogue no.)	Dilution
Actin	Rabbit	Sigma (A2066)	1:100
ADRP	Goat	Santa Cruz (sc-32450)	1:100
Caveolin-1	Mouse	Invitrogen (036000)	1:500
Clathrin	Goat	Santacruz (sc-6579)	1:1000
CP190	Rabbit	W. Whitfield, Dundee	1:250
Delta	Mouse	Hybridoma (C594.9B)	1:50
Dynamin 1	Goat	Santa Cruz (sc-6402)	1:500
H2B	Sheep	Abcam (ab9408)	1:100
H2B (Rabbit)	Rabbit	Abcam (ab1790)	1:100
H3K4dime	Rabbit	Abcam (ab7766)	1:3000
H3K4trime	Rabbit	Abcam (ab8580)	1:3000
H3K9/14Ac	Rabbit	Cell Signalling (9677)	1:1000
Invadolysin antibodies Ab4100 (*Dm*) Ab4101 (*Dm*) R1318 (*Hs*)	Rabbit	Heck laboratory	 1:500 1:500 1:250
Itch	Mouse	BD Biosciences (clone 32, 611198)	1:100
Non-stop antibodies Ab4890 (*Dm*) Ab4891 (*Dm*)	Rabbit	Heck laboratory	 1:500 1:500
Notch ECD	Mouse	Hybridoma (C458.2H)	1:50
Notch ICD	Mouse	Hybridoma (C17.9C6)	1:50
Rab11	Mouse	Upstate (clone 47, 05-853)	1:100
TIP47	Guinea pig	Progen (03-GP30)	1:100
Tubulin	Mouse	Sigma (B-5-1-2)	1:5000
Ubiquitin	Rabbit	Biomol (UG9510)	1:100
Ubiquitin	Rabbit	Sigma (U5379)	1:100

Secondary antibodies

Antibody	Host	Source	Dilution
Anti-mouse Alexa 488	Donkey	Molecular Probes (A21202)	1:500
Anti-mouse Alexa 594	Donkey	Molecular Probes (A21203)	1:500
Anti-rabbit Alexa 488	Donkey	Molecular Probes (A21206)	1:500
Anti-rabbit Alexa 594	Donkey	Molecular Probes (A21207)	1:500
Anti-goat Alexa 594	Donkey	Jackson Immunoresearch (705-075-147)	1:50
Anti-guinea pig Alexa 594	Donkey	Jackson Immunoresearch (706-075-148)	1:50
Anti-mouse HRP	Sheep	Amersham (NA931)	1:10,000
Anti-rabbit HRP	Donkey	Amersham (NA934)	1:10,000
Anti-goat/sheep HRP	Donkey	Santa Cruz (sc-2020)	1:10,000

Chapter 3: Second site non-complementation screen to identify interactors of *IX-14/invadolysin*

Introduction

Synthetic lethality has been widely used in yeast genetic screens to identify functional relationships between genes. It has also been used for large scale array screenings in yeast for functional profiling of genes (Ooi *et al.*, 2006). In *Drosophila* it was used to study the functional relationship of a collection of mutations for the first time in 1968 (Lucchesi, 1968). It is termed as second site non-complementation or modified synthetic lethal screen in *Drosophila.* Second site non-complementation screens have identified many interacting partners of various proteins (Fuller *et al.*, 1989).

The previous work in Heck laboratory on Invadolysin (IX-14) focussed on characterizing the *IX-14/invadolysin* mutation in flies and preliminary studies on the functional aspects of it. Despite detailed characterization of the mitotic phenotypes of the *IX-14* mutation, little was known about the protein's precise molecular role. To identify genetic interactors of *IX-14*, I performed a second site non-complementation screen taking advantage of the Drosdel collection of deficiencies that cover more than two thirds of the genome (Ryder *et al.*, 2007).

Deficiency Screen

In yeast, which lives predominantly as a haploid organism, and in which most of the genes are non-essential, synthetic lethality has been a powerful approach to evaluate protein function (Tong *et al.*, 2001) (Figure 3.1). Mutations or deletions of

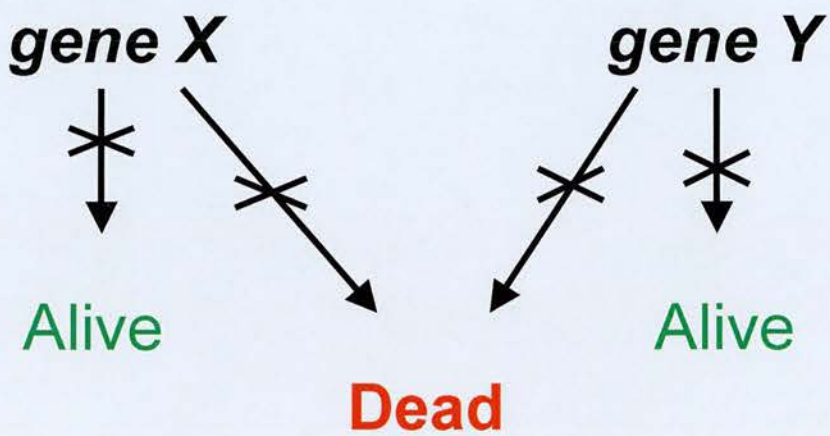

Figure 3.1. Schematic of the concept of synthetic lethality in yeast.
"Synthetic lethality" is a concept widely used to study redundant functional relationships of genes. The genes X and Y in the above schematic represent two genes where their individual deletions are viable, but in combination they are lethal. The lethality emphasizes that these two genes are either redundant or involved in similar processes in parallel pathways.

two genes X and Y are viable on their own but lethal when the two mutations are brought together implying that the two genes may be playing redundant functions for an essential pathway. *Drosophila* is a diploid organism. In *Drosophila* failure of complementation between heterozygous mutations at separate loci (second site non-complementation) has been used to identify genes that encode for interacting proteins (Hays *et al.*, 1989). Therefore we designed a screen where *IX-14* heterozygous mutants were crossed to the Drosdel deficiency kit and the trans-heterozygous progeny of flies were scored based on viability. I performed approximately 200 crosses as illustrated in the figure (Figure 3.2).

The original *IX-14*^{1} allele balanced over the TM3 third chromosome balancer was crossed to Drosdel deficiency lines. The deficiency stocks are balanced with an appropriate balancer chromosome depending on the chromosome from which the genes are deleted. For example, the third chromosome balancers were either TM6C or TM2. When the *IX-14* mutation was crossed to a deficiency stock located on the third chromosome (*Df*/TM6C, where *Df* could be one or more genes deleted), four different progeny were obtained. The progeny could be distinguished with regard to the presence or absence of balancers. The progeny that did not contain any balancers brought together the *IX-14*^{1} mutation with the deletion (*Df*). These progeny were viable, lethal or semilethal based on the interaction between *IX-14* mutation and *Df* (Figure 3.2).

Deficiency kit

I chose to use the Drosdel deficiency kit, and not the Bloomington deficiency kit, as the Drosdel kit had molecularly defined maps for each deficiency as shown in

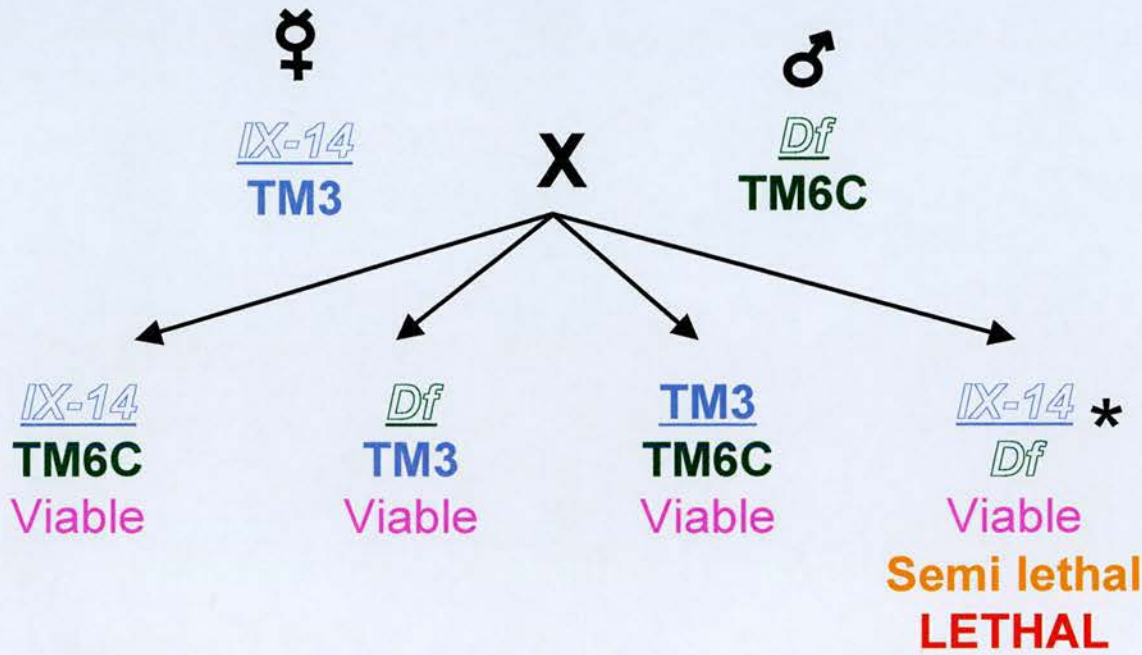

Figure 3.2. Schematic representation of second site non-complementation screen. *IX-14* mutants balanced over TM3 (represented in blue) were crossed to Drosdel deficiencies (eg. *Df*, represented in green) balanced over an appropriate balancer depending on the chromosome. The progeny were scored for the presence or absence of balancers. The flies with no balancer* will be viable, semi-lethal or lethal based on the interaction between *IX-14* and genes deleted within the deficiency tested.

the figure (Figure 3.3). In figure 3.3, the X chromosome deficiencies are represented (taken from Drosdel website). The cytological map of the X-chromosome is graphically represented at the top and the bottom of the figure and the deficiencies are represented as green blocks along the X-chromosome. Each deficiency has its limits between two particular regions of the X-chromosome and the number of genes deleted by each deficiency varies from a few to a couple of hundreds.

The deficiency crosses were performed using 5-10 virgin females from the *IX-14* mutant allele and 2-3 males from the deficiency stock. The males and females were mated in a fresh vial and left to produce progeny for 5 days at room temperature. After 5 days, the parents were removed from the vials and the progeny were left to emerge. Once all the progeny emerged the flies were counted with reference to the presence or absence of balancers. Males and females were counted separately in order to investigate if there was any male or female specific phenotype.

Results of Deficiency screen

As a result of the screening performed, one completely lethal (*Df(3L)ED225*) and three semilethal lines (*Df(3R)ED5071, Df(2R)ED1552, Df(2L)ED695*) were identified (Figure 3.4). The list of all the results of the crosses is in table 3.4A. The lethal deficiency *Df(3L)ED225*, was present on the left arm of the third chromosome whereas the *IX-14* mutation was present on the right arm of the third chromosome. This eliminated the possibility of the *IX-14* gene being present within *Df(3L)ED225*. The lethal deficiency uncovered the region between 75C and 75D on the cytological map. It completely deleted 23 genes and partially another gene, as listed in the figure (Figure 3.5). These genes included some well-studied genes as well as genes

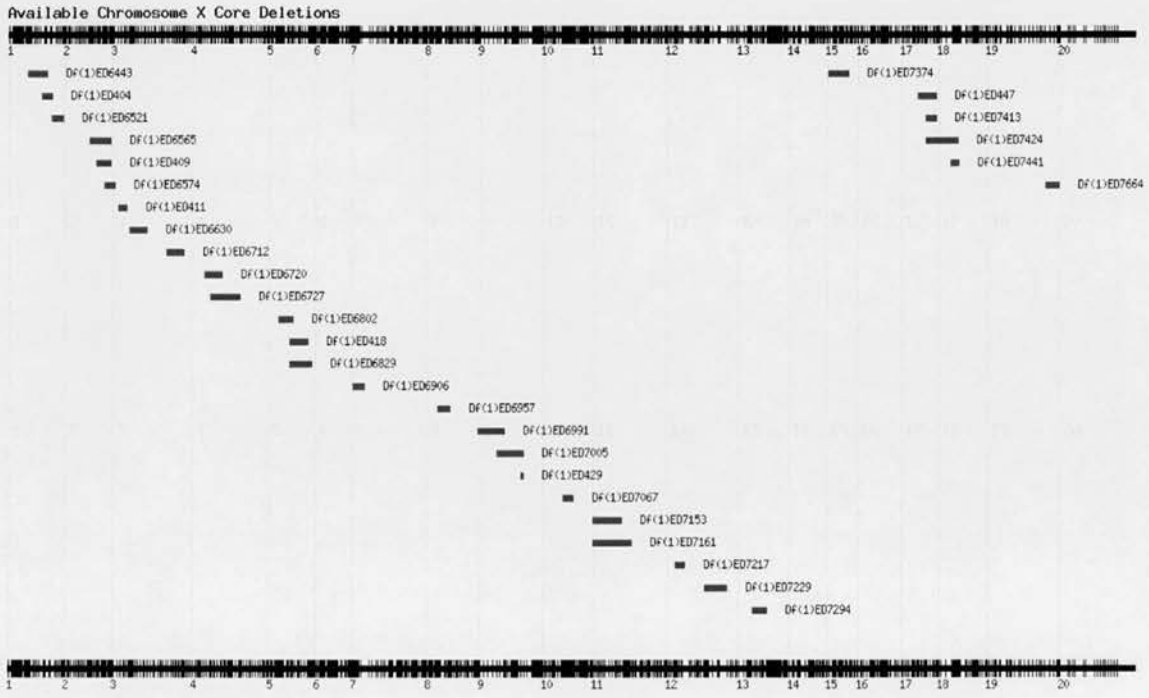

Figure 3.3. Schematic representation of the Drosdel deficiency kit.
The collection of deficiency lines for the X-chromosome is represented. The genes included in the area represented by green blocks are deleted in the corresponding deficiency.

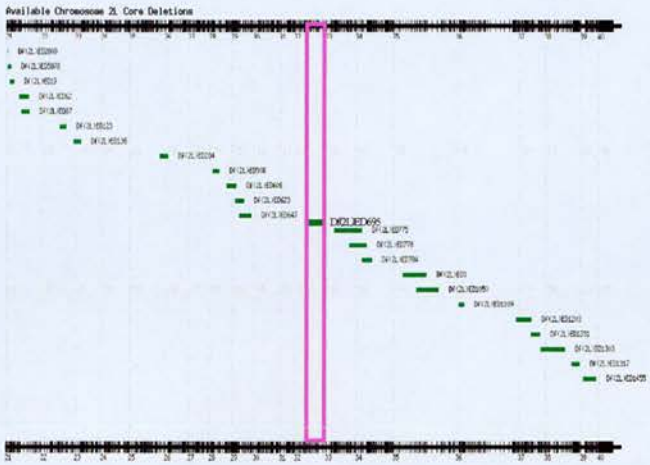

Chromosome 2L - *Df(2L)ED695*

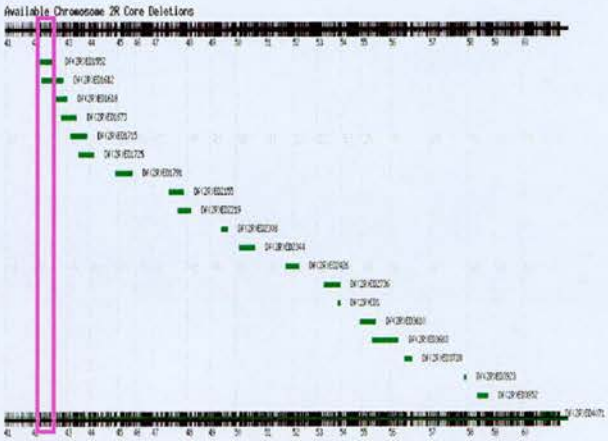

Chromosome 2R - *Df(2R)ED1552*

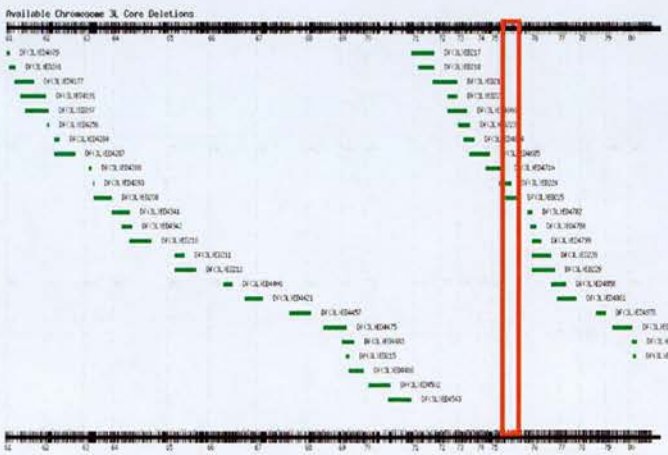

Chromosome 3L - *Df(3L)ED225*

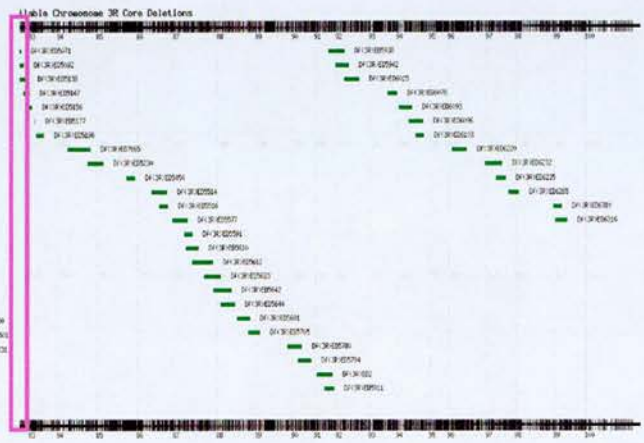

Chromosome 3R - *Df(3R)5071*

Figure 3.4. Drosdel deficiencies that showed interaction with *IX-14^1*.
Four deficiencies, *Df(2L)ED695*, *Df(2R)ED1552*, *Df(3L)ED225* and *Df(3R)5071,* showed genetic interactions with *IX-14^1*. Of these *Df(3L)ED225* (indicated in red) was lethal and the remaining three were semi-lethal (indicated in magenta) when in combination with *IX-14^1*.

Gene	Functions
CG7320	-
CG13700	-
CG13701 (skl)	apoptosis, induction of apoptosis
CG18064	-
CG32198	-
CG4216 (term)	DNA binding, zinc ion binding
CG18233	oxidoreductase activity, protein metabolism, protein modification
CG32199	procollagen-proline 4-dioxygenase activity
CG7313 (Che75a)	-
CG4345 (grim)	NOT nurse cell apoptosis, central nervous system metamorphosis
CG32196	-
CG32197	-
CG7285 (star1)	neuropeptide, somatostatin, allatostatin receptor activity
CG4174	procollagen-proline 4-dioxygenase activity
CG18231	oxidoreductase activity
CG13380	-
CG5103	transketolase activity
CG4319 (rpr)	NOT nurse cell apoptosis, response to DNA damage stimulus
CG4306	-
CG13702 (A1CR2)	neuropeptide, somatostatin, allatostatin receptor activity
CG7271	nucleic acid binding, zinc ion binding
CG18234	oxidoreductase activity
CG32201	procollagen-proline 4-dioxygenase activity
Partial coverage	
CG4166 (not)	nucleic acid binding, ubiquitin-specific protease activity, zinc ion binding

Figure 3.5. List of genes uncovered by *Df(3L)ED225*.
The deficiency Df(3L)ED225 uncovered 24 genes (23 complete and 1 partial-CG4166). The genes and their known or predicted functions are listed in the table above.

whose functions were unknown. There were apoptotic genes such as *rpr*, *grim* and ubiquitin proteases such as *non-stop* and other enzymes.

In an attempt to identify the gene responsible for the lethal interaction, deficiency lines containing overlapping regions were tested for lethality with the *IX-14* mutation. Firstly, the neighbouring deficiency *Df(3L)ED224*, which deleted some of the genes also deleted by *Df(3L)ED225*, complemented *IX-14*. These genes were eliminated from being the potential interactors. This left 15 genes of *Df(3L)ED225* as possible interactors. Deficiencies *Df(3L)H99* and *Df(3L)Exel6134* were tested- these also overlapped with *Df(3L)ED225*. Of these, *Df(3L)H99* was viable and *Df(3L)Exel6134* was lethal. This narrowed the number of potential interacting genes to 13. Due to the unavailability of smaller deficiencies uncovering these 13 genes, individual mutants had to be tested (Figure 3.6).

Four of the 13 genes were represented by mutant alleles available in the Bloomington stock centre. (CG13702, CG32197, CG18231 and CG4166) (Figure 3.6). These mutations tested for lethality in combination with the *IX-14* mutation. Of these lines, only CG4166 was lethal in combination with *IX-14* mutation. CG4166 was originally named as *non-stop* or *not* (Martin *et al.*, 1995). I also tested the other mutant *IX-14* allele ($IX\text{-}14^{4Y7}$) for interaction with CG4166. But surprisingly, it was not lethal in combination. This could be attributed to the different molecular nature of the mutations. $IX\text{-}14^{4Y7}$ is P-element insertion 40 bp upstream of the transcription start region. Hence $l(3)IX\text{-}14^{4Y7}$ could be a hypomorphic allele and the amount of IX-14/Invadolysin in the transheterozygotes might be enough for the viability of transheterozygotes.

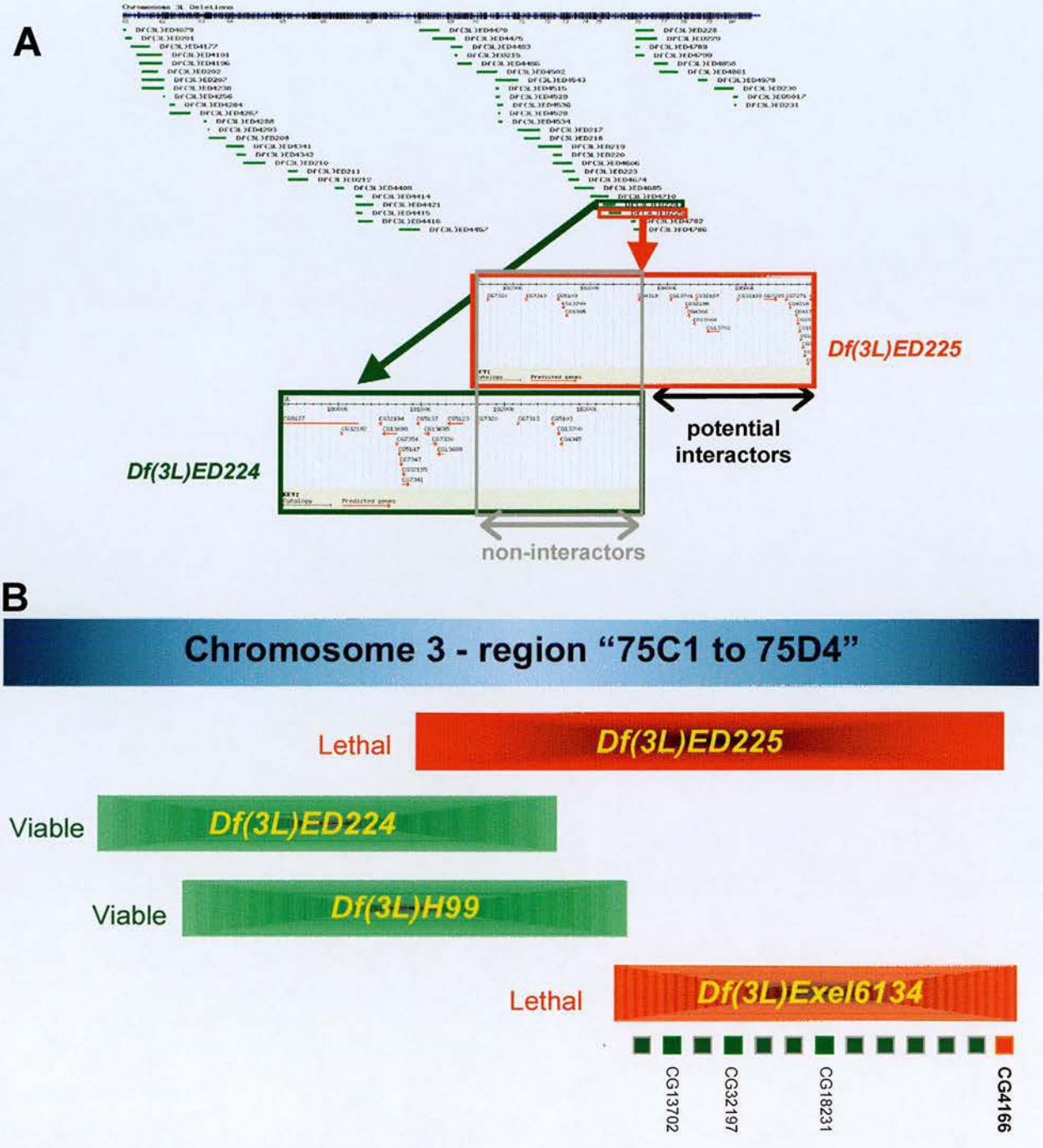

Figure 3.6. Schematic representation of narrowing down genetic interactors to one gene.
A. The potential interactors of *IX-14[1]* from the pool of 24 genes (uncovered by *Df(3L)ED225* were narrowed down by crossing *IX-14[1]* to overlapping deficiency *Df(3L)ED224*. 7 genes were ruled out as *Df(3L)ED224* complemented *IX-14[1]*.
B. Deficiencies *Df(3L)H99* and *Df(3L)Exel6134* were tested to further narrow down the number of potential interacting genes. Individual mutant alleles within *Df(3L)Exel6134* were tested for lethality and the mutation in the gene CG4166 was lethal in combination with *IX-14[1]*. In the above figure, lethal interactions are represented in red and non-lethal are represented in green.

Identification of *non-stop* as an interacting gene

In order to confirm the interaction between *lX-14* and *non-stop*, the two available mutant alleles for *non-stop*, not^{1} and not^{2} (also termed not^{02069}) tested for lethality with the $lX\text{-}14^{1}$ mutant. Both were completely lethal.

Non-stop is a ubiquitin specific protease or a deubiquitinating enzyme (Poeck *et al.*, 2001). Ubiquitin specific proteases are an essential regulatory component of both protein degradation by the proteasome, and of other ubiquitin-dependent processes, by virtue of their ability to regulate protein ubiquitination in a target-specific manner (Soboleva and Baker, 2004). Consistent with *non-stop* functioning as a ubiquitin protease, immunoblots of *non-stop* homozygous mutant third instar larvae showed an accumulation of three ubiquitinated proteins ~ at 29, 55 and 200 kDa size that are undetectable in wild type third instar larval extracts (Poeck *et al.*, 2001).

The *lX-14/non-stop* transheterozygotic animals die as pupae (Figure 3.7). It is interesting to note that *lX-14* mutant animals die as early third instar larvae and the *non-stop* homozygotes pupate. The transheterozygotes are rescued until pupation but after that they fail to develop and eclose as adult flies. The detailed interaction between *lX-14* and *non-stop* is characterized in the next chapter (Chapter 4).

Semilethal deficiencies *Df(3R)ED5071, Df(2R)ED1552, Df(2L)ED695*

I attempted to narrow down interacting genes from the semilethal deficiencies. However, due to the unavailability of smaller overlapping deficiencies uncovering the parts of original deficiencies, a complete analysis could not be made. However, all available individual mutations and smaller deficiencies were tested for

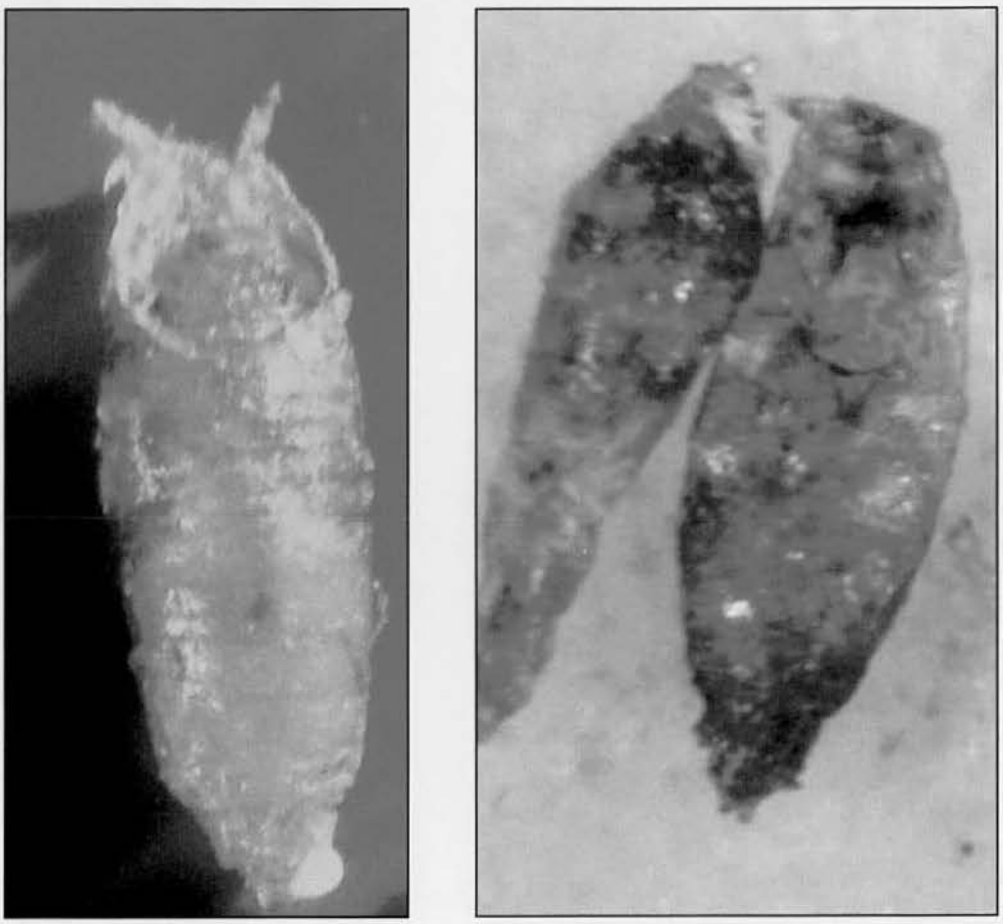

Figure 3.7. *IX-14*^{1}*/non-stop* trans-heterozygote pupae.
The *IX-14* and *non-stop* trans-heterozygote animals die as pupae. They do not metamorphosize and die in the pupal cases in contrast to wild type pupae.

lethality. There was no individual smaller deficiency or individual genes that were lethal or semilethal in combination with *IX-14.*

Table 3.4A. Results of second site complementation screen - (*IX-14*^{1}/TM3) crossed to Deficiency stocks

1st chromosome

Deficiency	Female w/o balancers	Females with balancers	% Non-balancer flies
Df (1) ED 404	14	42	33.33
Df (1) ED 6630	22	25	88
Df (1) ED 418	4	19	21.05
Df (1) ED 6957	25	50	50
Df (1) ED 429	23	56	41.07
Df (1) ED 7161	12	22	54.55
Df (1) ED 7217	18	39	46.15
Df (1) ED 7374	22	54	40.74
Df (1) ED 447	20	40	50
Df (1) ED 7413	26	72	36.11
Df (1) ED 7441	14	29	48.28
Df (1) ED 7294	16	38	42.11

2nd chromosome left arm

Deficiency	Males w/o balancer	Males with balancer	Females w/o balancer	Females with balancers	% Males w/o balancers	% Females w/o balancers	% Total non-balancer flies
Df (2L) ED 2809	9	37	11	33	24.32	33.33	28.825
Df (2L) ED 5878	4	17	11	25	23.53	44	33.765
Df (2L) ED 62	3	16	8	17	18.75	47.06	32.905
Df (2L) ED 87	22	30	12	26	73.33	46.15	59.74
Df (2L) ED 123	4	11	4	10	36.36	40	38.18
Df (2L) ED 284	18	52	17	32	34.62	53.13	43.875
Df (2L) ED 508	8	19	7	21	42.11	33.33	37.72
Df (2L) ED 606	6	26	8	29	23.08	27.59	25.335
Df (2L) ED 629	13	52	10	33	25	30.3	27.65
Df (2L)ED 695	6	58	3	43	10.34	6.98	8.66
Df (2L) ED 647	12	35	15	38	34.29	39.47	36.88
Df (2L) ED 784	5	8	6	10	62.5	60	61.25
Df (2L) ED 3	13	48	25	53	27.08	47.17	37.125
Df (2L) ED 1050	13	18	14	25	72.22	56	64.11
Df (2L) ED 1109	3	8	3	9	37.5	33.33	35.415
Df (2L) ED 1203	12	39	24	48	30.77	50	40.385
Df (2L) ED 1303	12	16	12	21	75	57.14	66.07
Df (2L) ED 623	9	24	11	30	37.5	36.67	37.085
Df (2L) ED 695	10	9	1	12	111.11	8.33	59.72
Df (2L) ED 746	12	28	14	36	42.86	38.89	40.875

2nd chromosome right arm

Deficiency	Males w/o balancer	Males with balancer	Females w/o balancer	Females with balancers	% Males w/o balancers	% Females w/o balancers	% Total non-balancer flies
Df (2R) ED 1612	9	30	8	31	30	25.81	27.905
DF (2R) ED 1552	4	41	7	42	9.76	16.67	13.215
Df (2R) ED 1618	12	33	10	29	36.36	34.48	35.42
Df (2R) ED 1715	5	29	6	31	17.24	19.35	18.295
Df (2R) ED 1725	6	11	5	13	54.55	38.46	46.505
Df (2R) ED 1791	7	19	8	19	36.84	42.11	39.475
Df (2R) ED 2219	9	40	12	21	22.5	57.14	39.82
Df (2R) ED 2426	8	14	7	18	57.14	38.89	48.015
Df (2R) ED 2736	24	59	18	39	40.68	46.15	43.415
Df (2R) ED 3610	17	29	18	36	58.62	50	54.31
Df (2R) ED 3683	7	8	2	9	87.5	22.22	54.86
Df (2R) ED 3923	14	21	14	17	66.67	82.35	74.51
Df (2R) ED 4071	11	18	11	21	61.11	52.38	56.745
Df (2R) ED 2436	10	31	15	36	32.26	41.67	36.965

3rd chromosome left arm

Deficiency	Males w/o balancer	Males with balancer	Females w/o balancer	Females with balancers	% Males w/o balancers	% Females w/o balancers	% Total non-balancer flies
Df (3L) ED 4079	11	38	12	32	28.95	37.5	33.225
Df (3L) ED 201	12	29	10	21	41.38	47.62	44.5
Df (3L) ED 4177	16	27	13	27	59.26	48.15	53.705
Df (3L) ED 4191	2	8	2	12	25	16.67	20.835
Df (3L) ED 207	10	34	12	30	29.41	40	34.705
Df (3L) ED 4287	10	21	9	28	47.62	32.14	39.88
Df (3L) ED 4288	9	20	9	19	45	47.37	46.185
Df (3L) ED 208	7	13	5	16	53.85	31.25	42.55
Df (3L) ED 4342	21	36	24	52	58.33	46.15	52.24
Df (3L) ED 210	11	31	8	26	35.48	30.77	33.125
Df (3L) ED 211	11	31	19	40	35.48	47.5	41.49
Df (3L) ED 212	24	32	14	27	75	51.85	63.425
Df (3L) ED 4408	9	7	7	10	128.57	70	99.285
Df (3L) ED 4421	7	23	10	20	30.43	50	40.215
Df (3L) ED 4475	3	7	6	16	42.86	37.5	40.18
Df (3L) ED 4483	8	21	11	18	38.1	61.11	49.605
Df (3L) ED 215	15	34	14	39	44.12	35.9	40.01
Df (3L) ED 4486	8	9	5	27	88.89	18.52	53.705
Df (3L) ED 4502	23	25	18	15	92	120	106
Df (3L) ED 217	5	12	7	15	41.67	46.67	44.17
Df (3L) ED 218	12	18	10	10	66.67	100	83.335
Df (3L) ED 219	4	19	7	19	21.05	36.84	28.945
Df (3L) ED 220	18	22	28	16	81.82	175	128.41
Df (3L) ED 223	9	25	6	23	36	26.09	31.045
Df (3L) ED 4674	13	16	14	27	81.25	51.85	66.55
Df (3L) ED 4685	12	29	11	25	41.38	44	42.69
Df (3L) ED 4710	10	35	19	40	28.57	47.5	38.035
Df (3L) ED 224	17	18	10	15	94.44	66.67	80.555
Df (3L) ED 225	**0**	**38**	**0**	**32**	**0**	**0**	**0**

Df (3L) ED 4782	8	12	12	9	66.67	133.33	100
Df (3L) ED 4786	17	20	14	26	85	53.85	69.425
Df (3L) ED 4799	16	27	7	33	59.26	21.21	40.235
Df (3L) ED 228	6	10	16	18	60	88.89	74.445
Df (3L) ED 229	4	1	6	7	400	85.71	242.855
Df (3L) ED 4858	24	53	17	45	45.28	37.78	41.53
Df (3L) ED 4861	8	31	12	26	25.81	46.15	35.98
Df (3L) ED 4978	5	15	8	22	33.33	36.36	34.845
Df (3L) ED 230	8	15	5	16	53.33	31.25	42.29
Df (3L) ED 5017	6	20	4	16	30	25	27.5
Df (3L) ED 231	5	16	7	13	31.25	53.85	42.55
Df (3L) ED 4284	7	15	5	11	46.67	45.45	46.06
Df (3L) ED 4344	13	22	15	32	59.09	46.88	52.985
Df (3L) ED 4543	8	6	9	11	133.33	81.82	107.575

3rd chromosome right arm

Deficiency	Males w/o balancer	Males with balancer	Females w/o balancer	Females with balancers	% Males w/o balancers	% Females w/o balancers	% Total non-balancer flies
Df (3R) ED 5071	4	41	7	42	9.76	16.67	13.215
Df (3R) ED 5138	9	10	18	8	90	225	157.5
Df (3R) ED 5156	14	19	38	49	73.68	77.55	75.615
Df (3R) ED 5177	9	9	23	16	100	143.75	121.875
Df (3R) ED 5196	10	35	18	29	28.57	62.07	45.32
Df (3R) ED 5230	4	24	7	28	16.67	25	20.835
Df (3R) ED 5514	9	24	10	28	37.5	35.71	36.605
Df (3R) ED 5516	6	19	7	16	31.58	43.75	37.665
Df (3R) ED 5577	6	7	5	7	85.71	71.43	78.57
Df (3R) ED 5591	2	6	5	5	33.33	100	66.665
Df (3R) ED 5610	8	23	14	16	34.78	87.5	61.14
Df (3R) ED 5644	7	21	6	17	33.33	35.29	34.31
Df (3R) ED 5705	29	34	31	19	85.29	163.16	124.225
Df (3R) ED 5780	16	13	14	8	123.08	175	149.04
Df (3R) ED 2	14	36	20	24	38.89	83.33	61.11
Df (3R) ED 5911	11	20	9	18	55	50	52.5
Df (3R) ED 5942	12	16	9	18	75	50	62.5
Df (3R) ED 6025	12	21	10	17	57.14	58.82	57.98
Df (3R) ED 6076	7	30	11	29	23.33	37.93	30.63
Df (3R) ED 6096	6	13	8	21	46.15	38.1	42.125
Df (3R) ED 6103	5	25	15	24	20	62.5	41.25
Df (3R) ED 6220	12	25	13	17	48	76.47	62.235
Df (3R) ED 6232	22	21	16	24	104.76	66.67	85.715
Df (3R) ED 6235	3	21	4	28	14.29	14.29	14.29
Df (3R) ED 6265	12	24	5	19	50	26.32	38.16
Df (3R) ED 6310	4	11	2	8	36.36	25	30.68
Df (3R) ED 5622	6	21	7	19	28.57	36.84	32.705
Df (3R) ED 5412	12	25	8	22	48	36.36	42.18

Chapter 4: Characterization of the *invadolysin* and *non-stop* interaction

Introduction

Non-stop, an ubiquitin protease or deubiquitinating enzyme (DUB), was isolated as a genetic interactor of *IX-14/invadolysin* as described in the previous chapter (Chapter 3). The relationship between the two genes is studied in detail in this chapter with a thorough phenotypic analysis of the mutants. *non-stop* is a homozygous pupal lethal mutation called so because of its 'non-stop' axon guidance phenotype where it is required for the correct stopping of R1-R6 axons (Martin *et al.*, 1995; Poeck *et al.*, 2001). Immunoblots of *non-stop* homozygous mutant third instar larvae showed accumulation of three ubiquitinated proteins ~ at 29, 55 and 200 kDa size that are undetectable in the wild type third instar larval extracts (Poeck *et al.*, 2001).

Two of the previously studied mutants for *non-stop*, not^1 and not^2 (or not^{02069}) die as pupae although the not^2 mutant animals do not always pupate. not^2 die as late third instar larvae. The yeast homologue of *non-stop*, *ubp8*, is part of the SAGA transcription complex (Henry *et al.*, 2003). Non-stop is a 735 aa long protein with a peptidase domain at the C-terminus and a zinc finger motif in the middle (Figure 4.1A).

non-stop larvae accumulate melanotic masses and live longer than wild type

As stated above, *non-stop* mutant larvae are lethal. However the third instar larvae live a prolonged life. An aging assay was carried out to determine when exactly these larvae die. Wild type, *invadolysin* (*IX-14*^{4Y7}), and *non-stop* (*not*^{1} and *not*^{02069}/*not*^{2}) (mutant heterozygous stocks) flies were fed yeast paste for 2 days and left to lay eggs for a day in a fresh vial. The parents were removed and the viability of the third instar was determined daily. The wild type larvae lived as third instar larvae for 2-3 days, pupated and eclosed as adult flies 4-5 days later. The *not*^{1} larvae were alive for 9 days and died a day after they pupated. Most of the *not*^{2} larvae did not pupate but lived as third instar larvae for about 12 days. In contrast, *invadolysin* mutant larvae die as early third instars and live very short life. The *non-stop* larvae also accumulated black melanotic masses over time not only inside the body cavity but also right beneath the cuticle (Figure 4.1B). Such formation of melanotic masses occurs when signalling pathways are dis-regulated (Minakhina and Steward, 2006).

invadolysin larvae also show accumulation of ubiquitinated proteins

From the study characterizing *non-stop* (Poeck *et al.*, 2001), it was shown that ubiquitinated proteins at 29, 55 and 200 kDa accumulate in *non-stop* mutants. I wanted to examine if a similar ubiquitination pattern was evident in *invadolysin* mutant larvae. When larval extracts were immunoblotted with an antibody for ubiquitin, a band at ~29 kDa could only be seen in the *invadolysin* and *non-stop* larval extracts but not in wild type larval extract (Figure 4.2). This suggested that

Figure 4.1A. Domains of *Dm*Non-stop.
*Dm*Non-stop is a 735 aa acid enzyme belonging to C19 class of cysteine proteases, with a peptidase domain at the C-terminal. It also has a zing finger motif in the middle.

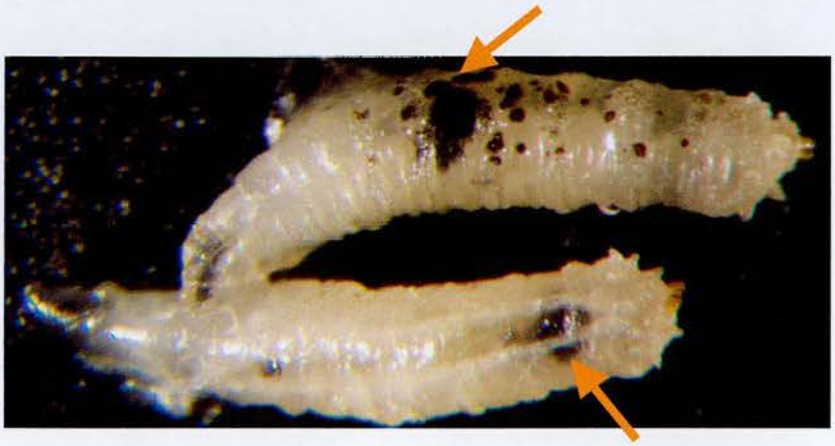

Figure 4.1B. Melanotic masses in *non-stop* larvae.
The *non-stop* mutant larvae contain melanotic masses both inside the body and on the cuticle. In the above picture the not^2 mutant larvae are shown and the melanotic masses are pointed using orange arrows. The larva on the top has melanotic depositions on its cuticle and the bottom one has them inside its body.

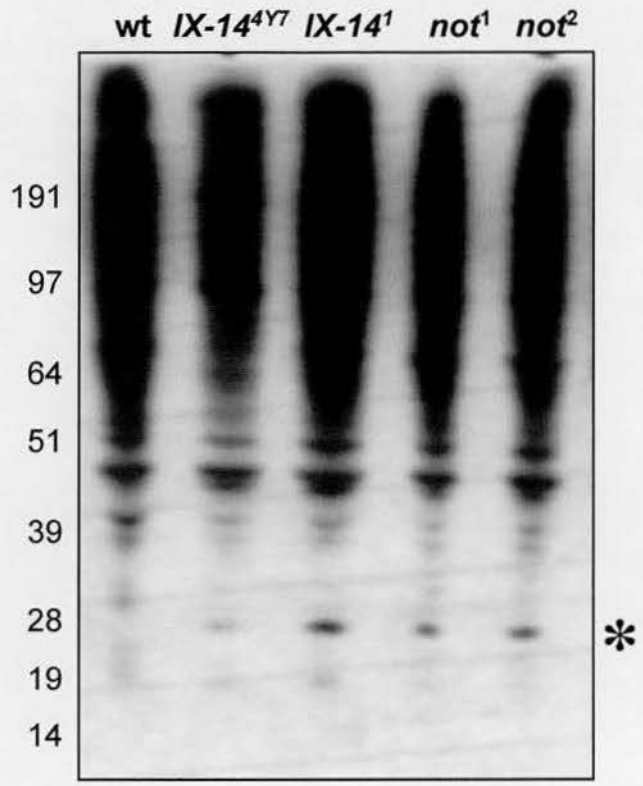

Figure 4.2. *invadolysin* and *non-stop* mutants show accumulation of ubiquitinated proteins.
Larval extracts were probed with an anti-ubiquitin polyclonal antibody (Biomol). Both *invadolysin* alleles (*IX-14*^{1} and *IX-14*^{4Y7}) *non-stop* alleles (*not*^{1} and *not*^{2}) show an accumulation of ubiquitinated proteins of 29 kDa pointed by an asterisk.

there might be accumulation of the same ubiquitinated protein at 29 kDa in both *invadolysin* and *non-stop* mutants. The higher molecular weight bands (55 and 200 kDa) couldn't be seen in the immunoblot due to high background or non-specificity of the antibody.

A second antibody for ubiquitin was tested on larval extracts as above. This time, 28 kDa and 55 kDa bands could be seen in both *invadolysin* and *non-stop* larval extracts but not in wild type larval extract (Figure 4.3). This antibody also showed high background and hence detection of 200 kDa band was not possible. Considering the similar size of the bands (29 and 55 kDa), I concluded that *invadolysin* and *non-stop* may be involved in the same or similar pathways, dis-regulation of which, in the mutant status brings about accumulation of particular ubiquitinated proteins.

The accumulation of ubiquitinated proteins is only detected in a small number of mutant larvae

During the course of several experiments carried out to examine the accumulation of ubiquitnated protein, I noted that only about 25% of the *invadolysin* mutant larvae showed the accumulation of the 28 and 55 kDa bands (Figure 4.4). They were never seen in the wild type larval extracts. This may be attributable to a dynamic nature of the ubiquitination status or it could also be that the larvae that are about to die specifically accumulate these bands. Immunoprecipitaiton experiments were attempted with anti-ubiquitin antibodies to isolate these proteins, but it was not successful due to the not surprisingly high background of proteins that were bound by ubiquitin antibodies.

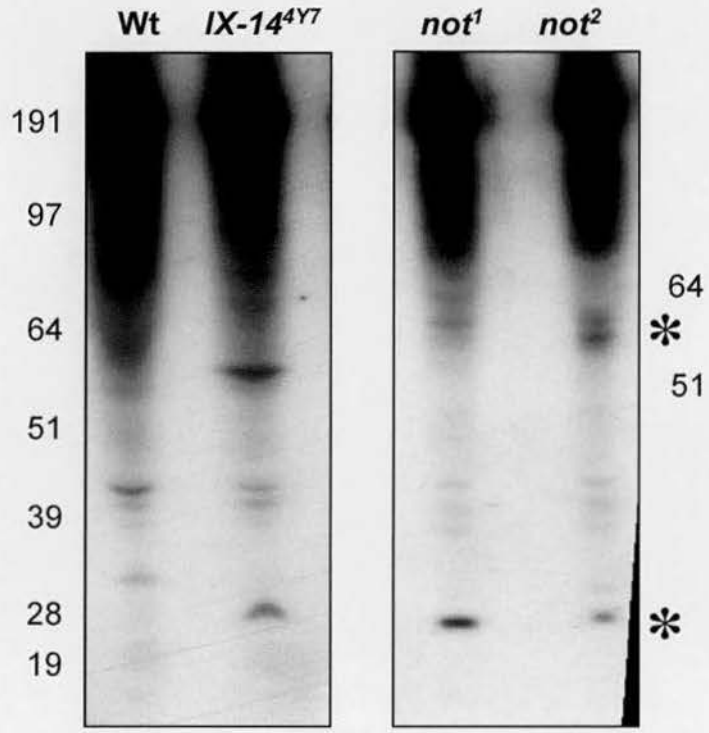

Figure 4.3. *invadolysin* and *non-stop* mutant alleles show accumulation of ubiquitinated proteins at 29 and 55 kDa.
Larval extracts were probed with an anti-ubiquitin polyclonal antibody (Sigma). Both *invadolysin* (*IX-14*^{4Y7}) *non-stop* alleles (*not*^{1} and *not*^{2}) show an accumulation of ubiquitinated proteins of 29 kDa and 55 kDa shown by asterisks.

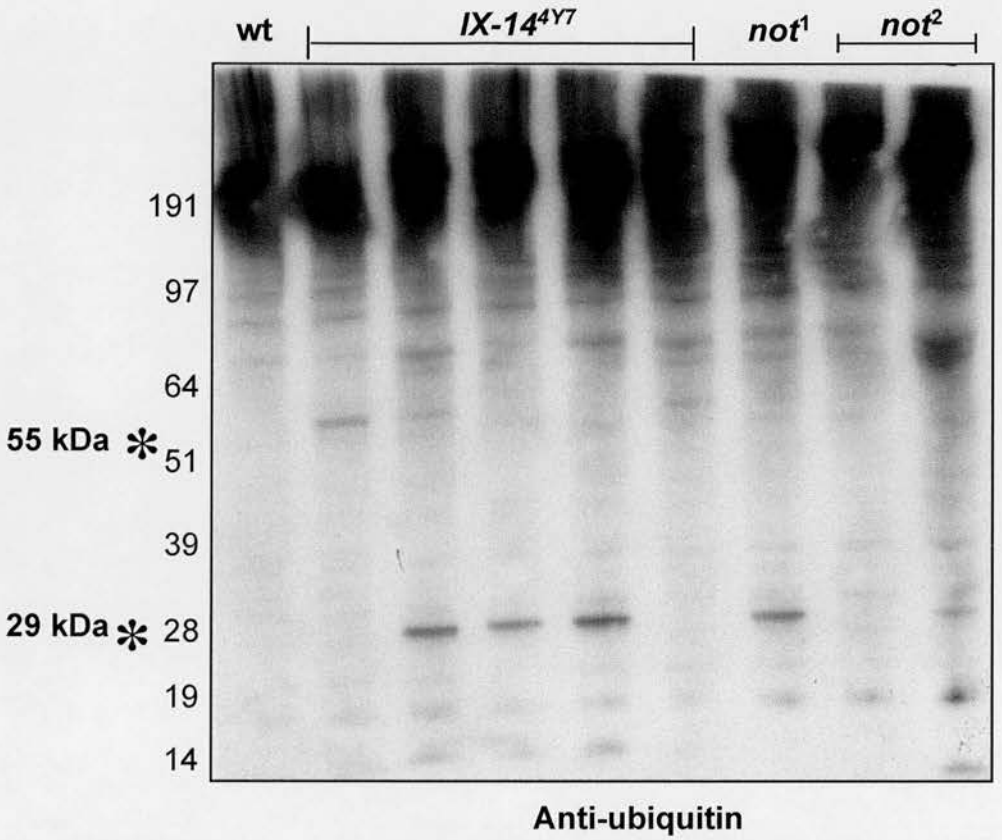

Figure 4.4. The accumulation of ubiquitinated proteins is only in some of the mutant larvae.

Individual larval extracts from wt and the *invadolysin* and *non-stop* mutants were probed with anti-ubiqutitin antibody (Sigma). Only some of the mutant *IX-14*^{4Y7} and *non-stop* mutants larvae showed an accumulation of ubiquitinated proteins at 29 kDa or 55 kDa (or both), indicated by asterisks.

Differences in phenotypes of *invadolysin* and *non-stop* mutants

On the other hand, *invadolysin* mutant larvae have very small brains and lack imaginal discs as expected for proliferation defects. *non-stop* larvae have a normal brain size (compared to wild type) and also possess imaginal discs (Figure 4.5). It is also worth noting that the size of the *non-stop* mutant larvae is similar to wild type. McHugh *et al.* showed that *invadolysin* mutants show an accumulation of nuclear envelope proteins such as lamin and otefin in neuroblasts (McHugh *et al.*, 2004). The *non-stop* mutants did not show an accumulation of these proteins. *invadolysin* mutant larvae possess germ cell migration defects and gonads fail to form. But the *non-stop* mutant larvae formed gonads, which were of similar size compared to wild type.

Mitotic chromosomes are hypercondensed in *non-stop* mutant neuroblasts

The original pheynotype described for the *invadolysin* mutants was the hypercondensed chromosomes in neuroblasts (Gatti and Baker, 1989; McHugh *et al.*, 2004). While mitotic chromosomes were hypercondensed in length, they were fuzzy. There were very few anaphases and the hypercondensation was not due to a mitotic arrest but rather a structural defect because allowing more time in mitosis with colchicine does not rescue the lateral condensation defect in *invadolysin/IX-14* mutant neuroblasts (McHugh *et al.*, 2004).

Interestingly both the not^{1} and not^{2} mutant alleles showed hypercondensed yet fuzzy chromosomes, which were very similar to *invadolysin*/($IX\text{-}14^{4Y7}$) mutants

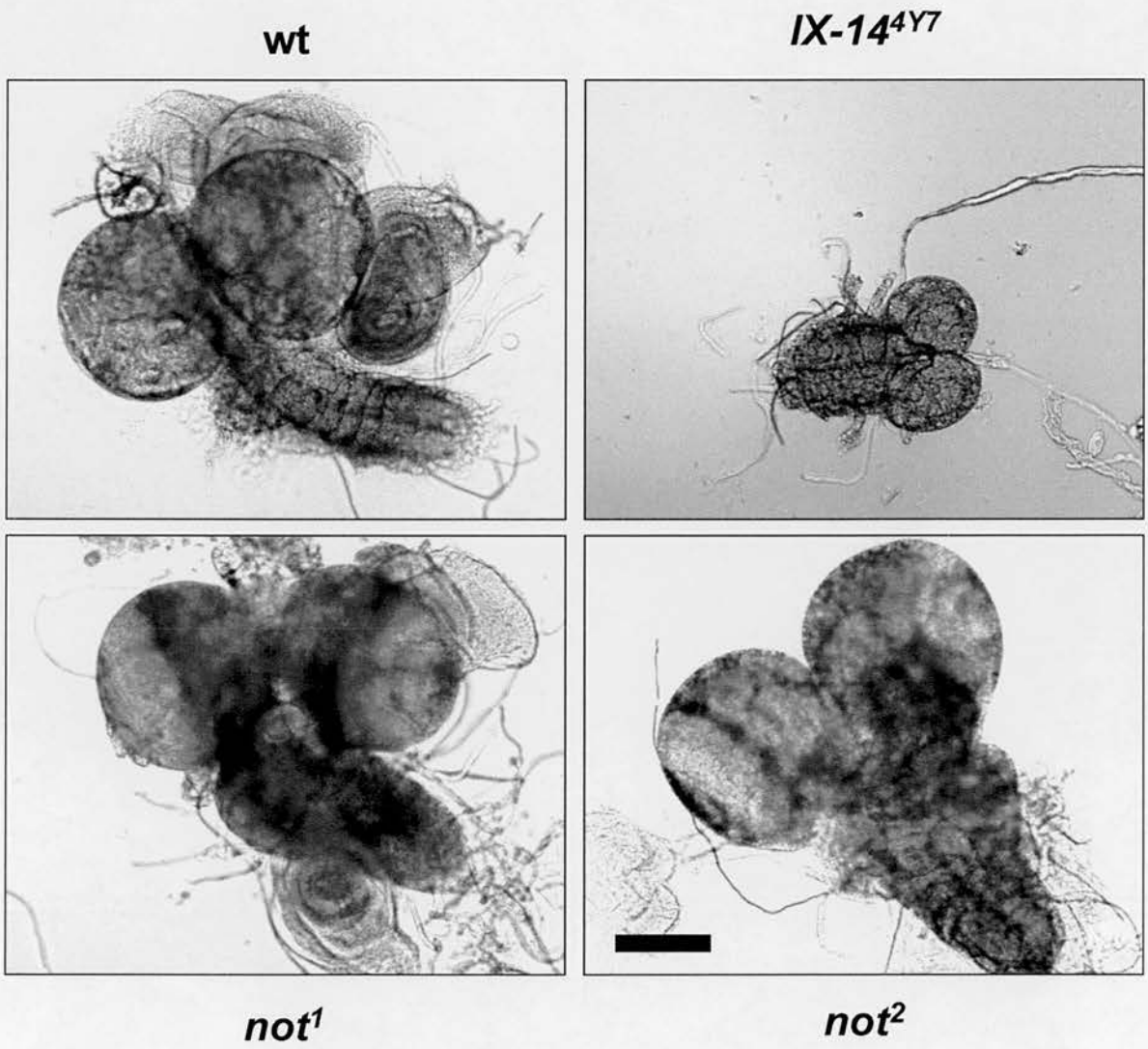

Figure 4.5. ***invadolysin*** **mutant brains are smaller but** ***non-stop*** **brains are normal size.** Brains from wild type and mutant (*invadolysin* and *non-stop)* third instar larvae were dissected and imaged by a bright field microscope. The *invadolysin* mutant brains were much smaller in size and lacked imaginal discs. The *non-stop* mutant brains were normal in size compared to wild type and contained imaginal discs (scale bar 100 μm).

(Figure 4.6). The number of hypercondensed chromosomes in *not*^{1} was less than that of *not*^{2}. *not*^{2} was a more severe mutant than *not*^{1}. In contrast to *invadolysin*/(*IX-14*) mutants, anaphases could be seen in both *not*^{1} and *not*^{2} mutants.

Mitotic index in *invadolysin* and *non-stop* mutants

The mitotic index is the percentage of mitotic cells in a group of cells. This gives an idea about the proliferation of cells in a tissue under growth. Mitotic index was measured for wild type, *invadolysin*/(*IX-14*) and *not*^{1} and *not*^{2} mutants. The mitotic index values for the mutants were much lower than those of wild type. For wild type it was about 1.5% and for *invadolysin* mutants, it was only about 0.5%. For *non-stop* mutants, the mitotic index was a little higher (about 0.7%) but still less than the wild type. This indicates that cell proliferation in *invadolysin* and *non-stop* mutants is defective (Figure 4.7).

Mitotic spindles in *non-stop* larvae

It was known from previous studies that the *invadolysin* neuroblasts contain abnormal spindles such as monopolar or asymmetric spindles. The centrosomes were not separated though the cells were in metaphase (McHugh *et al.*, 2004). I dissected brains from wild type, *invadolysin* and *non-stop* mutants to analyze for spindle shape and formation by using α-tubulin and CP-190, a marker for centrosomes (Whitfield *et al.*, 1995). The *invadolysin* mutants showed abnormal spindles whereas in *non-stop* larvae, spindles looked bipolar as in wild type for majority of the mitotic cells observed (Figure 4.8). The centrosomes were separated

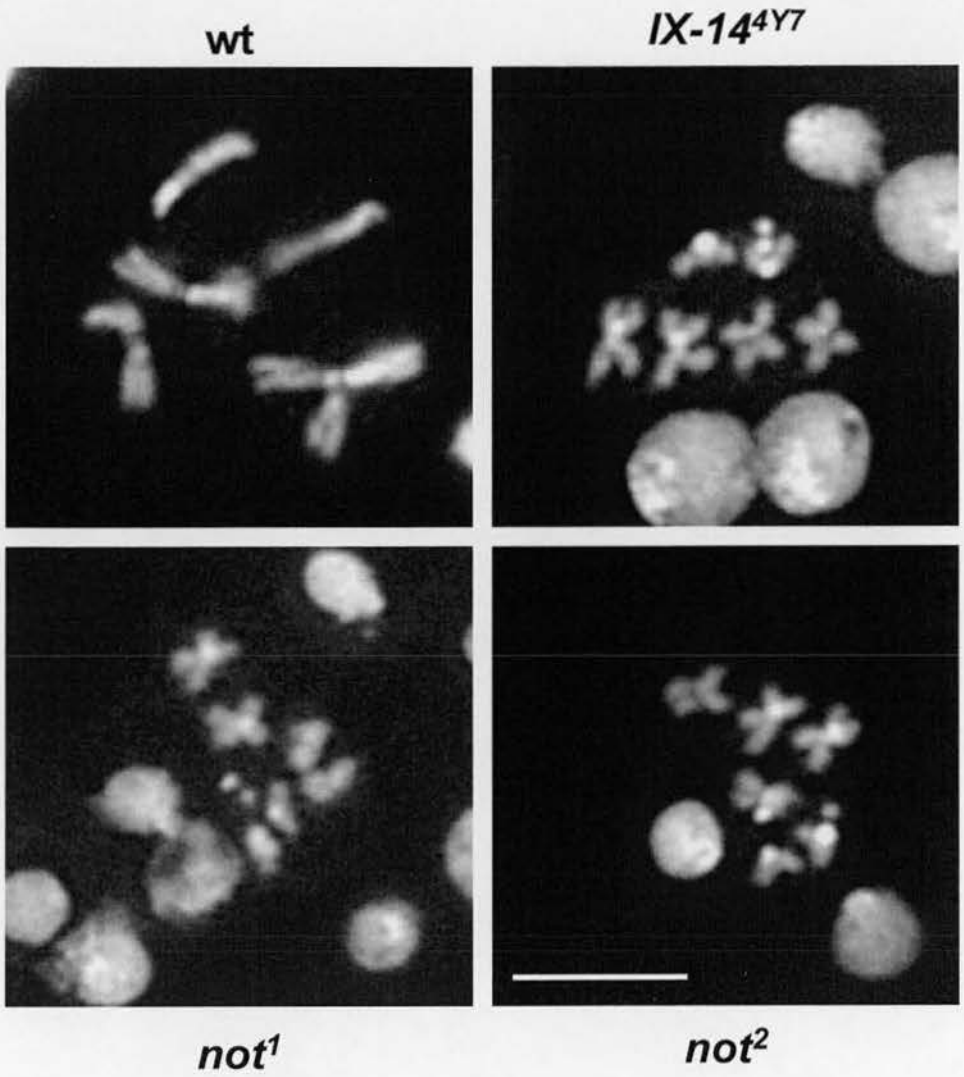

Figure 4.6. *invadolysin* and *non-stop* mutant neuroblast mitotic chromosomes are hypercondensed.
Brains from wild type and mutant (*invadolysin* and *non-stop*) third instar larvae were dissected, fixed and squashed to obtain a monolayer of neuroblasts. The neuroblasts were stained with DAPI and fluorescent images were obtained. Both *invadolysin* and *non-stop* mitotic chromosomes are hypercondensed and fuzzy (scale bar 5 μm).

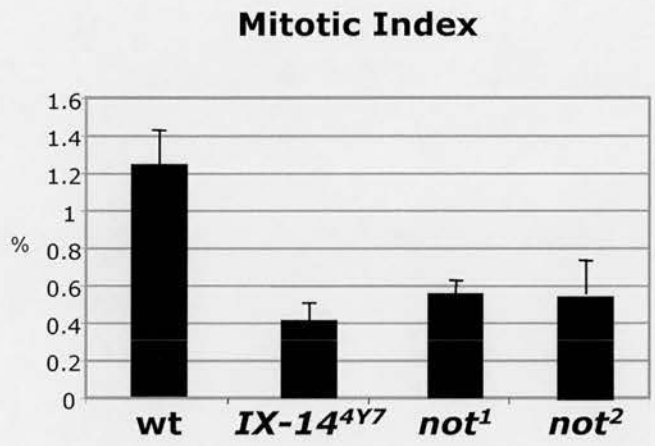

Figure 4.7. Mitotic index is low in *invadolysin* and *non-stop* mutant brains. Brains from wild type and mutant (*invadolysin* and *non-stop*) third instar larvae were dissected, fixed and squashed to obtain a monolayer of neuroblasts. Cells were counted from 10 fields each from 3 brains for all the genotypes and sample standard deviation was calculated. The mitotic index of mutants was lower than wild type, as shown above. This was further confirmed by performing a two-tailed Student's t-test, revealing that not^1 and not^2 were indistinguishable at the 5% significance level, but all mutants ($IX\text{-}14^{4Y7}$, not^1 and not^2 were significantly different from wild type.

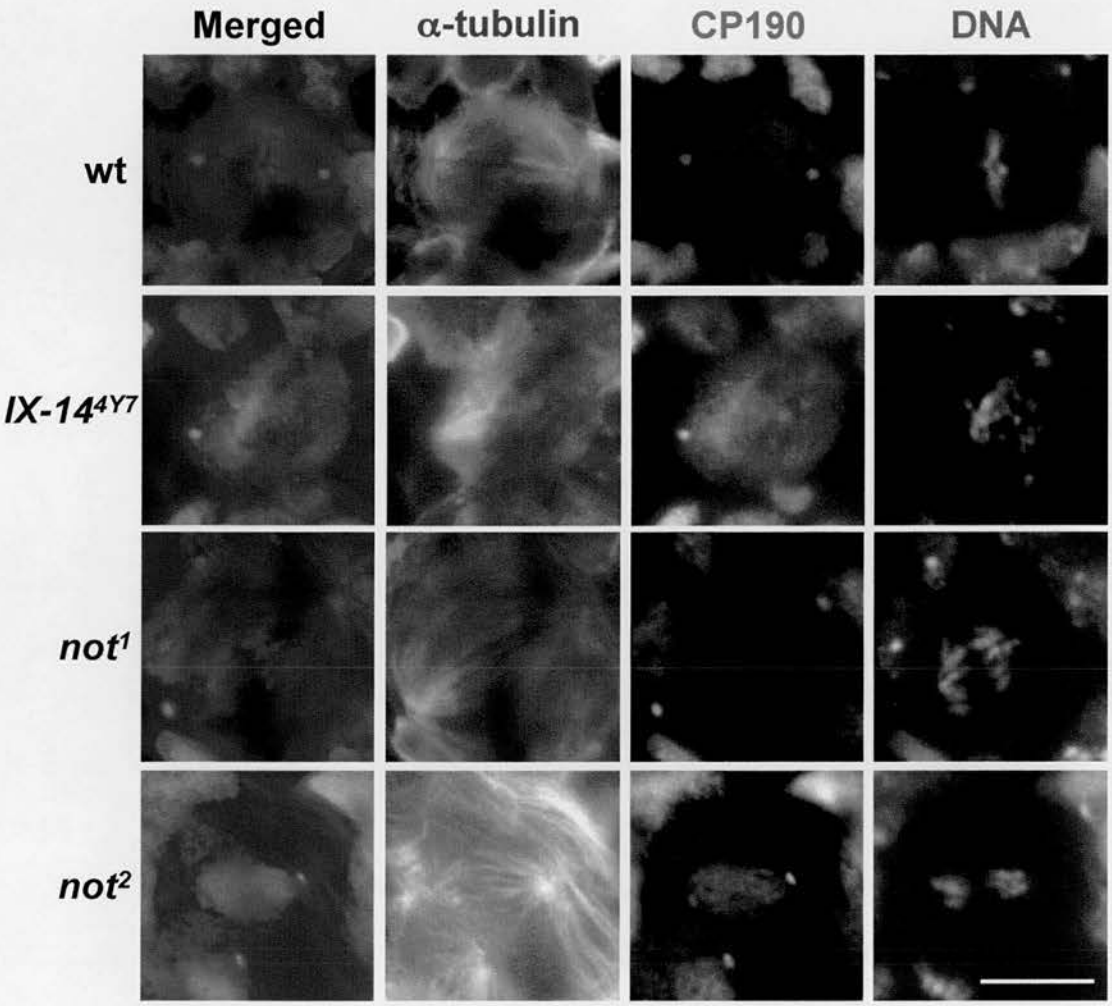

Figure 4.8. Spindle morphology and centrosomes are normal in *non-stop* mutants. Brains from wild type and mutant (*invadolysin* and *non-stop*) third instar larvae were dissected, fixed and squashed to obtain a monolayer of neuroblasts. Neuroblasts were stained with α-tubulin and CP190 antibodies to visualise spindle fibres and centrosomes. The *invadolysin* mutant spindles were abnormal (monopolar, asymmetric) but the *non-stop* spindles were normal compared to wild type (scale bar 10 μm).

and two foci for CP190 could be seen. This suggests that the *non-stop* and *invadolysin* mutants have separable phenotypes. Furthermore, I suggest that the hypercondsensed chromosome phenotype is not associated with spindles, because *non-stop* mutants form normal spindles even in presence of abnormal mitotic chromosomes.

Polytene chromosomes in *non-stop* larvae

Salivary glands of *D. melanogaster* contain huge polytene chromosomes. Polytene chromosomes are giant chromosomes formed by repeated replication of DNA and the fusion of the centromeres of all chromosomes to make a chromocentre. It was reported previously that *invadolysin* mutant salivary gland chromosomes are structurally defective (McHugh *et al.*, 2004). I wanted to examine if the *non-stop* mutants also have a similar defective polytene chromosome architecture. Indeed both not^1 and not^2 mutants had defective polytene chromosomes (Figure 4.9). The banding pattern was lost and chromocentre was not well defined. The chromosome arms seemed loosely arranged and fell apart easily. Consistent with the neuroblast mitotic phenotype, not^1 was not as severe as not^2 allele in this aspect also.

The chromosome structural defects might be related to histone ubiquitination

The yeast homologue of *non-stop*, *ubp8* is has been shown to deubiquitinate histone H2B (Henry *et al.*, 2003). Ubiquitination of H2B is reported to regulate transcription via H3 methylations (Henry *et al.*, 2003; Ng *et al.*, 2002; Sun and Allis, 2002; Turner *et al.*, 2002). I wanted to determine if one or more of

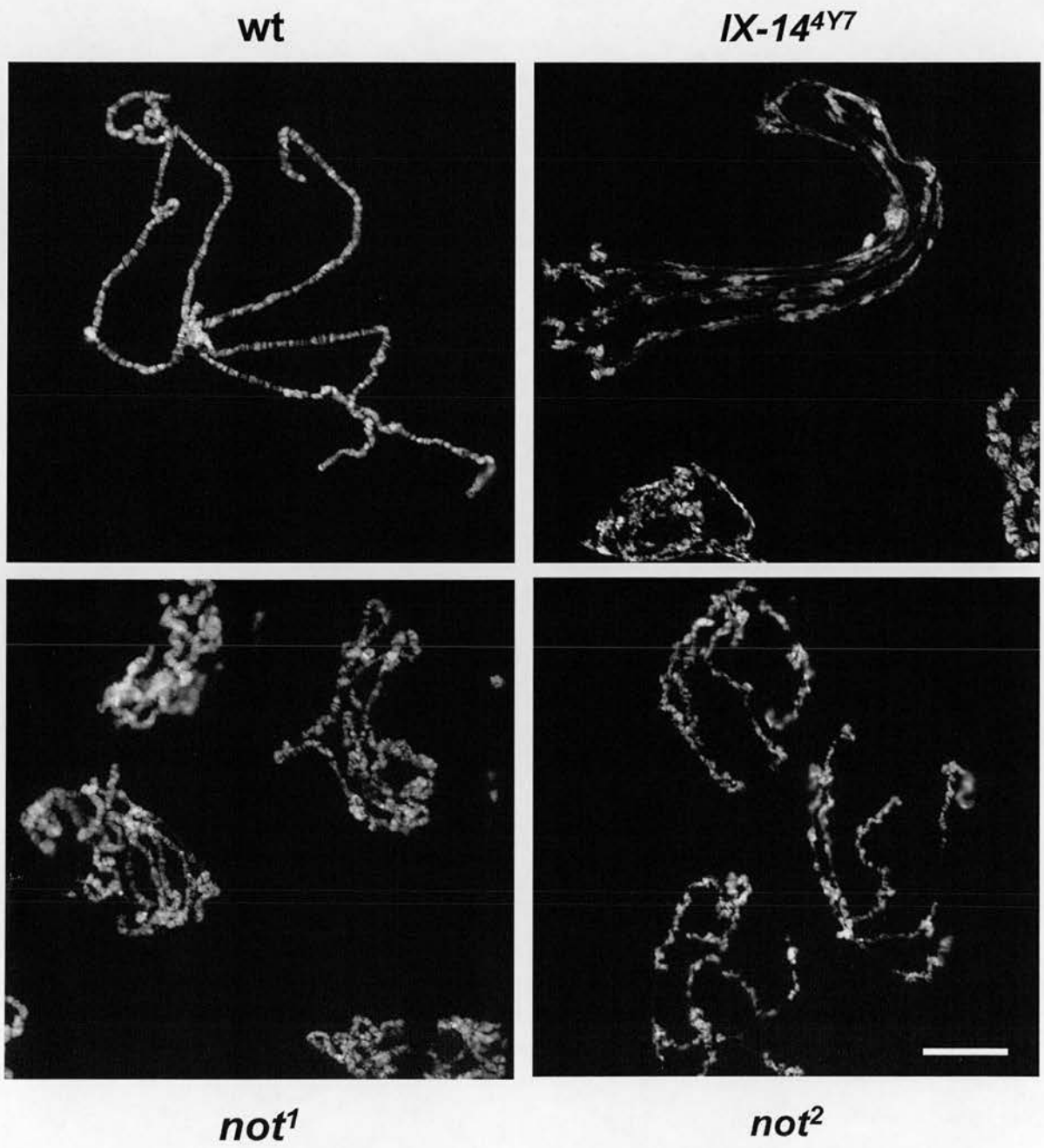

Figure 4.9. *invadolysin* and *non-stop* mutant salivary gland chromosomes are abnormal.

Salivary glands from wild type and mutant third instar larvae were dissected and squashed to release and spread the chromosomes. The chromosomes were stained with DAPI and fluorescent images were obtained. Both *invadolysin* and *non-stop* chromosomes were abnormal and had lost the characteristic banding pattern and obvious chromocentre as compared to wild type (scale bar is 20 μm).

the accumulated proteins in the *non-stop* and *invadolysin* mutants was H2B. When the third instar larval extracts were blotted with H2B antibody, there was a strong band at 55 kDa in *invadolysin* and *not*^{2} mutant extracts but very weakly in the wild type extract (Figure 4.10). The 14 kDa band for unmodified H2B was present in similar levels in both wild type and mutant extracts. This suggested that one of the ubiquitinated bands observed in larval extracts with the ubiquitin antibody might be H2B. H2B is known to be monoubiquitinated in yeast (Henry *et al.*, 2003), but poly ubiquitin chains also may be added depending on the purpose of modification, which might explain the 55 kDa band observed with H2B antibody.

It could be possible that the modified histones, particularly ubiquitinated-histones, are present in very low quantities in cells. Hence, it may be necessary to concentrate histones in order to better examine histone modifications. Histones were extracted by acid extraction method (Bonaldi *et al.*, 2004) and immunoblotted with two different H2B antibodies and the ubiquitin antibody (Sigma). Interestingly, both H2B antibodies recognised similar sized proteins compared to ubiquitin antibody (Figure 4.11). The 29 kDa band was recognised by both ubiquitin antibody and one of the H2B antibodies, and the 55 kDa band was recognised by ubiquitin and the other H2B antibody. However, the level of these modified proteins in the wild type was similar to that of the mutants. Unmodified H2B was used as the loading control. The difference between the levels of H2B originally observed in total larval extracts was not observed with histone extractions. This might be because of the enrichment of histones in a "histone extraction" or the saturation. However, these experiments suggest that one of the ubiquitin bands might represent ubiquitinated H2B.

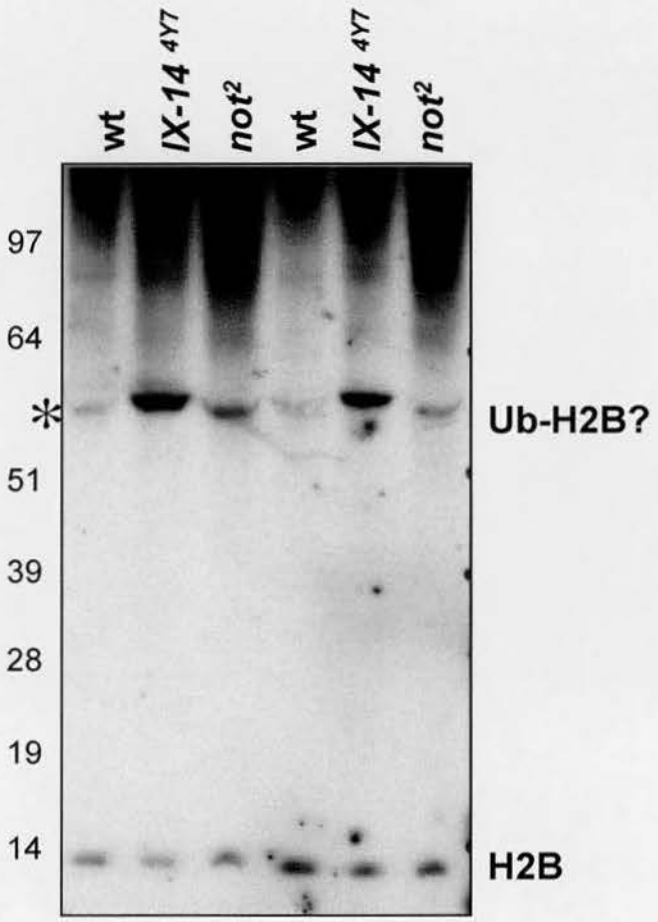

Figure 4.10. The accumulated ubiquitinated protein at 55 kDa might be histone H2B.

Wild type, *invadolysin* and *not*^{2} extracts were probed with anti-H2B antibody. A protein band at 55 kDa was detected in independent extracts (indicated by an asterisk) with greater intensity in the mutant extracts. The band was more intense in *invadolysin* mutants than *non-stop*.

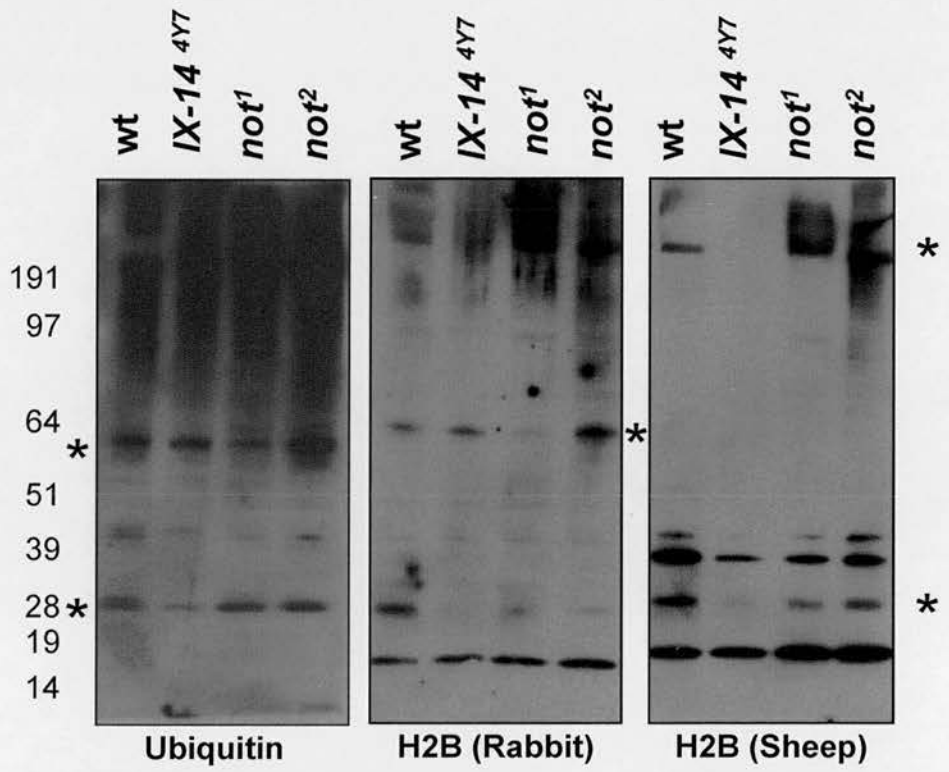

Figure 4.11. Histone extractions show 29, 55 and 200 kDa bands but no difference between wild type and the mutants.

Histones were extracted from wild type, *invadolysin* and *non-stop* mutant larvae and probed with ubiquitin and two histone 2B antibodies (made in Rabbit and Sheep, both abcam). 28, 55 and 200 kDa bands could be detected by both ubiquitin and histone antibodies. No difference in the levels of these bands between wild type and mutants was observed. However, this indicates that accumulated proteins observed in total larval extracts of both *invadolysin* and *non-stop* mutant larvae might be ubiquitinated H2B.

H3K4 methylations in *invadolysin* and *non-stop* mutants

Ubiquitination of H2B is shown to affect transcription by influencing H3K4 (histone H3, lysine 4) methylations, particularly di- and tri-methylations (Ng *et al.*, 2002; Sun and Allis, 2002). Hence, I next wanted to determine if the markers of transcriptional activation, such as specific histone methylations, are affected in the mutant animals. Histone H3 lysine 4 methylations (di- and tri-methylations) are widely used as markers for transcription activation (Schneider *et al.*, 2004). When larval extracts were immunoblotted with antibodies specific for H3K4 di- and tri-methylations, I found that the levels of both H3K4 di- and tri-methylations were higher in the *invadolysin* and *non-stop* mutants (Figure 4.12). The levels of H3 K9/14 acetylation were not affected in the mutants suggesting that only the modifications associated with H2B ubiquitination are affected in the mutants. Thus, upregulation of H3K4 methylations suggests that the level of transcription of certain genes might be upregulated in the mutants compared to the wild type.

Overexpression of H2B ubiquitin ligase Bre1

Since Non-stop (*ubp8*) is a ubiquitin protease and shown to deubiquitinate H2B, there should be a corresponding E3 ligase that ubiquitinates H2B. Invadolysin might be regulating that E3 ligase, considering my previous results showing H2B ubiquitination. Bre1 is the protein known to ubiquitinate H2B in yeast (Hwang *et al.*, 2003). It is also known to regulate Notch signalling by affecting transcription. (Bray *et al.*, 2005). Over expression of Bre1 might be expected to ubiquitinate H2B to higher levels and possibly resulting in chromosome condensation defects

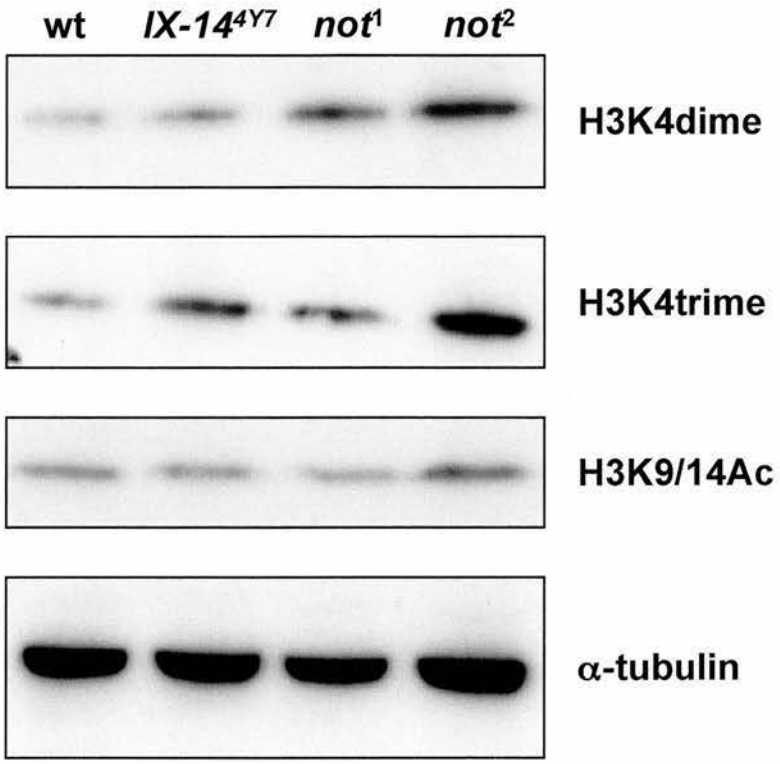

Figure 4.12. The levels of histone H3K4 di-and tri-methylations are higher in *invadolysin* and *non-stop* mutants.
Wild type, *invadolysin* and *not*^{2} extracts were probed with histone H3K4 di- and tri-methylation specific antibodies. The levels of di- and tri- methylation were more in both *invadolysin* and *non-stop* mutants compared to wild type. However, levels of acetylation on H3K9 and H3K14 were similar in wild type and the mutants. α-tubulin was used as a loading control.

phenocopying the defects observed in *invadolysin* or *non-stop* mutants. When *Drosophila* Bre1 was over-expressed ubiquitously (*UAS-Bre1* crossed to actin or tubulin Gal4 drivers), the neuroblast chromosomes were hypercondensed with a very similar appearance with *invadolysin* and *non-stop* mutants (Figure 4.13). This strongly indicated that the hypercondensed, yet fuzzy appearance of chromosomes was a direct or indirect result of the accumulation of ubiquitinated histone H2B.

Model for the role of Invadolysin in chromosome condensation

Based on the above results, the following model for the role of Invadolysin and Non-stop in chromosome condensation can be hypothesised. Invadolysin is either acting through the deubiquitinating enzyme Non-stop or the Ubiquitin ligase Bre1 to regulate chromosome condensation. When a higher level of ubiquitinated histone H2B is accumulated, chromosome structure is affected, which makes them fuzzy and hypercondensed (Figure 4.14). This also might bring about changes in transcription via H3K4 methylations.

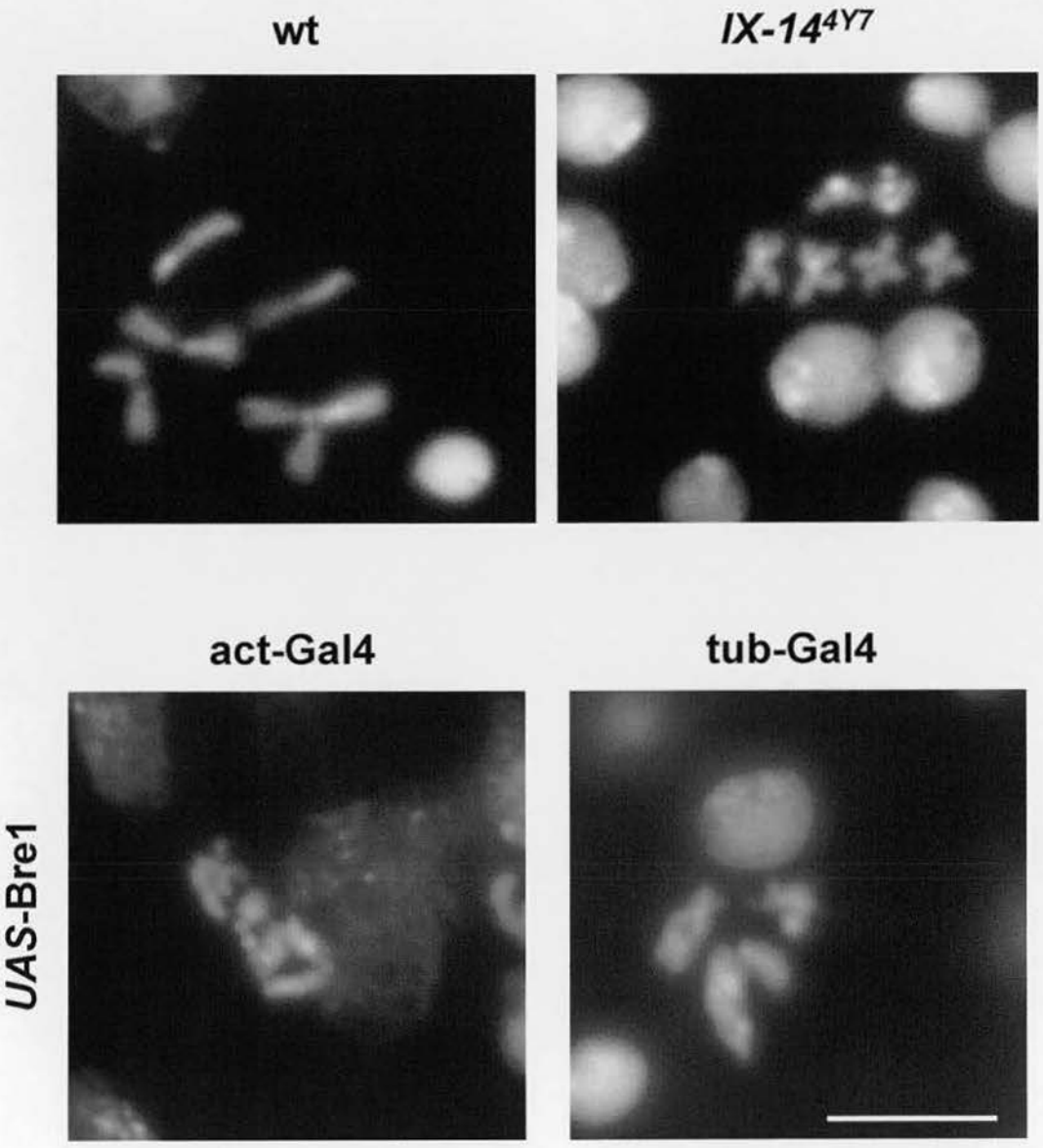

Figure 4.13. Bre1 overexpression causes mitotic chromosome hypercondensation phenotype.
Ubiquitin ligase Bre1 was overexpressed in flies using actin or tubulin Gal4 drivers. The mitotic chromosomes of neuroblasts were hypercondensed and fuzzy when Bre1 was overexpressed (lower panel) similar to *invadolysin* mutants (scale bar 5 μm).

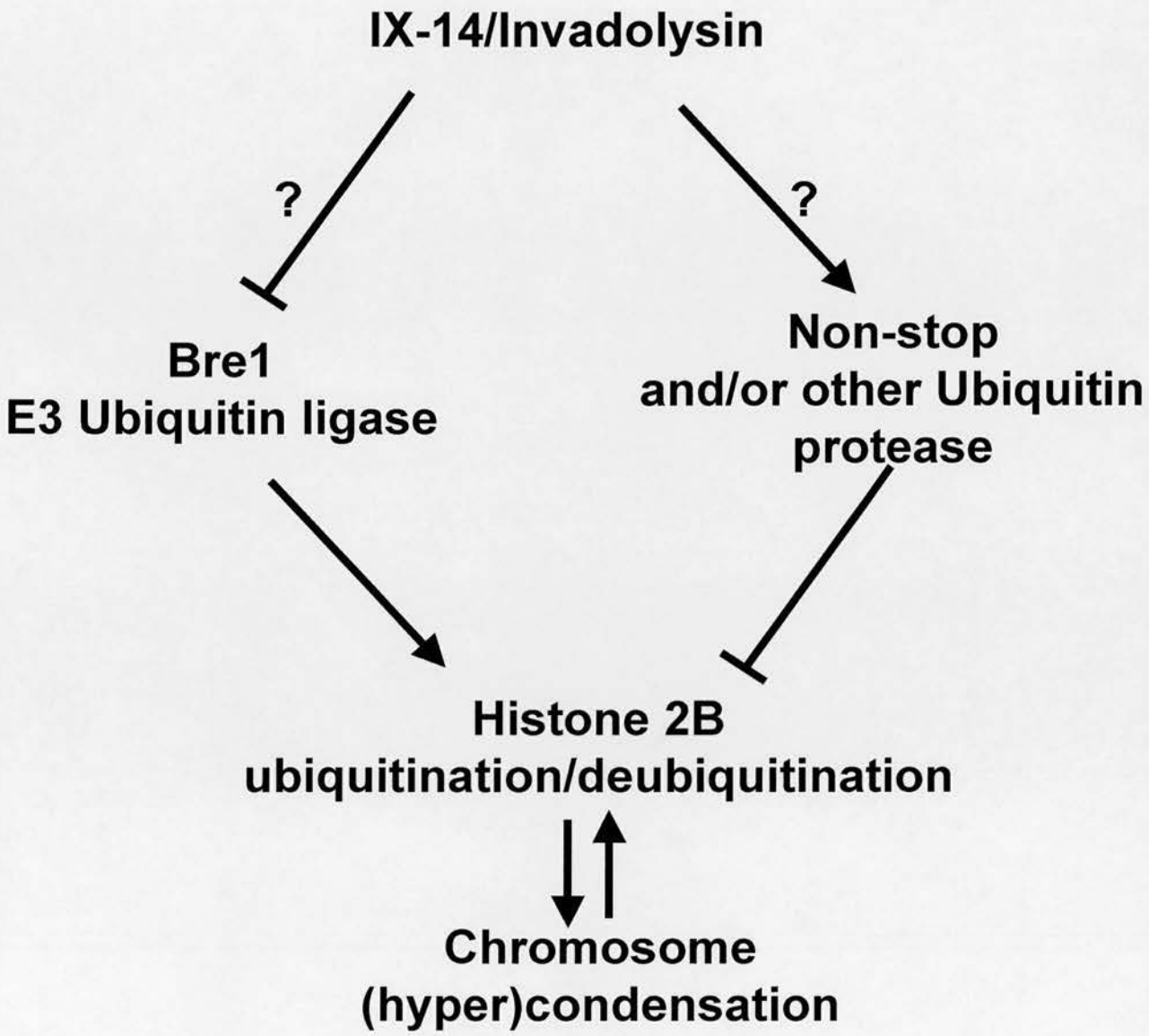

Figure 4.14. Model for the interaction between Invadolysin, Non-stop and Bre1. Invadolysin might be regulating higher order chromosome condensation through histone ubiquitination via ubiquitin ligases and proteases. Invadolysin might be upregulating the ubiquitin protease Non-stop or downregulating the ubiquitin ligase Bre1. Accumulation of ubiquitinated H2B might result in hypercondensed, fuzzy chromosomes.

Chapter 5: Invadolysin and Notch signalling

Introduction

Cell signalling is an important activity for cells allowing them to communicate with each other and respond to internal and external environments. One of the most important and well-known pathways involved in cell signalling is that of Notch signalling. Notch pathway components include the Notch receptor, Delta, Serrate and Scabrous ligands in flies (Delta-like and Jagged in mammals), and a number of regulators of the pathway (Baron, 2003). The main targets of Notch pathway are the Enhancer of Split (E(Spl)) or bHLH genes (Jennings *et al.*, 1994). The Notch pathway operates when the ligand in the signal donor cell binds the Notch receptor generally in the signal receiving cell. The Notch receptor is a transmembrane protein that spans the plasma membrane once to generate an extracellular and an intracellular domain (NECD and NICD respectively). The ligand binds to the NECD triggering the cleavage of the NICD that in turn gets cleaved again and translocates into nucleus, undergoing different levels of regulation depending on the requirements of the cell. In the nucleus, NICD triggers the transcription of its target genes. If the ligand in a cell binds the receptor on the same cell, then the signal is turned off by a phenomenon called *cis*-inactivation or *cis*-inhibition (Baron, 2003; Micchelli *et al.*, 1997).

Considering my previous results (identification of a ubiquitin protease, Non-stop, interacting with *invadolysin*), I expected that Invadolysin might also be part of a signalling cascade as deubiquitinating enzymes are involved in various signal transduction pathways (Wilkinson, 2000). This could well be one of the reasons for

the pleotropic phenotypes observed in the *invadolysin* mutants. The results in the previous chapter (Chapter 4) pointed towards Invadolysin being involved in histone ubiquitination and transcriptional regulation. *Drosophila* Bre1 is one of the players in histone ubiquitination and has also been shown to be a positive regulator of the Notch pathway (Bray *et al.*, 2005). On the other hand, Non-stop interacts with Pros26, a proteasome subunit, both genetically and physically, which is directly involved in Notch signalling (Giot *et al.*, 2003; Poeck *et al.*, 2001; Schweisguth, 1999). Hence I wanted to determine if there are any effects on the Notch pathway in the absence of *invadolysin*.

Levels of NECD and NICD in *invadolysin* mutants

invadolysin mutants have normal levels of NECD

The levels of NECD in *invadolysin* and *non-stop* mutants were analyzed by immnoblotting. A band above 200 kDa for NECD was detected in wild type and mutant extracts. The levels of NECD were comparable to wild type levels in both *invadolysin* and *non-stop* mutants by immunoblotting (Figure 5.1).

invadolysin mutants have reduced levels of NICD

I next examined the levels of NICD by immunoblotting the larval extracts. The levels of NICD were significantly lower in *invadolysin* mutants compared to wild type larval extracts. The not^1 and not^2 mutant alleles showed no significant change in the levels of NICD (Figure 5.2). The antibody to NICD detected a major band around 150 kDa with a few minor Notch derivative bands as described by Ye *et al.* (Ye *et al.*, 1999) in wild type and *non-stop* mutant larval extracts.

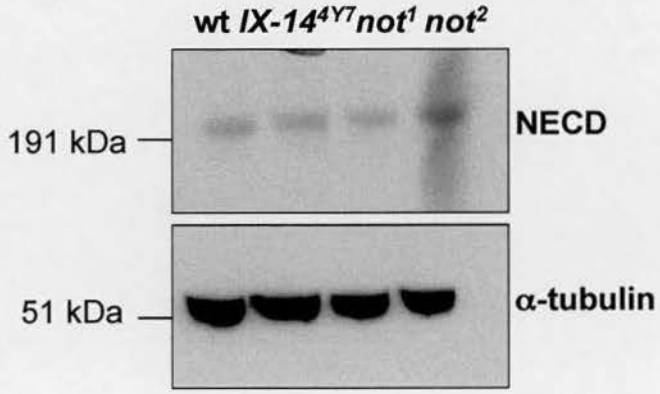

Figure 5.1. NECD levels are not altered in *invadolysin* and *non-stop* mutant larvae.
Extracts of whole third instar larvae (wt, *invadolysin* (*IX-14*^{4Y7}) and *non-stop*) were immunoblotted with NECD antibody. Overall levels of NECD were similar in wild type, *invadolysin* and *non-stop* mutants. α-tubulin was used as a loading control.

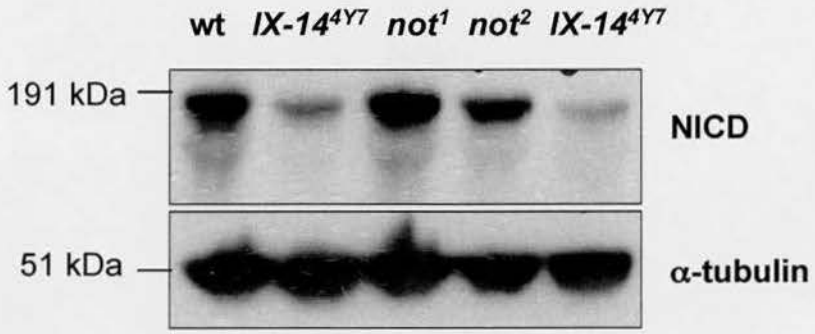

Figure 5.2. NICD levels are lower in *invadolysin* mutants.
Extracts of whole third instar larvae (wt, *invadolysin* (*IX-14*^{4Y7}) and *non-stop*) were immunoblotted with NICD antibody. Overall levels of NICD were reduced in the *invadolysin* mutants (*IX-14*^{4Y7}) but not in *non-stop* mutants. α-tubulin was used as a loading control.

I also examined the levels of the NICD in the wild type and *invadolysin* mutant neuroblasts. The neuroblasts of *invadolysin* mutants were stained for NICD specific antibody and DNA. The levels of NICD were lower in *invadolysin* mutant neuroblasts compared to wild type neuroblasts (Figure 5.3). The levels of NICD were not altered in both not^1 and not^2 mutants possibly represents a separate function of *invadolysin* from *non-stop*, or suggests that *non-stop* is downstream of *invadolysin*.

Other cell cycle mutant such as *kinesin KLP61F* does not show altered levels of NECD or NICD

To ensure that the reduced NICD level in *invadolysin* mutants was not a result of a general cell cycle defect, NICD levels were examined in another cell cycle mutant, *kinesin* (*KLP61F*) with hypercondensed chromosomes (Heck *et al.*, 1993). I observed that the levels of NICD were not reduced in the *KLP61F* mutants and the effect on NICD was thus *invadolysin* specific (Figure 5.4).

NECD and NICD levels remain unaltered throughout early development in wild type animals

To eliminate the possibility that the reduced NICD level in *invadolysin* mutants was due to *invadolysin* larvae being at an earlier developmental stage than wild type animals, protein extracts from wild type embryos, 1^{st}, 2^{nd}, 3^{rd} instar larvae and pupae were probed to detect the levels of NECD and NICD. Interestingly the

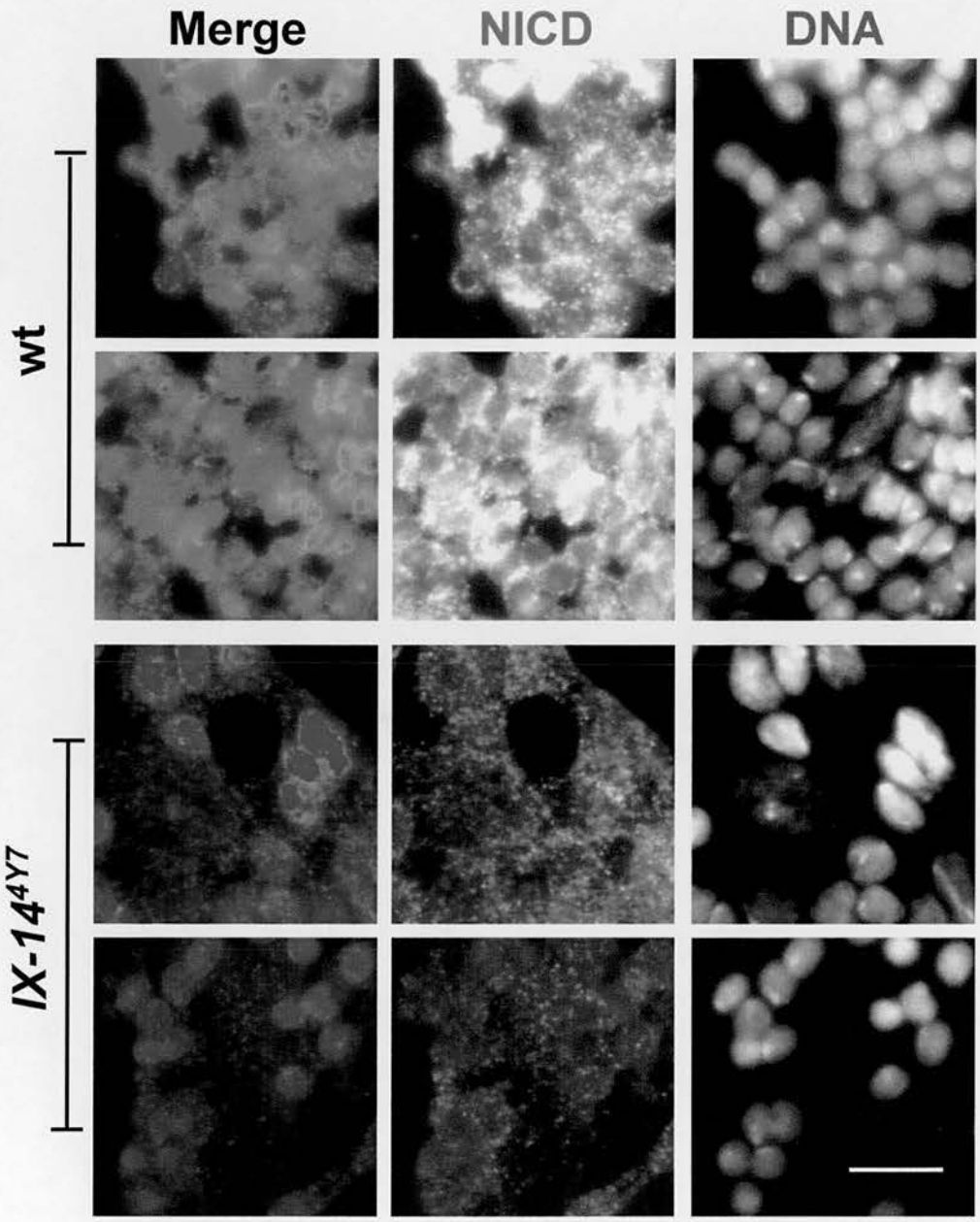

Figure 5.3. NICD levels are lower in *invadolysin* mutant neuroblasts. Neuroblasts of wild type and *invadolysin* mutant (*IX-14*^{4Y7}) third instar larvae were immunostained with NICD antibody (red). Fluorescent images were obtained using the same exposure time. NICD staining was reduced in the *invadolysin* mutants compared to wild type. DAPI was used to stain DNA (scale bar is 10 μm).

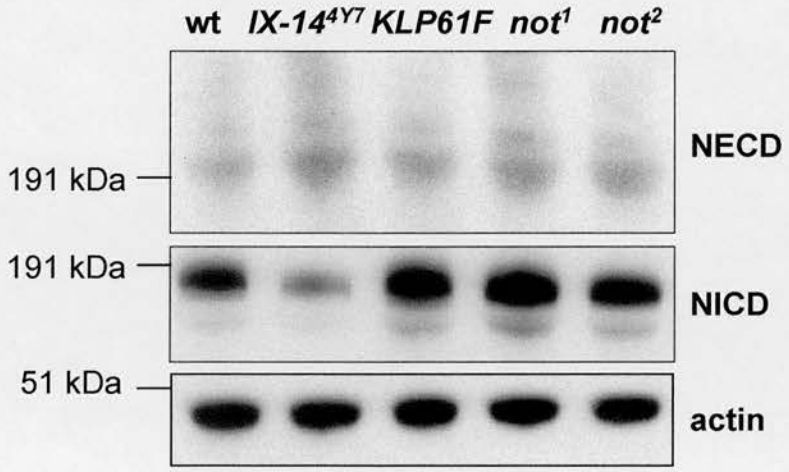

Figure 5.4. NICD levels are not altered in wild type and other cell cycle related mutation *KLP61F*.
Extracts of whole third instar larvae (wt, *invadolysin* (*IX-14*^{4Y7}), *non-stop* and *KLP61F*). were immunoblotted with NECD, NICD and actin antibodies. The levels of NICD were reduced only in the *invadolysin* mutant whereas NECD levels were similar in wild type and mutants tested. Actin was used as a loading control.

levels of both NECD and NICD remained similar throughout development in wild type animals, indicating that the decrease in NICD in *invadolysin* mutants was specifically due to the absence of *invadolysin* (Figure 5.5).

Delta levels are elevated in *invadolysin* mutants

One of the possible explanations for reduction in the level of NICD in *invadolysin* mutants is through *cis*-inactivation by Notch ligand(s). To test this hypothesis, I examined the levels of the Notch ligand Delta in wild type, *invadolysin* and *non-stop* mutants. Interestingly, while it was difficult to detect Delta in wild type and *non-stop* mutant animals, the levels of Delta were considerably increased in *invadolysin* mutant larvae (Figure 5.6). Delta could be detected as 100-200 kDa bands (including its presumed ubiquitinated forms) in the *invadolysin* mutants using a monoclonal antibody. Individual *invadolysin* mutant larvae were also examined to determine if the level of Delta was elevated in every individual. Indeed all the *invadolysin* mutant larvae showed an increase in Delta compared to very low levels of Delta in wild type larvae (Figure 5.7). The levels of Delta were also not elevated in *non-stop* mutants.

Delta transcript levels are not increased in *invadolysin* mutants

Since the protein level of Delta was increased in the *invadolysin* mutants, I wanted to examine if the increase was at the level of transcription or at the level of protein only. The Delta transcript level was detected by RT-PCR (through a range of PCR cycles to avoid saturation of the PCR product), using primers that amplify 190 bp of the Delta transcript. I found that the level of Delta mRNA was very

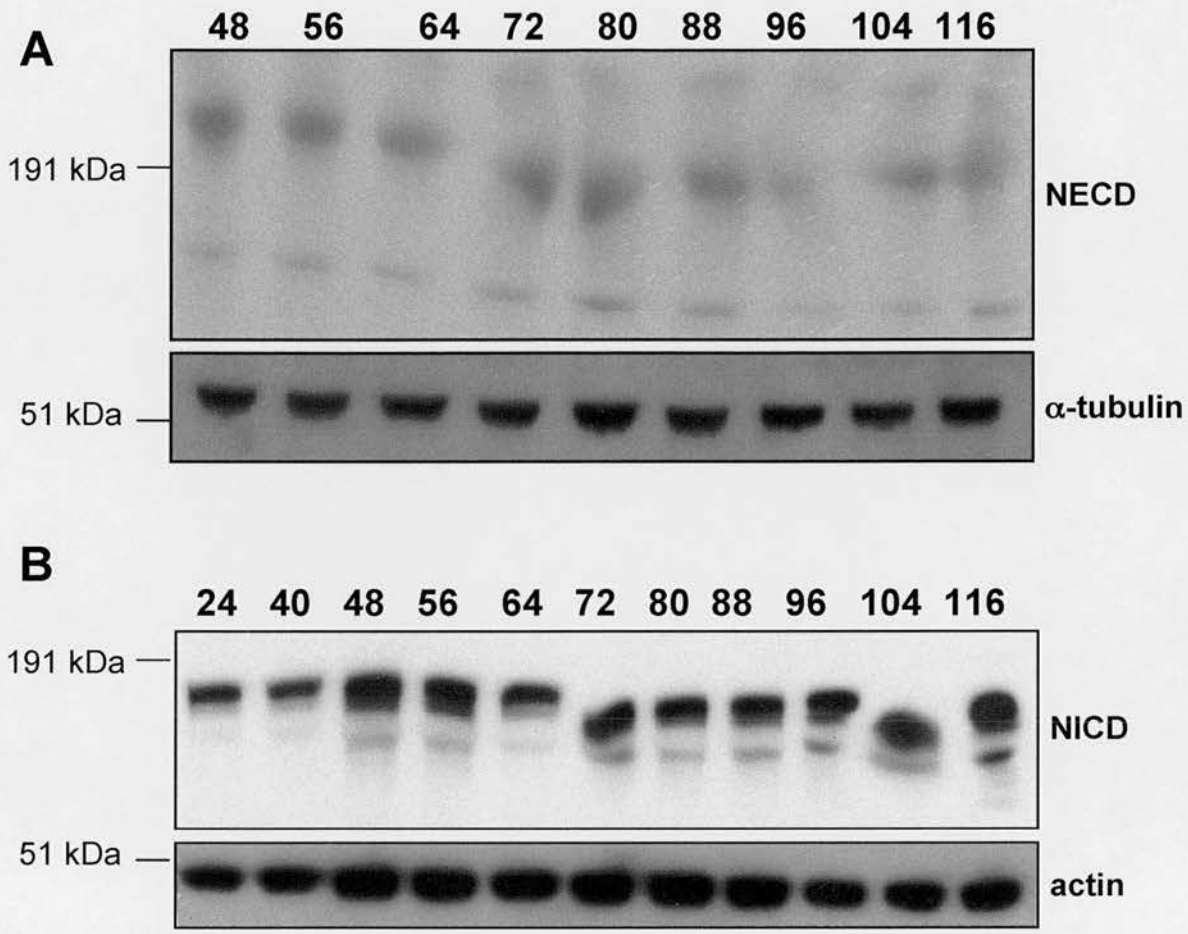

Figure 5.5. NECD and NICD levels do not vary throughout development for wild type larval extracts.

A. Immunoblotting with antibody for NECD in wild type larvae shows that the levels of NECD do not vary through development. Embryo, larvae, pupae were aged for the time indicated (in hrs) and the protein extracts were immunoblotted for NECD. Actin was used as a loading control.

B. Immunoblotting with antibody for NICD in wild type larvae shows that the levels of NICD do not vary through development. Embryo, larvae, pupae were aged for the time indicated (in hrs) and the protein extracts were immunoblotted for NICD. α-tubulin was used as a loading control.

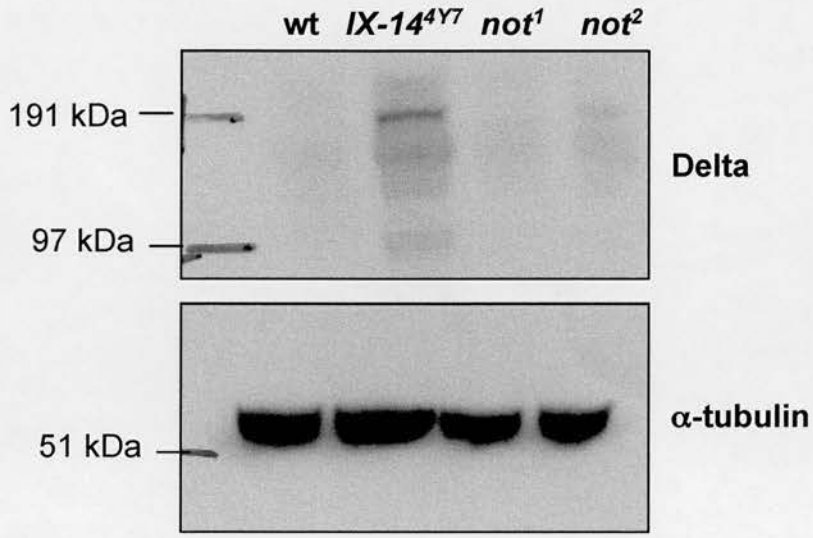

Figure 5.6. The level of Delta is greatly increased in *invadolysin* mutant extracts. Extracts of whole third instar larvae (wt, *invadolysin* (*IX-14*^{4Y7}) and *non-stop*) were immunoblotted for Delta. The overall level of Delta was increased in the *invadolysin* mutants but not in *non-stop* mutants. α-tubulin was used as a loading control.

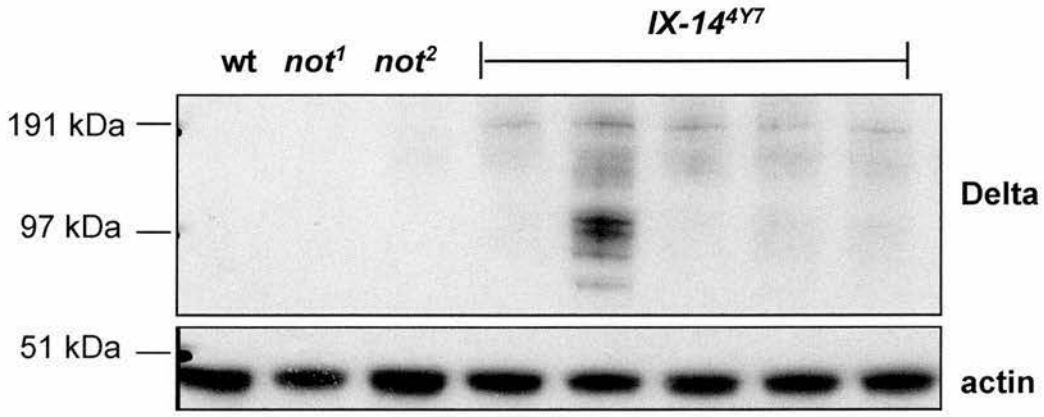

Figure 5.7. The level of Delta is upregulated in numerous individual *invadolysin* mutant larvae.
Extracts of individual third instar larvae (wt, *invadolysin* (*IX-14*^{4Y7}) and *non-stop*) were immunoblotted for Delta. The overall level of Delta was increased in the *invadolysin* mutants but not in *non-stop* mutants. Actin was used as a loading control.

similar to wild type in *invadolysin* mutants as compared to the control gene poly (Figure 5.8) suggesting that the elevated level of Delta in the *invadolysin* mutants was at the protein level and not due to an increase in the transcription of Delta. The levels of Delta mRNA in *non-stop* mutants also appeared to be the same as wild type and *invadolysin* mutants. It can be hypothesised from this result that in *invadolysin* mutants, Delta is not transcribed in excess but is rather stabilized and not degraded or it could be translated in excess. However, it is most likely that the accumulation of Delta could be due to a failure in the endocytosis of Delta and its subsequent degradation, a process in which Invadolysin might be playing a role. Delta protein accumulated at higher levels in *invadolysin* mutants might result in the *cis*-inactivation of Notch signalling.

E(Spl) levels are decreased in *invadolysin* mutant larvae

I also examined the transcript level of the Notch target gene Enhancer of split (E(Spl)) transcript in wild type, *invadolysin* and *non-stop* mutant larvae. E(Spl) transcripts were amplified using gene specific primers that amplify a 245 bp of the product. The level of E(Spl) was decreased only in the *invadolysin* mutants, compared to control gene poly, in consistent with the previous result that NICD was decreased in *invadolysin* mutants (Figure 5.9). A decrease in NICD suggests an inactivation of the Notch pathway itself and thereby a down-regulation of the Notch target genes is expected which might be responsible for the various phenotypes exhibited in the *invadolysin* mutants.

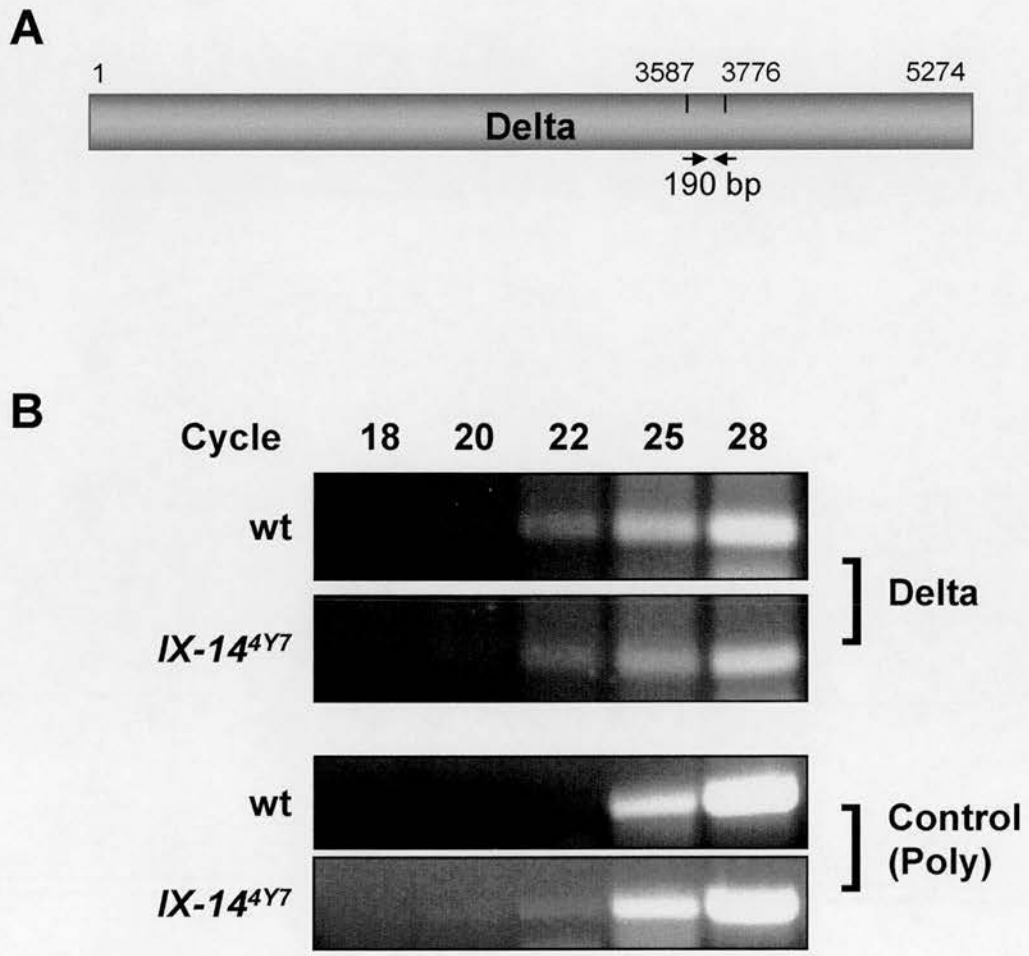

Figure 5.8. The transcript level of Delta is similar to wt in *invadolysin* mutants. Total RNA was extracted from whole wild type and *invadolysin* mutant larvae and RT-PCR was performed with Delta and control (Poly) specific primers. 190 bp of the Delta transcript was amplified as shown in A. RT-PCR was carried out using a range of cycles (18, 20, 22, 25, 28) to avoid saturation of the PCR product. Delta amplified in similar cycles in wild type and *invadolysin* mutants in comparison to control Poly indicating that Delta transcript level in *invadolysin* mutant extracts is similar to wild type level (B).

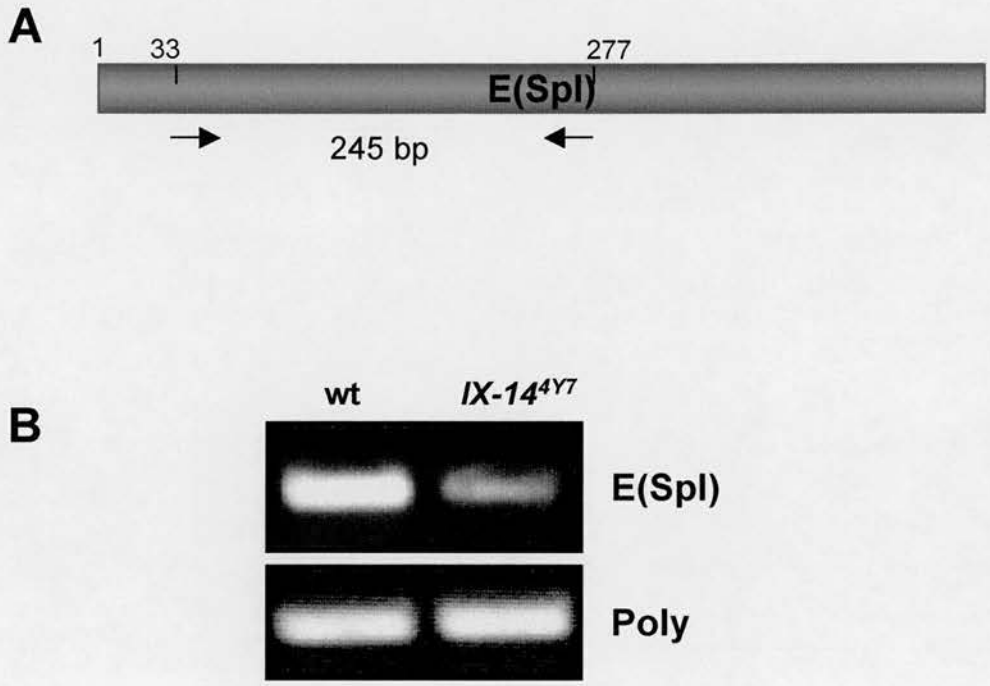

Figure 5.9. The transcript level of E(Spl) is decreased in *invadolysin* mutants.
Total RNA was extracted from whole wild type and *invadolysin* mutant larvae and RT-PCR was performed with E(Spl) and control (Poly) specific primers. 245 bp of the E(Spl) transcript was amplified as shown in A. The results show that the E(Spl) transcript level is decreased in *invadolysin* mutant extracts (B).

Human Invadolysin partially colocalizes with Notch pathway proteins

Invadolysin localized to ring-like structures in transformed human cells (McHugh *et al.*, 2004). I hypothesised that these ring-like structures may be a kind of endocytic vesicles. Several Notch pathway regulators such as Itch and Rab11 localize to endosomes (Angers *et al.*, 2004; Emery *et al.*, 2005). Rab11 regulates the endocytosis of Delta via recycling endosomes (Emery *et al.*, 2005), whereas the *Drosophila* homologue of Itch, Suppressor of deltex (Su(dx)) is a negative regulator of Notch function (Fostier *et al.*, 1998). Experiments in transformed human cells (A375 melanoma cells) suggested that the human Invadolysin partially co-localizes with Rab11 and Itch (Figure 5.10). These results suggested that Invadolysin might be interacting with some of these known Notch pathway proteins and thereby perhaps, in that way, play a role in the Notch pathway.

Interaction map for Invadolysin links Invadolysin to various Notch pathway proteins

Genome-wide yeast two-hybrid screens in *Drosophila* have identified protein-protein interactions (Giot *et al.*, 2003). 27 protein interactors of Invadolysin were identified in such genome-wide two-hybrid screens. An interaction map was drawn for Invadolysin using the Osprey software (http://www.thebiogrid.org/). This program allows the user to draw a network map with the interactors of interactors. The program uses the data from the Biogrid collection and integrates physical interaction data with genetic interactions identified from enhancer and suppressor screens in *Drosophila*. Based on these data, I compiled an interaction map for

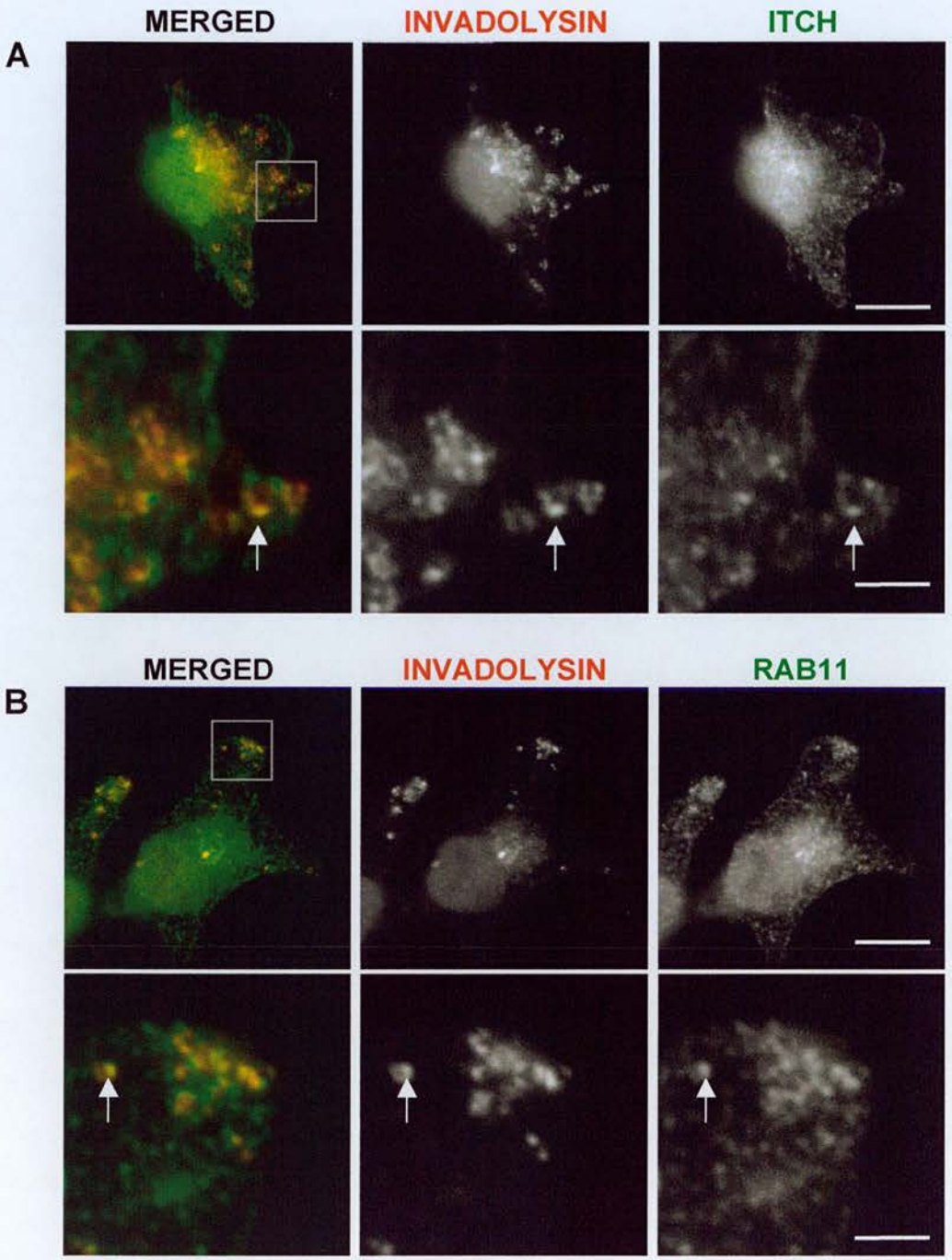

Figure 5.10. Invadolysin partially colocalizes with the Notch pathway proteins Itch and Rab11.

A. A375 cells were stained with Invadolysin (red) and Itch/Su(dx) (green) antibodies.
B. A375 cells were stained with Invadolysin (red) and Rab11 (green) antibodies.
Partial co-localization of Invadolysin can be observed with both Itch and Rab11. The grey boxed areas in the upper panels are enlarged in the lower panels to show colocalization (indicated by arrows). Scale bars are 10 μm in the upper panels and 2 μm in the lower panels.

Invadolysin (shown in Figure 5.11).

The map shows several interactors of Invadolysin and their interactors. Many of the interactors of Invadolysin such as mask, CG8942, CG6565, CG10032, tankyrase, CG10575, pnn, CG13114 (all shown in green) are linked to Notch pathway proteins (shown in black). This suggests that interactors of Invadolysin interact with Notch pathway proteins. For example, CG8942, a yeast two-hybrid interactor of Invadolysin, interacted with the Notch pathway proteins, Numb and Hairless. Another interactor of Invadolysin, mask, linked to Ras85D, which in turn links with Notch and Delta. Interestingly, Pros26, the yeast two-hybrid and genetic interactor of Non-stop, directly interacts with Notch protein itself. Brel also comes into the picture as it interacts with the Notch pathway (Bray *et al.*, 2005), and fur2 (a furin), which link it to Invadolysin indirectly. This interaction map suggests that Invadolysin may have close association with the Notch pathway through multiple nodes or routes.

A Model for Invadolysin in the Notch pathway

Based on the results presented in this chapter, I have shown that *invadolysin* mutants show a reduced level of NICD. *invadolysin* mutants also show a reduced level of transcription for E(Spl), a Notch target gene. *invadolysin* mutants show an increase in the level of the Notch ligand Delta protein but not at its mRNA. The reduced levels of Notch signalling in the *invadolysin* mutants could be attributed to the *cis*-inactivation of the signal by the presence of greater amounts of Delta. I propose that, in *invadolysin* mutants, Delta ligand is binding to the Notch receptor of

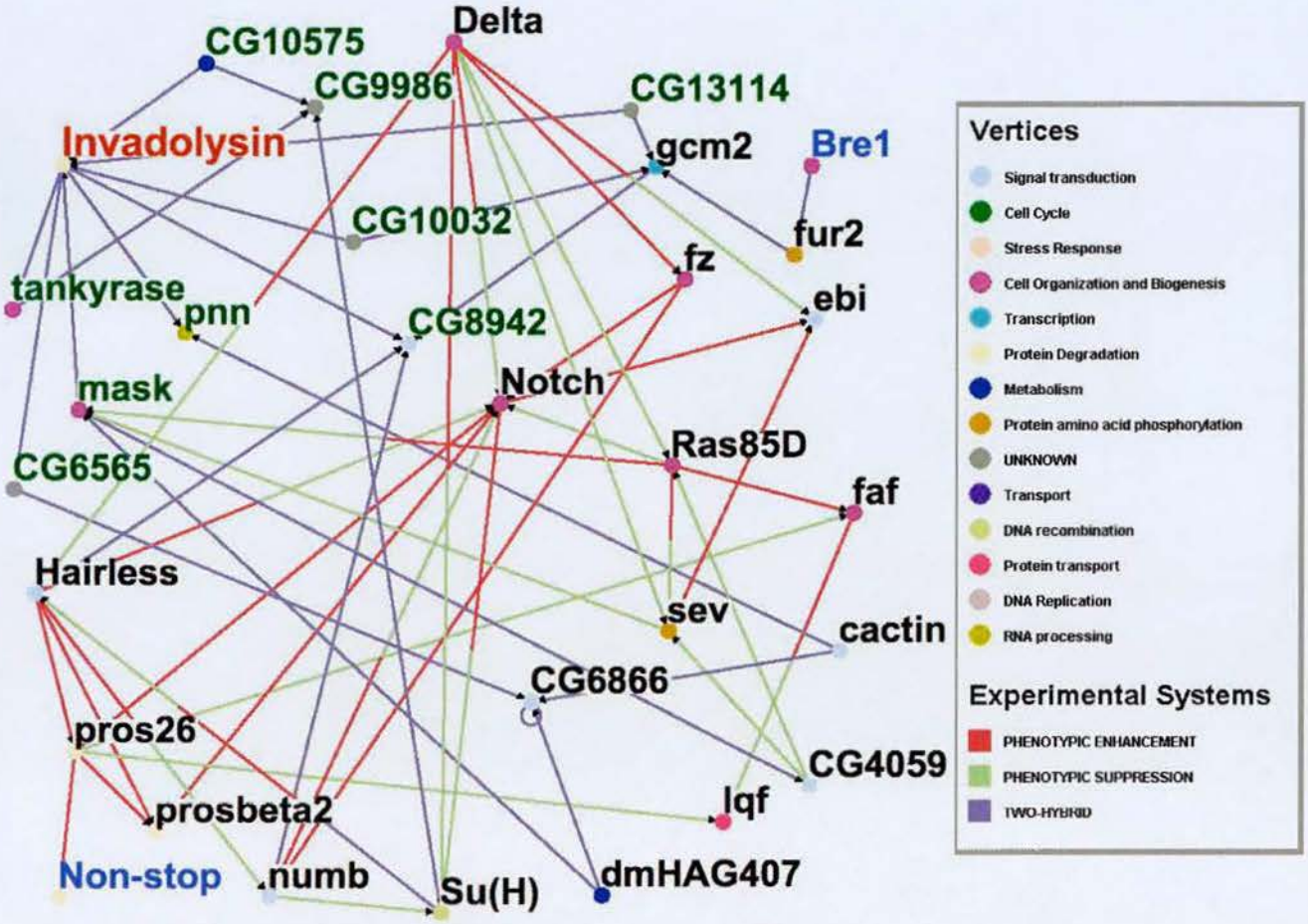

Figure 5.11. Osprey interaction map for Invadolysin and its interactors.
The Osprey interaction map shows that Invadolysin links to a number of the Notch pathway components through more than one link. Invadolysin is shown in red and its interactors are shown in green. The Notch pathway components are shown in black and Bre1 and Non-stop are shown in blue.

the same cell and bringing about *cis*-inactivation of the signal.

These results suggest that Invadolysin might be regulating the level or activity of Delta. This might be through inhibiting *cis*-inactivation by reducing the levels of Delta. Delta is normally endocytosed at the cell membrane and sorted in cellular compartments such as endosomes. It is then either degraded or recycled based on the requirements of the cell. Invadolysin might be regulating the endocytosis of Delta or the degradation of Delta in cellular compartments. This could also be through regulating the ubiquitin ligases Mind bomb and/or Neuralised which are important for Delta endocytosis (Le Borgne and Schweisguth, 2003). Localisation of Invadolysin with Rab11 supports the hypothesis that Invadolysin is involved in regulating the endocytosis of Delta. Delta endocytosis is important in Notch signal transduction (Chitnis, 2006).

A role for Invadolysin in vesicle trafficking or endocytosis remains to be deciphered. The antibodies for *Drosophila* Invadolysin are not available to be used this purpose. However, the hypothesis could be tested in human cells using the available human Invadolysin antibodies, and by knocking-down Invadolysin using siRNA. A direct role for Invadolysin in the Notch pathway is yet to be established. However, as shown in the model (Figure 5.12), I suggest that Invadolysin may promote Delta endocytosis. In absence of Invadolysin, *cis*-inactivation or *cis*-inhibition might occur due to accumulated Delta.

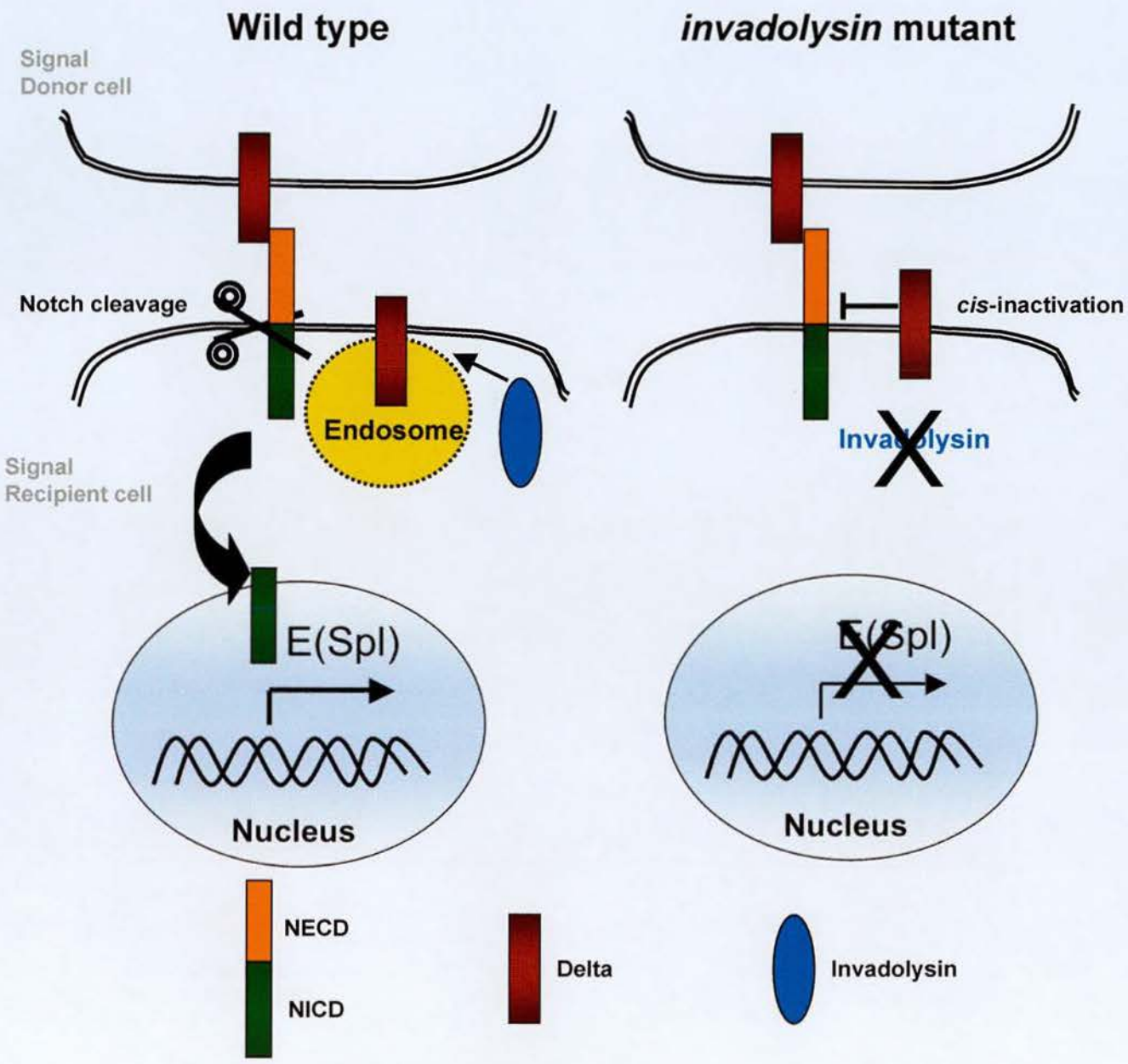

Figure 5.12. Model for Invadolysin in the Notch pathway.
According to the results presented in this chapter, Invadolysin is likely to be playing a role in the endocytosis of Delta directly or indirectly. In a wild-type situation, Delta in the signal donor cell binds the Notch receptor in the signal recipient cell which results in the cleavage of NICD from NECD. NICD translocates to the nucleus to bring about the transcription of its target gene E(Spl). Invadolysin might be triggering the endocytosis of Delta in the signal receiving cell to antagonize *cis*-inactivation, which occurs when Delta in the signal recipient cell binds the receptor on the same cell.
In the *invadolysin* mutants, Delta in the signal recipient cell accumulates and binds to the Notch receptor on the same cell bringing about *cis*-inactivation of the Notch signal, blocking the transcription of E(Spl).

Chapter 6: Characterization of human Invadolysin "ring-like" structures observed in human cultured cells

Introduction

Cytoplasmic "ring-like" structures were observed in cultured human cells with an antibody raised against the C-terminal half of human Invadolysin (McHugh *et al.*, 2004). GFP-, SBP- or HA-tagged constructs of human Invadolysin also resulted in similar localization patterns in human cells suggesting that tagged form of Invadolysin can also localize to similar structures (Heck lab, unpublished). These ring-like structures showed no significant colocalization with any of the organelle markers previously tested, such as proteasomes, signalosomes, Golgi, mitochondria or lysosomes. They appeared similar in appearance to invadopodia, found in many transformed cells and are important for extracellular matrix degradation (Baldassarre *et al.*, 2003; Buccione *et al.*, 2004). Invadopodia measure about 1 μm in diameter, which was similar to the measurements of the rings observed with the Invadolysin antibody. However, further functional experiments in the Heck laboratory suggested that the ring-like structures might not be invadopodia (Kathryn Marshall, personal communication). Invadolysin did not colocalize with cortactin (protein known to be enriched in invadopodia) and did not localize to the foci of matrix degradation. However, experiments carried out in *Drosophila* (described in the previous chapters, Chapters 4 and 5) suggested that Invadolysin might be a component of a vesicular pathway regulating endocytosis or receptor trafficking.

It was therefore important to determine the location of the protein in order to understand its function. To determine what the ring-like structures were, several co-localization studies were performed using cultured human cells. As described in chapter 5, the *Drosophila* Invadolysin is involved in the Notch pathway, possibly in regulating Delta endocytosis. I wanted to investigate in greater detail whether the Invadolysin ring-like structures are components of some endocytic machinery or receptor trafficking.

Invadolysin localizes to cytoplasmic ring-like structures

A375 cells (human melanoma) were fixed and stained for Invadolysin (antibody R1318, 1st bleed). The antibody distinctly stained ring-like structures in the cytoplasm (Figure 6.1). The antibody also stained the nucleus, but this was also observed with the pre-immune serum. When the antibody was affinity purified, the ring-like structures became more apparent. The nuclear staining was also removed when the antibody was purified (Francesca Di Cara, personal communication). Hence only the ring-like localization was considered as specific for the Invadolysin protein.

Ring-like structures were not found in all the cells all the time, suggesting that these are physiologically-active, dynamic organelles. The number of the rings varied greatly from cell to cell in A375 cells (and all the other cell lines tested so far), but the average size was around 1 μm for most of majority of the rings.

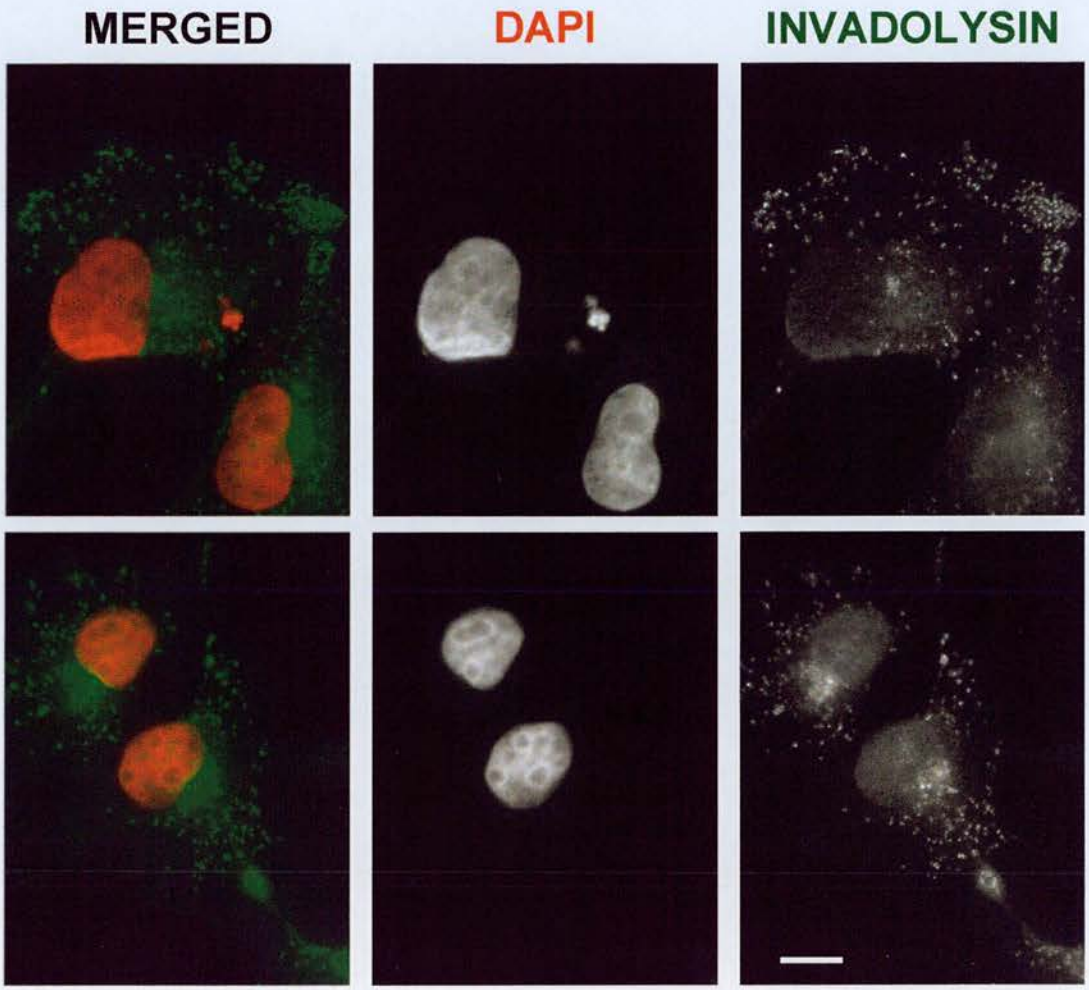

Figure 6.1. Localization of Invadolysin in A375 melanoma cells. A375 cells were stained with Invadolysin antibody (green) and DAPI to label DNA (red). Invadolysin localizes to distinct ring-like structures in the cytoplasm (scale bar is 10 μm).

Clathrin does not colocalize with Invadolysin rings

Since a role for Invadolysin in Delta endocytosis was suggested (Chapter 5), I examined if clathrin-coated endocytic pits colocalize with Invadolysin rings. A375 cells were co-stained for Clathrin and Invadolysin (Figure 6.2). I did not observe any colocalization between the two proteins, which suggests that Invadolysin rings are not Clathrin coated pits.

Dynamin 1 does not colocalize with Invadolysin rings

Dynamin is a protein involved in cell migration as well as mitosis (Konopka *et al.*, 2006; Kruchten and McNiven, 2006). An isoform of Dynamin, Dynamin 2 has been shown to be a component of invadopodia (Baldassarre *et al.*, 2003). Dynamin is also a component of the both clathrin and non-clathrin mediated endocytic machinery and plays an important role in the endocytosis of the Notch ligand Delta (Seugnet *et al.*, 1997). Experiments to determine if Dynamin 1 colocalized with Invadolysin rings were performed. However the proteins did not colocalize when A375 cells were co-stained for the two proteins (Figure 6.3).

Invadolysin rings are not involved in clathrin-mediated endocytosis

Cells uptake transferrin is via clathrin-mediated endocytosis (Dautry-Varsat, 1986). To confirm whether or not Invadolysin rings are involved in any kind of clathrin-mediated endocytosis, an endocytosis assay was carried out. A375 cells were serum starved for 30 min to treat with fluorescent transferrin in full medium for 10 minutes. Cells were then fixed and labelled for Invadolysin. Transferrin uptake

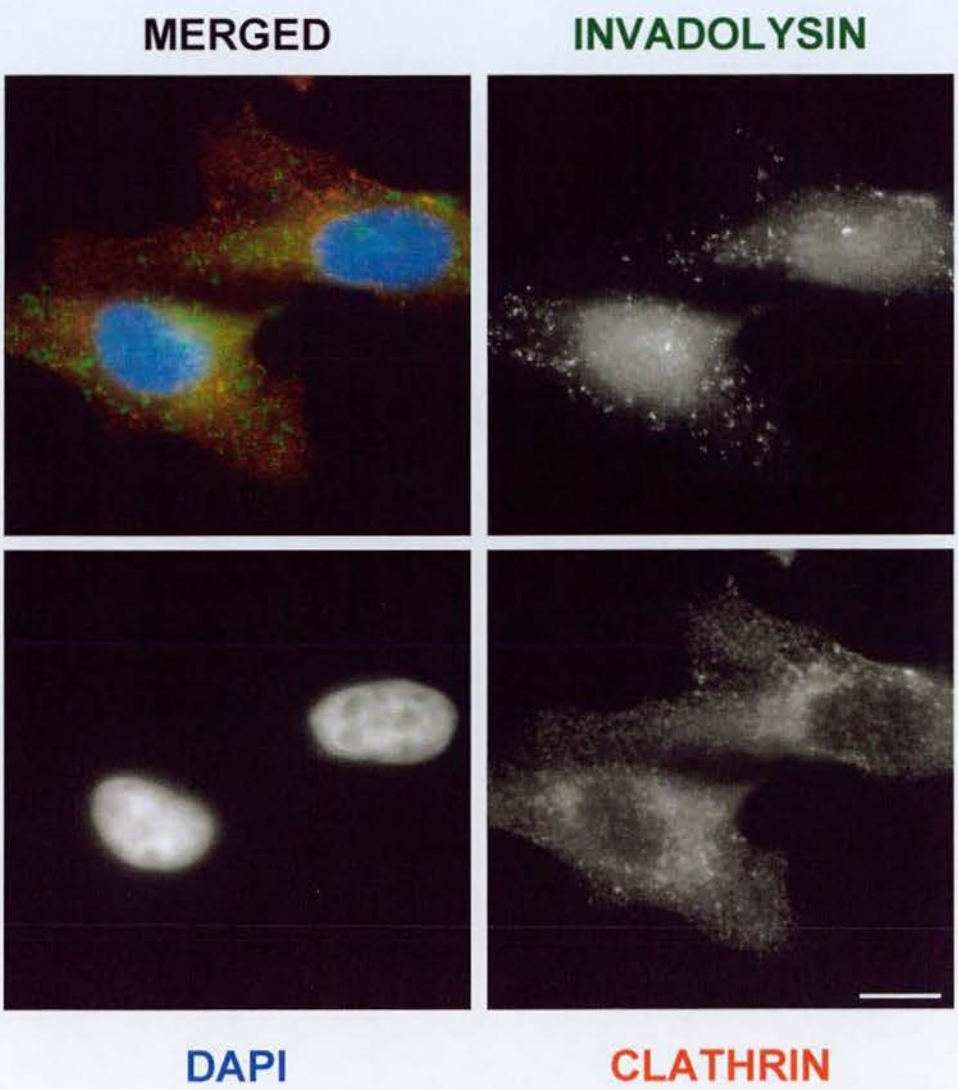

Figure 6.2. Invadolysin rings do not colocalize with Clathrin.
A375 cells were stained with Invadolysin (green) and Clathrin (red) antibodies, and DAPI (blue). Invadolysin rings do not colocalize with Clathrin spots (scale bar is 10 μm).

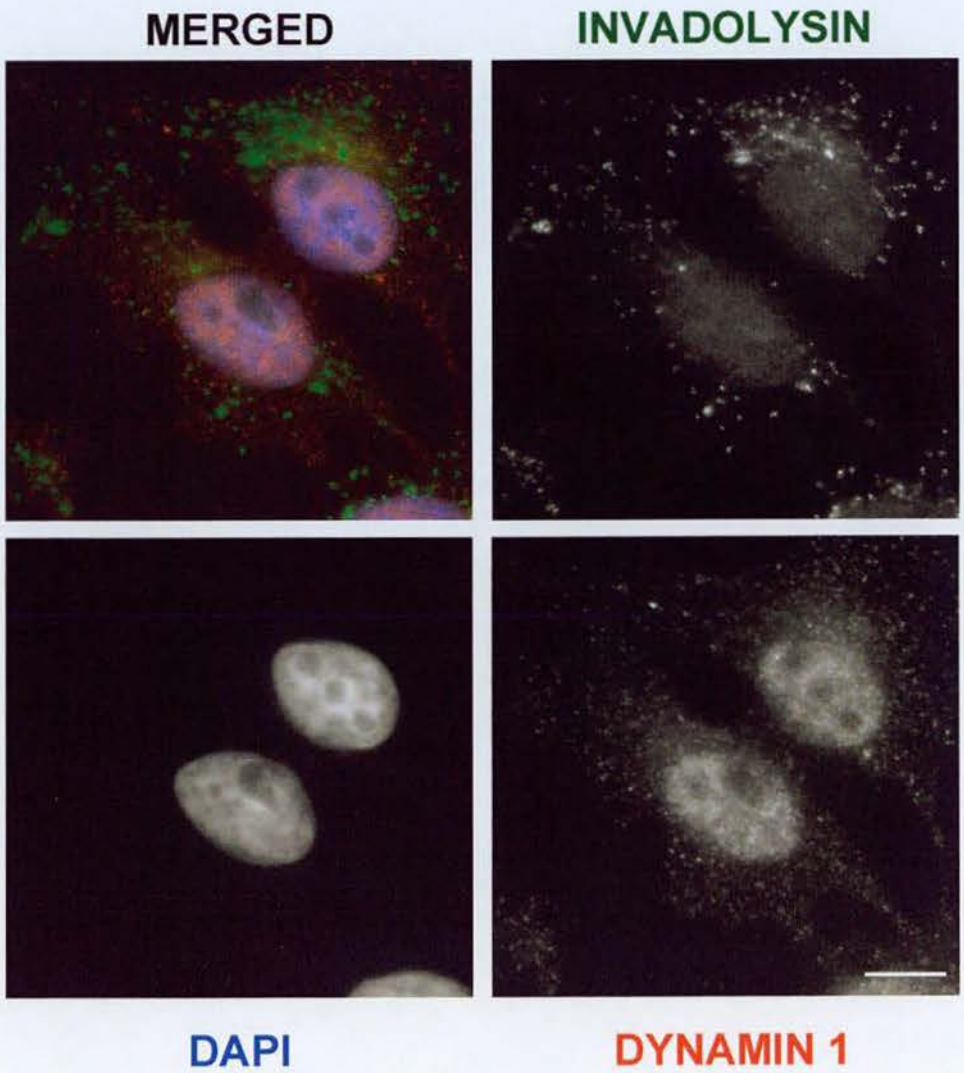

Figure 6.3. Invadolysin rings do not colocalize with Dynamin 1.
A375 cells were stained with Invadolysin (green) and Dynamin 1 (red) antibodies, and DAPI (blue). Invadolysin rings do not colocalize with Dynamin 1 (scale bar is 10 μm).

(though apparent) by the cells was not found inside the Invadolysin rings (Figure 6.4). This further dismissed the possibility of Invadolysin rings being related to clathrin-mediated endocytosis.

Cholera toxin-B localizes inside the Invadolysin rings

Fluorescently labelled cholera toxin-B (CTxB) is widely used to study non-clathrin mediated endocytosis, particularly caveolar endocytosis (Montesano *et al.*, 1982). CTxB binds GM1 gangleosides and is taken into cells mainly by caveolae-mediated endocytosis. A375 cells were serum starved and treated with CTxB in full medium for 10 minutes to determine if Invadolysin rings are related to caveolar endocytosis. Cells were then fixed and labelled with Invadolysin antibodies. CTxB was present outside the rings but it seemed to accumulate to a higher level inside the Invadolysin rings. It was notable that CTxB appeared inside most of the Invadolysin rings (Figure 6.5). This suggested that the inner volume of the rings might be a lipid based entity. This also suggested that CTxB had an affinity for some kind of lipids present in the Invadolysin rings or the Invadolysin rings are involved in the uptake of CTxB from the cell membrane as a part of caveolar endocytosis.

Caveolin-1 decorates Invadolysin rings

The endocytosis assay with CTxB suggested that at least some of Invadolysin may be associated with caveolae. Caveolae are plasma membrane domains involved in exo-and endo-cytosis, and in lipid regulation (Parton and Simons, 2007). Hence co-localization studies were performed in A375 cells with Caveolin 1 (Cav-1), a

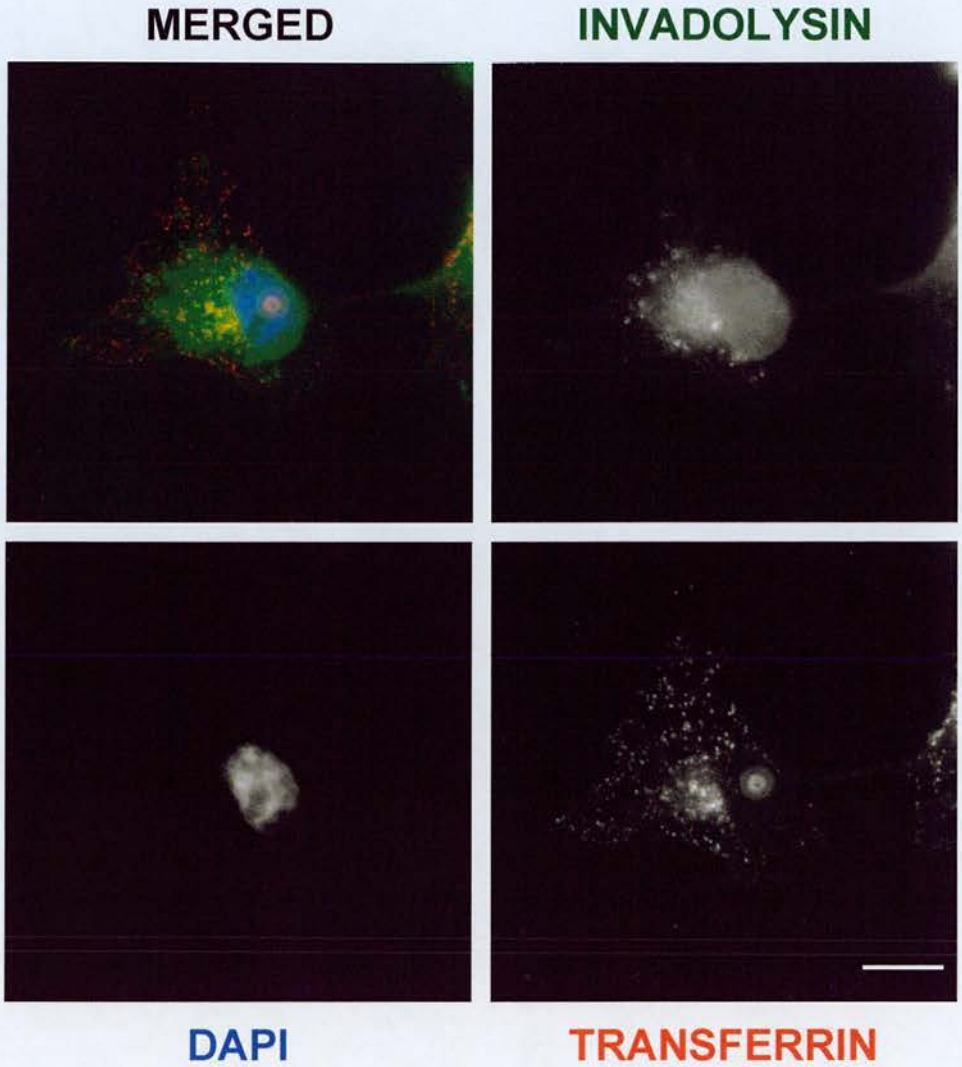

Figure 6.4. Transferrin does not localize with Invadolysin rings.
A375 cells were treated with fluorescent transferrin (red) and stained with Invadolysin antibody (green) and DAPI (blue). Invadolysin rings do not appear to contain transferrin (scale bar is 10 μm).

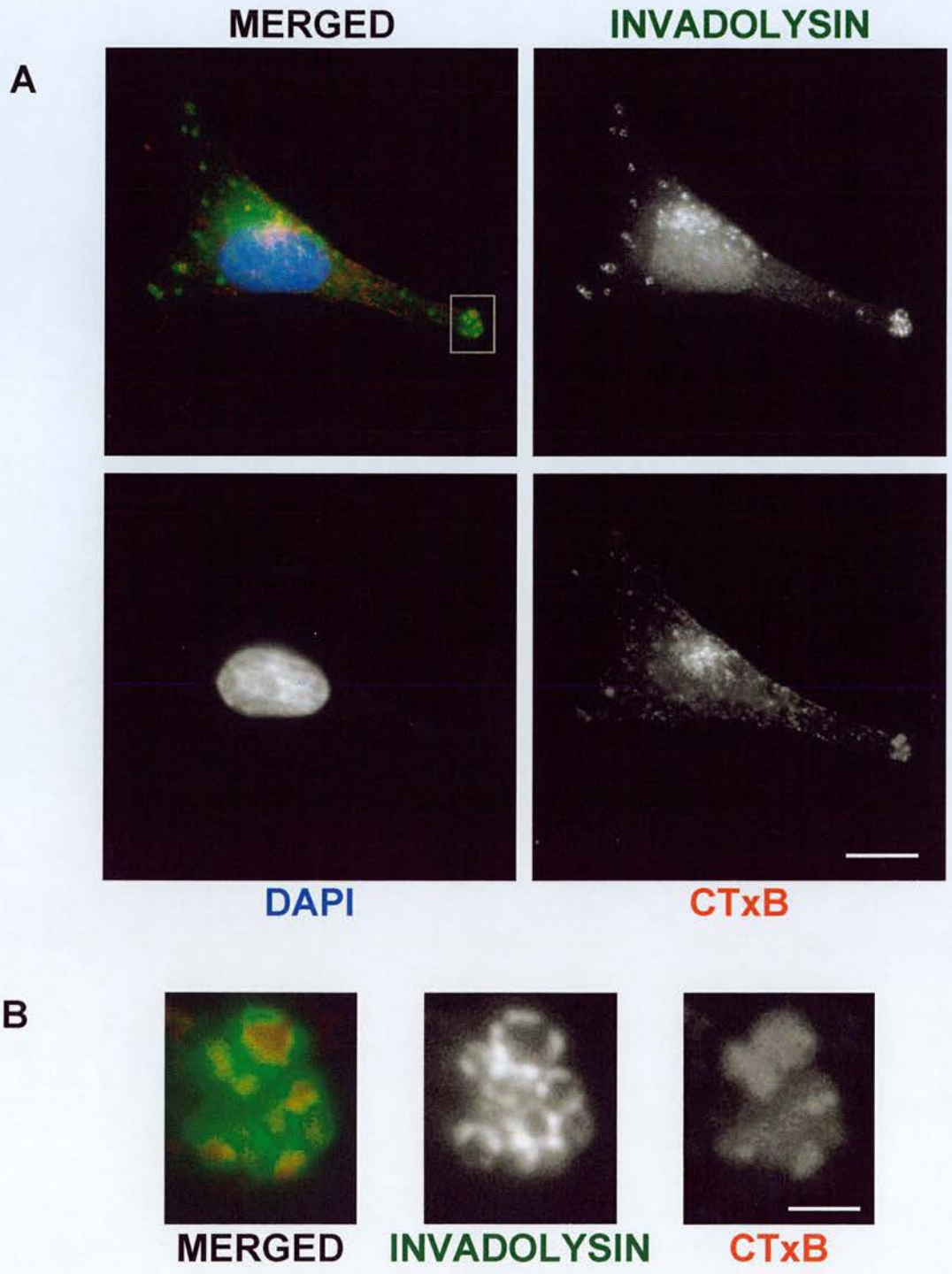

Figure 6.5. Cholera toxin B can be found inside Invadolysin rings.
A. A375 cells were treated with fluorescent cholera toxin B (CTxB, red), and stained for Invadolysin antibody (green) and DAPI (blue). Invadolysin rings appeared to contain CTxB (scale bar is 10 μm).
B. The grey boxed area in A is enlarged to show the rings and the CTxB inside them (scale bar is 2 μm).

component of caveolae. Caveolin-1 appeared to decorate the Invadolysin rings (Figure 6.6). Caveolin-1 is known to be an integral component of caveolae, which are small, 50-70 nm structures. However, caveolin-1 also associates with lipid droplets (Robenek *et al.*, 2004), and is enriched upon brefeldin A treatment (Ostermeyer *et al.*, 2004) or mutant caveolin transfection (Pol *et al.*, 2001). These experiments indicated that the Invadolysin rings were possibly lipid-associated structures such as lipid droplets.

Oleic acid manipulation of lipid droplets

Oleic acid is a mono un-saturated omega-9 fatty acid found in various vegetable and animal sources. When cells are treated with oleic acid, they take it in and store it in lipid droplets, which grow in size. To test the hypothesis that Invadolysin might be on lipid based organelle lipid droplets, cells were treated with oleic acid. Cells were plated on coverslips and treated with 0, 100, 400 or 600 μM oleic acid (coupled to BSA) for 21 hours. Oleic acid was added to the normal growth medium of the cells (DMEM with 10% foetal bovine serum). After treatment, cells were fixed and stained with Invadolysin antibodies. Invadolysin rings were of normal size (1 μm) in the cells treated with no or 100 μM oleic acid. However in cells treated with 400 or 600 μM oleic acid, the rings had roughly doubled in size (about 2-3 μm) (Figure 6.7). Rings also appeared in clusters, many accumulated at the periphery of the nucleus (possibly near Golgi-ER network). These data indicate that the Invadolysin rings could be lipid droplets and oleic acid treatment could increase the diameter of lipid droplets by two-fold. The number of the rings also seemed to have increased after oleic acid treatment. However, a

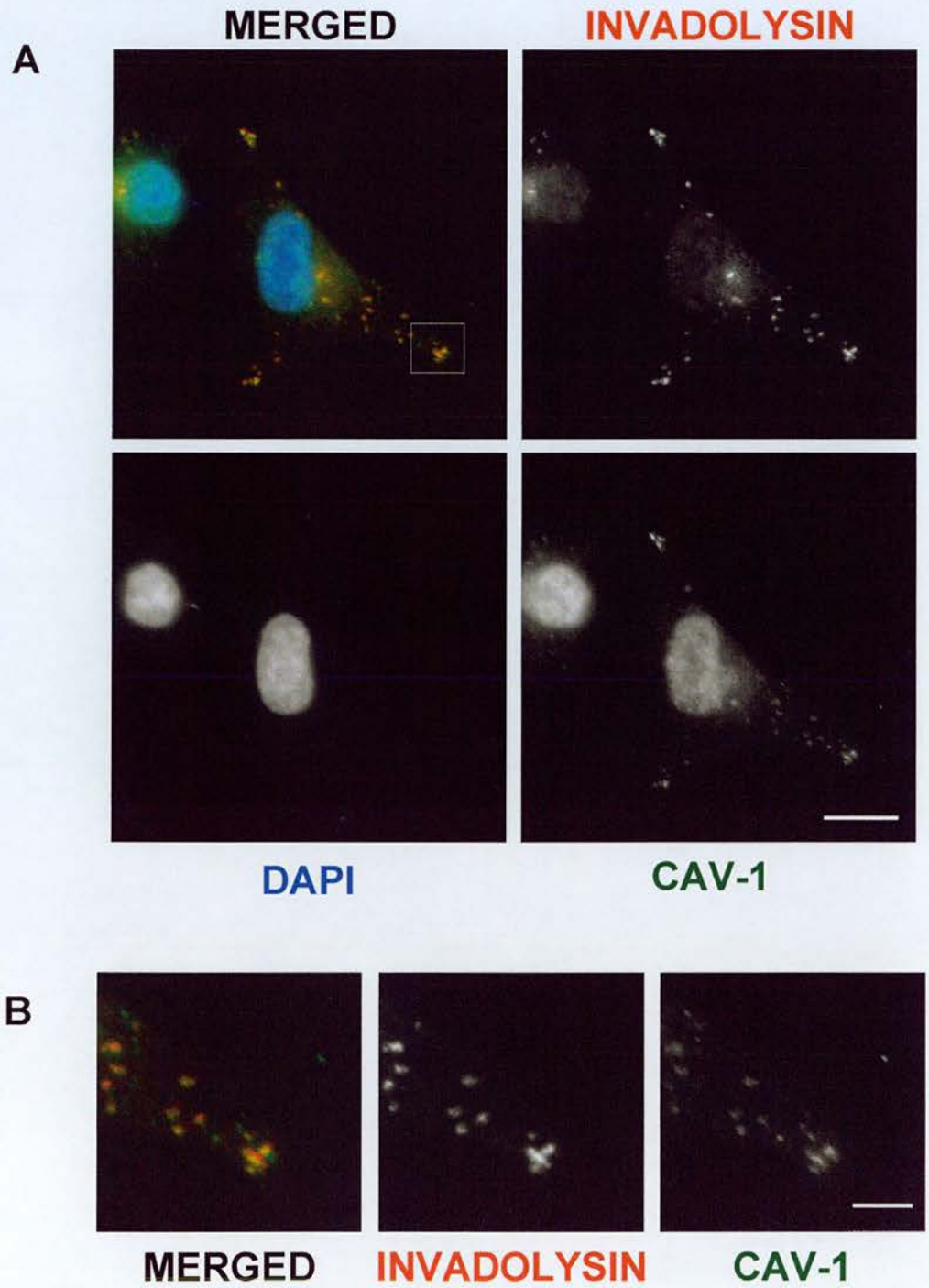

Figure 6.6. Caveolin-1 colocalizes with Invadolysin rings.
A. A375 cells were stained with Invadolysin (red), Caveolin-1 (green) antibodies, and DAPI (blue). Caveolin-1 appeared to colocalize with Invadolysin rings (scale bar is 10 μm).
B. The grey boxed area in A is enlarged to show colocalization (scale bar is 2 μm).

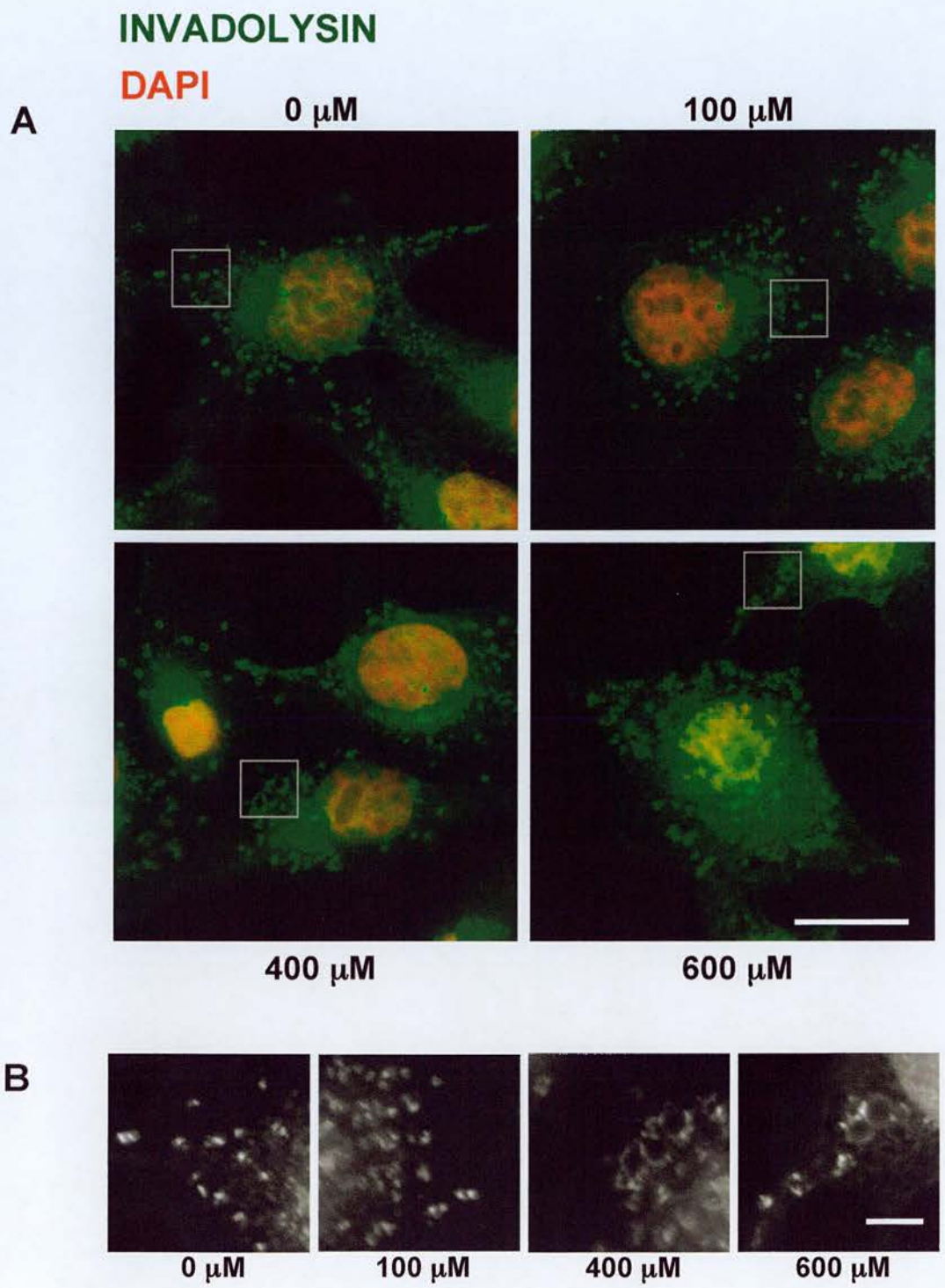

Figure 6.7. Oleic acid treatment increases the size of Invadolysin rings.
A. A375 cells were treated with oleic acid (100, 400 and 600 μM) for 21 hrs and stained with Invadolysin antibody (green) and DNA (red). The size of the Invadolysin rings increased approximately 2-3 fold with 400 and 600 μM oleic acid (scale bar is 10 μm). **B**. The grey boxed areas in A are enlarged to show the increase in size of the rings (scale bar is 2 μm).

definitive quantification could not be made due to the inherent variability from cell to cell in the numbers of rings in control as well as oleic acid treated cells. Similar experiments were performed in other cells lines such as HeLa and PEO14. I observed that the ring like structures could also be modulated using oleic acid in these cells. Rings in HeLa cells appeared to show a more dramatic increase in Invadolysin ring size and number with 600 μM oleic acid. The rings in PEO14 cells only appeared bigger when oleic acid was increased to 1.8mM.

Invadolysin rings resemble rings observed with lipid droplet proteins

Lipid droplets are important organelle for lipid metabolism in cells. They occur in organisms ranging from yeast to human (Murphy 2001). They are known to contain a core of neutral lipids where triglycerides and cholesteryl esters are stored. They are surrounded by a lipid monolayer and until now, very few proteins have been characterized as components of this lipid monolayer membrane. PAT family proteins ADRP (Adipose Differentiation Related Protein), perilipins, TIP47 are the most well known of these (Martin and Parton, 2006). I wanted to examine the localization of proteins such as ADRP and TIP47 in A375 melanoma cells. I also wanted to determine if Invadolysin colocalized with these proteins. Previous research on lipid droplet proteins suggests that they may be washed off from lipid droplets very easily and hence the specific fixation and permeabilization conditions are critical for the maintenance of the integrity of this organelle during immunofluorescence experiments (Ohsaki *et al.*, 2005). ADRP and TIP47 localization have only been observed only when permiabilization reagents such as digitonin or saponin are used.

When A375 cells were stained for ADRP or TIP47 using digitonin as a permeabilization agent, both proteins appeared as ring-like structures strikingly similar in appearance to those of Invadolysin (Figure 6.8). However, colocalization experiments for Invadolysin with ADRP or TIP47 was not possible, as the Invadolysin or its antibody did not tolerate digitonin or saponin permeabilization. Due to the similarity in localization pattern, it could be hypothesised that ADRP, TIP47 and Invadolysin were localized to the same compartment of the cultured cells (i.e., lipid droplets).

Direct labelling of lipid droplets with BODIPY

To further confirm that Invadolysin rings were on the surface lipid droplets, BODIPY, a neutral lipid binding dye, was used. BODIPY 493/503 (8-bromomethyl-4,4-difluoro-1,3,5,7- tetramethyl-4-bora-3a,4a-diaza-*s*-indacene) is a fluorescent dye that has a very sharp excitation emission curve and binds neutral lipids. It has been widely used to label lipid droplets. Lipid droplet proteins ADRP and TIP47 label the surface of BODIPY spots in cells (Ohsaki *et al.*, 2005). Such staining for TIP47 is shown in the figure (Figure 6.9).

A375 cells were fixed and stained with Invadolysin antibodies and BODIPY. BODIPY labelled the inside of every invadolysin ring confirming that the Invadolysin rings indeed surrounded lipid droplets (Figure 6.10).

HeLa and PEO14 cells were also examined for Invadolysin rings and BODIPY. In all cells, BODIPY stained the inside of Invadolysin rings present in these cells (Figure 6.11).

A375 cells were also treated with oleic acid and stained for Invadolysin along

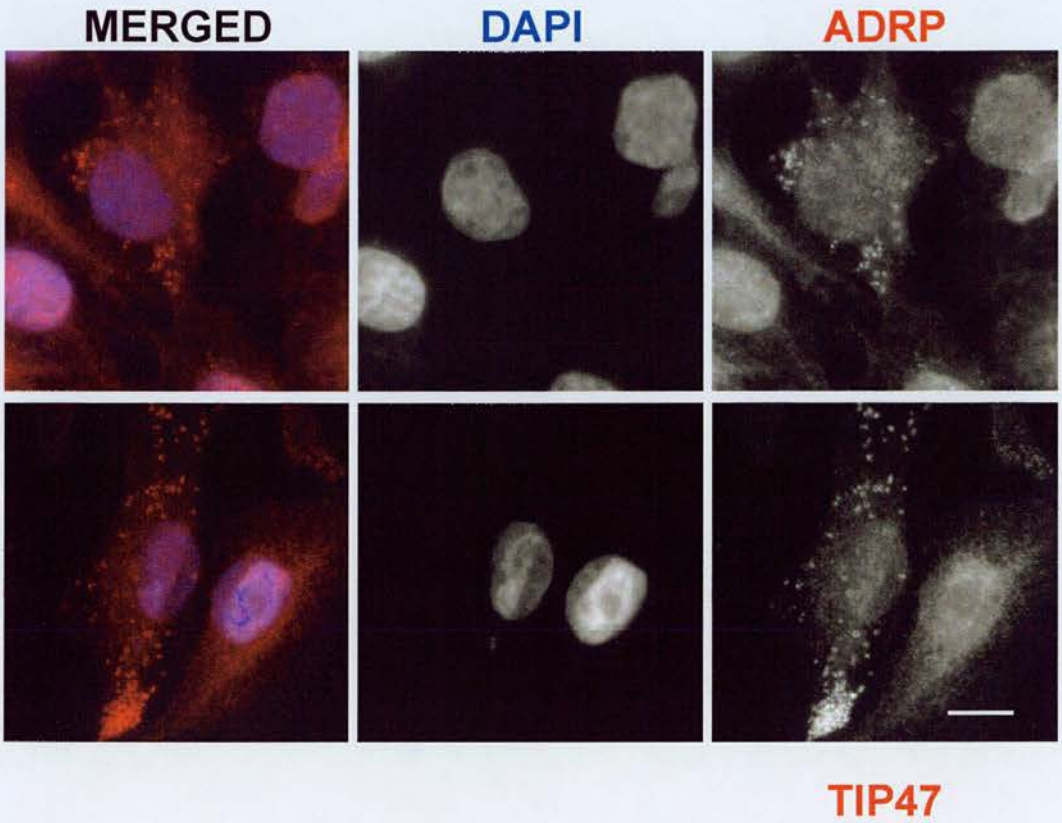

Figure 6.8. Invadolysin rings are similar to the rings of other lipid droplet proteins.
A375 cells were stained with antibodies for lipid droplet proteins (red). DNA is stained with DAPI (blue). Both ADRP and TIP47 stain ring-like structures similar in appearance to Invadolysin (scale bar is 10 μm).

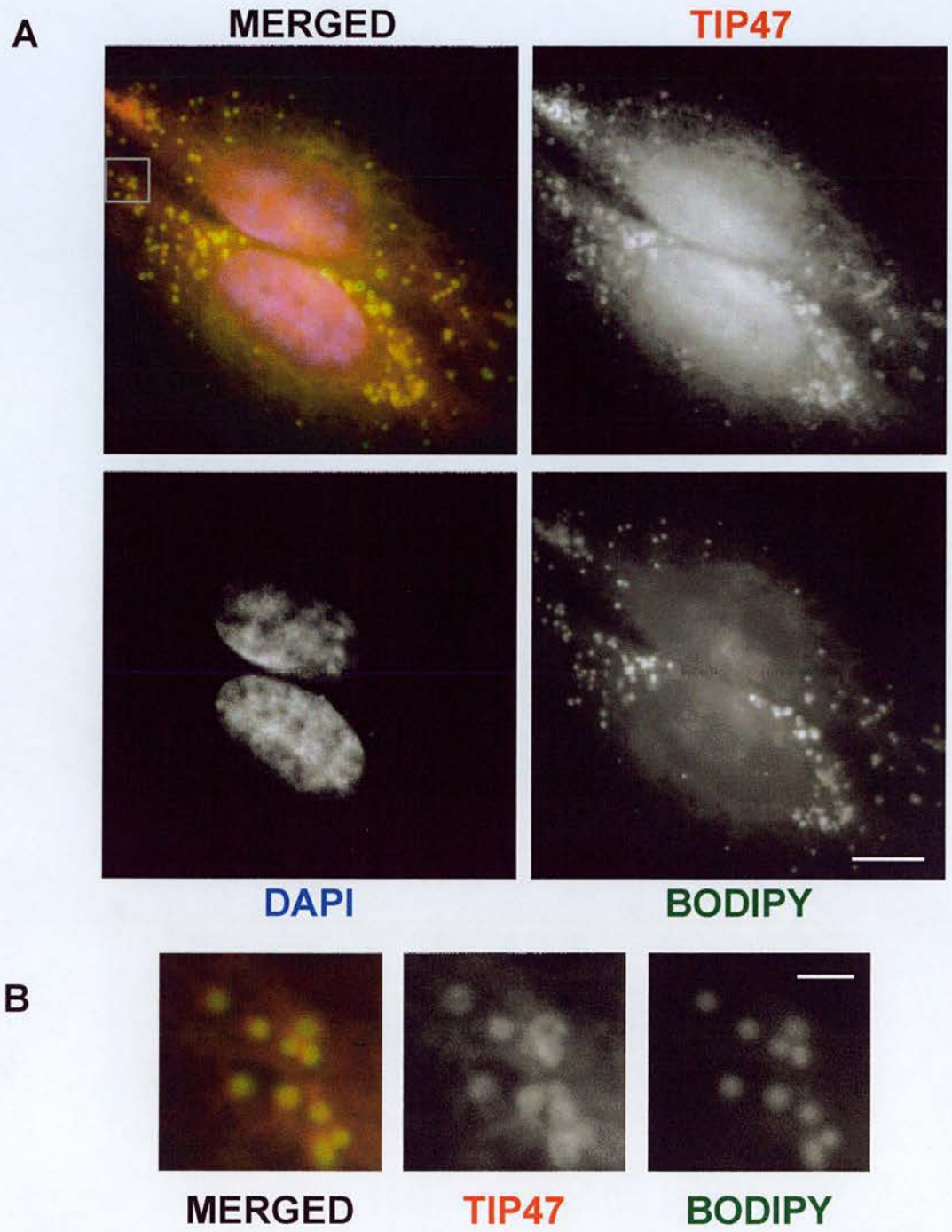

Figure 6.9. BODIPY stains the interior of TIP47 rings.
A. A375 cells were stained with TIP47 antibody (red), BODIPY to stain lipid droplets (green) and DAPI (blue). BODIPY staining was always surrounded by TIP47 rings (scale bar is 10 μm).
B. The grey boxed area in A is enlarged to show TIP47 rings with BODIPY staining inside of them (scale bar is 2 μm).

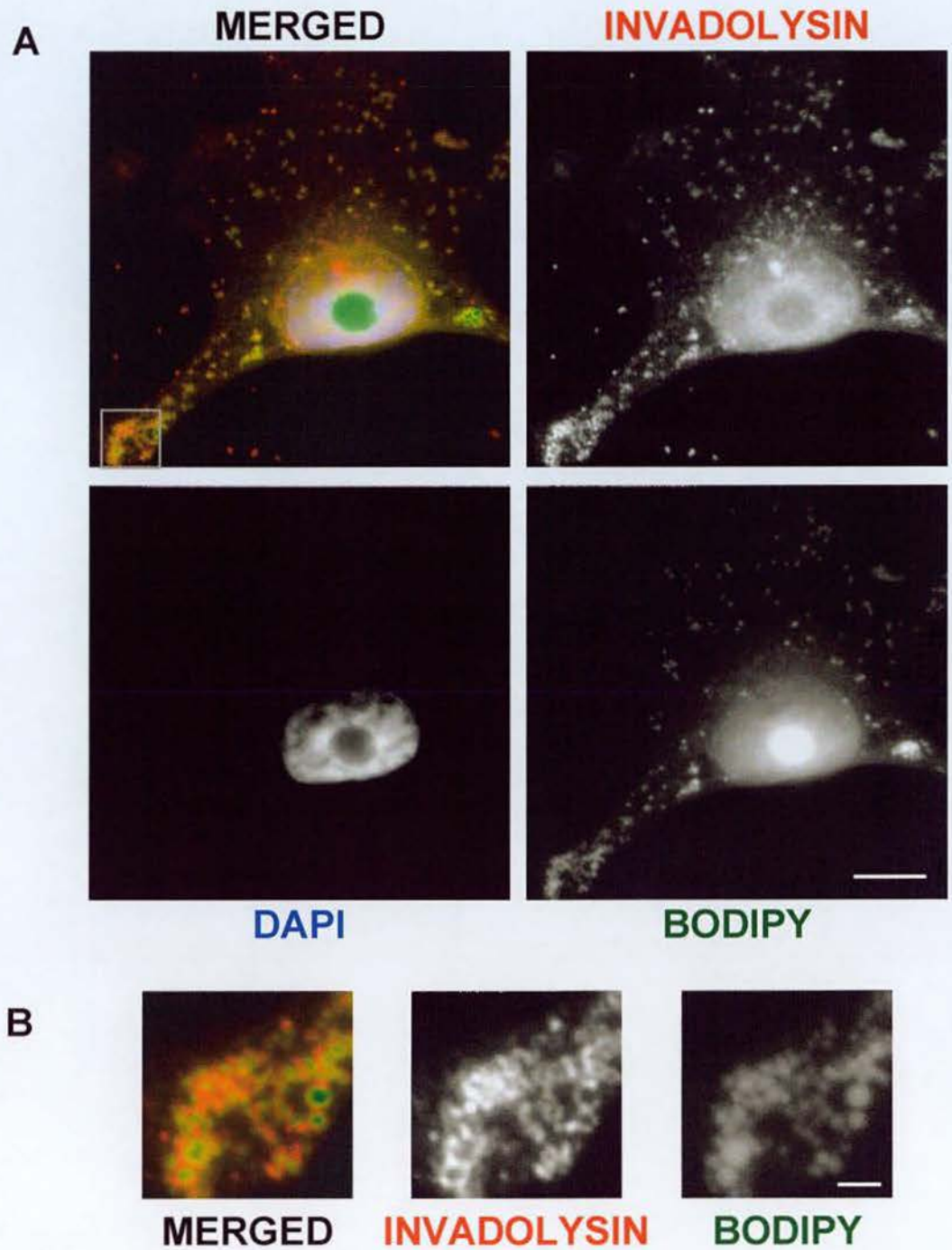

Figure 6.10. Invadolysin stains the surface of BODIPY spots.
A. A375 cells were stained with Invadolysin antibody (red), BODIPY (green) and DAPI (blue). BODIPY staining was always surrounded by Invadolysin rings indicating that Invadolysin is localized on the surface of lipid droplets (scale bar is 10 μm).
B. The grey boxed area in A is enlarged to show the Invadolysin rings with BODIPY staining inside of them (scale bar is 2 μm).

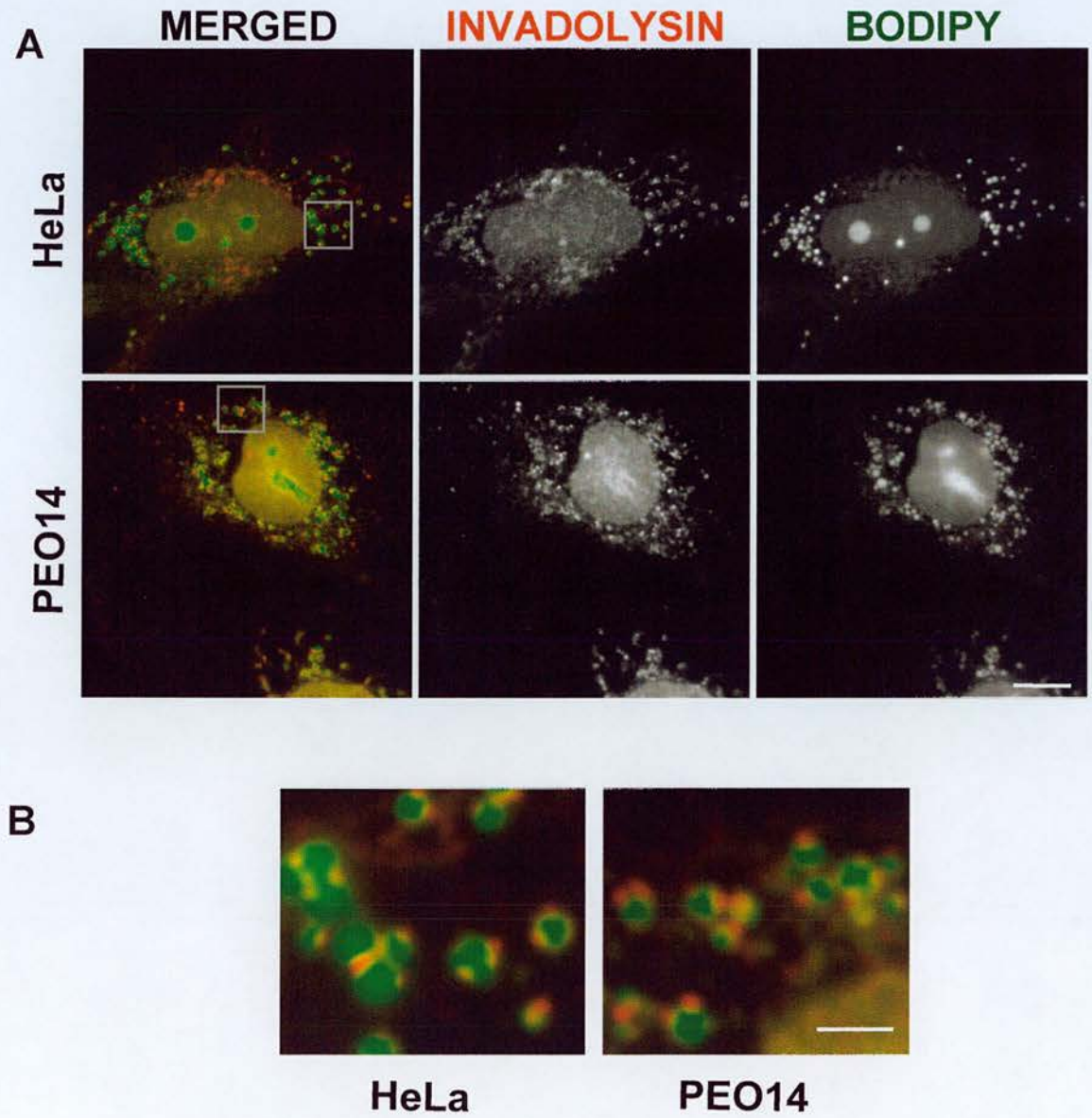

Figure 6.11. BODIPY stains the inside of Invadolysin rings in other cell lines.
A. HeLa and PEO14 cells were stained with Invadolysin antibody (red) and BODIPY (green). BODIPY staining was always surrounded by Invadolysin rings (scale bar is 10 μm).
B. The grey boxed areas in A are enlarged to show the Invadolysin rings with BODIPY staining inside of them (scale bar is 2 μm).

with BODIPY. The size of rings as visualized with BODIPY and Invadolysin staining increased in size and number in most of the cells (Figure 6.12). In summary, I conclude that Invadolysin in a component of the membrane surrounding lipid droplets.

Lipid droplets in Huh7 cells

Human hepatoma cells (Huh7), which are known to contain a large amount of lipid droplets (Targett-Adams *et al.*, 2003) were analysed for the presence of Invadolysin rings along with BODIPY. Huh7 cells contained numerous BODIPY-stained lipid droplets and Invadolysin always surrounded these BODIPY stained spots (Figure 6.13). This showed the presence of Invadolysin in Huh7 cells and furthermore demonstrated the presence of Invadolysin on the surface of lipid droplets in these cells too. Further experiments are being performed in the lab to analyze the protein and transcript levels of Invadolysin in these cells.

Identifying what the Invadolysin rings were was important to understand what this metalloprotease might be doing in the cell. A role for Invadolysin in endocytosis and vesicular trafficking were two cellular activities suggested by result chapter 5. Clathrin-dependent endocytosis markers did not colocalize with Invadolysin, but markers of non-clathrin mediated endocytosis did, suggesting a lipid-based target. Other lipid droplet proteins (ADRP, TIP47) showed a very similar localization to Invadolysin and oleic acid could modulate ring-like structures. Finally, oleic acid manipulation of the lipid droplets and staining with the neutral lipid dye BODIPY consolidated the hypothesis that Invadolysin was indeed present on the surface of LDs.

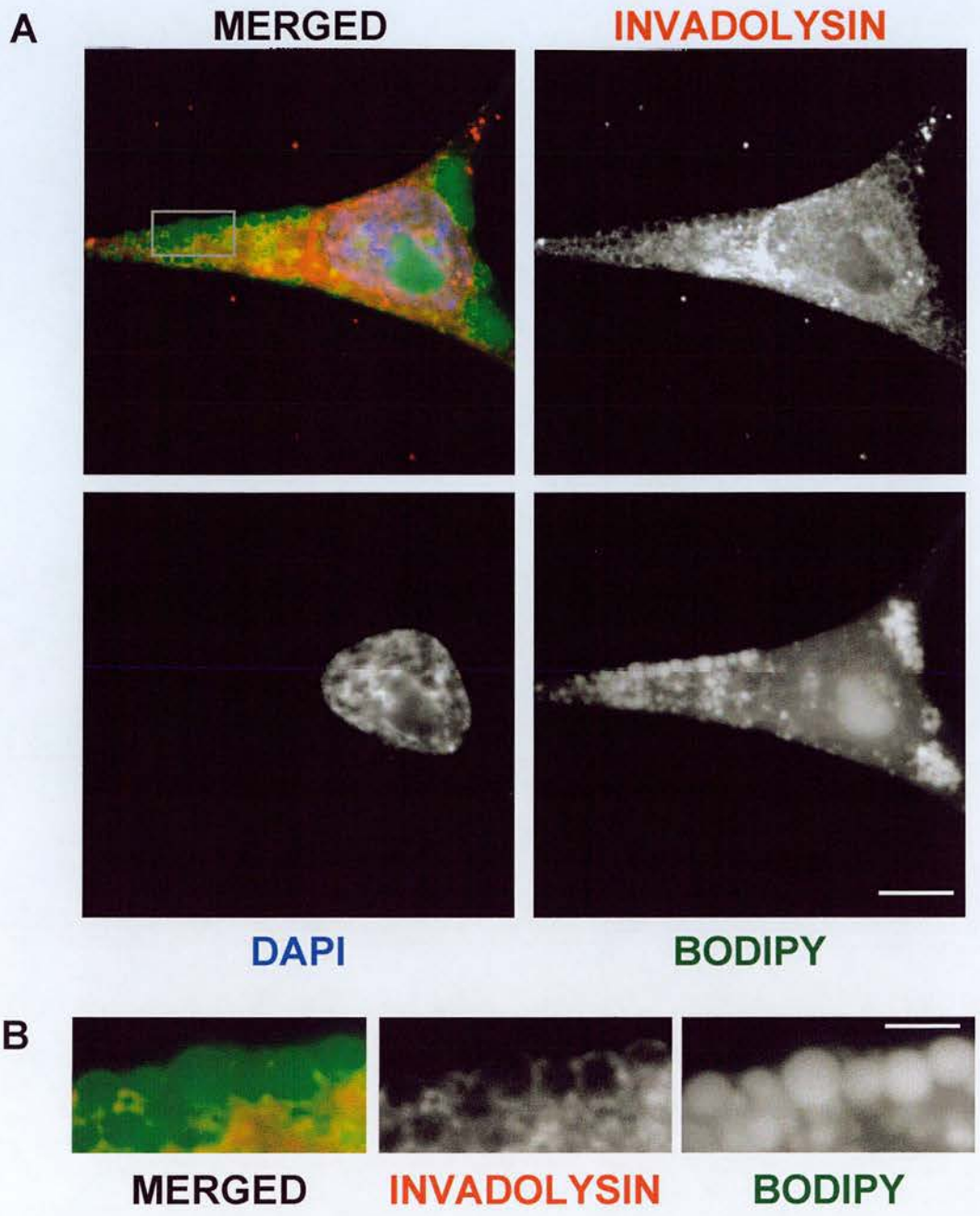

Figure 6.12. Lipid droplets increase in size after oleic acid treatment as detected by BODIPY and Invadolysin.

A. A375 cells were treated with oleic acid (600 μM) for 21 hrs and stained with Invadolysin antibody (red), BODIPY (green) and DAPI (blue). The size of the lipid droplets increased approximately 2-fold which could be detected by both BODIPY and Invadolysin (scale bar is 10 μm).

B. The grey boxed area in A is enlarged to show Invadolysin rings with BODIPY staining inside of them (scale bar is 2 μm).

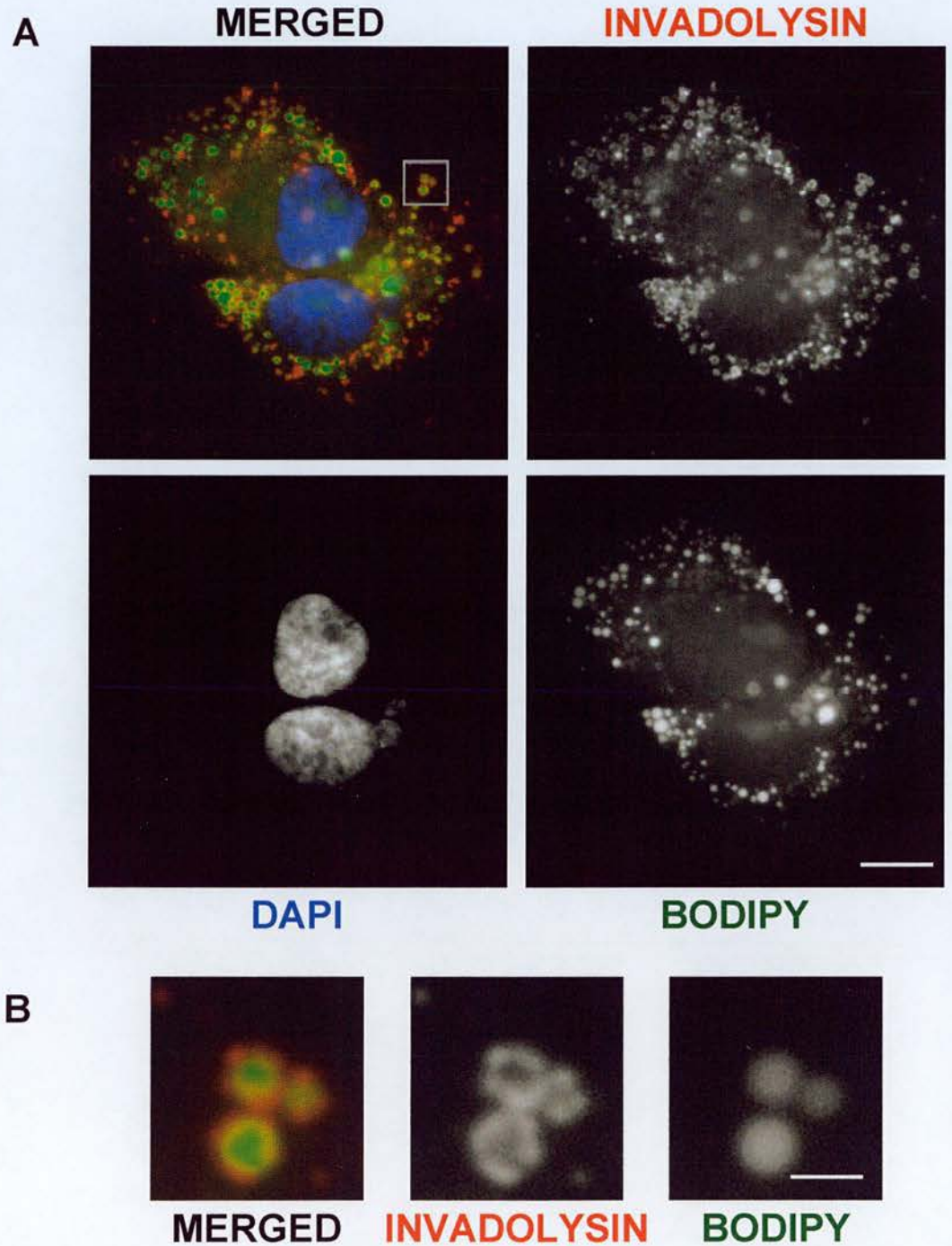

Figure 6.13. Invadolysin localization in Huh7 cells.
A. Huh7 (human hepatoma) cells were stained with Invadolysin antibody (red), BODIPY (green) and DAPI (blue). BODIPY staining was always surrounded by Invadolysin rings indicating that Invadolysin is localized on the surface of lipid droplets (scale bar is 10
μm).
B. The grey boxed area in A is enlarged below to show Invadolysin rings with BODIPY staining inside of them (scale bar is 2 μm).

Chapter 7: Generation of reagents for the study of Invadolysin

Introduction

In biological research, reagents such as antibodies and plasmid constructs are essential to carry out experiments. A part of my PhD project focussed on generating and characterizing antibodies for *Drosophila* Invadolysin, make certain plasmid constructs and standardizing conditions for genetic experiments. I will be describing this work collectively in this chapter.

Antibodies

Antibodies are used for experiments such as immunoblotting, immunofluorescence, immunoprecipitation and protein purification. These are all useful techniques to analyze a protein's localization and function. Antibodies previously generated for the *Drosophila* Invadolysin protein were raised against the C-terminal half of the protein using a bacterially expressed His-tagged protein (Brian McHugh). These antibodies recognised a number of unspecific proteins in addition to Invadolysin. Hence, in an attempt generate additional antibodies against Invadolysin, a peptide antibody approach was used. Peptide antibodies were also generated for the protein Non-stop, the genetic interactor of Invadolysin described previously (chapter 4). Peptides (15-20 amino acid length) are generated synthetically and injected into animals to elicit immune response. Generating peptide antibodies is less laborious compared to making fusion protein antibodies. Our lab has had previous success using peptide antibodies for a non-SMC protein (CAP-D2) of the condensin complex (Savvidou *et al.*, 2005).

Previous work aimed at expressing full length Invadolysin in bacteria had been difficult and inconsistent (Bin Yu, Ching-Wen Chang). N and C-term tags seem to be cleaved which could be attributed to Invadolysin being a protease cleaving itself. Protease activity was minimal with bacterial-expressed proteins suggesting the protein might be misfolded or requires post-translational cleavage or modification for its activity. This was another reason to attempt to generate peptide antibodies to Invadolysin.

The *Drosophila invadolysin* gene encodes a 683 amino acid long protein (predicted) (Figure 7.1A). It is homologous to Leishmanolysin, whose crystal structure has been solved (Schlagenhauf *et al.*, 1998). When the sequence of Invadolysin was threaded on the structure of Leishmanolysin, there were 9 regions found only in the higher eukaryotic sequences which were predicted to be on the surface of the protein (McHugh *et al.*, 2004). It is reasonable to predict that residues lying on the surface of the protein should provide an accessible epitope within the cell. Hence a unique peptide sequence of 15 amino acids from "loop 2" was selected for antibody generation. The position of this sequence is indicated on the modeled structure with a blue arrow (Figure 7.1B). This peptide sequence CNATGQNCRIDSNTQ was synthesized by Genosphere Biotechnologies (Paris) and injected into two rabbits. Serum was collected from rabbits before and after the immunization.

Drosophila Non-stop is a protein predicted to be of 735 amino acids in length (Figure 7.2A). It is an ubiquitin protease belonging to the C19 class of cysteine proteases with a zinc finger UBP motif (Figure 7.2B). Since the structure of Non-stop or its homologues has not been solved, 'EMBOSS antigenic' programme was

A

MAKTPPLRPHGNMAKFLAALGICSWLLVSATAHNCQHQHPKAHEVVHGVR
IQLADSEDDSAGDPARHSVRRRSVAAEQPLRILLVYDESVYRLEEEKFNL
INDTVLPEAVQFWEQALMVRETKGVIRLNRKCDSTQVYVKNGHTHCIDHC
KATTMCGEVQVPDAHLDVCRVCNATGQNCRIDSNTQPGEGIENADFVFYV
SARQTQRCFKGLTVAYAAHCQQEAALDRPIAGHANLCPESISTKPQELQT
LISTVKHEILHALGFSVSLYAFFRDDDGKPRTPRKLDTGKPYLNEKLQIH
QWSNETIRKVVRENWSVRGGHVNKVVDMMVTPRVIAEVRAHFNCNKLEGA
ELEDQGGEGTALTHWEKRILENEAMTGTHTQSPVFSRITLALMEDSGWYR
ANYSMATPLTWGKGLGCAFAMRSCKDWIQYNHARGRSIHPFCSKVKQDPL
QTECTDDRNSVALCNLIRHEFELPKGYQNFDSLNHVKDGEEGFYGGSVSL
ADHCPYIQEFTWRSKNVIVRGSHCRFTENNPRPEKNFALESYGEGAKCFD
HSESMWEERSCHQTREWQHWGSGCYKYDCFDGRLHILVGNYSYKCSFPGQ
KLSIRIAANGWLHKGAIMCPPCHELCGAQFAAQGKQCRPGEEPDPLNKYP
RDNLACGAGSEKSRSVAIITAVLLLFGLRWGF

B

Figure 7.1. Generation of peptide antibodies for Invadolysin.
A. Amino acid sequence of *Drosophila* Invadolysin protein. The peptide sequence used to generate antibodies is highlighted in blue. This peptide was unique to *Dm*Invadolysin. The protease motif (HEXXH) is highlighted in magenta.
B. Predicted structure of Invadolysin modeled on the crystal structure of Leishmanolysin protein. The peptide sequence chosen for antibody generation lies at loop 2 (as indicated by black circle pointed to by a blue arrow), which should be at the exposed surface of the protein, thus being accessible to antibody binding.

used to identify a suitable peptide sequence of Non-stop to use as an antigen. The sequence THMRACVCVCVQCE was chosen from the N-terminus of the protein as indicated by an asterisk (Figure 7.2B). These antibodies were also generated using the service offered by the company Genosphere Biotechnologies.

The preimmune serum, test bleeds and the immune bleeds for antibodies against both Invadolysin and Non-stop were tested by immunoblotting against larval extracts from wild type and mutant third instar larvae. Two rabbits each were injected with the peptide antigens described above and the Invadolysin peptide antibodies were named Ab4100 and Ab4101 whereas the Non-stop antibodies generated were termed Ab4890 and Ab4891.

To test for reactivity on immunoblots, antibodies were tested at 1: 500 dilution on wild type extracts using a slot blotter. Ab4100 showed a prominent band at 70 kDa, close to the expected size of Invadolysin. The Ab4101 antibody showed a prominent band at 51 kDa (Figure 7.3). These bands were not observed with the pre-immune serum. However, these bands were also apparent in the *invadolysin* homozygous mutant larval extracts and hence no definitive conclusions could be made about the 70 kDa band being Invadolysin. Individual larval extracts were prepared from a number of wild type and mutant larvae and probed with Ab4100. The 70 kDa band appeared in most of the mutant larvae (Figure 7.4). The *invadolysin* mutant larvae do not express Invadolysin mRNA by both RT-PCR and northern blot (McHugh *et al.*, 2004). I propose that no protein should be expressed or synthesized in the *invadolysin* mutant larvae, which may be responsible for their lethality as third instar larvae. However, the protein seen in the mutants could be maternally loaded and loss of the protein in certain essential tissues or cells only

A

MFQYSYIRKIPMPTSEYDFATGHTDSCLLFTHMRACVCVCVQCEETRKASEKSQK
FTKKKPNYFQNWAARRRTAKVAKIRRKQRKCDKAFVPLQSSAKRAKTKENSVDSN
TSVFSSSSSSSSGRSFGRGTERWAVGAEAGRGTAENETLAVAAAAATTTNAGRFI
TADLIKTVNSDKQRDRVAKGHRDAKNPLDATKHLRLSDCLRTVQKLAIELESADAG
SDASAQANASADASSAVMSETGCRHYQSYVKEHSYDTFRVIDAYFAACVNRDAR
ERKAIHCNCFECGSYGIQLYACLHCIYFGCRGAHITSHLRSKKHNVALELSHGTLYC
YACRDFIYDARSREYALINRKLEAKDLQKSIGWVPWVPTTKETNLLLANARRRLVR
PNQTIGLRGLLNLGATCFMNCIVQALVHTPLLSDYFMSDRHDCGSKSSHKCLVCEV
SRLFQEFYSGSRSPLSLHRLLHLIWNHAKHLAGYEQQDAHEFFIATLDVLHRHCVK
AKAEHESKSNSSGSGSGTNSSNSSSSHCYGQCNCIIDQIFTGMLQSDVVCQACNG
VSTTYDPFWDISLDLGETTTHGGVTPKTLIDCLERYTRAEHLGSAAKIKCSTCKSYQ
ESTKQFSLRTLPSVVSFHLKRFEHSALIDRKISSFIQFPVEFDMTPFMSEKKNAYGD
FRFSLYAVVNHVGTIDTGHYTAYVRHQKDTWVKCDDHVITMASLKQVLDSEGYLLF
YHKNVLEYE

B

Figure 7.2. Generation of peptide antibodies for Non-stop.
A. Amino acid sequence of *Drosophila* Non-stop protein. The peptide sequence used to generate antibodies is highlighted in blue. This peptide sequence is unique to Non-stop and identified using 'EMBOSS antigenic' programme.
B. Schematic representation of Non-stop. Non-stop is a 735 amino acid long protein. It has a zinc finger UBP domain and a C19 class peptidase domain. The blue asterisk indicates the region of the protein used for generating antibodies.

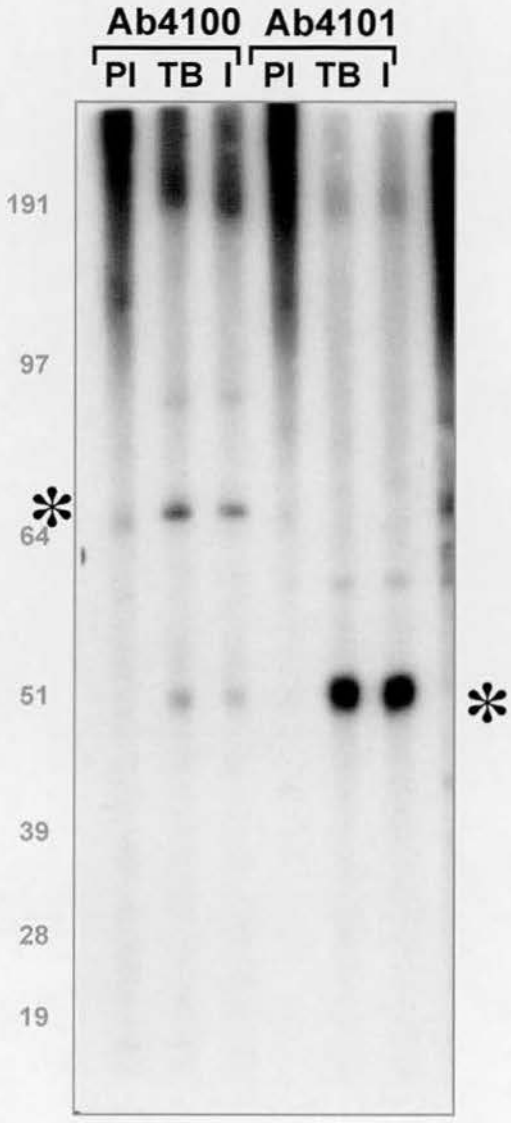

Figure 7.3. Characterization of peptide antibodies Ab4100 and Ab4101 generated against *Dm*Invadolysin.

A band at 70 kDa (expected size for Invadolysin, shown with an asterisk) is seen with Ab4100 that is absent in the pre-immune serum. However the Ab4101 recognises a band near 51 kDa. All the sera were used at 1:500 dilution. PI - Preimmune serum, TB - Test Bleed, I - Immune serum.

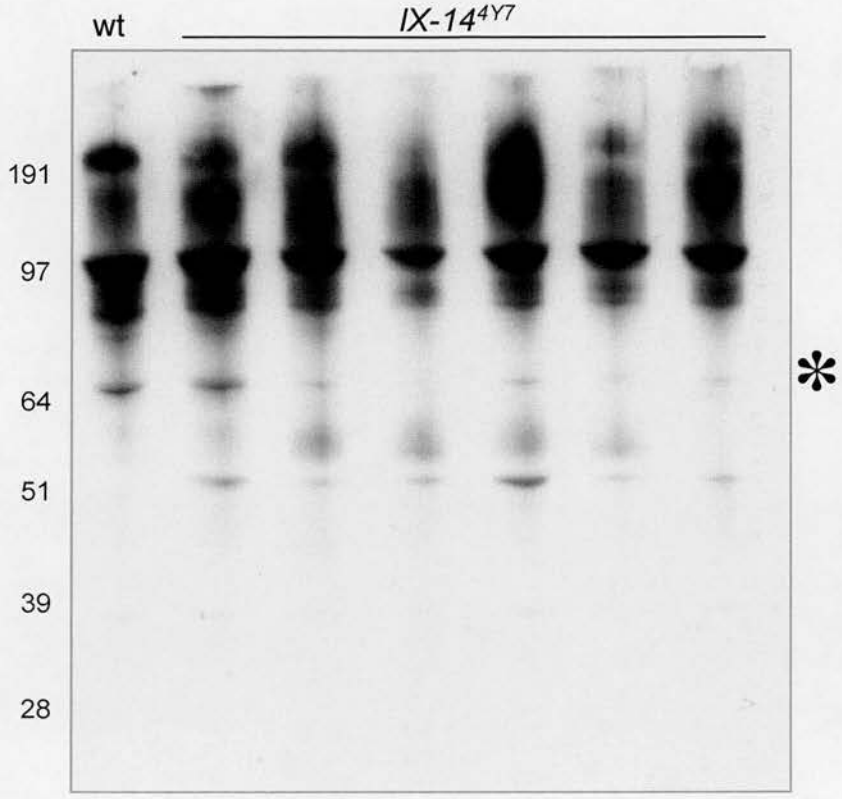

Figure 7.4. Antibody characterization using single larval extracts.
Antibody 4100 on single larval extracts of wild type (only half of one larva was loaded for wild type since mutant larvae are approximately half the size of wild type) and mutant larvae (*IX-14^{4Y7}*) show a band at around 65-70 kDa (shown with an asterisk). This band is weak or absent in the mutants implying that Invadolysin may be present at low level in some of the *IX-14^{4Y7}* mutants.

could be responsible for lethality in the mutant status or the *IX-14*^{4Y7} allele might be hypomorphic. Purification of the antibodies was attempted using the peptide, but was unsuccessful as no bands of the expected size were observed after the purification. More optimization of these methods needs to be done in order to make definitive conclusions.

The Non-stop antibodies Ab4890 and Ab4891 showed no differences between wild type and *non-stop* (*not*^{1} and *not*^{2}) mutant extracts when tested by immunoblotting. However, a surprising observation was made when these antibodies were probed against *invadolysin* mutant larval extracts. There was a prominent band observed with Ab4890 in the *invadolysin* mutant extracts. This 40 kDa band was absent in wild type or *non-stop* mutants. This 40 kDa band was also observed with the Ab4891 antibody but was less prominent due to the presence of other bands (Figure 7.5). This band was repeatedly observed with many independently prepared extracts suggesting that it is not an artifact. This 40 kDa band observed only in *invadolysin* mutants could potentially be an aberrantly accumulated form of Non-stop due to the absence of Invadolysin. Immunoprecipitations using Ab4890 could be used to identify this protein by mass spectrometry.

A screen for modifiers of Invadolysin function

Another side project of my PhD involved planning an overexpression screen in *Drosophila* to identify potential regulators of Invadolysin function. The *UAS*-GAL4 system allows overexpression of a gene of interest in a specific tissue and also at a specific time (Duffy, 2002). GAL4 is a yeast transcription factor that can

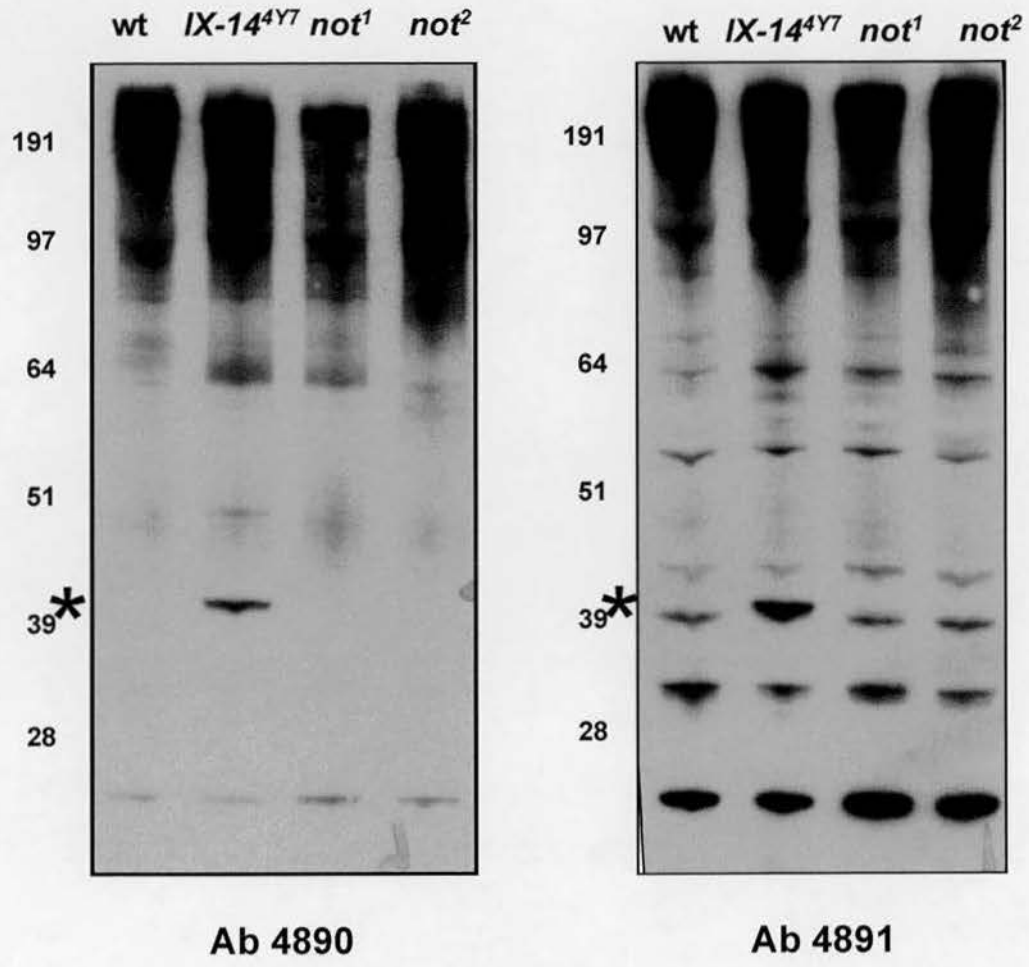

Figure 7.5. Characterization of antibodies 4890 and 4891 for Non-stop.
Antibody 4890 and 4891 were generated using the peptide shown in Fig 7.2 and tested on wild type, *IX-14*^{4Y7}, *not*^{1} and *not*^{2} mutant larval extracts. No difference was observed between wild type and *not* mutants but there was a conspicuous band in the *IX-14*^{4Y7} mutants ~ at 40 kDa (indicated by an asterisk) seen with both Non-stop antibodies. However the band was clearer with Ab4890.

bind *UAS* (Upstream Activating Sequence) and activate the transcription of any gene behind *UAS*. If the gene of interest downstream of *UAS*, its expression can be driven using GAL4. The expression of GAL4 itself can be timed and tissue-specified using a tissue specific promoter. Thus the gene of interest can be overexpressed in a particular tissue at a particular time. Such overexpression in fly tissue might result in a phenotype such as rough eyes, wing notches or wing blisterings. A visible phenotype can be modified by crossing the overexpression flies to mutants or other overexpression flies. An overexpression screen would involve crossing the flies that overexpress Invadolysin to genome-wide deficiencies and identifying which deficiency modifies (enhances or suppressors) the phenotype caused by the overexpression of Invadolysin. The potential modifier gene can be identified by narrowing down the list of genes uncovered by that deficiency.

To carry out this screen, it was important to choose the right GAL4 driver that can drive the overexpression of Invadolysin in an easy-to-screen organ giving a visible and scorable phenotype. The *UAS-IX-14* flies were generated in the Heck laboratory. I wanted to determine whether these flies overexpress Invadolysin when induced by GAL4. To do this, *UAS-IX-14* homozygous flies were crossed to heat-shock GAL4 flies and the progeny larvae were heat shocked at 37 $^{\circ}$C for 1 hr each day for 3 days. Larvae were collected each day after heat shock and total RNA was prepared. RT-PCR was carried out using *invadolysin* primers and a control set of primers (poly). Invadolysin transcript was clearly overexpressed compared to the control poly transcript levels (Figure 7.6). These results indicated that Invadolysin was being overexpressed. However, this could not be confirmed at the protein level due to the unavailability of Invadolysin specific antibody.

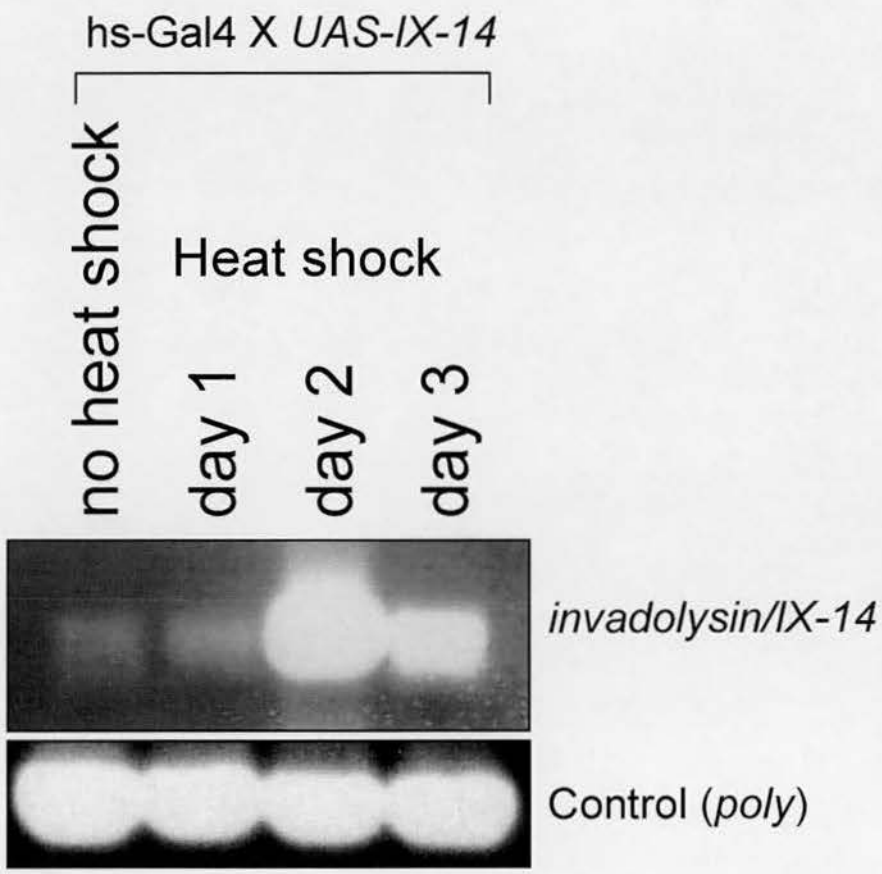

Figure 7.6. Invadolysin overexpression in flies using the *UAS*-GAL4 system. Homozygous *UAS-1X-14* flies were crossed to *heatshock-GAl4* to determine whether *invadolysin/IX-14* can be over expressed. Upon heat shock, *invadolysin* mRNA accumulates to greater levels in *UAS-IX-14* larvae compared to the non heat shocked control animals (detected using RT-PCR). The expression is maximal on day 2. *Poly* is used as a control for total RNA levels.

Initially, ey-GAL4 and GMR-GAL4 were crossed *Dm*Invadolysin over expressing flies at 25 °C. No rough eye phenotype was observed in the progeny. Therefore, various temperatures were tested: 18, 25, 27 and 29°C. Temperatures above 29°C could compromise the physiology of the flies and hence temperatures higher than 29°C were not used. GMR-GAL4 (no.15) with *UAS-IX-14* driver resulted in a slight rough eye phenotype at 29°C compared to the wild type flies crossed with GMR-GAL4 (Figure 7.7). Invadolysin overexpressing eyes were rougher than the wild type and this phenotype did not enhance significantly over time. The overexpressing flies died between days 28-30 where as the wild type flies were still alive. Female flies seemed to have rougher eyes than the male flies. Similar experiments conducted at lower temperatures showed no phenotype in the eyes. This experiment was performed twice and the same results were obtained. This established that the GMR-GAL4#15 driver could be used at 29°C for an overexpression screen.

The overexpression screen would be carried out as illustrated in the figure (Figure 7.8). The first step is to cross the homozygous viable GMR-GAL4 flies to homozygous viable *UAS-IX-14* flies. The crosses are easier to carry out because both of the plasmid integrations are on the second chromosome (*UAS-IX-14* and *GMR-GAL4*). The resulting flies will have rough eyes and the females can be chosen among this progeny and balanced with a balancer chromosome. Recombination events take place only in females and 50% of these females should have the GMR-GAL4 and *UAS-IX-14* on the same homologous chromosome. This recombination can be confirmed when balanced flies still have rough eyes. This can also be confirmed by RT-PCR for Invadolysin or PCR for to amplify *GAL4* sequence or

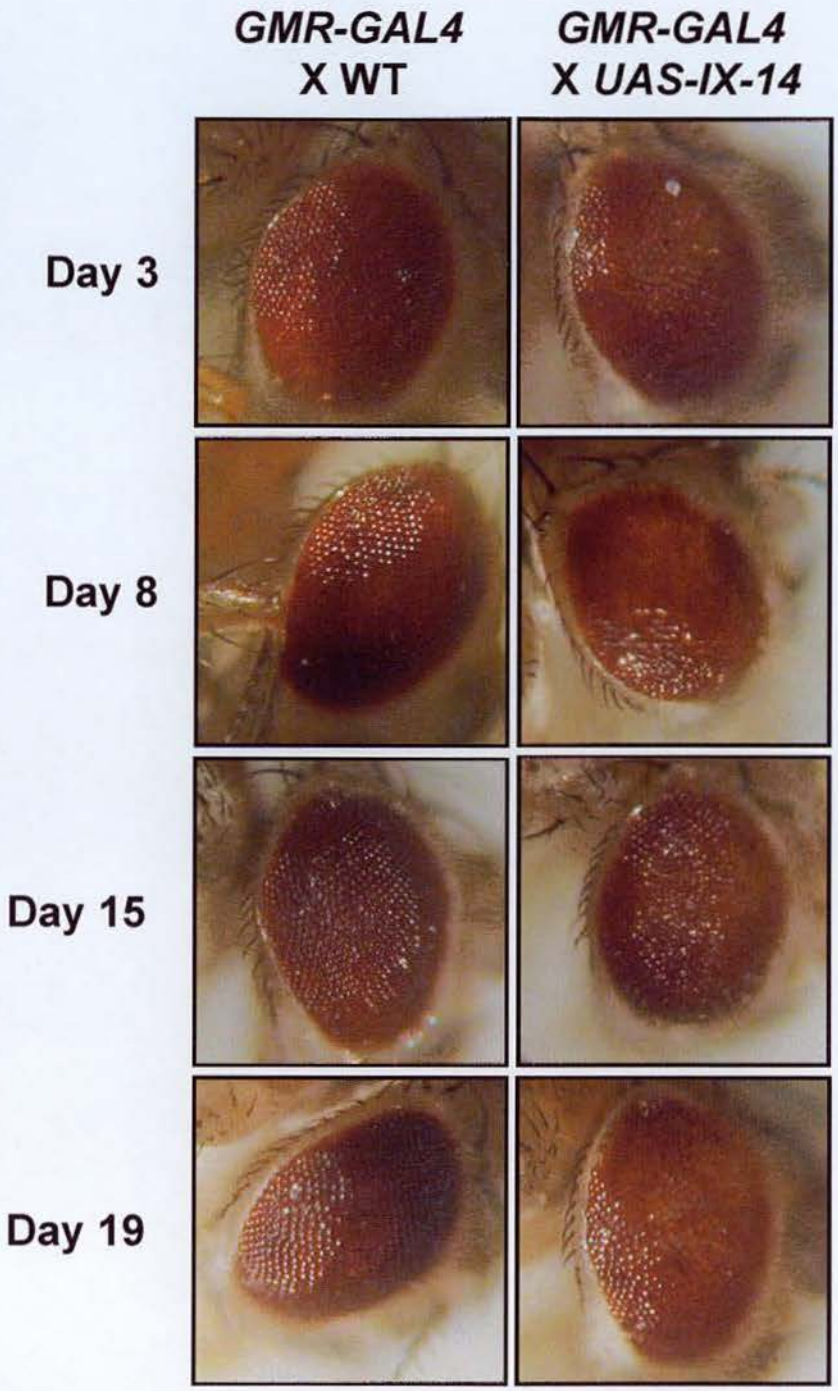

Figure 7.7. Invadolysin over expression in eyes gives slightly roughened eye phenotype. Homozygous *UAS-1X-14* flies were crossed to *GMR-GAL4#15* flies to obtain flies overexpressing *invadolysin*. The progeny showed slight degeneration of the eye from day 1 after eclosion compared to control wild type crossed to *GMR-Gal4#15*. Representative images of eyes from days 3, 8, 15 and 19 are shown in the above figure for wild type crossed to *GMR-Gal4#15* and Invadolysin overexpression flies.

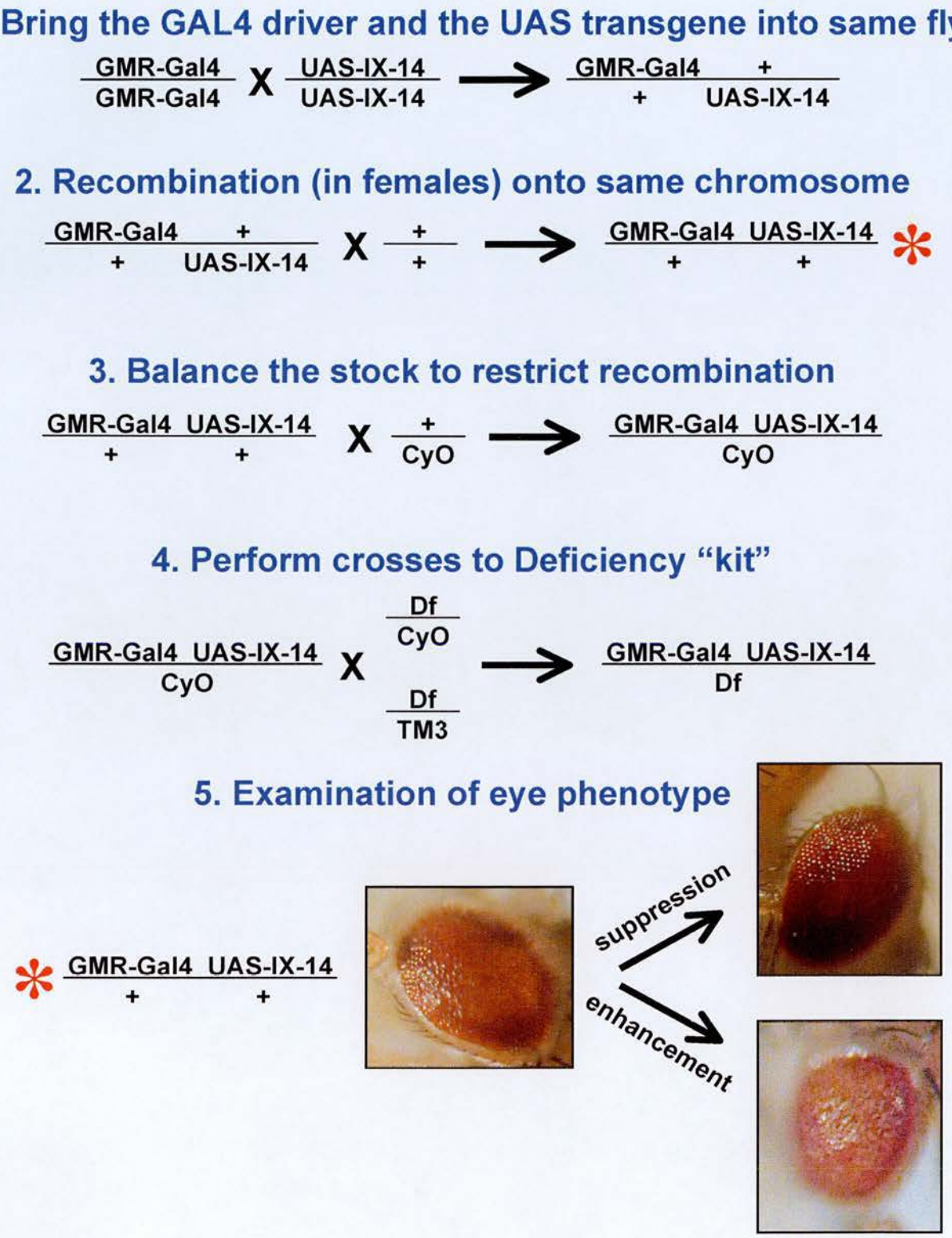

Figure 7.8. Scheme for Invadolysin overexpression screen.
The homozygous *UAS-1X-14* will be crossed to *GMR-GAL4* to obtain flies overexpressing Invadolysin. These flies will then be screened with deficiency lines to identify the potential regulators of Invadolysin activity or level. The deficiencies that can enhance eye degradation are "down regulators" and those that suppress the rough eye phenotype should be "up regulators" of Invadolysin activity or level.

UAS sequence (or the vector specific primers). The above balancing would involve a second chromosome balancer (e.g. SM5 Curly O) as both *UAS-IX-14* and *GMR-GAL4* are on the second chromosome. These balanced flies can subsequently be crossed to deficiencies and the progeny flies, without any balancer, can be scored for their eye phenotype. There should be three different kinds of phenotype. One is the original rough eye phenotype is unaffected. Second is that the rough eye phenotype looks more wild type in appearance because of suppression of the phenotype as the result of deletion of a gene in the deficiency. The third possibility is that the rough eye phenotype is worsened via enhancement of phenotype due to a gene deleted in the deficiency.

Suppression of the eye phenotype indicates that the gene responsible in the deficiency is a positive regulator of Invadolysin level or activity. Invadolysin is not able to cause rough eye phenotype in absence of that gene. Enhancement of the eye phenotype indicates that the gene involved in the deficiency is a negative regulator of Invadolysin level or activity. Invadolysin expression is making the eyes rougher in the absence of that gene. This screen for modifiers of Invadolysin overexpression in the eye is currently being perfomed in the lab.

FLAG-tagged constructs for Invadolysin

The final side project of my PhD course involved generating tagged constructs for Invadolysin. Another way of identifying interacting proteins of Invadolysin is to immunoprecipitate Invadolysin specifically and analyze the binding partners. One way to do this is with tagged proteins. C-term FLAG Tag constructs have been engineered into the pCaSpeR vector (Figure 7.9). The FLAG tag DYKD

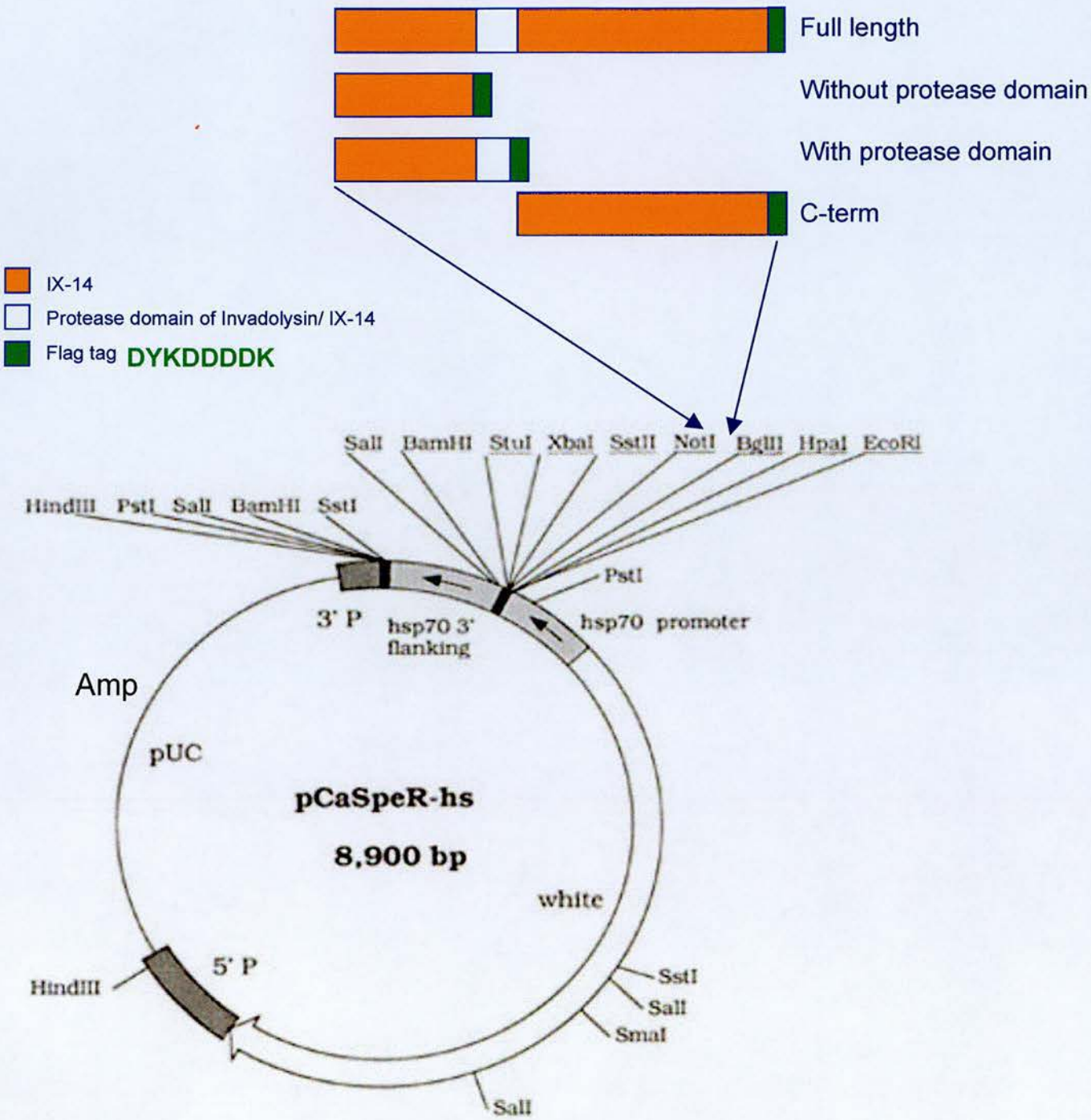

Figure 7.9. Scheme for FLAG tagged constructs of Invadolysin.
Full length and different fragments of Invadolysin/IX-14 have been cloned into pCasper vector into *Bgl*II-*Not*I sites. The FLAG tag is at the C-terminus. These constructs can be used to generate flies with FLAG tagged full length or a part of Invadolysin.

(new version DYKDDDDK is used in my experiments) has been widely used (Slootstra *et al.*, 1997; Weihe *et al.*, 2001). Invadolysin constructs include a full length a C-terminal and two N-terminal constructs with and without the catalytically active domain. A control construct with FLAG sequence in the pCaSpeR vector was also made. These constructs can be transfected into cultured S2 cells along with the control FLAG vector. Immunoprecipitations can be done using anti-FLAG antibody and the co-immunoprecipitated proteins can be electrophoresed and observed with colloidal Coomassie Blue or silver stain. The bands can be excised and identified by mass spectrometry to identify potential physical interactors of Invadolysin. A Yeast two-hybrid data set for Invadolysin (FLY GRID) lists 27 potential binding proteins (Giot *et al.*, 2003). Any overlap in data will lend further credibility to physiological relevance. In case the FLAG-tagged constructs result in high background, TAP (tandem affinity purification) tags could be employed as an alternative (Puig *et al.*, 2001). FLAG (or TAP) constructs can also be injected into flies and flies containing these tagged constructs can be generated and the above mentioned biochemical experiments could be carried out using fly tissues. Further experiments with these constructs will be carried out by other people in the lab.

All the reagents described in this chapter have been used in the ongoing experiments or potentially play a critical role in future experiments in the lab.

Chapter 8: Discussion

During the three years of my Ph.D. research, I have attempted to study the localization and function, and identify interactors of the novel metalloprotease Invadolysin. These experiments should shed light on the pathways in which Invadolysin might be playing a role. It was known from previous studies that Invadolysin should be involved in processes such as mitosis and cell migration (McHugh *et al.*, 2004). However, very little was known about the precise molecular role of Invadolysin. The evidence that it was an essential gene in *Drosophila* clearly suggested that Invadolysin has important functions.

Second-site non-complementation screen identified *non-stop* as a genetic interactor of *invadolysin*

I started with the objective of identifying potential interactors of *invadolysin* to aid in understanding its cellular function. Second site non-complementation screening in *Drosophila* identified *non-stop* as a genetic interactor of *invadolysin* (Chapter 3). This was a result of narrowing down the genes uncovered by the lethal deficiency *Df(3L)ED225*. The semi-lethal deficiencies identified in this screen uncovered a large number of genes and not all the mutants were available at the *Drosophila* stock centres. However, with an increasing number of deficiencies being maintained at stock centres, it could be possible to narrow down additional potential interactors out of semi-lethal deficiencies in the future.

Phenotypic comparison of *non-stop* and *invadolysin* mutants

non-stop encodes a deubiquitinating enzyme and ubiquitinated proteins accumulate in the *non-stop* mutant larvae (Poeck *et al.*, 2001). The fact that *invadolysin* mutants also showed similar accumulation of ubiquitinated proteins suggests that the two proteins are functioning in the same or similar pathways regulating an essential process. The other very interesting observation supporting this hypothesis was the hypercondensation phenotype observed in *non-stop* mutants, which was very similar to that observed in *invadolysin* mutants. Salivary gland chromosomes also shared similar mutant phenotypes. However, the extent of the defects was less pronounced in *non-stop* mutants compared to *invadolysin* mutants, suggesting that *invadolysin* mutants might be acting upstream in the pathway and hence resulting in more severe defects. *non-stop* mutants showed normal spindles and centrosomes in neuroblasts in contrast to *invadolysin* mutants, which contain abnormal spindles and centrosomes. Hence the spindle and centrosome phenotypes exhibited by *invadolysin* mutants are independent of *non-stop*. *non-stop* mutants formed gonads whereas *invadolysin* mutants never formed gonads due to defective germ cell migration. This suggests that germ cell migration in *non-stop* mutants should be normal. Further experiments involving real time study of germ cell migration in both the mutants are ongoing in collaboration with Dr. Ivan Clark (Dundee).

Several other phenotypes found in *invadolysin* mutants were not observed in *non-stop* mutants. *non-stop* mutant brains were of wild type size compared to the small brains of *invadolysin* mutants. Imaginal discs developed in *non-stop* mutants

in contrast to *invadolysin* mutants. *non-stop* mutants could pupate where as *invadolysin* mutants died as early third instar larvae suggesting that *non-stop* is not essential until metamorphosis events. This also suggests that *invadolysin* is acting earlier than *non-stop*, affecting the viability of larvae in its absence. Non-stop is known to influence glial cell migration during eye development in *Drosophila* (Poeck *et al.*, 2001). This could not be tested in *invadolysin* mutants as they do not form eye discs. Mosaic analysis or inducible RNAi in flies should allow us to determine if Invadolysin plays a role in glial cell migration.

non-stop mutants also showed certain phenotypes that were not observed in *invadolysin* mutants. *non-stop* mutant larvae form melanotic masses in their larval cavity. *non-stop* mutant larvae live up to 13 days as third instar larvae and die either by pupating or as third instar larvae. The not^2 larvae can often be seen with melanotic masses whereas this is observed very occasionally in not^1 mutants. The not^1 lesion is an EMS-induced point mutation (Poeck *et al.*, 2001), but the transcript is still expressed in these mutants, where as not^2 is a P-element insertion allele that completely abolishes expression of the gene product. This is one of the probable reasons why not^2 mutants are more severe than not^1 mutants in exhibiting phenotypes.

Melanotic masses are reported to be caused by about 30 gene mutations in *Drosophila* as a result of disruption of signalling pathways (Minakhina and Steward, 2006). Melanotic masses are not observed in *invadolysin* mutants, possibly because they do not have an extended larval life. From these observations, I concluded that *invadolysin* is playing a more important role than *non-stop* in the pathways affected

resulting in the phenotypes observed.

Thus *non-stop* mutants share a number of similarities with *invadolysin* mutants, while other phenotypes of *invadolysin* are not affected by *non-stop*. One of the ways to study the functions of Invadolysin at later developmental stages would be by clonal analysis or inducible RNAi techniques.

Invadolysin might be regulating histone ubiquitination

The yeast homologue of Non-stop (Ubp8) is known to deubiquitinate histone H2B and regulate transcription (Henry *et al.*, 2003). UBP8 also associates with the transcription co-activator SAGA complex (Grant *et al.*, 1997; Lee *et al.*, 2005). Ubiquitination of H2B promotes activation of transcription (Henry *et al.*, 2003; Ng *et al.*, 2002; Sun and Allis, 2002). Non-stop along with the SAGA complex is known to control axon guidance in *Drosophila* via histone deubiquitination (Poeck *et al.*, 2001; Weake *et al.*, 2008). We can predict that *Drosophila* Non-stop might be involved in regulation of transcription by deubiquitinating H2B. Therefore, when H2B antibodies were used to probe extracts of larval proteins, bands at 55 kDa were found to be accumulated in the extracts for both *invadolysin* and *non-stop* mutants. This could be a ubiquitinated form of H2B. Similar sized bands were also observed with anti-ubiquitin antibodies, suggesting that those bands might also have been ubiquitinated. Invadolysin might be playing a role in regulating Non-stop and thereby affecting the deubiquitination of H2B.

Another player in the H2B ubiquitination-deubiquitination process is an E3

ubiquitin ligase. In yeast, this ubiquitin ligase has been identified as Bre1 (Hwang *et al.*, 2003; Wood *et al.*, 2003). Both *invadolysin* and *non-stop* showed a hypercondensed chromosome phenotype. I proposed that this phenotype could be related to the increased ubiquitination of H2B. If so, over-expression of the H2B ubiquitin ligase Bre1 should also result in increased ubiquitination of H2B and possibly a hypercondensed chromosome phenotype. When *Drosophila* Bre1 was overexpressed, it resulted in hypercondensed mitotic chromosomes in the neuroblasts, consistent with the hypothesis that the phenotype was a consequence of the accumulation of histone ubiquitination. H2B ubiquitination can influence transcription by regulating methylation on H3 lysine 4 (di- and tri-methylation) (Shahbazian *et al.*, 2005). When lysine di and tri-methylation on H3 was examined, both *invadolysin* and *non-stop* mutants showed an increase in this modification of histone H3 (Chapter 3). These modifications on histone H3 are linked to transcriptional activation (Schneider *et al.*, 2004). Hence we can suggest can be concluded that both *invadolysin* and *non-stop* mutants may show aberrant patterns or levels of transcription.

Invadolysin in Notch signalling

Drosophila Bre1 has also been implicated in the regulation of Notch signalling (Bray *et al.*, 2005). Non-stop genetically and physically interacts with a component of the proteasome complex known as Pros26 (Poeck *et al.*, 2001). Pros26 is a proteasome subunit which is involved in regulating the Notch pathway (Giot *et al.*, 2003). Hence there were multiple lines of evidence suggesting a

possible role for Invadolysin in the Notch pathway.

I thus decided to investigate the role of Invadolysin in Notch pathway. The important experiment that showed a link between the Notch pathway and Invadolysin was that the Notch intracellular domain was decreased in level in *invadolysin* mutants but not in *non-stop* mutants. The levels of Notch extracellular domain in *invadolysin* mutants and wild type larvae were the same, but the intracellular domain decrease could be observed both by immunoblotting and immunofluorescence experiments suggesting an inhibition of the Notch signalling. I further confirmed that Notch signalling was downregulated in *invadolysin* mutants by analysing the expression of the Notch target gene "Enhancer of Split" (E(Spl)). I found that the expression of E(Spl) was greatly reduced in the *invadolysin* mutants. The possibility that down-regulation of the Notch intracellular domain was due to the developmental stage of the larvae was eliminated by careful temporal staging of wild type larvae and immunoblotting the extracts with Notch intracellular and extracellular domain antibodies. This showed that the levels of Notch signalling remained similar throughout development, indicating that the down-regulation observed in *invadolysin* mutants was specific to the *invadolysin* mutant phenotype.

It was important to discover if Invadolysin played a role in regulating the intracellular domain of Notch or its ligand Delta to modulate signalling activity. The striking accumulation of the Notch ligand Delta clearly showed that Invadolysin was acting at the level of Delta and not at the level of the Notch receptor itself.
The increase in levels of Delta was easily observed in the *invadolysin* mutants but it

was difficult to even detect a considerable amount of Delta in wild type larvae. This suggested that Delta was stabilized in *invadolysin* mutants and in a wild type situation, Invadolysin should be somehow involved in the downregulation of Delta.

Suggested involvement of Invadolysin in the endocytosis of Delta

The endocytosis of Delta is very important for Notch signalling activity (Chitnis, 2006). When Delta is stabilized on the plasma membrane, it binds to the Notch receptor on the same cell to bring about *cis*-inactivation of the signal. *cis*-inactivation inhibited by endocytosis of Delta, which involves the action of ubiquitin ligases such as Neuralised (Bardin and Schweisguth, 2006) and Mind bomb (Baron, 2003; Koo *et al.*, 2005). This step might be inhibited in the *invadolysin* mutants. Invadolysin might be playing a role directly or indirectly to promote the endocytosis of Delta. Delta accumulation in the mutants appeared to be the result of increase at the protein level rather than an upregulation at the transcript level as the Delta mRNA levels in *invadolysin* mutants were not upregulated. This also suggested that Invadolysin might be playing a role in bringing down the levels of Delta.

In cultured human cells, Invadolysin was shown to localize to ring-like structures (McHugh *et al.*, 2004). I hypothesised that these ring-like structures might be a kind of endocytic vesicles. Rab11 regulates the endocytosis of Delta via recycling endosomes (Emery *et al.*, 2005) whereas the *Drosophila* homologue of Itch, *suppressor of deltex* (*Su(dx)*) is a negative regulator of Notch function (Fostier *et al.*, 1998), also localizes to early endosomes (Angers *et al.*, 2004). When examined for colocalization, both Rab11 and Itch/AIP4 partially colocalized with

Invadolysin in cultured human cells. Invadolysin might be predicted to regulate the endocytosis of Delta by interacting with Rab11 and/or Itch on the early endosomes.

Another ubiquitin protease Fat Facets regulates the levels of Liquid Facets which in turn promotes Delta endocytosis (Overstreet *et al.*, 2003; Overstreet *et al.*, 2004). Therefore, one of the possible ways that Invadolysin might act on Delta may be through this deubiquitinating enzyme Fat Facets. One way to examine this would be to determine the levels of Liquid Facets in *invadolysin* mutants. It could also be possible that Invadolysin might also be a general regulator of ubiquitin ligases and/or ubiquitin proteases.

It is important to note that *non-stop* mutants did not show decrease in Notch signaling and this might be due to Invadolysin acting upstream of Non-stop in the pathway affecting chromosome phenotypes. However, Non-stop might also be acting on Notch pathway by a different route. Notch and another protein in the Notch pathway, Numb, a negative regulator of the Notch pathway (Frise *et al.*, 1996), are linked to glial cell migration in *Drosophila* (Edenfeld *et al.*, 2007). Non-stop is also known to be important for glial cell migration (Poeck *et al.*, 2001).

Thus I speculated that Invadolysin may play a role in Delta endocytosis. This suggested that Invadolysin might be located on endocytic vesicles. Unfortunately due to the poor quality of *Drosophila* Invadolysin antibodies, it was not possible to conclusively analyze the localization of Invadolysin in *Drosophila* cells. Hence I decided to examine the localization of Invadolysin in cultured human cells.

Examination of Invadolysin localization in cultured human cells

It was previously shown that an antibody raised against the C-terminal half of human Invadolysin recognised ring-like structures in cultured human cells (McHugh *et al.*, 2004). These structures did not seem to colocalize with peroxisomes, signalosomes, proteasomes or lysosomes in previous studies, but they were predicted to be invadopodia considering the demonstrated role of Invadolysin in cell migration and similar appearance to invadopodia in size and shape.

Invadopodia are actin based projections that protrude from the cells to degrade the extracellular matrix and play a role in the invasion of cancer cells (Weaver, 2006). Dynamin 2, a protein involved in mitosis and migration was also shown to be in invadopodia (Baldassarre *et al.*, 2003). However, detailed experiments carried out in the Heck lab showed that Invadolysin rings were not invadopodia (Dr. Kathryn Marshall). I considered that these ring-like structures could be a part of some vesicular transport or endo-exocytosis system based on a possible role for Invadolysin in the endocytosis of Delta. Hence, I attempted colocalization experiments in order to establish the identity of the ring-like structures. From my initial analysis, these ring-like structures seemed to be distributed all over the cell rather than being concentrated to the basal part of the cell to which invadopodia localize in contact with the extracellular matrix. Furthermore, actin or cortactin did not show significant colocalization with the rings, both of which are essential components of invadopodia.

When the member proteins for clathrin-mediated endocytosis were examined, clathrin and dynamin, did not colocalize with the Invadolysin rings. However, cholera toxin B, a marker for caveolar endocytosis was found inside the Invadolysin

rings in a number of experiments, suggesting that these structures might be some lipid related structures. Caveolin-1 protein, a marker for caveolar endocytosis, showed partial colocalization with Invadolysin rings, which further strengthened the hypothesis that these rings are lipid-based structures.

Invadolysin localizes to the surface of lipid droplets

Lipid droplets are organelles that store lipids and found in various cell types (Murphy, 2001). PAT family proteins such as Perilipin, ADRP and TIP47, found on the membranes of lipid droplets also localize as ring-like structures similar to Invadolysin (Martin and Parton, 2006). Caveolins are also targeted to lipid droplets (Martin and Parton, 2005). The size of lipid droplets can be modulated using oleic acid and I found that Invadolysin rings could also be modulated by adding oleic acid to the culture media. Invadolysin rings grew bigger with increasing concentrations of oleic acid. These experiments suggested that Invadolysin was also present on the surface of lipid droplets. BODIPY localization, a dye binding neutral lipids present in lipid droplets, was found exclusively within Invadolysin rings suggesting that Invadolysin rings were indeed lipid droplets. Tagged constructs of human Invadolysin can also localize to ring-like structures that are recognised by the antibody mentioned above (Brian McHugh, Ching-Wen Chang, Heck lab). These observations also supported the concept that Invadolysin localized to the surface of lipid droplets.

The localization of Invadolysin on the surface of lipid droplets might be through a GPI-anchor. The protein sequence of Invadolysin suggests a possibility of a GPI-anchor (Heck lab, unpublished). GPI-anchored proteins also associate with

the monolayer membrane of lipid droplets (Muller *et al.*, 2008) which might also be the case for Invadolysin.

Lipid droplets are not just organelles for storing fat. They have been recently implicated as protein storage depots (Cermelli *et al.*, 2006; Welte, 2007). Rab GTPases have been shown to lie in close proximity to lipid droplets, with some Rabs found on to the surface of lipid droplets (Martin *et al.*, 2005). Intriguingly, Rabs are also involved in Delta endocytosis (Emery *et al.*, 2005). Several mass spectrometric analyses of lipid droplets have identified histones in the lipid droplets (Beller *et al.*, 2006; Binns *et al.*, 2006; Cermelli *et al.*, 2006; Wan *et al.*, 2007). It will be interesting to discover if histone ubiquitination-deubiquitination process has any link to lipid droplets. If so, what is the role of the metalloprotease Invadolysin in histone storage in lipid droplets? Lipid droplets have also known to be involved in phospholipids recycling membrane traffic (Liu *et al.*, 2004), autophagy and proteasomal activity (Ohsaki *et al.*, 2006). In addition, they are also important organelles for hepatitis C virus production (Miyanari *et al.*, 2007). The number of lipid droplets has been shown to be enhanced in certain cancer cells (Ohsaki *et al.*, 2006). Lipid droplets are also associated with other cellular organelles such as endosomes (Bartz *et al.*, 2007), peroxisomes (Binns *et al.*, 2006) and could be speculated to play a dynamic role in variety of cellular processes. Invadolysin might be involved in one or more of these above mentioned functions associated with lipid droplets.

In a brief conclusion, as illustrated in figure 8.1, I summarize my findings. I have shown that the *Drosophila* Invadolysin interacts genetically with the ubiquitin

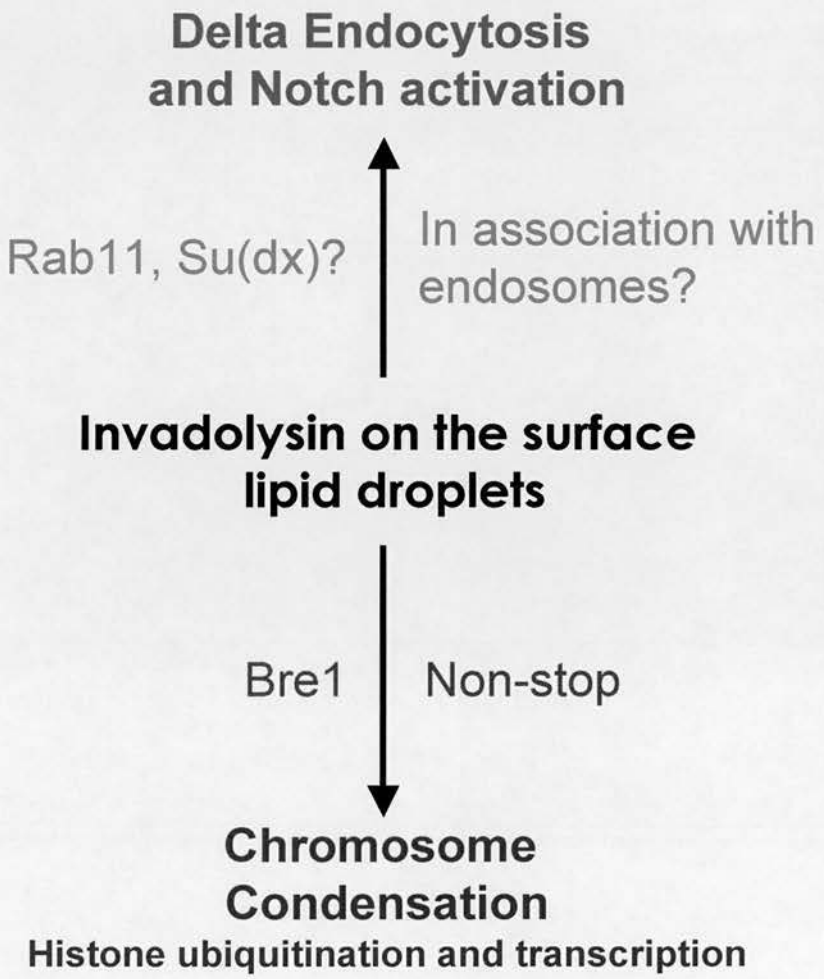

Figure 8.1. Model for the roles of Invadolysin.
Based on the results presented in this thesis, Invadolysin, a metalloprotease present on the surface of lipid droplets regulates chromosome condensation via Bre1 and/or Non-stop. Invadolysin also regulates Delta endocytosis possibly through its association with endosomes.

protease Non-stop. This interaction is reflected by similar phenotypes in the two mutants. Invadolysin together with Non-stop and Brel, might be regulating chromosome condensation and/or transcription via histone modifications. In addition, *Drosophila* Invadolysin might be regulating Delta, a ligand in the Notch pathway. Finally, I have shown that Invadolysin localizes to the surface of lipid droplets in human cells.

Future Work

More research needs to be carried out on all the aspects of this research to further understand molecular roles of Invadolysin. Regarding the interaction between Invadolysin and Non-stop, it will be important to see if Invadolysin interacts physically with Non-stop and/or Bre1. Non-stop, Bre1 and Invadolysin could be cloned into appropriate expression vectors and an *in vitro* binding assay could be performed to address this. The other way of doing this is to further characterize the antibodies mentioned in the Reagents Result Chapter (Chapter 7) or to generate new antibodies. FLAG-, GFP/RFP- or HA-tagged Invadolysin flies can also be used for the same purpose. Since Non-stop is associated with transcription via histone ubiquitination, histone modifications could be further studied in *invadolysin* and *non-stop* mutant backgrounds to analyse which modifications are affected specifically in the mutants.

Generating "conditional knock-down" flies using FLP/FRT or inducible RNAi technologies for *invadolysin* could be a useful tool to analyse Notch signalling at cellular level. One of the limitations with my study of Invadolysin and the Notch pathway was that all my experiments were done at a tissue or whole organism level. Studies at cellular level using mutant clones could help to narrow down the involvement of Invadolysin in the Notch pathway to a definitive step. Mutant clones could be stained for different Notch pathway proteins involved in the endocytosis of Delta to determine which protein is affected in *invadolysin* mutant background.

Another way to further study the interaction between Invadolysin and the Notch pathway is by overexpressing Invadolysin in fly organs. Invadolysin

overexpressing flies could be used in an enhancer/suppressor screen for genetic interactions between the Notch pathway and Invadolysin. Screening for interaction could also be done using the mutants of Invadolysin and the Notch pathway. Notch signalling is known to regulate cell migration (Six *et al.*, 2003). Thus the germ cell migration defect, seen in *Drosophila invadolysin* mutants, could be a consequence of Notch pathway aberrations.

Invadolysin localizing to the surface of the lipid droplets is an exciting discovery, which sheds light on unanticipated functions suggested by this localization. Lipid droplets could be isolated from *Drosophila* embryos, tissues or human cells following various treatments to analyse the effect of these reagents on the localization and activity of Invadolysin. Notch signalling is also known to affect lipid droplets, where intriguingly Notch 1 over-expression has been shown to increase lipid droplets in murine ST-2 cells promoting adipogenesis (Sciaudone *et al.*, 2003). The relationship between Notch signalling and lipid droplets has not been explored in any depth and would be an interesting direction for analysis.

Certain cancer cells are known to have increased lipid droplets (Ohsaki *et al.*, 2006). Normal vs. transformed tissues could be examined for the levels and localization of Invadolysin. The localization of Invadolysin is observed on most of the large number of lipid droplets observed in Huh7 cells (hepatocarcinoma). A comparative study of Invadolysin expression in normal liver cells vs. Huh7 cells could be carried out.

It would also be interesting to understand how lipid metabolism is affected in the presence or absence of Invadolysin. siRNA knock-down in cultured cells would

be the a method of choice for these studies. A triglyceride assay can be carried out in wt vs. mutant flies to determine if Invadolysin influences lipid storage and levels.

Considering the functional consequences of the loss of Invadolysin, it is possible that Invadolysin is playing a protein trafficking role at the surface of lipid droplets. Since lipid droplets are in dynamic association with endosomes, it could be possible that Invadolysin is regulating a membrane signalling receptor or ligand (such as Notch and Delta), which might transiently localize to the lipid droplets.

More evidence is being accumulated to show how one protein can be involved in diverse processes. For example, integrins, present on cell membranes, known to perform extra-cellular matrix functions and signalling activities, are now also are known to regulate centrosome function, assembly of the mitotic spindle and cytokinesis (Reverte *et al.*, 2006). Invadolysin might be such a protein regulating diverse processes such as endocytosis and chromosome condensation.

My PhD work has been a brief study of the functional roles of Invadolysin in various processes. More work needs to be carried out to establish clear molecular roles of Invadolysin. However, I believe that my studies have put forward a foundation and opened many avenues to study this versatile and essential metalloprotease, Invadolysin.

Bibliography

Adams, M.D., S.E. Celniker, R.A. Holt, C.A. Evans, J.D. Gocayne, P.G. Amanatides, S.E. Scherer, P.W. Li, R.A. Hoskins, R.F. Galle, R.A. George, S.E. Lewis, S. Richards, M. Ashburner, S.N. Henderson, G.G. Sutton, J.R. Wortman, M.D. Yandell, Q. Zhang, L.X. Chen, R.C. Brandon, Y.H. Rogers, R.G. Blazej, M. Champe, B.D. Pfeiffer, K.H. Wan, C. Doyle, E.G. Baxter, G. Helt, C.R. Nelson, G.L. Gabor, J.F. Abril, A. Agbayani, H.J. An, C. Andrews-Pfannkoch, D. Baldwin, R.M. Ballew, A. Basu, J. Baxendale, L. Bayraktaroglu, E.M. Beasley, K.Y. Beeson, P.V. Benos, B.P. Berman, D. Bhandari, S. Bolshakov, D. Borkova, M.R. Botchan, J. Bouck, P. Brokstein, P. Brottier, K.C. Burtis, D.A. Busam, H. Butler, E. Cadieu, A. Center, I. Chandra, J.M. Cherry, S. Cawley, C. Dahlke, L.B. Davenport, P. Davies, B. de Pablos, A. Delcher, Z. Deng, A.D. Mays, I. Dew, S.M. Dietz, K. Dodson, L.E. Doup, M. Downes, S. Dugan-Rocha, B.C. Dunkov, P. Dunn, K.J. Durbin, C.C. Evangelista, C. Ferraz, S. Ferriera, W. Fleischmann, C. Fosler, A.E. Gabrielian, N.S. Garg, W.M. Gelbart, K. Glasser, A. Glodek, F. Gong, J.H. Gorrell, Z. Gu, P. Guan, M. Harris, N.L. Harris, D. Harvey, T.J. Heiman, J.R. Hernandez, J. Houck, D. Hostin, K.A. Houston, T.J. Howland, M.H. Wei, C. Ibegwam, et al. 2000. The genome sequence of *Drosophila melanogaster*. *Science*. 287:2185-95.

Adams, R.R., M. Carmena, and W.C. Earnshaw. 2001. Chromosomal passengers and the (aurora) ABCs of mitosis. *Trends Cell Biol.* 11:49-54.

Alberts, B., D. Bray, J. Lewis, M. Raff, K. Roberts, and J.D. Watson. 1994. Molecular Biology of the Cell. Garland Publishing Inc., New York, United States of America.

Angers, A., A.R. Ramjaun, and P.S. McPherson. 2004. The HECT domain ligase itch ubiquitinates endophilin and localizes to the trans-Golgi network and endosomal system. *J Biol Chem*. 279:11471-9.

Ashburner, A., K.G. Golic, and R.S. Hawley. 2005. *Drosophila* A Laboratory handbook. Cold Spring Harbor Laboratory Press, Cold Spring Harbor, New York, United States of America.

Ault, J.G., and C.L. Rieder. 1994. Centrosome and kinetochore movement during mitosis. *Curr Opin Cell Biol.* 6:41-9.

Baldassarre, M., A. Pompeo, G. Beznoussenko, C. Castaldi, S. Cortellino, M.A. McNiven, A. Luini, and R. Buccione. 2003. Dynamin participates in focal extracellular matrix degradation by invasive cells. *Mol Biol Cell*. 14:1074-84.

Barbero, P., L. Bittova, and S.R. Pfeffer. 2002. Visualization of Rab9-mediated vesicle transport from endosomes to the trans-Golgi in living cells. *J Cell Biol*. 156:511-8.

Bardin, A.J., and F. Schweisguth. 2006. Bearded family members inhibit Neuralized-mediated endocytosis and signaling activity of Delta in Drosophila. *Dev Cell*. 10:245-55.

Baron, M. 2003. An overview of the Notch signalling pathway. *Semin Cell Dev Biol*. 14:113-9.

Bartz, R., J.K. Zehmer, M. Zhu, Y. Chen, G. Serrero, Y. Zhao, and P. Liu. 2007. Dynamic activity of lipid droplets: protein phosphorylation and GTP-mediated protein translocation. *J Proteome Res.* 6:3256-65.

Bate, M., and A.M. Arias. 1993. The development of *Drosophila melanogaster.* Cold Spring Harbor Laboratory Press, New York.

Beckman, M. 2006. Cell biology. Great balls of fat. *Science.* 311:1232-4.

Beller, M., D. Riedel, L. Jansch, G. Dieterich, J. Wehland, H. Jackle, and R.P. Kuhnlein. 2006. Characterization of the *Drosophila* lipid droplet subproteome. *Mol Cell Proteomics.* 5:1082-94.

Belmont, A.S. 2002. Mitotic chromosome scaffold structure: new approaches to an old controversy. *Proc Natl Acad Sci U S A.* 99:15855-7.

Belmont, A.S. 2006. Mitotic chromosome structure and condensation. *Curr Opin Cell Biol.* 18:632-8.

Belmont, A.S., and K. Bruce. 1994. Visualization of G1 chromosomes: a folded, twisted, supercoiled chromonema model of interphase chromatid structure. *J Cell Biol.* 127:287-302.

Berechid, B.E., M. Kitzmann, D.R. Foltz, A.H. Roach, D. Seiffert, L.A. Thompson, R.E. Olson, A. Bernstein, D.B. Donoviel, and J.S. Nye. 2002. Identification and characterization of presenilin-independent Notch signaling. *J Biol Chem.* 277:8154-65.

Bhat, M.A., A.V. Philp, D.M. Glover, and H.J. Bellen. 1996. Chromatid segregation at anaphase requires the barren product, a novel chromosome-associated protein that interacts with Topoisomerase II. *Cell.* 87:1103-14.

Binns, D., T. Januszewski, Y. Chen, J. Hill, V.S. Markin, Y. Zhao, C. Gilpin, K.D. Chapman, R.G. Anderson, and J.M. Goodman. 2006. An intimate collaboration between peroxisomes and lipid bodies. *J Cell Biol.* 173:719-31.

Blanchette-Mackie, E.J., N.K. Dwyer, T. Barber, R.A. Coxey, T. Takeda, C.M. Rondinone, J.L. Theodorakis, A.S. Greenberg, and C. Londos. 1995. Perilipin is located on the surface layer of intracellular lipid droplets in adipocytes. *J Lipid Res.* 36:1211-26.

Blow, J.J., and A. Dutta. 2005. Preventing re-replication of chromosomal DNA. *Nat Rev Mol Cell Biol.* 6:476-86.

Blow, J.J., and T.U. Tanaka. 2005. The chromosome cycle: coordinating replication and segregation. Second in the cycles review series. *EMBO Rep.* 6:1028-34.

Bonaccorsi, S., M.G. Giansanti, and M. Gatti. 2000. Spindle assembly in Drosophila neuroblasts and ganglion mother cells. *Nat Cell Biol.* 2:54-6.

Bonaldi, T., A. Imhof, and J.T. Regula. 2004. A combination of different mass spectroscopic techniques for the analysis of dynamic changes of histone modifications. *Proteomics.* 4:1382-96.

Borodovsky, A., B.M. Kessler, R. Casagrande, H.S. Overkleeft, K.D. Wilkinson, and H.L. Ploegh. 2001. A novel active site-directed probe specific for deubiquitylating enzymes reveals proteasome association of USP14. *Embo J.* 20:5187-96.

Bouvier, J., P. Schneider, and R. Etges. 1995. Leishmanolysin: surface metalloproteinase of *Leishmania. Methods Enzymol.* 248:614-33.

Brand, A.H., and N. Perrimon. 1993. Targeted gene expression as a means of altering cell fates and generating dominant phenotypes. *Development.* 118:401-15.

Brasaemle, D.L., G. Dolios, L. Shapiro, and R. Wang. 2004. Proteomic analysis of proteins associated with lipid droplets of basal and lipolytically stimulated 3T3-L1 adipocytes. *J Biol Chem*. 279:46835-42.

Brasaemle, D.L., B. Rubin, I.A. Harten, J. Gruia-Gray, A.R. Kimmel, and C. Londos. 2000. Perilipin A increases triacylglycerol storage by decreasing the rate of triacylglycerol hydrolysis. *J Biol Chem*. 275:38486-93.

Bray, S., H. Musisi, and M. Bienz. 2005. Bre1 is required for Notch signaling and histone modification. *Dev Cell*. 8:279-86.

Brou, C., F. Logeat, N. Gupta, C. Bessia, O. LeBail, J.R. Doedens, A. Cumano, P. Roux, R.A. Black, and A. Israel. 2000. A novel proteolytic cleavage involved in Notch signaling: the role of the disintegrin-metalloprotease TACE. *Mol Cell*. 5:207-16.

Buccione, R., J.D. Orth, and M.A. McNiven. 2004. Foot and mouth: podosomes, invadopodia and circular dorsal ruffles. *Nat Rev Mol Cell Biol*. 5:647-57.

Cermelli, S., Y. Guo, S.P. Gross, and M.A. Welte. 2006. The lipid-droplet proteome reveals that droplets are a protein-storage depot. *Curr Biol*. 16:1783-95.

Chitnis, A. 2006. Why is delta endocytosis required for effective activation of notch? *Dev Dyn*. 235:886-94.

Clague, M.J., and S. Urbe. 2006. Endocytosis: the DUB version. *Trends Cell Biol*. 16:551-9.

Clemens, J.C., C.A. Worby, N. Simonson-Leff, M. Muda, T. Maehama, B.A. Hemmings, and J.E. Dixon. 2000. Use of double-stranded RNA interference in *Drosophila* cell lines to dissect signal transduction pathways. *Proc Natl Acad Sci U S A*. 97:6499-503.

Cobbe, N., and M.M. Heck. 2000. Review: SMCs in the world of chromosome biology- from prokaryotes to higher eukaryotes. *J Struct Biol*. 129:123-43.

Corradin, S., A. Ransijn, G. Corradin, M.A. Roggero, A.A. Schmitz, P. Schneider, J. Mauel, and G. Vergeres. 1999. MARCKS-related protein (MRP) is a substrate for the Leishmania major surface protease leishmanolysin (gp63). *J Biol Chem*. 274:25411-8.

Coussens, L.M., B. Fingleton, and L.M. Matrisian. 2002. Matrix metalloproteinase inhibitors and cancer: trials and tribulations. *Science*. 295:2387-92.

Cupers, P., M. Bentahir, K. Craessaerts, I. Orlans, H. Vanderstichele, P. Saftig, B. De Strooper, and W. Annaert. 2001. The discrepancy between presenilin subcellular localization and gamma-secretase processing of amyloid precursor protein. *J Cell Biol*. 154:731-40.

Dai, J., S. Sultan, S.S. Taylor, and J.M. Higgins. 2005. The kinase haspin is required for mitotic histone H3 Thr 3 phosphorylation and normal metaphase chromosome alignment. *Genes Dev*. 19:472-88.

Dautry-Varsat, A. 1986. Receptor-mediated endocytosis: the intracellular journey of transferrin and its receptor. *Biochimie*. 68:375-81.

de la Pompa, J.L., A. Wakeham, K.M. Correia, E. Samper, S. Brown, R.J. Aguilera, T. Nakano, T. Honjo, T.W. Mak, J. Rossant, and R.A. Conlon. 1997. Conservation of the Notch signalling pathway in mammalian neurogenesis. *Development*. 124:1139-48.

Deblandre, G.A., E.C. Lai, and C. Kintner. 2001. *Xenopus* neuralized is a ubiquitin ligase that interacts with XDelta1 and regulates Notch signaling. *Dev Cell*. 1:795-806.

Desjeux, P. 2001. The increase in risk factors for leishmaniasis worldwide. *Trans R Soc Trop Med Hyg*. 95:239-43.
Diffley, J.F., and K. Labib. 2002. The chromosome replication cycle. *J Cell Sci*. 115:869-72.
Donoviel, D.B., A.K. Hadjantonakis, M. Ikeda, H. Zheng, P.S. Hyslop, and A. Bernstein. 1999. Mice lacking both presenilin genes exhibit early embryonic patterning defects. *Genes Dev*. 13:2801-10.
Doree, M., and T. Hunt. 2002. From Cdc2 to Cdk1: when did the cell cycle kinase join its cyclin partner? *J Cell Sci*. 115:2461-4.
Doxsey, S.J. 2001. Centrosomes as command centres for cellular control. *Nat Cell Biol*. 3:E105-8.
Duffy, J.B. 2002. GAL4 system in *Drosophila*: a fly geneticist's Swiss army knife. *Genesis*. 34:1-15.
Earnshaw, W.C., B. Halligan, C.A. Cooke, M.M. Heck, and L.F. Liu. 1985. Topoisomerase II is a structural component of mitotic chromosome scaffolds. *J Cell Biol*. 100:1706-15.
Earnshaw, W.C., and M.M. Heck. 1985. Localization of topoisomerase II in mitotic chromosomes. *J Cell Biol*. 100:1716-25.
Edenfeld, G., B. Altenhein, A. Zierau, D. Cleppien, K. Krukkert, G. Technau, and C. Klambt. 2007. Notch and Numb are required for normal migration of peripheral glia in *Drosophila*. *Dev Biol*. 301:27-37.
Egeblad, M., and Z. Werb. 2002. New functions for the matrix metalloproteinases in cancer progression. *Nat Rev Cancer*. 2:161-74.
Elledge, S.J. 1996. Cell cycle checkpoints: preventing an identity crisis. *Science*. 274:1664-72.
Emery, G., A. Hutterer, D. Berdnik, B. Mayer, F. Wirtz-Peitz, M.G. Gaitan, and J.A. Knoblich. 2005. Asymmetric Rab 11 endosomes regulate delta recycling and specify cell fate in the *Drosophila* nervous system. *Cell*. 122:763-73.
Emre, N.C., K. Ingvarsdottir, A. Wyce, A. Wood, N.J. Krogan, K.W. Henry, K. Li, R. Marmorstein, J.F. Greenblatt, A. Shilatifard, and S.L. Berger. 2005. Maintenance of low histone ubiquitylation by Ubp10 correlates with telomere-proximal Sir2 association and gene silencing. *Mol Cell*. 17:585-94.
Etges, R. 1992. Identification of a surface metalloproteinase on 13 species of *Leishmania* isolated from humans, *Crithidia fasciculata*, and *Herpetomonas samuelpessoai*. *Acta Trop*. 50:205-17.
Feany, M.B., and W.W. Bender. 2000. A Drosophila model of Parkinson's disease. *Nature*. 404:394-8.
Fischle, W., B.S. Tseng, H.L. Dormann, B.M. Ueberheide, B.A. Garcia, J. Shabanowitz, D.F. Hunt, H. Funabiki, and C.D. Allis. 2005. Regulation of HP1-chromatin binding by histone H3 methylation and phosphorylation. *Nature*. 438:1116-22.
Flemming, W. 1879. Ueber das Verhalten des Kerns bei der Zellteilung und über die Bedeutung mehrkerniger Zellen. *Arch. Pathol. Anat.* 77:1-28.
Foe, V.E. 1989. Mitotic domains reveal early commitment of cells in Drosophila embryos. *Development*. 107:1-22.
Fostier, M., D.A. Evans, S. Artavanis-Tsakonas, and M. Baron. 1998. Genetic characterization of the Drosophila melanogaster Suppressor of deltex gene: A regulator of notch signaling. *Genetics*. 150:1477-85.

Frise, E., J.A. Knoblich, S. Younger-Shepherd, L.Y. Jan, and Y.N. Jan. 1996. The Drosophila Numb protein inhibits signaling of the Notch receptor during cell-cell interaction in sensory organ lineage. *Proc Natl Acad Sci U S A.* 93:11925-32.

Fryer, C.J., E. Lamar, I. Turbachova, C. Kintner, and K.A. Jones. 2002. Mastermind mediates chromatin-specific transcription and turnover of the Notch enhancer complex. *Genes Dev.* 16:1397-411.

Fujimoto, Y., H. Itabe, J. Sakai, M. Makita, J. Noda, M. Mori, Y. Higashi, S. Kojima, and T. Takano. 2004. Identification of major proteins in the lipid droplet-enriched fraction isolated from the human hepatocyte cell line HuH7. *Biochim Biophys Acta.* 1644:47-59.

Fuller, M.T., C.L. Regan, L.L. Green, B. Robertson, R. Deuring, and T.S. Hays. 1989. Interacting genes identify interacting proteins involved in microtubule function in *Drosophila. Cell Motil Cytoskeleton.* 14:128-35.

Gao, J., and G. Serrero. 1999. Adipose differentiation related protein (ADRP) expressed in transfected COS-7 cells selectively stimulates long chain fatty acid uptake. *J Biol Chem.* 274:16825-30.

Gasser, S.M., T. Laroche, J. Falquet, E. Boy de la Tour, and U.K. Laemmli. 1986. Metaphase chromosome structure. Involvement of topoisomerase II. *J Mol Biol.* 188:613-29.

Gassmann, R., A. Carvalho, A.J. Henzing, S. Ruchaud, D.F. Hudson, R. Honda, E.A. Nigg, D.L. Gerloff, and W.C. Earnshaw. 2004. Borealin: a novel chromosomal passenger required for stability of the bipolar mitotic spindle. *J Cell Biol.* 166:179-91.

Gatti, M., and B.S. Baker. 1989. Genes controlling essential cell-cycle functions in *Drosophila melanogaster. Genes Dev.* 3:438-53.

Gerbi, S.A., and A.K. Bielinsky. 2002. DNA replication and chromatin. *Curr Opin Genet Dev.* 12:243-8.

Giot, L., J.S. Bader, C. Brouwer, A. Chaudhuri, B. Kuang, Y. Li, Y.L. Hao, C.E. Ooi, B. Godwin, E. Vitols, G. Vijayadamodar, P. Pochart, H. Machineni, M. Welsh, Y. Kong, B. Zerhusen, R. Malcolm, Z. Varrone, A. Collis, M. Minto, S. Burgess, L. McDaniel, E. Stimpson, F. Spriggs, J. Williams, K. Neurath, N. Ioime, M. Agee, E. Voss, K. Furtak, R. Renzulli, N. Aanensen, S. Carrolla, E. Bickelhaupt, Y. Lazovatsky, A. DaSilva, J. Zhong, C.A. Stanyon, R.L. Finley, Jr., K.P. White, M. Braverman, T. Jarvie, S. Gold, M. Leach, J. Knight, R.A. Shimkets, M.P. McKenna, J. Chant, and J.M. Rothberg. 2003. A protein interaction map of *Drosophila melanogaster. Science.* 302:1727-36.

Girard, F., B. Bello, U.K. Laemmli, and W.J. Gehring. 1998. In vivo analysis of scaffold-associated regions in *Drosophila*: a synthetic high-affinity SAR binding protein suppresses position effect variegation. *Embo J.* 17:2079-85.

Gomis-Ruth, F.X. 2003. Structural aspects of the metzincin clan of metalloendopeptidases. *Mol Biotechnol.* 24:157-202.

Grant, P.A., L. Duggan, J. Cote, S.M. Roberts, J.E. Brownell, R. Candau, R. Ohba, T. Owen-Hughes, C.D. Allis, F. Winston, S.L. Berger, and J.L. Workman. 1997. Yeast Gcn5 functions in two multisubunit complexes to acetylate nucleosomal histones: characterization of an Ada complex and the SAGA (Spt/Ada) complex. *Genes Dev.* 11:1640-50.

Greenspan, R.J. 1997. Fly Pushing: The Theory and Practice of *Drosophila* Genetics. Cold Spring Harbor Laboratory Press, Cold Spring Harbor, New York, United States of America.

Gross, J., and C.M. Lapiere. 1962. Collagenolytic activity in amphibian tissues: a tissue culture assay. *Proc Natl Acad Sci U S A*. 48:1014-22.

Gruber, S., C.H. Haering, and K. Nasmyth. 2003. Chromosomal cohesin forms a ring. *Cell*. 112:765-77.

Guacci, V. 2007. Sister chromatid cohesion: the cohesin cleavage model does not ring true. *Genes Cells*. 12:693-708.

Guacci, V., D. Koshland, and A. Strunnikov. 1997. A direct link between sister chromatid cohesion and chromosome condensation revealed through the analysis of MCD1 in S. cerevisiae. *Cell*. 91:47-57.

Gupta-Rossi, N., O. Le Bail, H. Gonen, C. Brou, F. Logeat, E. Six, A. Ciechanover, and A. Israel. 2001. Functional interaction between SEL-10, an F-box protein, and the nuclear form of activated Notch1 receptor. *J Biol Chem*. 276:34371-8.

Gupta-Rossi, N., E. Six, O. LeBail, F. Logeat, P. Chastagner, A. Olry, A. Israel, and C. Brou. 2004. Monoubiquitination and endocytosis direct gamma-secretase cleavage of activated Notch receptor. *J Cell Biol*. 166:73-83.

Haass, C., and B. De Strooper. 1999. The presenilins in Alzheimer's disease--proteolysis holds the key. *Science*. 286:916-9.

Haering, C.H., J. Lowe, A. Hochwagen, and K. Nasmyth. 2002. Molecular architecture of SMC proteins and the yeast cohesin complex. *Mol Cell*. 9:773-88.

Handsley, M.M., and D.R. Edwards. 2005. Metalloproteinases and their inhibitors in tumor angiogenesis. *Int J Cancer*. 115:849-60.

Hays, T.S., R. Deuring, B. Robertson, M. Prout, and M.T. Fuller. 1989. Interacting proteins identified by genetic interactions: a missense mutation in alpha-tubulin fails to complement alleles of the testis-specific beta-tubulin gene of Drosophila melanogaster. *Mol Cell Biol*. 9:875-84.

Heck, M.M. 1997. Condensins, cohesins, and chromosome architecture: how to make and break a mitotic chromosome. *Cell*. 91:5-8.

Heck, M.M., A. Pereira, P. Pesavento, Y. Yannoni, A.C. Spradling, and L.S. Goldstein. 1993. The kinesin-like protein KLP61F is essential for mitosis in Drosophila. *J Cell Biol*. 123:665-79.

Henry, K.W., A. Wyce, W.S. Lo, L.J. Duggan, N.C. Emre, C.F. Kao, L. Pillus, A. Shilatifard, M.A. Osley, and S.L. Berger. 2003. Transcriptional activation via sequential histone H2B ubiquitylation and deubiquitylation, mediated by SAGA-associated Ubp8. *Genes Dev*. 17:2648-63.

Hirano, T. 2002. The ABCs of SMC proteins: two-armed ATPases for chromosome condensation, cohesion, and repair. *Genes Dev*. 16:399-414.

Hirano, T., R. Kobayashi, and M. Hirano. 1997. Condensins, chromosome condensation protein complexes containing XCAP-C, XCAP-E and a Xenopus homolog of the *Drosophila* Barren protein. *Cell*. 89:511-21.

Hirano, T., and T.J. Mitchison. 1994. A heterodimeric coiled-coil protein required for mitotic chromosome condensation in vitro. *Cell*. 79:449-58.

Hirota, T., D. Gerlich, B. Koch, J. Ellenberg, and J.M. Peters. 2004. Distinct functions of condensin I and II in mitotic chromosome assembly. *J Cell Sci.* 117:6435-45.

Hofmann, I., and S. Munro. 2006. An N-terminally acetylated Arf-like GTPase is localised to lysosomes and affects their motility. *J Cell Sci.* 119:1494-503.

Hooper, N.M. 1994. Families of zinc metalloproteases. *FEBS Lett.* 354:1-6.

Hu, M., P. Li, L. Song, P.D. Jeffrey, T.A. Chenova, K.D. Wilkinson, R.E. Cohen, and Y. Shi. 2005. Structure and mechanisms of the proteasome-associated deubiquitinating enzyme USP14. *Embo J.* 24:3747-56.

Hudson, D.F., P. Vagnarelli, R. Gassmann, and W.C. Earnshaw. 2003. Condensin is required for nonhistone protein assembly and structural integrity of vertebrate mitotic chromosomes. *Dev Cell.* 5:323-36.

Hwang, W.W., S. Venkatasubrahmanyam, A.G. Ianculescu, A. Tong, C. Boone, and H.D. Madhani. 2003. A conserved RING finger protein required for histone H2B monoubiquitination and cell size control. *Mol Cell.* 11:261-6.

Imamura, M., T. Inoguchi, S. Ikuyama, S. Taniguchi, K. Kobayashi, N. Nakashima, and H. Nawata. 2002. ADRP stimulates lipid accumulation and lipid droplet formation in murine fibroblasts. *Am J Physiol Endocrinol Metab.* 283:E775-83.

Irniger, S. 2002. Cyclin destruction in mitosis: a crucial task of Cdc20. *FEBS Lett.* 532:7-11.

Ito, T. 2007. Role of histone modification in chromatin dynamics. *J Biochem (Tokyo).* 141:609-14.

Jennings, B., A. Preiss, C. Delidakis, and S. Bray. 1994. The Notch signalling pathway is required for Enhancer of split bHLH protein expression during neurogenesis in the Drosophila embryo. *Development.* 120:3537-48.

Jiang, H., J. He, S. Pu, C. Tang, and G. Xu. 2007. Heat shock protein 70 is translocated to lipid droplets in rat adipocytes upon heat stimulation. *Biochim Biophys Acta.* 1771:66-74.

Kadesch, T. 2004. Notch signaling: the demise of elegant simplicity. *Curr Opin Genet Dev.* 14:506-12.

Kee, Y., N. Lyon, and J.M. Huibregtse. 2005. The Rsp5 ubiquitin ligase is coupled to and antagonized by the Ubp2 deubiquitinating enzyme. *Embo J.* 24:2414-24.

Kennerdell, J.R., and R.W. Carthew. 1998. Use of dsRNA-mediated genetic interference to demonstrate that frizzled and frizzled 2 act in the wingless pathway. *Cell.* 95:1017-26.

Kidd, S., and T. Lieber. 2002. Furin cleavage is not a requirement for *Drosophila* Notch function. *Mech Dev.* 115:41-51.

Konopka, C.A., J.B. Schleede, A.R. Skop, and S.Y. Bednarek. 2006. Dynamin and cytokinesis. *Traffic.* 7:239-47.

Koo, B.K., K.J. Yoon, K.W. Yoo, H.S. Lim, R. Song, J.H. So, C.H. Kim, and Y.Y. Kong. 2005. Mind bomb-2 is an E3 ligase for Notch ligand. *J Biol Chem.* 280:22335-42.

Kouzarides, T. 2007. Chromatin modifications and their function. *Cell.* 128:693-705.

Krause, S.A., M.L. Loupart, S. Vass, S. Schoenfelder, S. Harrison, and M.M. Heck. 2001. Loss of cell cycle checkpoint control in *Drosophila* Rfc4 mutants. *Mol Cell Biol.* 21:5156-68.

Kruchten, A.E., and M.A. McNiven. 2006. Dynamin as a mover and pincher during cell migration and invasion. *J Cell Sci.* 119:1683-90.

Lai, E.C. 2002. Protein degradation: four E3s for the notch pathway. *Curr Biol.* 12:R74-8.

Lam, G., and C.S. Thummel. 2000. Inducible expression of double-stranded RNA directs specific genetic interference in *Drosophila*. *Curr Biol.* 10:957-63.

Le Borgne, R., and F. Schweisguth. 2003. Notch signaling: endocytosis makes delta signal better. *Curr Biol.* 13:R273-5.

Lee, K.K., L. Florens, S.K. Swanson, M.P. Washburn, and J.L. Workman. 2005. The deubiquitylation activity of Ubp8 is dependent upon Sgf11 and its association with the SAGA complex. *Mol Cell Biol.* 25:1173-82.

Lee, L.A., L.K. Elfring, G. Bosco, and T.L. Orr-Weaver. 2001. A genetic screen for suppressors and enhancers of the *Drosophila* PAN GU cell cycle kinase identifies cyclin B as a target. *Genetics.* 158:1545-56.

Leopold, P., and N. Perrimon. 2007. Drosophila and the genetics of the internal milieu. *Nature.* 450:186-8.

Levitan, D., and I. Greenwald. 1995. Facilitation of lin-12-mediated signalling by sel-12, a *Caenorhabditis elegans* S182 Alzheimer's disease gene. *Nature.* 377:351-4.

Lewis, C.D., and U.K. Laemmli. 1982. Higher order metaphase chromosome structure: evidence for metalloprotein interactions. *Cell.* 29:171-81.

Li, Y., and N.E. Baker. 2004. The roles of cis-inactivation by Notch ligands and of neuralized during eye and bristle patterning in Drosophila. *BMC Dev Biol.* 4:5.

Liu, P., Y. Ying, Y. Zhao, D.I. Mundy, M. Zhu, and R.G. Anderson. 2004. Chinese hamster ovary K2 cell lipid droplets appear to be metabolic organelles involved in membrane traffic. *J Biol Chem.* 279:3787-92.

Llano, E., G. Adam, A.M. Pendas, V. Quesada, L.M. Sanchez, I. Santamaria, S. Noselli, and C. Lopez-Otin. 2002. Structural and enzymatic characterization of *Drosophila* Dm2-MMP, a membrane-bound matrix metalloproteinase with tissue-specific expression. *J Biol Chem.* 277:23321-9.

Llano, E., A.M. Pendas, P. Aza-Blanc, T.B. Kornberg, and C. Lopez-Otin. 2000. Dm1-MMP, a matrix metalloproteinase from *Drosophila* with a potential role in extracellular matrix remodeling during neural development. *J Biol Chem.* 275:35978-85.

Logeat, F., C. Bessia, C. Brou, O. LeBail, S. Jarriault, N.G. Seidah, and A. Israel. 1998. The Notch1 receptor is cleaved constitutively by a furin-like convertase. *Proc Natl Acad Sci U S A.* 95:8108-12.

Losada, A., and T. Hirano. 2001. Shaping the metaphase chromosome: coordination of cohesion and condensation. *Bioessays.* 23:924-35.

Loupart, M.L., S.A. Krause, and M.S. Heck. 2000. Aberrant replication timing induces defective chromosome condensation in *Drosophila* ORC2 mutants. *Curr Biol.* 10:1547-56.

Lucchesi, J.C. 1968. Synthetic lethality and semi-lethality among functionally related mutants of Drosophila melanfgaster. *Genetics.* 59:37-44.

Lukas, J., C. Lukas, and J. Bartek. 2004. Mammalian cell cycle checkpoints: signalling pathways and their organization in space and time. *DNA Repair (Amst).* 3:997-1007.

MacCallum, D.E., A. Losada, R. Kobayashi, and T. Hirano. 2002. ISWI remodeling complexes in Xenopus egg extracts: identification as major chromosomal components that are regulated by INCENP-aurora B. *Mol Biol Cell.* 13:25-39.

Maresca, T.J., and R. Heald. 2006. The long and the short of it: linker histone H1 is required for metaphase chromosome compaction. *Cell Cycle.* 5:589-91.

Martin, K.A., B. Poeck, H. Roth, A.J. Ebens, L.C. Ballard, and S.L. Zipursky. 1995. Mutations disrupting neuronal connectivity in the Drosophila visual system. *Neuron.* 14:229-40.

Martin, S., K. Driessen, S.J. Nixon, M. Zerial, and R.G. Parton. 2005. Regulated localization of Rab18 to lipid droplets: effects of lipolytic stimulation and inhibition of lipid droplet catabolism. *J Biol Chem.* 280:42325-35.

Martin, S., and R.G. Parton. 2005. Caveolin, cholesterol, and lipid bodies. *Semin Cell Dev Biol.* 16:163-74.

Martin, S., and R.G. Parton. 2006. Lipid droplets: a unified view of a dynamic organelle. *Nat Rev Mol Cell Biol.* 7:373-8.

Matesic, L.E., D.C. Haines, N.G. Copeland, and N.A. Jenkins. 2006. Itch genetically interacts with Notch1 in a mouse autoimmune disease model. *Hum Mol Genet.* 15:3485-97.

McGuire, S.E., G. Roman, and R.L. Davis. 2004. Gene expression systems in *Drosophila*: a synthesis of time and space. *Trends Genet.* 20:384-91.

McHugh, B., S.A. Krause, B. Yu, A.M. Deans, S. Heasman, P. McLaughlin, and M.M. Heck. 2004. Invadolysin: a novel, conserved metalloprotease links mitotic structural rearrangements with cell migration. *J Cell Biol.* 167:673-86.

Micchelli, C.A., E.J. Rulifson, and S.S. Blair. 1997. The function and regulation of cut expression on the wing margin of Drosophila: Notch, Wingless and a dominant negative role for Delta and Serrate. *Development.* 124:1485-95.

Minakhina, S., and R. Steward. 2006. Melanotic mutants in *Drosophila*: pathways and phenotypes. *Genetics.* 174:253-63.

Mirkovitch, J., M.E. Mirault, and U.K. Laemmli. 1984. Organization of the higher-order chromatin loop: specific DNA attachment sites on nuclear scaffold. *Cell.* 39:223-32.

Miura, S., J.W. Gan, J. Brzostowski, M.J. Parisi, C.J. Schultz, C. Londos, B. Oliver, and A.R. Kimmel. 2002. Functional conservation for lipid storage droplet association among Perilipin, ADRP, and TIP47 (PAT)-related proteins in mammals, *Drosophila*, and *Dictyostelium*. *J Biol Chem.* 277:32253-7.

Miyanari, Y., K. Atsuzawa, N. Usuda, K. Watashi, T. Hishiki, M. Zayas, R. Bartenschlager, T. Wakita, M. Hijikata, and K. Shimotohno. 2007. The lipid droplet is an important organelle for hepatitis C virus production. *Nat Cell Biol.* 9:1089-97.

Miyanari, Y., M. Hijikata, M. Yamaji, M. Hosaka, H. Takahashi, and K. Shimotohno. 2003. Hepatitis C virus non-structural proteins in the probable membranous compartment function in viral genome replication. *J Biol Chem.* 278:50301-8.

Montesano, R., J. Roth, A. Robert, and L. Orci. 1982. Non-coated membrane invaginations are involved in binding and internalization of cholera and tetanus toxins. *Nature.* 296:651-3.

Morgan, D.O. 1997. Cyclin-dependent kinases: engines, clocks, and microprocessors. *Annu Rev Cell Dev Biol.* 13:261-91.

Muller, G., S. Over, S. Wied, and W. Frick. 2008. Association of (c)AMP-Degrading Glycosylphosphatidylinositol-Anchored Proteins with Lipid Droplets Is Induced by Palmitate, H(2)O(2) and the Sulfonylurea Drug, Glimepiride, in Rat Adipocytes. *Biochemistry.*

Mumm, J.S., and R. Kopan. 2000. Notch signaling: from the outside in. *Dev Biol.* 228:151-65.

Murphy, D.J. 2001. The biogenesis and functions of lipid bodies in animals, plants and microorganisms. *Prog Lipid Res.* 40:325-438.

Murray, H.W., J.D. Berman, C.R. Davies, and N.G. Saravia. 2005. Advances in leishmaniasis. *Lancet.* 366:1561-77.

Nakamura, N., Y. Banno, and K. Tamiya-Koizumi. 2005. Arf1-dependent PLD1 is localized to oleic acid-induced lipid droplets in NIH3T3 cells. *Biochem Biophys Res Commun.* 335:117-23.

Ng, H.H., R.M. Xu, Y. Zhang, and K. Struhl. 2002. Ubiquitination of histone H2B by Rad6 is required for efficient Dot1-mediated methylation of histone H3 lysine 79. *J Biol Chem.* 277:34655-7.

Nijman, S.M., M.P. Luna-Vargas, A. Velds, T.R. Brummelkamp, A.M. Dirac, T.K. Sixma, and R. Bernards. 2005. A genomic and functional inventory of deubiquitinating enzymes. *Cell.* 123:773-86.

Nusslein-Volhard, C., and E. Wieschaus. 1980. Mutations affecting segment number and polarity in *Drosophila. Nature.* 287:795-801.

Ohsaki, Y., J. Cheng, A. Fujita, T. Tokumoto, and T. Fujimoto. 2006. Cytoplasmic lipid droplets are sites of convergence of proteasomal and autophagic degradation of apolipoprotein B. *Mol Biol Cell.* 17:2674-83.

Ohsaki, Y., T. Maeda, and T. Fujimoto. 2005. Fixation and permeabilization protocol is critical for the immunolabeling of lipid droplet proteins. *Histochem Cell Biol.* 124:445-52.

Ooi, S.L., X. Pan, B.D. Peyser, P. Ye, P.B. Meluh, D.S. Yuan, R.A. Irizarry, J.S. Bader, F.A. Spencer, and J.D. Boeke. 2006. Global synthetic-lethality analysis and yeast functional profiling. *Trends Genet.* 22:56-63.

Ostermeyer, A.G., L.T. Ramcharan, Y. Zeng, D.M. Lublin, and D.A. Brown. 2004. Role of the hydrophobic domain in targeting caveolin-1 to lipid droplets. *J Cell Biol.* 164:69-78.

Overstreet, E., X. Chen, B. Wendland, and J.A. Fischer. 2003. Either part of a Drosophila epsin protein, divided after the ENTH domain, functions in endocytosis of delta in the developing eye. *Curr Biol.* 13:854-60.

Overstreet, E., E. Fitch, and J.A. Fischer. 2004. Fat facets and Liquid facets promote Delta endocytosis and Delta signaling in the signaling cells. *Development.* 131:5355-66.

Ozeki, S., J. Cheng, K. Tauchi-Sato, N. Hatano, H. Taniguchi, and T. Fujimoto. 2005. Rab18 localizes to lipid droplets and induces their close apposition to the endoplasmic reticulum-derived membrane. *J Cell Sci.* 118:2601-11.

Page-McCaw, A. 2007. Remodeling the model organism: Matrix metalloproteinase functions in invertebrates. *Semin Cell Dev Biol.*

Page-McCaw, A., A.J. Ewald, and Z. Werb. 2007. Matrix metalloproteinases and the regulation of tissue remodelling. *Nat Rev Mol Cell Biol.* 8:221-33.

Page-McCaw, A., J. Serano, J.M. Sante, and G.M. Rubin. 2003. *Drosophila* matrix metalloproteinases are required for tissue remodeling, but not embryonic development. *Dev Cell*. 4:95-106.

Pan, D., and G.M. Rubin. 1997. Kuzbanian controls proteolytic processing of Notch and mediates lateral inhibition during *Drosophila* and vertebrate neurogenesis. *Cell*. 90:271-80.

Panakova, D., H. Sprong, E. Marois, C. Thiele, and S. Eaton. 2005. Lipoprotein particles are required for Hedgehog and Wingless signalling. *Nature*. 435:58-65.

Parks, A.L., K.M. Klueg, J.R. Stout, and M.A. Muskavitch. 2000. Ligand endocytosis drives receptor dissociation and activation in the Notch pathway. *Development*. 127:1373-85.

Parton, R.G., and K. Simons. 2007. The multiple faces of caveolae. *Nat Rev Mol Cell Biol*. 8:185-94.

Paulson, J.R., and U.K. Laemmli. 1977. The structure of histone-depleted metaphase chromosomes. *Cell*. 12:817-28.

Pender, S.L., and T.T. MacDonald. 2004. Matrix metalloproteinases and the gut - new roles for old enzymes. *Curr Opin Pharmacol*. 4:546-50.

Pflumm, M.F. 2002. The role of DNA replication in chromosome condensation. *Bioessays*. 24:411-8.

Pintar, A., A. De Biasio, M. Popovic, N. Ivanova, and S. Pongor. 2007. The intracellular region of Notch ligands: does the tail make the difference? *Biol Direct*. 2:19.

Poeck, B., S. Fischer, D. Gunning, S.L. Zipursky, and I. Salecker. 2001. Glial cells mediate target layer selection of retinal axons in the developing visual system of Drosophila. *Neuron*. 29:99-113.

Pol, A., R. Luetterforst, M. Lindsay, S. Heino, E. Ikonen, and R.G. Parton. 2001. A caveolin dominant negative mutant associates with lipid bodies and induces intracellular cholesterol imbalance. *J Cell Biol*. 152:1057-70.

Pollard, T.D., and W.C. Earnshaw. 2007. Cell Biology. SAUNDERS, An imprint of Elsevier Science, Philadelphia, United States of America.

Puente, X.S., and C. Lopez-Otin. 2004. A genomic analysis of rat proteases and protease inhibitors. *Genome Res*. 14:609-22.

Puig, O., F. Caspary, G. Rigaut, B. Rutz, E. Bouveret, E. Bragado-Nilsson, M. Wilm, and B. Seraphin. 2001. The tandem affinity purification (TAP) method: a general procedure of protein complex purification. *Methods*. 24:218-29.

Rawlings, N.D., F.R. Morton, C.Y. Kok, J. Kong, and A.J. Barrett. 2008. MEROPS: the peptidase database. *Nucleic Acids Res*. 36:D320-5.

Reiter, L.T., L. Potocki, S. Chien, M. Gribskov, and E. Bier. 2001. A systematic analysis of human disease-associated gene sequences in Drosophila melanogaster. *Genome Res*. 11:1114-25.

Reverte, C.G., A. Benware, C.W. Jones, and S.E. LaFlamme. 2006. Perturbing integrin function inhibits microtubule growth from centrosomes, spindle assembly, and cytokinesis. *J Cell Biol*. 174:491-7.

Robenek, H., M.J. Robenek, and D. Troyer. 2005. PAT family proteins pervade lipid droplet cores. *J Lipid Res*. 46:1331-8.

Robenek, M.J., N.J. Severs, K. Schlattmann, G. Plenz, K.P. Zimmer, D. Troyer, and H. Robenek. 2004. Lipids partition caveolin-1 from ER membranes into lipid droplets: updating the model of lipid droplet biogenesis. *Faseb J.* 18:866-8.

Roberts, D.B. 1998. *Drosophila* A Practical approach. Oxford University Press Inc., New York, United States of America.

Rooke, J., D. Pan, T. Xu, and G.M. Rubin. 1996. KUZ, a conserved metalloprotease-disintegrin protein with two roles in *Drosophila* neurogenesis. *Science.* 273:1227-31.

Russell, D.G., and H. Wilhelm. 1986. The involvement of the major surface glycoprotein (gp63) of *Leishmania* promastigotes in attachment to macrophages. *J Immunol.* 136:2613-20.

Ryder, E., M. Ashburner, R. Bautista-Llacer, J. Drummond, J. Webster, G. Johnson, T. Morley, Y.S. Chan, F. Blows, D. Coulson, G. Reuter, H. Baisch, C. Apelt, A. Kauk, T. Rudolph, M. Kube, M. Klimm, C. Nickel, J. Szidonya, P. Maroy, M. Pal, A. Rasmuson-Lestander, K. Ekstrom, H. Stocker, C. Hugentobler, E. Hafen, D. Gubb, G. Pflugfelder, C. Dorner, B. Mechler, H. Schenkel, J. Marhold, F. Serras, M. Corominas, A. Punset, J. Roote, and S. Russell. 2007. The DrosDel Deletion Collection: A *Drosophila* Genomewide Chromosomal Deficiency Resource. *Genetics.* 177:615-29.

Ryder, E., F. Blows, M. Ashburner, R. Bautista-Llacer, D. Coulson, J. Drummond, J. Webster, D. Gubb, N. Gunton, G. Johnson, C.J. O'Kane, D. Huen, P. Sharma, Z. Asztalos, H. Baisch, J. Schulze, M. Kube, K. Kittlaus, G. Reuter, P. Maroy, J. Szidonya, A. Rasmuson-Lestander, K. Ekstrom, B. Dickson, C. Hugentobler, H. Stocker, E. Hafen, J.A. Lepesant, G. Pflugfelder, M. Heisenberg, B. Mechler, F. Serras, M. Corominas, S. Schneuwly, T. Preat, J. Roote, and S. Russell. 2004. The DrosDel collection: a set of P-element insertions for generating custom chromosomal aberrations in *Drosophila melanogaster. Genetics.* 167:797-813.

Saitoh, N., I.G. Goldberg, E.R. Wood, and W.C. Earnshaw. 1994. ScII: an abundant chromosome scaffold protein is a member of a family of putative ATPases with an unusual predicted tertiary structure. *J Cell Biol.* 127:303-18.

Savvidou, E., N. Cobbe, S. Steffensen, S. Cotterill, and M.M. Heck. 2005. Drosophila CAP-D2 is required for condensin complex stability and resolution of sister chromatids. *J Cell Sci.* 118:2529-43.

Schlagenhauf, E., R. Etges, and P. Metcalf. 1998. The crystal structure of the *Leishmania* major surface proteinase leishmanolysin (gp63). *Structure.* 6:1035-46.

Schneider, R., A.J. Bannister, F.A. Myers, A.W. Thorne, C. Crane-Robinson, and T. Kouzarides. 2004. Histone H3 lysine 4 methylation patterns in higher eukaryotic genes. *Nat Cell Biol.* 6:73-7.

Schweisguth, F. 1999. Dominant-negative mutation in the beta2 and beta6 proteasome subunit genes affect alternative cell fate decisions in the Drosophila sense organ lineage. *Proc Natl Acad Sci U S A.* 96:11382-6.

Schweisguth, F. 2004. Regulation of notch signaling activity. *Curr Biol.* 14:R129-38.

Sciaudone, M., E. Gazzerro, L. Priest, A.M. Delany, and E. Canalis. 2003. Notch 1 impairs osteoblastic cell differentiation. *Endocrinology.* 144:5631-9.

Seki, T., and J.F. Diffley. 2000. Stepwise assembly of initiation proteins at budding yeast replication origins in vitro. *Proc Natl Acad Sci U S A.* 97:14115-20.

Semple, C.A. 2003. The comparative proteomics of ubiquitination in mouse. *Genome Res.* 13:1389-94.

Seugnet, L., P. Simpson, and M. Haenlin. 1997. Requirement for dynamin during Notch signaling in Drosophila neurogenesis. *Dev Biol.* 192:585-98.

Shahbazian, M.D., K. Zhang, and M. Grunstein. 2005. Histone H2B ubiquitylation controls processive methylation but not monomethylation by Dot1 and Set1. *Mol Cell.* 19:271-7.

Shearn, A., T. Rice, A. Garen, and W. Gehring. 1971. Imaginal disc abnormalities in lethal mutants of *Drosophila. Proc Natl Acad Sci U S A.* 68:2594-8.

Shi, S.T., S.J. Polyak, H. Tu, D.R. Taylor, D.R. Gretch, and M.M. Lai. 2002. Hepatitis C virus NS5A colocalizes with the core protein on lipid droplets and interacts with apolipoproteins. *Virology.* 292:198-210.

Shogren-Knaak, M., H. Ishii, J.M. Sun, M.J. Pazin, J.R. Davie, and C.L. Peterson. 2006. Histone H4-K16 acetylation controls chromatin structure and protein interactions. *Science.* 311:844-7.

Six, E., D. Ndiaye, Y. Laabi, C. Brou, N. Gupta-Rossi, A. Israel, and F. Logeat. 2003. The Notch ligand Delta1 is sequentially cleaved by an ADAM protease and gamma-secretase. *Proc Natl Acad Sci U S A.* 100:7638-43.

Slootstra, J.W., W.C. Puijk, G.J. Ligtvoet, D. Kuperus, W.M. Schaaper, and R.H. Meloen. 1997. Screening of a small set of random peptides: a new strategy to identify synthetic peptides that mimic epitopes. *J Mol Recognit.* 10:217-24.

Smirnova, E., E.B. Goldberg, K.S. Makarova, L. Lin, W.J. Brown, and C.L. Jackson. 2006. ATGL has a key role in lipid droplet/adiposome degradation in mammalian cells. *EMBO Rep.* 7:106-13.

Soboleva, T.A., and R.T. Baker. 2004. Deubiquitinating enzymes: their functions and substrate specificity. *Curr Protein Pept Sci.* 5:191-200.

Spradling, A.C., D. Stern, A. Beaton, E.J. Rhem, T. Laverty, N. Mozden, S. Misra, and G.M. Rubin. 1999. The Berkeley *Drosophila* Genome Project gene disruption project: Single P-element insertions mutating 25% of vital *Drosophila* genes. *Genetics.* 153:135-77.

St Johnston, D. 2002. The art and design of genetic screens: *Drosophila melanogaster. Nat Rev Genet.* 3:176-88.

Stocker, W., F. Grams, U. Baumann, P. Reinemer, F.X. Gomis-Ruth, D.B. McKay, and W. Bode. 1995. The metzincins--topological and sequential relations between the astacins, adamalysins, serralysins, and matrixins (collagenases) define a superfamily of zinc-peptidases. *Protein Sci.* 4:823-40.

Strahl, B.D., and C.D. Allis. 2000. The language of covalent histone modifications. *Nature.* 403:41-5.

Strick, R., and U.K. Laemmli. 1995. SARs are cis DNA elements of chromosome dynamics: synthesis of a SAR repressor protein. *Cell.* 83:1137-48.

Struhl, G., and I. Greenwald. 1999. Presenilin is required for activity and nuclear access of Notch in *Drosophila. Nature.* 398:522-5.

Sun, X., and S. Artavanis-Tsakonas. 1997. Secreted forms of DELTA and SERRATE define antagonists of Notch signaling in *Drosophila. Development.* 124:3439-48.

Sun, Z.W., and C.D. Allis. 2002. Ubiquitination of histone H2B regulates H3 methylation and gene silencing in yeast. *Nature.* 418:104-8.

Sundaram, M., H.W. Cook, and D.M. Byers. 2004. The MARCKS family of phospholipid binding proteins: regulation of phospholipase D and other cellular components. *Biochem Cell Biol.* 82:191-200.

Swank, R.A., J.P. Th'ng, X.W. Guo, J. Valdez, E.M. Bradbury, and L.R. Gurley. 1997. Four distinct cyclin-dependent kinases phosphorylate histone H1 at all of its growth-related phosphorylation sites. *Biochemistry.* 36:13761-8.

Swedlow, J.R., and T. Hirano. 2003. The making of the mitotic chromosome: modern insights into classical questions. *Mol Cell.* 11:557-69.

Targett-Adams, P., D. Chambers, S. Gledhill, R.G. Hope, J.F. Coy, A. Girod, and J. McLauchlan. 2003. Live cell analysis and targeting of the lipid droplet-binding adipocyte differentiation-related protein. *J Biol Chem.* 278:15998-6007.

Tauchi-Sato, K., S. Ozeki, T. Houjou, R. Taguchi, and T. Fujimoto. 2002. The surface of lipid droplets is a phospholipid monolayer with a unique Fatty Acid composition. *J Biol Chem.* 277:44507-12.

Tenenbaum, D. 2003. What's All the Buzz? Fruit Flies Provide Unique Model for Cancer Research. *J Natl Cancer Inst.* 95:1742-4.

Theodosiou, N.A., and T. Xu. 1998. Use of FLP/FRT system to study *Drosophila* development. *Methods.* 14:355-65.

Tio, M., C. Ma, and K. Moses. 1996. Extracellular regulators and pattern formation in the developing Drosophila retina. *Biochem Soc Symp.* 62:61-75.

Tong, A.H., M. Evangelista, A.B. Parsons, H. Xu, G.D. Bader, N. Page, M. Robinson, S. Raghibizadeh, C.W. Hogue, H. Bussey, B. Andrews, M. Tyers, and C. Boone. 2001. Systematic genetic analysis with ordered arrays of yeast deletion mutants. *Science.* 294:2364-8.

Toone, W.M., B.L. Aerne, B.A. Morgan, and L.H. Johnston. 1997. Getting started: regulating the initiation of DNA replication in yeast. *Annu Rev Microbiol.* 51:125-49.

Turner, S.D., A.R. Ricci, H. Petropoulos, J. Genereaux, I.S. Skerjanc, and C.J. Brandl. 2002. The E2 ubiquitin conjugase Rad6 is required for the ArgR/Mcm1 repression of ARG1 transcription. *Mol Cell Biol.* 22:4011-9.

Vagnarelli, P., D.F. Hudson, S.A. Ribeiro, L. Trinkle-Mulcahy, J.M. Spence, F. Lai, C.J. Farr, A.I. Lamond, and W.C. Earnshaw. 2006. Condensin and Repo-Man-PP1 co-operate in the regulation of chromosome architecture during mitosis. *Nat Cell Biol.* 8:1133-42.

Van Wart, H.E., and H. Birkedal-Hansen. 1990. The cysteine switch: a principle of regulation of metalloproteinase activity with potential applicability to the entire matrix metalloproteinase gene family. *Proc Natl Acad Sci U S A.* 87:5578-82.

Vaquero, A., M.B. Scher, D.H. Lee, A. Sutton, H.L. Cheng, F.W. Alt, L. Serrano, R. Sternglanz, and D. Reinberg. 2006. SirT2 is a histone deacetylase with preference for histone H4 Lys 16 during mitosis. *Genes Dev.* 20:1256-61.

Vass, S., S. Cotterill, A.M. Valdeolmillos, J.L. Barbero, E. Lin, W.D. Warren, and M.M. Heck. 2003. Depletion of Drad21/Scc1 in Drosophila cells leads to instability of the cohesin complex and disruption of mitotic progression. *Curr Biol.* 13:208-18.

Vernos, I., J. Raats, T. Hirano, J. Heasman, E. Karsenti, and C. Wylie. 1995. Xklp1, a chromosomal *Xenopus* kinesin-like protein essential for spindle organization and chromosome positioning. *Cell.* 81:117-27.

Wan, H.C., R.C. Melo, Z. Jin, A.M. Dvorak, and P.F. Weller. 2007. Roles and origins of leukocyte lipid bodies: proteomic and ultrastructural studies. *Faseb J.* 21:167-78.

Wang, J.C. 2002. Cellular roles of DNA topoisomerases: a molecular perspective. *Nat Rev Mol Cell Biol.* 3:430-40.

Wasserman, Z.R. 2005. Making a new turn in matrix metalloprotease inhibition. *Chem Biol.* 12:143-4.

Weake, V.M., K.K. Lee, S. Guelman, C.H. Lin, C. Seidel, S.M. Abmayr, and J.L. Workman. 2008. SAGA-mediated H2B deubiquitination controls the development of neuronal connectivity in the Drosophila visual system. *Embo J.* 27:394-405.

Weaver, A.M. 2006. Invadopodia: specialized cell structures for cancer invasion. *Clin Exp Metastasis.* 23:97-105.

Wei, S., Z. Xie, E. Filenova, and K. Brew. 2003. *Drosophila* TIMP is a potent inhibitor of MMPs and TACE: similarities in structure and function to TIMP-3. *Biochemistry.* 42:12200-7.

Weihe, U., M. Milan, and S.M. Cohen. 2001. Regulation of Apterous activity in Drosophila wing development. *Development.* 128:4615-22.

Welte, M.A. 2007. Proteins under new management: lipid droplets deliver. *Trends Cell Biol.* 17:363-9.

Weng, A.P., and J.C. Aster. 2004. Multiple niches for Notch in cancer: context is everything. *Curr Opin Genet Dev.* 14:48-54.

Whitfield, W.G., M.A. Chaplin, K. Oegema, H. Parry, and D.M. Glover. 1995. The 190 kDa centrosome-associated protein of Drosophila melanogaster contains four zinc finger motifs and binds to specific sites on polytene chromosomes. *J Cell Sci.* 108 (Pt 11):3377-87.

Wilkinson, K.D. 2000. Ubiquitination and deubiquitination: targeting of proteins for degradation by the proteasome. *Semin Cell Dev Biol.* 11:141-8.

Wolins, N.E., B.K. Quaynor, J.R. Skinner, M.J. Schoenfish, A. Tzekov, and P.E. Bickel. 2005. S3-12, Adipophilin, and TIP47 package lipid in adipocytes. *J Biol Chem.* 280:19146-55.

Wood, A., N.J. Krogan, J. Dover, J. Schneider, J. Heidt, M.A. Boateng, K. Dean, A. Golshani, Y. Zhang, J.F. Greenblatt, M. Johnston, and A. Shilatifard. 2003. Bre1, an E3 ubiquitin ligase required for recruitment and substrate selection of Rad6 at a promoter. *Mol Cell.* 11:267-74.

Woodcock, C.L., and S. Dimitrov. 2001. Higher-order structure of chromatin and chromosomes. *Curr Opin Genet Dev.* 11:130-5.

Wu, X., L. Yen, L. Irwin, C. Sweeney, and K.L. Carraway, 3rd. 2004. Stabilization of the E3 ubiquitin ligase Nrdp1 by the deubiquitinating enzyme USP8. *Mol Cell Biol.* 24:7748-57.

Yamaguchi, T., N. Omatsu, E. Morimoto, H. Nakashima, K. Ueno, T. Tanaka, K. Satouchi, F. Hirose, and T. Osumi. 2007. CGI-58 facilitates lipolysis on lipid droplets but is not involved in the vesiculation of lipid droplets caused by hormonal stimulation. *J Lipid Res.* 48:1078-89.

Yao, C., J.E. Donelson, and M.E. Wilson. 2003. The major surface protease (MSP or GP63) of *Leishmania* sp. Biosynthesis, regulation of expression, and function. *Mol Biochem Parasitol.* 132:1-16.

Ye, Y., N. Lukinova, and M.E. Fortini. 1999. Neurogenic phenotypes and altered Notch processing in Drosophila Presenilin mutants. *Nature.* 398:525-9.

Zhang, H. 2007. Life without kinase: cyclin E promotes DNA replication licensing and beyond. *Mol Cell.* 25:175-6.